



12-2007

Integrating Mass Spectrometry Based Proteomics and Bioinformatics Technologies for the Molecular Level Characterization of *Shewanella oneidensis* to Chromate Exposure

Melissa Renee Thompson
University of Tennessee - Knoxville

Recommended Citation

Thompson, Melissa Renee, "Integrating Mass Spectrometry Based Proteomics and Bioinformatics Technologies for the Molecular Level Characterization of *Shewanella oneidensis* to Chromate Exposure." PhD diss., University of Tennessee, 2007.
https://trace.tennessee.edu/utk_graddiss/318

This Dissertation is brought to you for free and open access by the Graduate School at Trace: Tennessee Research and Creative Exchange. It has been accepted for inclusion in Doctoral Dissertations by an authorized administrator of Trace: Tennessee Research and Creative Exchange. For more information, please contact trace@utk.edu.

To the Graduate Council:

I am submitting herewith a dissertation written by Melissa Renee Thompson entitled "Integrating Mass Spectrometry Based Proteomics and Bioinformatics Technologies for the Molecular Level Characterization of *Shewanella oneidensis* to Chromate Exposure." I have examined the final electronic copy of this dissertation for form and content and recommend that it be accepted in partial fulfillment of the requirements for the degree of Doctor of Philosophy, with a major in Life Sciences.

Robert L. Hettich, Major Professor

We have read this dissertation and recommend its acceptance:

Dorothea Thompson, Elizabeth Howell, Loren Hauser, Frank Larimer

Accepted for the Council:

Carolyn R. Hodges

Vice Provost and Dean of the Graduate School

(Original signatures are on file with official student records.)

To the Graduate Council:

I am submitting herewith a dissertation written by Melissa Renee Thompson entitled “Integrating Mass Spectrometry Based Proteomics and Bioinformatics Technologies for the Molecular Level Characterization of *Shewanella oneidensis* to Chromate Exposure”. I have examined the final electronic copy of this dissertation for form and content and recommended that it be accepted in partial fulfillment of the requirements for the degree of Doctor of Philosophy, with a major in Life Sciences.

Robert L. Hettich
Major Professor

We have read this dissertation
and recommended its acceptance:

Dorothea Thompson

Elizabeth Howell

Loren Hauser

Frank Larimer

Accepted for the Council:

Carolyn R. Hodges
Vice Provost and
Dean of the Graduate School

“Original signatures are on file with official student records.”

**INTEGRATING MASS SPECTROMETRY BASED PROTEOMICS
AND BIOINFORMATICS TECHNOLOGIES FOR THE
MOLECULAR LEVEL CHARACTERIZATION OF *SHEWANELLA*
ONEIDENSIS TO CHROMATE EXPOSURE**

A Dissertation Presented for the Doctor of Philosophy Degree
The University of Tennessee, Knoxville

Melissa Renee Thompson
December, 2007

DEDICATION

This dissertation is dedicated to everyone who helped me along the way from childhood to adulthood. I specifically wish to thank my husband, Brad, who has supported me during my entire graduate school career and sacrificed a great deal for me. I also wish to thank my family Bob and Brenda Rugen, Michelle Rugen, Brett and Kristin Rugen, H.C. Rugen, Jr., Ruth Dove, Gertrude Connor, and Lendell and Janet Thompson. To Seymore and Putty, who are the best support and distraction after a long day in the laboratory or writing at the computer. I would like to dedicate this work in memory of my grandfather Charles Dove and grandmother Maxine Dove. Finally, I would like to dedicate this work in memory of my grandmother, Eleanor Rugen, who was a great source of encouragement of my dreams and goals during her life.

ACKNOWLEDGMENT

I would like to thank the many people who have assisted me in the completion of the work presented in this dissertation. I would like to thank my advisor, Dr. Robert Hettich for providing guidance in my doctoral studies. I would also like to thank Dr. Dorothea Thompson, Dr. Elizabeth Howell, Dr. Frank Larimer, and Dr. Loren Hauser for serving on my dissertation committee and providing guidance in the pursuit of my degree. I would like to acknowledge the Organic and Biological Mass Spectrometry group at Oak Ridge National Laboratory for providing a place to pursue my research endeavors. I specifically like to thank Becky Maggard, who without her kindness and never ending help this dissertation would not have been possible. I would also like to thank Dr. Nathan VerBerkmoes, Dr. Hayes McDonald, Dr. Vilmos Kertesz, and Dr. Greg Hurst for providing useful guidance and discussions about my dissertation work. I would like to thank my mom, Brenda Rugen, for reading correcting this dissertation and in a tireless effort to help me succeed. I would like to thank Dr. Steven Brown, Dr. Karuna Chourey, and Dr. Dorothea Thompson for providing cellular material for the work presented in this dissertation. I would specifically like to thank Dr. Karuna Chourey for providing guidance and support in microbiology and cell culture. Finally, I would like to acknowledge financial support from the Graduate School of Genome Science and Technology (University of Tennessee-Knoxville) and the Environmental Remediation Sciences Program of the Office of Science at the Department of Energy, which made the research presented here possible.

ABSTRACT

The research outlined in this dissertation involves the development and demonstration of a mass spectrometry-based proteomics approach to characterize the global level molecular response of *Shewanella oneidensis* MR-1 to chromate exposure. The proteomics approach is centered on a high performance technique of multi-dimensional on-line liquid chromatographic separations with subsequent tandem mass spectrometric detection. Since very complex proteome samples are digested into peptides and then directly measured by MS, this technique is termed shotgun proteomics. This approach affords the identification and quantification of complex mixtures by directly analyzing their proteolytic peptides and then using computational techniques to reassemble the protein information. The research goals for this dissertation project were two-fold: (1) enhancement of the experimental and computational methodologies to permit deeper and more confident proteome characterizations, and (2) demonstration of this optimized approach for the comprehensive investigation of the molecular level response of the bacterium *S. oneidensis* to chromate insult. To address research needs, we developed a single-tube lysis method for cell lysis-proteome digestion to enable investigations of small amounts of cellular biomass, and identified suitable bioinformatic approaches to mine post-translational modifications from proteome datasets. These advancements were then utilized to examine the molecular level response of *S. oneidensis* to chromate insult, which was accomplished by varying chromate concentrations, dosages, and time points. These measurements provided the first global proteome-level observation of the dynamic changes of *S. oneidensis* in response to chromate insult.

TABLE OF CONTENTS

Chapter 1- Introduction to <i>Shewanella oneidensis</i> Microbiology with respect to Chromate Exposure using Mass Spectrometry Technology	1
Chapter 2- Experimental Design of Shotgun Proteomics Experiments and Bioinformatic Platforms using Multidimensional Protein Identification Technology	22
Chapter 3- Understanding Global Chromate Response of <i>Shewanella oneidensis</i> MR-1 under Acute and Chronic Exposure Using Shotgun Proteomics	51
Chapter 4- Dosage-Dependent Proteome Response of <i>Shewanella oneidensis</i> MR-1 to Acute Chromate Challenge	85
Chapter 5- Systematic Assessment of the Benefits and Caveats in Mining Microbial Post-Translational Modifications from Shotgun Proteomic Data; Response of <i>Shewanella oneidensis</i> to Chromate Exposure	126
Chapter 6- Proteomic Comparison of <i>Shewanella oneidensis</i> MR-1 Wild-Type and a Response Regulator Deletion Strain under Conditions of Chromate Transformation	162
Chapter 7- An Experimental Approach for Large-Scale Proteome Measurements from Small-Scale Amounts of Microbial Cultures and Communities	204
Chapter 8- Conclusions	226
List of References	241
Appendix	279
Vita	358

LIST OF TABLES

Table 2.1. The Consecutive LC Steps Employed in the Two-Dimensional Separation	31
Table 3.1. Proteome Analysis of Chromate-Shocked <i>S. oneidensis</i> MR-1	56
Table 3.2. Functional Categories of Identified Proteins with at Least Two Peptides.....	58
Table 3.3. Up-Regulated Proteins Identified in the 90 min Chromate-Shocked Samples	60
Table 3.4. Down-Regulated Proteins Identified in the 90 min Chromate-Shocked Samples	62
Table 3.5. Functional Distribution of the Observed and Predicted MR-1 Proteomes	71
Table 3.6. Relative Expression of Up-regulated mRNA and Corresponding Proteins in Response to 24-h Chromate Exposure	74
Table 3.7. Relative Expression of Down-regulated Proteins and Corresponding mRNA Levels after 24-h Exposure to Chromate	80
Table 4.1. Global Proteome Analysis of Chromate Dose on <i>S. oneidensis</i>	93
Table 4.2. False Peptide and Protein Identifications with a LCQ and a LTQ.....	97
Table 4.3. Selected Differentially Expressed Proteins Identified after Treatment with 0.3 mM K ₂ CrO ₄	104
Table 4.4. Selected Differentially Expressed Proteins Identified after Treatment with 0.5 mM K ₂ CrO ₄	106
Table 4.5. Selected Differentially Expressed Proteins Identified after Treatment with 1 mM K ₂ CrO ₄	108
Table 5.1. Amino Acid Residues and Corresponding Post-translational Modifications	133

Table 5.2. False Discovery Rates for 45min Control Run1 Dataset at Various Filter Threshold Levels	136
Table 5.3. Number of Post-Translationally Modified Peptides Identified in Each Dataset Searched using DBDigger.....	140
Table 5.4. Sequest Peptide Identifications from a Subset of MS/MS Spectra First Identified by DBDigger	142
Table 5.5. FDRs for Total and PTM Peptide Identifications with InsPecT	146
Table 5.6. Identification of Chemoreceptors using DBDigger and InsPecT from the 45 and 90 min Datasets	154
Table 6.1. Total Proteins Identified by Strains MR-1 and $\Delta 2426$ at Each Time Point.....	173
Table 6.2. Up-Regulated Proteins from MR-1 Cultures Versus $\Delta 2426$ Cultures	178
Table 6.3. Down-Regulated Proteins in MR-1 Cultures Versus $\Delta 2426$ Cultures	181
Table 6.4. Proteins Identified as Up-Regulated upon Cr(VI) Exposure in MR-1 Cultures	190
Table 6.5. Proteins Identified as Down-Regulated upon Cr(VI) Exposure in MR-1 Cultures	193
Table 6.6. InsPecT p-value Thresholds and Corresponding FDRs for Strain MR-1 PTMs	197
Table 7.1. Protein Identifications Made Using the LCQ Ion Trap	215
Table 7.2. Functional Category Distribution for <i>S. oneidensis</i> MR-1 LTQ Dataset.....	217
Table 7.3. Functional Category Distribution for <i>R. palustris</i> LTQ Dataset.....	222
Table 7.4. AMD Biofilm Proteome Measurements using DBDigger with the LTQ	223

LIST OF FIGURES

Figure 1.1. An integrated approach to understand chromate exposure in <i>S. oneidensis</i>	2
Figure 1.2. Original design of the electrospray ionization source	6
Figure 1.3. Flowchart diagram of the proteome studies of <i>S. oneidensis</i> Cr(VI) exposure	19
Figure 1.4. Representative shotgun proteomics experimental design.....	20
Figure 2.1. Schematic diagram of the two-dimensional column setup.....	29
Figure 2.2. TIC and base peak chromatograms from selected chromatography steps	33
Figure 2.3. Instability diagram of the three-dimensional ion trap	36
Figure 2.4. A MS/MS from a low-abundant peptide using the LTQ.....	39
Figure 2.5. Flow diagram outlining the scheme of the gitinspect.pl perl script	45
Figure 2.6. Predicted the protein FDR based on the peptide FDR classification	49
Figure 4.1. MS/MS from a peptide of SO3585 identified in the 0.3 mM dosage.....	96
Figure 4.2. Functional category distribution for each dosage and the control condition	100
Figure 4.3. Venn diagrams of dosage response proteome samples for the LTQ and LCQ	102
Figure 4.4. Proteins demonstrating dosage-dependent up-regulation.....	123
Figure 4.5. Dosage dependent abundance of proteins between 0.3 and 1 mM dosages	124
Figure 5.1. A Venn diagram comparing peptide identifications.....	138
Figure 5.2. Identification of PTM peptides using (A) DBDigger and (B) InsPecT	148

Figure 5.3. A sequence tree (or dendogram) depicting sequence similarity	153
Figure 5.4. A MS/MS for SO3642, a chemoreceptor, confirms a C-terminal peptide	157
Figure 5.5. A Venn diagram comparing DBDigger and InsPecT PTM peptides	159
Figure 6.1. A sequence tree aligning the protein sequences of SO2426 and SO4477.....	169
Figure 6.2. Transformation of 0.3 mM Cr(VI) in the form of K ₂ CrO ₄	171
Figure 6.3. Functional category distribution of proteins from strains MR-1 and Δ2426.....	175
Figure 6.4. Post-translationally modified peptides identified by InsPecT for strain MR-1	199
Figure 6.5. A peptide MS/MS from SO2426 with confirmed modifications.....	203
Figure 7.1. Schematic of the traditional sonication versus the single tube lysis method	209
Figure 7.2. BCA protein quantification assay for different amounts of wet cell pellets	213
Figure 8.1. The sulfur metabolism pathway of <i>S. oneidensis</i> MR-1.....	232

LIST OF SYMBOLS AND ABBREVIATIONS

µg	Micrograms
µL	Microliter
µm	Micrometer
2-D	Two dimensional
2D-PAGE	Two-dimensional polyacrylamide gel electrophoresis
Å	Angstrom
AC	Alternating current
ACN	Acetonitrile
AFM	Atomic Force Microscopy
AMD	Acid mine drainage
AMT	Accurate mass and time
AQUA	Absolute quantification isotopically labelled peptides
b ion	Fragmentation of a peptide from the N-terminus between the carboxy and amide bonds
BCA	Bicinchoninic acid solution
CaCl ₂	Calcium chloride
CID	Collision induced dissociation fragmentation method
cm	Centimeter
Cr	Chromium
Cr(III)	Trivalent chromium
Cr(V)	Pentavalent chromium
Cr(VI)	Hexavalent chromium
Cr ₂ O ₇ ²⁻	Dichromate
CrO ₄ ²⁻	Chromate
Da	Dalton
DC	Direct current
DMSO	Dimethyl sulfoxide
DNA	Deoxyribonucleic acid
DOE	Department of Energy
DOM	Dissolved organic matter
DPC	Diphenylcarbazide
DTA	Flat file of MS/MS spectrum converted from RAW file
DTT	Dithiothreitol
EDTA	Ethylenediaminetetraacetic acid
ESI	Electrospray ionization
FA	Formic acid
FASTA	Text file containing a nucleotide or amino acid sequence
FDR	False discovery rate
Fe(II)	Divalent iron
Fe(III)	Trivalent iron
FT-ICR	Fourier transform ion cyclotron resonance
FTICR MS	Fourier transform ion cyclotron resonance mass spectrometry

g	Gravity
h or hr	Hour
HCl	Hydrogen chloride
H ₂ O	Chemical formula for water
HPLC	High performance liquid chromatography
ICAT	Isotope coded affinity tags for peptide/protein quantification
ID	Internal diameter or identification
IEF	Isoelectric focusing
iTRAQ	Isobaric amine-reactive tagging reagent
K ₂ CrO ₄	Potassium chromate
KEGG	Kyoto encyclopedia of genes and genomes
kDa	Kilodaltons
kV	Kilovolts
L	Liter
LB	Luria-Bertani medium
LC	Liquid chromatography
LC/LC-MS/MS	2-dimensional liquid chromatography tandem mass spectrometry
LC-MS	Liquid chromatography-mass spectrometry
LC-MS/MS	Liquid chromatography-tandem mass spectrometry
LCQ	Liquid chromatography quadrupole ion trap, 3-D ion trap
LTQ	Linear trapping quadrupole
LTQ-FTICR	Linear trapping quadrupole Fourier transform ion cyclotron resonance hybrid mass spectrometer
LTQ-MS	Linear trapping quadrupole mass spectrometry
M	Molarity
m/z	Mass to charge ratio
MALDI	Matrix assisted laser desorption ionization
MALDI-MS	Matrix assisted laser desorption ionization mass spectrometry
MASPIC	DBDigger scorer
mg	Milligrams
MIC	Minimum inhibitory concentration
min	Minute
mL	milliLiters
mM	Millimolar
Mn(IV)	Tetravalent manganese
MS	Mass spectrometry
MS/MS	Tandem mass spectrometry
ms2	Flat file of MS/MS data converted from RAW file
MudPIT	Multidimensional protein identification technology
mzXML	Flat file of MS/MS data converted from RAW file
NA or N/A	Not available
NaCl	Sodium Chloride
nL	Nanoliter
OD	Optical density
ORF	Open reading frame
ORNL	Oak Ridge National Laboratory

pH	Measure of the acidity of a solution
pI	Isoelectric point
PMF	Peptide mass fingerprinting
ppm	Parts per million
PTM(s)	Post translational modification(s)
p-value	Probability value that MS/MS identification is true
QIT	Quadrupole ion trap
QTOF	Quadrupole time of flight
RF	Radio frequency
RNA	Ribonucleic acid
rpm	Revolutions per minute
ROS	Reactive oxygen species
RP	Reverse phase
s	Second
SCX	Strong cation exchange
SDS	Sodium dodecyl sulphate
SDS-PAGE	Sodium dodecyl sulphate polyacrylamide gel electrophoresis
sqt	Results file of MS/MS data searched with database or de novo
TCA	Tricarboxylic acid cycle
TFE	Tetrafluoroethylene
TIC	Total ion current
TIGR	The Institute for Genome Research
TOF	Time of flight
Tris	Trishydroxymethylaminomethane
txt	Text file
$U - V \cos \Omega t$	Equation for the DC and RF voltage of a quadrupole ion trap
UV	Ultraviolet radiation
w/w	Weight for weight
WT	Wild-type
Xcorr	SEQUEST cross-correlation score
y ion	Fragmentation of a peptide from the C-terminus between the carboxy and amide bonds
ΔCN or $DelCN$ or $\Delta DeltaCN$	Sequest delta correlation score

Chapter 1

Introduction to *Shewanella oneidensis* Microbiology with Respect to Chromate

Exposure using Mass Spectrometry Technology

Introduction

Utilizing mass spectrometry technology to decipher global metabolic pathways and regulatory networks has increased understanding of these cellular processes in biological systems. The application of mass spectrometry based proteomics falls under the area of systems biology. Systems biology as defined by Ideker *et al* [1] is the integration of data from a number of technologies in order to build a comprehensive model to predict cellular pathway responses in a variety of organisms. This approach generally utilizes metabolomic, genomic, transcriptomic, and proteomic datasets in some fashion in order to catalog potential metabolic pathway members. The proteomics portion of systems biology encompasses three areas of emerging technology (1) improvement of mass spectrometry instrumentation, (2) improvements in separation of complex mixtures, and (3) continuous advancement in the computational software utilized for mining the resulting datasets. The research in this dissertation contributed to a Department of Energy (DOE) project designed to utilize a systems biology approach with the proteomics portion of the project presented in this dissertation. The goal of this dissertation is to understand the chromate response in *Shewanella oneidensis* (Figure 1.1) for the purposes of bioremediation.

The use of proteomics based analyses began with two-dimensional polyacrylamide gel electrophoresis (2-D PAGE) in 1975 [2]. This method separates

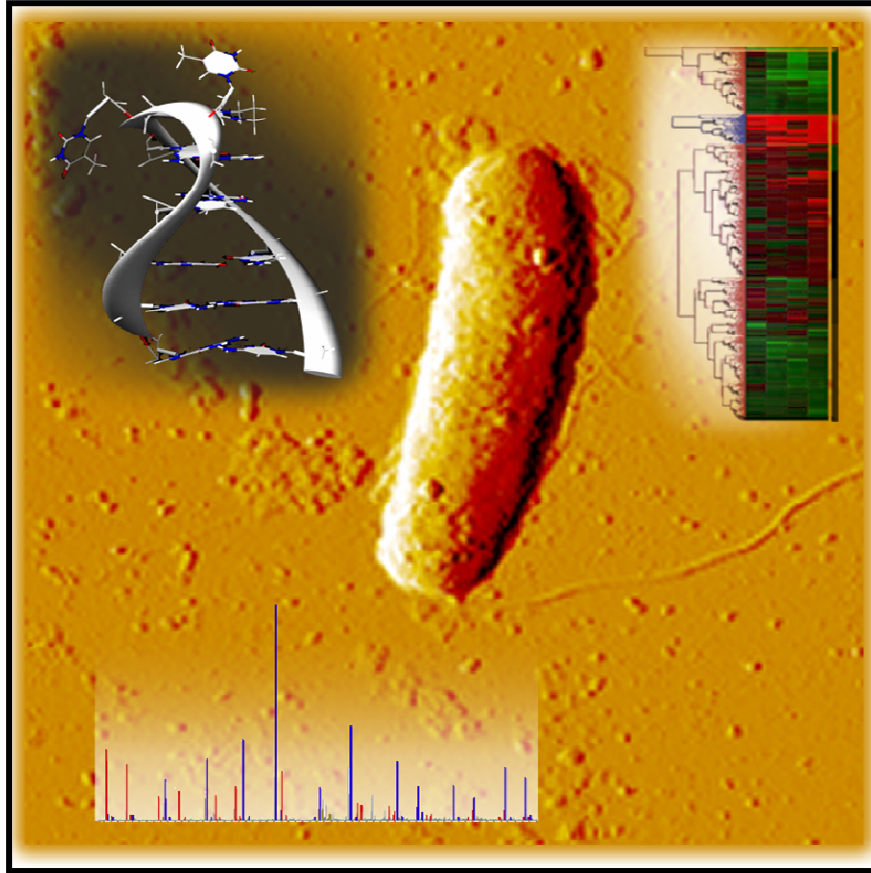


Figure 1.1. An integrated approach to understand chromate exposure in *S. oneidensis*. The dissertation comprised the proteomic portion of the project depicted by the tandem mass spectrum in the figure. The bacterial cell is *S. oneidensis* imaged by atomic force microscopy (AFM) (courtesy of K. Chourey). The double helix DNA strand depicts the availability of the genome sequence (courtesy of G. Wickham) and the RNA expression cluster depicts the transcriptomic portion of the project (courtesy of D. Thompson).

mixtures of proteins first by the isoelectric point of each individual protein and then by the molecular mass of the protein [2-4]. This initial work demonstrated the utility of separating complex mixtures of proteins in order to answer questions pertaining to the expression levels and subsequent metabolic pathway information of cellular proteins responding to a perturbation. The initial work with 2-D PAGE was limited by the inability to identify the differential spots on the gel easily. Identification of the protein species was accomplished initially by N-terminal Edman degradation [5, 6]. Edman degradation was developed by Edman and Begg [6] and operates by progressively cleaving the N-terminal amino acid residue from the protein. This residue is then separated chromatographically in order to determine its identity. The first application of Edman degradation required 5.0 mg of purified protein [6].

Mass Spectrometry Based Proteomics

Mass Spectrometry was not originally amenable to working with more fragile biomolecules such as proteins due to limitations in the types of ionization sources used previously (i.e. chemical and electron ionization [7]). Electron ionization was the first ionization source created for mass spectrometric detection of organic molecules and was developed in the late 1920's [8]. This ionization method employs the use of electrons ejected off a heated filament which bombards a gas phase analyte that has been injected into the ionization space. This method of ionization works well for molecules that have a high vapor pressure [8]. The mechanism of chemical ionization occurs through the interaction of the sample analyte desorbed from a probe with ions that are produced in the source (i.e. a reagent gas) leading to a reduction in the fragmentation of the molecular

species [8]. This method of ionization was created to circumvent the harshness of electron ionization, which fragmentation of the molecular species is common.

During the early 1990's, Hillenkamp *et al* [9] described a new, more gentle means of creating ionized proteins, defined as matrix assisted laser desorption ionization (MALDI). Now, gel spots identified in the 2-D PAGE gels could be excised, the protein(s) digested, and analyzed using MALDI-MS with a method designated as peptide mass fingerprinting (PMF). The number of intact unique peptide masses to be identified for a given protein can be as few as three to four using PMF [10]. This method works well for less complex mixtures such as gel spots, however, this methodology is not amenable to complex mixtures of proteins without the initial 2-D PAGE separation of the proteins. Therefore, a gel-free methodology was developed due to the cumbersome nature of 2-D PAGE.

In MALDI, the peptides/proteins are spotted onto a conductive metal plate and dried within the embedded matrix that is ablated by a laser [9]. The laser causes ionization of the matrix, which is generally an acid, creating positively charged ions by desorbing both the matrix and the embedded analyte off the surface. Following desorption, there are ion-molecule reactions between the matrix (the ion) and the analyte (the molecule), resulting in an ionized analyte. The charged analyte can now be injected into the mass analyzer for subsequent detection. Primarily, MALDI ionization is conducted under vacuum [8], however, there is an atmospheric pressure source available that was developed by Laiko *et al* [11].

Electrospray is also a gentle ionization source similar to MALDI-MS, but the peptides/proteins remain in solution. Electrospray ionization (ESI) was first described

and developed by Fenn *et al* [12] as a method of atmospheric ionization for large biomolecules such as DNA and proteins. ESI is a solution-based ionization method and creates ions by applying high voltage (in the range of kilovolts) to a silica capillary causing ionized droplets to be sprayed from the tip of the silica [8]. Due to Columbic repulsion of the ionized analyte within the droplet, each droplet formed breaks apart into smaller droplets causing desolvation of the ionized analyte and creating a Taylor cone. With respect to electrospray ionization in mass spectrometry, the Taylor cone is a plume of charged droplets emitted from the electrospray tip. The droplets form due to the voltage difference between the electrospray tip and the opening of the mass spectrometer [8]. The droplets undergo further desolvation within a heated metal capillary that transfers the ions into the vacuum of the mass spectrometer [8] (Figure 1.2). This method of ionization is easily coupled to a number of mass spectrometers as described below. In addition, the primary advantage of this ionization technique for analysis of biomolecules is the ability to couple this ionization source directly to the chromatographic separation of complex mixtures of proteins/peptides as discussed below [13-16].

There are a number of mass spectrometer designs amenable to acquiring large amounts of data on peptides or proteins with a relatively rapid data acquisition speed. However, the mass spectrometer chosen for a given proteomics experiment is dependent on the properties of the sample to be analyzed (intact proteins or digested peptides) and the capabilities of the mass analyzer such as the ability to perform data-dependent MS/MS, the mass resolution, the dynamic range, and the mass range. Data-dependent MS/MS allows for an unbiased selection of ions to be isolated and subsequently fragmented. This capability is necessary when attempting to catalog the members of a

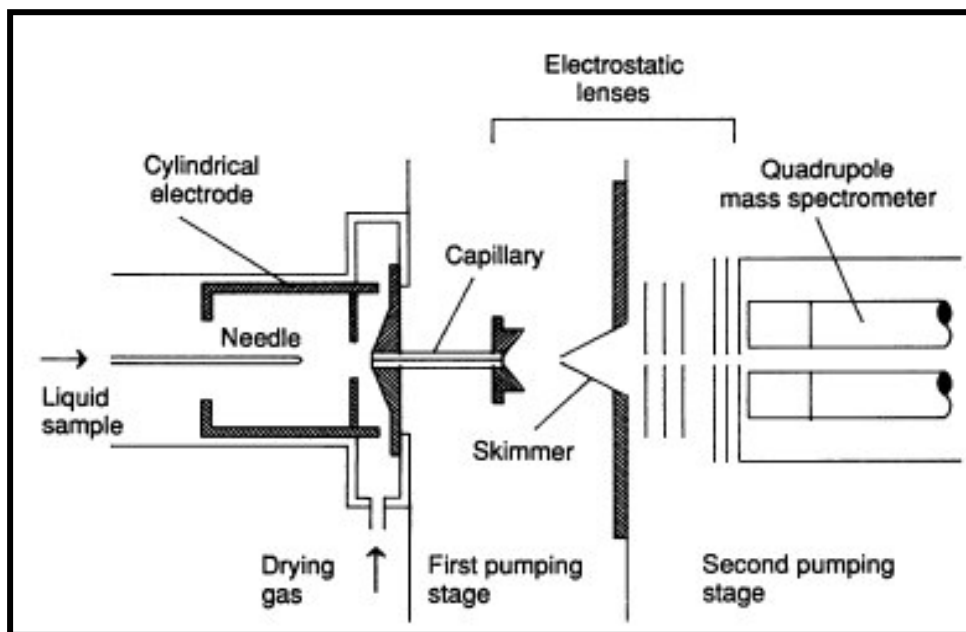


Figure 1.2. Original design of the electrospray ionization source.

Reprinted Figure 1 from *Science*, Vol. 246, Fenn *et al*, Electrospray ionization for mass spectrometry of large biomolecules, pages 64-71, Copyright 1989 with permission from AAAS.

complex mixture (i.e. a proteome). The mass resolution for a mass analyzer is defined as the peak width at half of the maximum height for that peak [17, 18]. The dynamic range is the ability of an ion lower in concentration compared to another ion to be detected in concurrence with the abundant ion within the same experiment [19, 20]. The mass range of a mass analyzer is a continuum of m/z values from lower m/z to greater m/z detected by the mass spectrometer and determines the type of biomolecule, intact protein or digested peptide, which can be utilized for an experiment.

Mass analyzers that have the ability to detect and analyze intact proteins include the Fourier transform ion cyclotron resonance (FT-ICR) [21, 22], Orbitrap [23], and time of flight (TOF) [24]. The benefits of using an FT-ICR include the high mass accuracy (in the ppm range), high mass resolution, and ability to be coupled with chromatographic separation [25, 26]. In addition, the FT-ICR has been coupled to the linear trapping quadrupole (LTQ) to form a hybrid instrument with enhanced capabilities [22]. The Orbitrap operates in a similar fashion as the FT-ICR, utilizing the ions' oscillation frequency as the method of detection. This mass analyzer differs from the FT-ICR in the respect that the Orbitrap does not use a super-conducting magnet. The Orbitrap is also interfaced as a hybrid instrument with the LTQ, allowing high resolution full mass spectra to be acquired in the Orbitrap and ion fragmentation with subsequent MS/MS to be acquired in the LTQ. The time of flight mass analyzer is also found as a hybrid instrument with a quadrupole or an ion trap [27, 28].

Some mass analyzers do not have the capability to detect intact proteins, but are very useful for peptide detection and analysis, including the three-dimensional ion trap (LCQ) [29] and the LTQ [30]. The LTQ is a second generation design based on the

principles of the LCQ. Improvements made by Stafford *et al* [29] allowed the LCQ to be coupled readily with peptide detection. The LCQ has been used in many studies on shotgun proteomics due to its capabilities of data-dependent MS/MS, dynamic range, and data acquisition speed allowing the LCQ to be coupled to liquid chromatographic separation. However, improvements to the design of the ion trap led to the commercialization of the LTQ [30]. The LTQ improves on the capabilities of the LCQ with an even faster data acquisition speed leading to the detection of more than five times as many protein identifications and four times as many MS/MS spectra acquired during the same time period [31, 32]. The increased dynamic range observed with the LTQ in comparison to the LCQ is due to the increased data acquisition speed and the increased trapping volume leading to a larger ion population without the space-charging effects of the three dimensional ion trap [30].

Liquid Chromatographic Separation of Biomolecules

The development of electrospray led to improvements in the second area of proteomics: separation of complex mixtures of peptides/proteins. Electrospray allows for online separation of peptides/proteins to be coupled to mass spectrometry. This gel-free method of separating complex mixtures is less time consuming, more sensitive, and more reproducible than gel-based methods. A large number of studies published in proteomics utilize reverse phase (RP) separation online with mass spectrometry. This is due to the liquid phase used in RP separation consisting of an aqueous to organic gradient. These two types of solvents readily disperse into droplets that desolvate in the heated capillary rapidly. The addition of strong cation exchange (SCX) online with RP was introduced by Washburn *et al* [33]. This allowed unbiased separation of peptides

first based on their affinity for the negatively charged resin of the SCX column followed by separation based on hydrophobicity. 2-D PAGE separation is limited based on the protein molecular weight (proteins > 180 kDa) and isoelectric point (pI within the range of 5-10) [33]. The unbiased separation of peptides/proteins is required for global detection studies like shotgun proteomics experiments. Another form of separation, isoelectric focusing (IEF), has emerged as an alternative to SCX as the second dimension of separation [34, 35]. This form of separation is performed with either intact proteins or peptides. This is a gel-based method predominantly [34] utilizing IPG strips available commercially, but can also be liquid-based with a commercially available apparatus (i.e. the MicroRotor cell from Bio-Rad, Hercules, CA).

Advancements in Computational Biology

Computational biology or algorithm development is an emerging area of development due to the large advancements described above, however there is still more progress that must be made in order increase the confidence of subsequent MS/MS data analysis. The development of data-dependent MS/MS coupled to liquid chromatographic separation increased the number of acquired spectra [36, 37] so now the average LC-MS experiment acquires hundreds of thousands of MS/MS [20, 38]. Due to the large number of MS/MS acquired, manual interpretation of spectra is unfeasible. Therefore, the development of computational algorithms created an automated approach for MS/MS data analysis.

The algorithm Sequest [39] was the first written for mining peptide identifications from data-dependent MS/MS. This algorithm requires the presence of a database that contains the predicted protein sequences present in the complex peptide mixture being

analyzed. Subsequent to the release of Sequest, a number of other algorithms have been released freely or commercially packaged [40-44]. The key for an algorithm to be deemed successful is based on a number of criteria including (1) accuracy of MS/MS identification, (2) the length of time for searching a MS/MS, (3) ease of setting the criteria parameters for an algorithm, and (4) availability of the algorithm for use to the general scientific community. Each subsequent algorithm attempts to improve on the speed and accuracy of matching the MS/MS acquired against a theoretical spectrum generated from the provided protein database. Increasing the accuracy of matching the MS/MS acquired has been a challenge with respect to identifying post-translational modified proteins [45]. Three search algorithms, DBDigger [44], InsPecT [40], and Sequest [39] are evaluated in this dissertation and their abilities to search shotgun proteomics data for post-translational modifications (PTMs) are discussed in detail in Chapters 2 and 5.

PTMs are chemical modifications found on the amino acid residues of proteins and can be due to consequences of either biological or inorganic chemical processes [46-51]. These modifications, when due to an enzymatic process, are sometimes involved in cellular signaling and transcriptional activation control [52-55]. Oxidation is an example of an inorganic chemical modification process and can be due to an increase in the presence of free radicals within the cytosol that are subsequently quenched by proteins [46, 47]. Determining the identity and relative stoichiometry of the modified version of the residue in contrast to the unmodified counterpart is an emerging challenge in mass spectrometry based proteomics [45, 56]. This area is an emerging challenge due to advancements that have led to the routine cataloguing of the unmodified protein

complement in both bacterial cultures and tissue samples. However, the low stoichiometry of the modified counterpart has led to a large effort in enriching for the PTM of interest [55, 57, 58]. There are efforts being made to determine from a global proteome dataset the identity of post-translationally modified proteins [59, 60].

Bacteria are amenable subjects for large-scale studies, such as the shotgun proteomics studies described in this dissertation for a number of reasons. First, many bacterial lab strains are easily cultivatable under laboratory conditions, where cellular material is not a limiting factor. Second, the environmental importance of a growing list of bacterial species have been implicated in biogeochemical cycling [61-65] and fouling of energy pipelines [66]. Finally, a large number of bacteria have been characterized both physiologically and biochemically creating a vast literature database to search. In addition, the availability of an immense number of bacterial genome sequences from both isolates and environmental communities [67-78] is required for properly searching the MS/MS data.

***Shewanella oneidensis* MR-1**

S. oneidensis MR-1 is a gram-negative γ -proteobacteria first isolated from Lake Oneida, NY by Myers and Nealson [61] as *Alteromonas putrefaciens*. *A. putrefaciens* was renamed *Shewanella putrefaciens* by Myers and Nealson [79]. Then, in 1999 *S. putrefaciens* was renamed *S. oneidensis* MR-1 by Venkataswaran *et al* [80]. *S. oneidensis* was enriched from the lake sediments as a manganese and iron reducing bacterial species. The genome was published by Heidelberg *et al* [69], which facilitated work in better understanding the metabolic capabilities of this bacterium. *S. oneidensis* is facultatively anaerobic indicating that the bacterium prefers molecular oxygen as the

terminal electron acceptor for respiration; however, a number of electron acceptors can be utilized under anaerobic growth conditions [61]. In addition to manganese and iron, *S. oneidensis* was found to utilize many other compounds as terminal electron acceptors for respiration under anaerobic conditions [81-86]. Some other electron acceptors found to be utilized by *S. oneidensis* include fumarate and nitrate [81], elemental sulfur [85], and nitrite [87]. In fact, as a result of other unpublished work, the estimation is that of over a dozen electron acceptors may be utilized by *S. oneidensis* [88, 89]. The energetics of various electron acceptors have been determined with oxygen being most favorable followed by trivalent iron, nitrate, tetravalent manganese, and nitrite [90].

Since *S. oneidensis* has such a vast repertoire of electron acceptors for utilization, there must be an extensive regulatory and sensory system in place for recognizing this array of respiratory molecules. Upon completion of the genome sequence annotation [69], the identification of a large number of genes involved in environmental responses were identified. This included the annotation of 88 two-component response regulatory genes [69], three separate pathways for chemotaxis signaling, and 29 methyl-accepting chemotaxis protein receptors (chemoreceptors) [91]. The large number of response regulatory proteins is expected to be due to the diverse environments in which *S. oneidensis* may be found including marine, freshwater, and soil sediments [69]. Nealson *et al* [88] performed the first comprehensive study on chemotaxis response in *S. oneidensis*. The authors found *S. oneidensis* responded dramatically to the presence of nitrate and nitrite by accumulating around wells containing the electron acceptors [88]. In addition, the authors found that the bacterium did not demonstrate any type of response to the transition metals Mn(IV) oxide and Fe(III) citrate. However, a

subsequent study by Bencharit and Ward [92] found that *S. oneidensis* indeed demonstrates a chemotactic response using swarm plate assays to a variety of transition metals utilized as terminal electron acceptors including Mn(IV) and Fe(III).

S. oneidensis also contains a number of transcriptional regulatory proteins that have been elucidated in a number of studies [93-97]. Understanding the role of transcriptional regulators in response to gene expression is necessary to understand global regulatory and metabolic pathway function. EtrA, electron transport regulator A, was found to be 73.6% identical to the *Escherichia coli* protein Fnr, fumarate/nitrate regulator, and was found to functionally complement the *fnr* mutant in *E. coli* [93]. Another study using a gene replacement strategy [94] knocked out *etrA* in *S. oneidensis* and found that growth with fumarate and nitrate as terminal electron acceptors was reduced in the mutant cultures. The corresponding terminal reductase activities for the electron acceptors was also reduced in the mutant strain, indicating that EtrA may control transcription of the corresponding reductase genes [94]. A comparative transcriptomic study found that the mutant strain of the *etrA* gene knockout affected the transcriptional levels of 69 genes in *S. oneidensis* [95]. In addition, putative regulatory sequences demonstrating conservation with *fnr* regulatory sequences were identified upstream of 26 operons with affected transcript levels. The corresponding mRNAs from fumarate reductase were not only found to be repressed in the mutant strain, but contained a putative *fnr* sequence as well [94]. Another global regulator, Fur (ferric uptake regulator), has been studied in detail by transcriptomics and proteomics [96, 97]. These studies identified that Fur was involved in the negative regulation of iron transport genes and a putative Fur box was identified upstream of a number of affected genes [96].

Therefore, the presence of perhaps other transcriptional regulators, which respond to transition metals, is likely to be encoded in the genome as well.

As a result of the apparent respiratory versatility of *S. oneidensis*, initial work focused on understanding the enzymatic mechanism involved in using these transition metals as electron acceptors [66, 79, 81-84, 90, 98-103]. This work included attempts to isolate and characterize the terminal electron acceptor reductases [86, 102, 104-110]. First, prior to isolation of *S. oneidensis* MR-1, the utilization of metals for growth was not known to occur. Myers and Nealson [79] determined that a proton motive force was being generated, which is direct evidence for respiratory growth in response to reduction of Mn(IV) and Fe(III) when added as the sole electron acceptors to the growth media. Now, that growth coupled to metal reduction was known, the next step was to determine the enzymes involved in the direct reduction of the metals. A number of studies followed that demonstrated the role of a number of cytochromes and reductases from *S. oneidensis* that were essential to the electron transport chain activated in response to Mn(IV) and Fe(III) [81, 100, 102, 104-119]. Primarily, the identification of outer membrane cytochromes that were required for metal reduction indicated that *S. oneidensis* may require direct contact with the surface for reduction to occur [104-107]. After the genome sequence had been published [69], Meyer *et al* [117] and Yang *et al* [119] found that the *S. oneidensis* genome encodes a large number of cytochromes. In addition, terminal reductase activity for a number of electron acceptors was also found to be located in membrane protein preparations [86, 102, 120]. Direct contact with the surface may explain the lack of metal ion transporters in the genome compared to other bacterial species [69].

***S. oneidensis* Cr(VI) Toxicity and Transformation**

Another transition metal utilized as a reductant by *S. oneidensis* is the hexavalent species of chromium [Cr(VI)] in the form of chromate (CrO_4^{2-}) or dichromate ($\text{Cr}_2\text{O}_7^{2-}$) [86]. Chromate is a serious pollutant caused by human activities and discharged as liquid waste at many industrial and governmental facilities [121-123]. Traditionally, the process for remediating these contaminated waste sites has involved costly chemical methods [124, 125]. Therefore, the idea of using a natural environmental bacterium that demonstrates an enzymatic ability to reduce Cr(VI) to insoluble Cr(III) hydroxides in addition to a tolerance for various concentrations of Cr(VI) is more economical and environmentally friendly [126]. The use of bacteria for remediation has been proposed and implemented on a number of pollutants in the United States [126-131].

S. oneidensis has demonstrated Cr reductase activity in the cytoplasmic membrane [86], however, there are not any known reports on the growth of *S. oneidensis* utilizing Cr(VI) as the sole electron acceptor [132]. Myers *et al* [86] demonstrated the Cr reductase activity in anaerobically grown cultures utilizing fumarate as the electron acceptor with Cr(VI) added to the purified membrane fractions subsequently. The hypothesized pathway for reduction of Cr(VI) proceeds first via a one electron transfer yielding Cr(V) [86]. This is based on evidence from Myers *et al* [86], which found the reductase activity was inhibited by substances known to inhibit members of multi-component electron transport chains. In addition, Viamajala *et al* [133] demonstrated that the kinetic activity of the Cr reductase in *S. oneidensis* must involve at least three separate enzymes. The three enzymes are unknown, but one is described as being relatively slow and there are two that are enzymatically fast but susceptible to inhibition

by nitrite when nitrate is used as the electron acceptor [133]. This indicates that Cr reductase activity in *S. oneidensis* may be non-specific. These kinetics measurements were taken on *S. oneidensis* grown anaerobically with nitrate or fumarate as the electron acceptor. Direct evidence for Cr(VI) reduction in *S. oneidensis* was accomplished by Daulton *et al* [134] identifying extracellular precipitates of Cr(III) surrounding the outside of the bacterial cells. In addition, Cr(III) precipitates in the cytoplasm of *S. oneidensis* have been imaged by transmission electron microscopy [135]. However, there is also evidence that Cr(VI) reduction may occur indirectly via reduction of Fe(III) to Fe(II) first [131, 136, 137].

Cr reductase activity is not novel to *S. oneidensis*, rather a number of other bacteria have shown this activity previously. This includes *S. alga* BrY, a relative of *S. oneidensis*, where *S. alga* was found to be proficient in Cr(VI) reduction following a starvation period [137]. The starvation period causes the cells to decrease in volume allowing them to penetrate further into subsurface environments where Cr(VI) concentrations may be greater. In addition to *S. alga*, other bacterial species encode soluble Cr(VI) reductase proteins that have been purified, including *Pseudomonas putida* MK1 [138], *P. putida* PRS2000 [139], and *Pseudomonas ambigua* G-1 [140].

Even though many bacterial species have demonstrated either direct enzymatic or indirect chemical reduction of Cr(VI), the bacterial species must demonstrate a minimum level of resistance to Cr(VI) toxicity in order to be used as an agent of bioremediation. The toxic effects of Cr(VI) include inhibition of sulfate uptake [141] and the generation of reactive oxygen species (ROS). The ROS cause oxidative damage to DNA [126] leading to mutations that can manifest as cancer in humans [142, 143]. Therefore, a great

deal of work has been dedicated to understanding the mechanisms of resistance in addition to the level of resistance of various bacterial species [144-146].

The minimum inhibitory concentration (MIC) for aerobically grown *S. oneidensis* was found to be 2 mM [147]. For anaerobically grown *S. oneidensis*, inhibition was found to be at a much lower concentration [135]. An extensive physiological study on the toxicity effects of Cr(VI) and Cr(III) was performed by Viamajala *et al* [146]. This study found that cultures grown under aerobic or anaerobic conditions would cease to divide at a measurable rate until all Cr(VI) had been reduced; indicating an inhibition of some metabolic process caused by the presence of Cr(VI). Interestingly, the authors hypothesize that the primary toxicity of Cr may be due to the trivalent species remaining bound to the reductases and causing precipitates to form in the cytoplasm [146].

S. oneidensis is not the only bacterium that demonstrates resistance to Cr toxicity. Members of the genus *Pseudomonas* have demonstrated resistance to Cr(VI) toxicity via chromosomal and plasmid-borne genes [148-153]. In addition, members of the genus *Alcalignes* were also found to demonstrate Cr(VI) resistance via plasmid-borne genes [154, 155]. Specifically, the ChrA gene was isolated from *Pseudomonas* and *Alcalignes* as responsible for chromate resistance [151, 155] and may encode an active efflux pump that expels Cr(VI) from the bacterium. There is a protein, SO0986, encoded in the genome of *S. oneidensis* that demonstrates significant sequence similarity to the ChrA gene in *Pseudomonas aeruginosa*, however, there is no expression evidence to indicate that active efflux of Cr(VI) is used as the mechanism in *S. oneidensis*. In fact, as described above, the molecular mechanisms involved in chromate toxicity and reduction in *S. oneidensis* remain largely unknown.

Due to the fact that very little is known at the molecular level about chromate exposure in *S. oneidensis*, the first goal of the dissertation involved the completion of a number of proteomic studies to improve understanding regarding chromate exposure in *S. oneidensis* (Figure 1.3). This was accomplished by first a global study of acute chromate shock found in Chapter 3 in order to understand the initial response of *S. oneidensis* to sub-lethal levels of chromate. Also in Chapter 3, a global chronic exposure study is outlined demonstrating how the bacterium might respond to sub-lethal concentrations of chromate over an extended period of time. This work was followed by a dosage response study in Chapter 4, the purpose of which was to understand how the bacterium responds to various levels of sub-lethal concentrations of chromate. Finally in Chapter 6, the time during transformation of chromate from the hexavalent species to the trivalent species is explored; giving possible evidence of proteins that may be transporting and reducing the sub-lethal concentration of chromate in wildtype and $\Delta 2426$ mutant cultures. The $\Delta 2426$ mutant was created based on evidence from previous studies [147, 156] that the protein, SO2426, was highly up-regulated in response to acute chromate exposure. In addition, Cr(VI) reduction assays indicated that the $\Delta 2426$ mutant was deficient in Cr(VI) transformation in addition to a number of other transition metals [157].

The second goal of the work was more technology driven and focused on different method development areas to build upon the proteomics pipeline developed at Oak Ridge National Laboratory. Improvements to two of the technologically challenged areas of proteomics (sample preparation for proteome analysis and computational analysis of MS/MS data) enhanced both the experimental design and the resulting information obtained from performing shotgun proteomics experiments. Figure 1.4

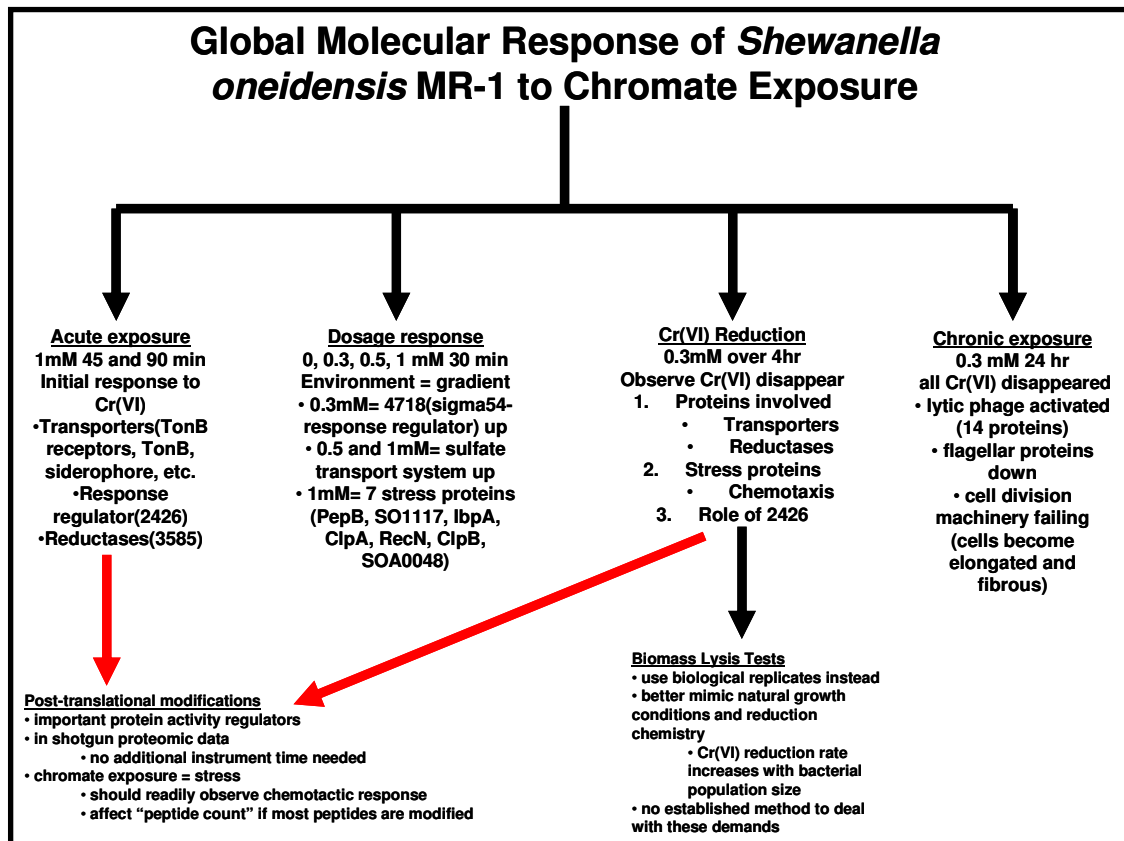


Figure 1.3. Flowchart diagram of the proteome studies of *S. oneidensis* Cr(VI) exposure.

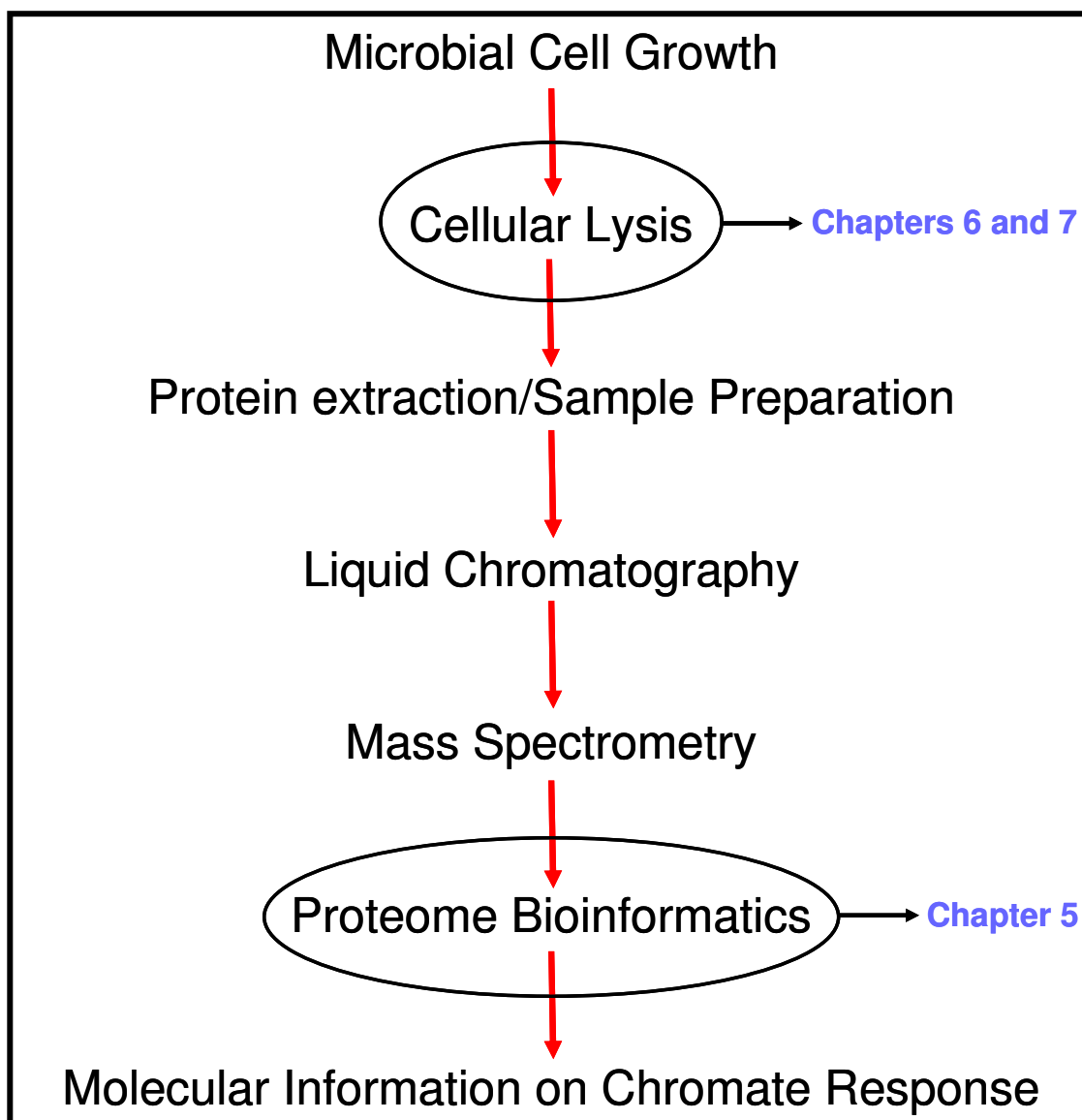


Figure 1.4. Representative shotgun proteomics experimental design.

Outlined in the flow chart are the steps in a representative experiment from whole-cell lysate to the resulting data analysis of the acquired MS/MS data. Improvements to the setup are highlighted and details are outlined in Chapters 5, 6, and 7.

depicts the steps involved in a conventional shotgun proteomics experiment and is representative of the pipeline used at Oak Ridge National Laboratory from cell lysis to data analysis. Highlighted are the method development areas described in this dissertation that have been accomplished to improve on the design of the experimental setup. Chapter 5 demonstrates a novel systematic study of mining shotgun proteomics data for PTMs. This was accomplished by comparing the performance of three algorithms (DBDigger [44], InsPecT [40], and Sequest [39]) by searching MS/MS data from whole-cell lysates of *S. oneidensis* for PTMs. Chapter 6 is not only about understanding chromate transformation in *S. oneidensis*, but comprises one of the first comprehensive proteome measurements from biological replicate cultures of a bacterium. In addition, Chapter 7 describes a novel single-tube lysis method that has been successfully applied in the results of Chapter 6. The single-tube lysis method permits global proteome detection from a few milliliters of bacterial cell culture versus the traditional liters of cell culture. This is a greater than 1000x reduction in the amount of cellular material needed for proteome detection and characterization. All of the research described in this dissertation comprises both novel and thorough evaluations performed to understand acute and chronic chromate exposure as well as during chemical transformation of chromate at the molecular level utilizing methodologies in the systems biology area of shotgun proteomics.

Chapter 2

Experimental Design of Shotgun Proteomics Experiments and Bioinformatic

Platforms using Multidimensional Protein Identification Technology

Introduction

The work presented in this dissertation utilized a mass spectrometry based platform for global protein characterization from microbial isolate cultures and a natural microbial community. This chapter describes the experimental details and components of this platform utilized for large scale proteome measurements. Each chapter summarizes the specific mass spectrometry method used (i.e. LCQ or LTQ), with this chapter describing the overall methodological approach explored and developed. The instruments utilized during the course of the dissertation were a LCQ (liquid chromatography quadrupole ion trap, three-dimensional ion trap) and a LTQ (linear trapping quadrupole) coupled to an online two-dimensional chromatography method. In addition to acquisition of mass spectrometry data, the lack of a feasible means of searching the data for post-translational modifications was addressed through optimizing the scoring filters from three bioinformatics platforms and adapting an in-house script.

Microbial Cultures and Communities

Microbial cultures (Chapters 3-7) were obtained from isolates stored as glycerol stocks at -80 °C and were provided by Dr. Dorothea Thompson from Purdue University (*Shewanella oneidensis* MR-1) and Dr. Dale Pelletier from the Biosciences Division at Oak Ridge National Laboratory (*Rhodospseudomonas palustris* CGA0010). The acid mine drainage biofilm microbial community used in Chapter 7 was a gift from Dr. Jillian

Banfield at University of Berkley. *S. oneidensis* was cultivated in batch culture under aerobic conditions and *R. palustris* was cultivated under photoheterotrophic conditions. *S. oneidensis* was grown in 500 mL cultures for [147, 156, 158] or 100 mL cultures for [159] under aerobic conditions to mid-exponential phase (A_{600} , 0.5) followed by continued monitored growth or the addition of K_2CrO_4 for a given period of time. For cellular harvest, cells were pelleted by centrifugation (5,000 x *g* for 5 min), resuspended in ice-cold LB medium, washed two times in 50 mM Tris, 10 mM EDTA (pH 7.6), and centrifuged at 5,000 x *g* for 10 min. The cell pellets were stored at -80 °C until cellular lysis and digestion. Details of microbial growth can also be found in [147, 156, 158-160].

Preparation of Proteomes for HPLC-MS/MS Analysis

All chemical reagents were obtained from Sigma unless stated otherwise. Modified sequencing grade trypsin (Promega, Madison, WI) was used in all digestions. The modified trypsin used for digestion was methylated on lysines and arginines, thereby reducing the autolytic behavior of the enzyme, which may interfere with detection of the peptides of interest [161]. HPLC grade water and acetonitrile were acquired from Burdick & Jackson (Muskegon, MI), and 99% formic acid was purchased from EM Science (Darmstadt, Germany).

Lysis by Sonication and Tryptic Digestion

For proteome analyses in Chapters 3, 4, 5, and 7, the *S. oneidensis* cells were placed on ice and lysed by sonication using a microprobe at high power with 30-s pulses five times with a 30-s cooling period between each sonication. *R. palustris* and the acid mine drainage biofilm in chapter 7 were also lysed by sonication, however due to the

invaginated membrane of *R. palustris* and the cellulose matrix structure of the biofilm, there were ten 30-s sonication pulses followed by the 30-s cooling period. Cellular debris was removed by centrifugation at 5,000 x g for 10 min. The supernatant was centrifuged at 100,000 x g for 60 min in an ultracentrifuge to separate a soluble fraction from a pellet for Chapters 3, 4, and 5. The pellet (membrane fraction) was washed with 50 mM Tris, 10 mM EDTA (pH 7.6) and centrifuged at 100,000 x g for 60 min; this fraction was then resuspended in 50 mM Tris, 10 mM EDTA (pH 7.6) by brief sonication. Both proteome fractions were quantified using bicinchoninic acid (BCA) analysis [162], aliquoted, and stored at -80 °C until ready for digestion. Approximately 2 mg of each proteome fraction (soluble and membrane) was denatured and disulfide bonds reduced in 6 M guanidine and 10 mM DTT (60 °C for 1 h). The denatured/reduced proteome mixture was diluted 6-fold with 50 mM Tris, 10 mM CaCl₂ (pH 7.8), and sequencing grade trypsin was added at 1:100 [protease/protein (w/w)]. The digestions were run with gentle shaking at 37 °C for 18 h, followed by a second addition of trypsin at 1:100 and an additional 5 h incubation. The samples were treated with 20 mM DTT for 1 h at 37 °C as a final reduction step to remove remaining disulfide bonds and then immediately desalted using Sep-Pak Plus C18 solid phase extraction (Waters, Milford, MA). A second reduction step with DTT was performed instead of using the cysteine alkylation reagent iodoacetemide. Iodoacetemide blocks the cysteine residues through the addition of a carboxymethyl group (57 Da), which will appear as a static modification in the resulting MS/MS searches. The added complexity of this modification in the resulting data filter levels must be taken into consideration as described below for PTMs. All samples were concentrated and solvent-exchanged into 0.1% formic acid in water by centrifugal

evaporation to ~10 µg/µl starting material, filtered, aliquoted, and stored at -80 °C until ready for LC-MS/MS analysis.

Single-Tube Lysis and Tryptic Digestion

For the proteome analyses presented in Chapters 6 and 7, a single-tube lysis method was employed. This method differs from the above sonication method and was performed as follows. Microbial cell pellets ranging in size from 1 mg to ~200 mg were lysed using 6 M Guanidine/10 mM DTT dissolved in 50 mM Tris/ 10 mM CaCl₂ pH 7.6 (Tris Buffer). The Ca²⁺ ion is necessary to enhance activity by promoting autocatalytic activity converting trypsinogen into trypsin, the active enzyme [163]. In addition, the resulting protein content is denatured with the guanidine and the mixture was incubated overnight at 37 °C. Following lysis, the samples were diluted 6-fold with the Tris Buffer and trypsin was added in an optimized amount for 6 hr at 37 °C with gentle rocking followed by a second trypsin aliquot overnight. The optimized amount of trypsin was determined in order to obtain the fewest autolytic tryptic peptide identifications after the LC-MS/MS experiment. When too much trypsin is added, the resulting proteome dataset will have greater than 50% sequence coverage of trypsin identified in the resulting dataset, in contrast to the ~20% sequence coverage observed if an optimized amount is used. A final 20 mM DTT reduction step was performed following the proteolytic digestion for 2 hr at 37 °C with gentle rocking. After lysis, proteolytic digestion, and the final reduction step a high speed centrifugal step was performed to pellet cellular debris. Samples were then desalted with a Sep-Pak C₁₈ Lite or Plus cartridge and solvent exchanged into 100% H₂O, 0.1% formic acid; followed by filtration using an Ultrafree-MC centrifugal filter device (Millipore, Billerica, MA) and stored at -80 °C until LC/LC-

MS/MS analysis. The final filtration step is necessary to remove any aggregate cellular material that will clog the subsequent LC column.

Lysis using Tetrafluoroethylene (TFE) was performed in the same manner as the Guanidine HCl method, except TFE was added initially at a concentration of 50:50 TFE:Tris Buffer/10 mM DTT. For the microbial community (acid mine drainage biofilm) discussed in Chapter 7, a different single-tube lysis method, freeze/grinding, was attempted. The freeze/grinding method was accomplished by first flash-freezing the biofilm in liquid nitrogen, followed by mechanical grinding of the sample into a fine powder. Then, the cell pellets were resuspended in 6 M Guanidine/10 mM DTT in Tris Buffer with the remaining steps being as above for the Guanidine lysis method.

Small Sample Lysis by Bead-Beating

The bead-beating method of lysis [164] is not a single-tube lysis method, however bead-beating is similar in the respect that a smaller than traditional amount of biomass can be lysed with this method. The bead-beating method used 0.5 mm glass beads (Biospec Products, Bartlesville, OK) first sterilized in HPLC-grade methanol (Burdick and Jackson) overnight. Next, an approximately similar amount of glass beads as the cell pellet for lysis is transferred to a separate 2 mL eppendorf tube with a spatula cleaned with methanol. About 250 μ L of 6 M Guanidine/10 mM DTT is added to the glass beads and vortexed. The biofilm (as in Chapter 7) is transferred to the glass beads and vortexed 5 times for 30 s with a 30 s cooling period. The biofilm/glass bead slurry is then incubated over night at 37 °C. Following this step, the Guanidine is diluted to 1 M with 50 mM Tris/10 mM CaCl₂ and centrifuged to pellet the glass beads. The supernatant is transferred to a separate eppendorf tube and 10-20 μ g of trypsin was added for 5 hr at 37

°C with gentle rocking, and another aliquot of trypsin was added with an overnight incubation. Finally, a final reduction step for 2 hr with 20 mM DTT, followed by centrifugation to pellet debris, and the samples were then desalted with a Sep-Pak C18 Plus cartridge. As described in Chapter 7, this method has not been optimized and the results for this method are worse than the other lysis methods due to the buoyancy of the biofilm floating on the top of the glass beads.

Liquid Chromatographic Separation of Peptides

Separation of complex mixtures of peptides using an online two-dimensional liquid chromatographic separation has many advantages over other methods of separation. In particular, the use of orthogonal separations such as strong cation exchange (SCX) and reverse phase (RP) provides coupled but independent separation dimensions. An orthogonal separation method is defined as use of two or more chromatography types, which separate peptides based on two or more different chemical properties (i.e. hydrophobicity, size, ionic properties, etc.). There are other methods of two-dimensional separation available (see Chapter 1 for discussion); however the coupling of SCX and RP online with mass spectrometry analysis of peptides has become the most successful implementation of two-dimensional orthogonal online separation of peptides. SCX separates peptides based on their affinity for the negatively charged benzene sulfonic acid bonded resin and RP separates peptides based on their affinity for a highly hydrophobic 18-carbon chain bound resin. The traditional method of SCX separation is not considered to be compatible with mass spectrometry due to the use of a strong salt (i.e. NaCl) for peptide elution. However, the work demonstrated here utilizes the volatile salt ammonium acetate, which exhibits greater compatibility with MS

allowing for online separation. In addition, the total capacity of the column must be considered prior to loading the peptides. Overloading leads to diminished separation of the peptides, as well as a decreased confidence in the prediction of the elution time.

The proteome fractions (soluble and membrane) prepared from control and chromate-treated samples were analyzed in duplicate for Chapters 3, 4, and 5 and from whole cell lysates in triplicate for samples in Chapters 6 and 7 via a 24-hr two-dimensional (2-D) LC-MS/MS experiment using an Ultimate HPLC system (LC Packings, a division of Dionex, San Francisco, CA). The HPLC pump provided a flow rate of $\sim 100 \mu\text{L}/\text{min}$ that was split pre-column using a fused silica setup as shown in Figure 2.1 to achieve a final flow rate of $\sim 300 \text{ nL}/\text{min}$ at the nanospray tip. The flow at the tip was measured using a $5 \mu\text{L}$ capacity calibrated micropipet (Drummond Scientific Company, Broomall, PA) with $1 \mu\text{L}$ increments over at least a 3 min time frame. This was chosen due to the flow rate variation over time and so an average flow rate is taken over the specified time period. A split phase column ($150 \mu\text{m}$ inner diameter fused silica) was packed via a pressure injection platform (New Objective, Woburn, MA) as follows: first with $\sim 3.5 \text{ cm}$ of strong cation exchange (Luna SCX, $5 \mu\text{m}$ particle size, 100 \AA distance between particles when packed together; Phenomenex, Torrance, CA) followed by $\sim 3.5 \text{ cm}$ of C_{18} reverse phase (Aqua C18, $5 \mu\text{m}$, 200 \AA ; Phenomenex). Subsequently, $\sim 500 \mu\text{g}$ of proteolytic peptide sample was loaded onto the split phase column via the pressure injection platform. The sample size of $500 \mu\text{g}$ was chosen in order to take advantage of the dynamic range capabilities of the ion trap mass spectrometers used. This amount of protein slightly overloads the theoretical capacity of the column, but allows us to identify proteins that may be present at a concentration of

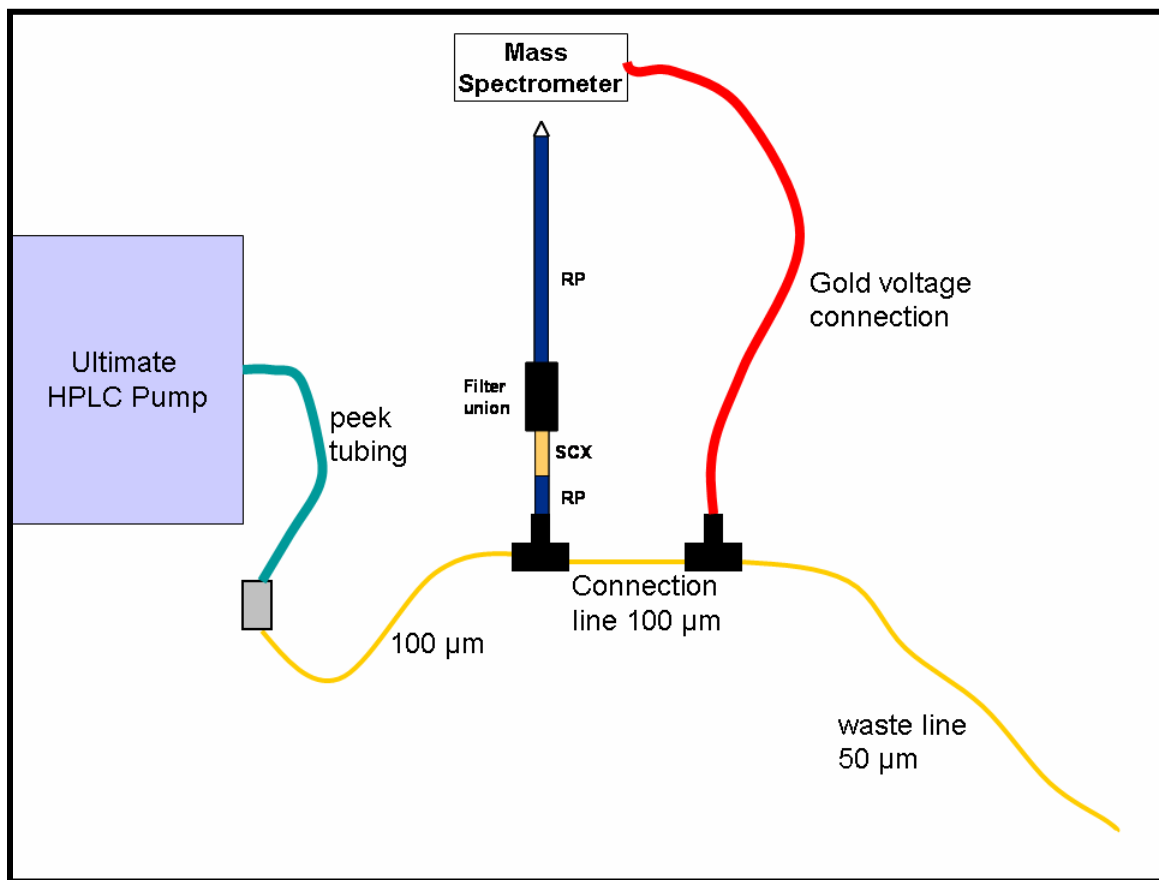


Figure 2.1. Schematic diagram of the two-dimensional column setup.

The Ultimate pump is connected to the two dimensional nanocolumn via peek tubing connected to 100 µm fused silica by a metal fitting, which acts as a ground for the voltage. The 50 µm waste line is depicted as well extending from the second micro tee connecting the mass spectrometer voltage to the nanocolumn.

nanograms per milliliter [165]. The loaded split phase column was then inserted behind a PicoFrit tip (100 μm inner diameter, 15 μm inner diameter at the tip; New Objective) packed via the pressure injection platform with ~15 cm of C₁₈ reverse phase (Jupiter C18, 5 μm , 300 Å or Aqua C18, 5 μm , 200 Å; Phenomenex). The C₁₈ reverse phase resin on the split phase column acts as a trapping cartridge for the peptides to initially bind to, with the first chromatographic step being a desalting step as described by McDonald *et al* [166]. This acts to remove impurities from the sample preparation process and move the peptides during the gradient [100% Buffer A (95% H₂O, 5% ACN, 0.1% formic acid) to 100% Buffer B (30% H₂O, 70% ACN, 0.1% formic acid)] from the C₁₈ resin to the SCX resin for subsequent separation based on charge affinity.

Following the first chromatographic step (the desalting step), proteome fractions (Chapters 3, 4 and 5) or cell lysates (Chapters 6 and 7) were separated using the orthogonal methods of SCX followed by RP for 11 subsequent salt steps (a step gradient). Table 2.1 depicts the time and amount of ammonium acetate added to dislodge peptides from the SCX resin for each salt step and subsequent organic phase separation. The chromatographic separation of each salt step is as follows: 2 min of Buffer A for re-equilibration of the column followed by 2 min (steps 2-11) of the specified amount of salt or 10 min for step 12. After the salt step, there was another Buffer A equilibration period of 5-10 min followed by the Buffer A to Buffer B RP separation. The re-equilibration period with the second Buffer A step is critical; if this step is not performed the salt introduced will precipitate out of solution in the presence of organic solvent. This RP separation method consisted of the gradient from 100% Buffer A to 50% Buffer B for steps 2-11 and 100% Buffer A to 100% Buffer B for step 12. The goal of step 12 is to

Table 2.1. The Consecutive LC Steps Employed in the Two-Dimensional Separation

Chromatography Step	Time (min)	Ammonium Acetate Added (mM)
1	60	0
2	120	50
3	120	75
4	120	100
5	120	125
6	120	150
7	120	175
8	120	200
9	120	225
10	120	250
11	120	300
12	100	500

remove all peptides that may still be binding to the resin following step 11, which explains the longer salt step followed by the complete organic phase endpoint during the RP separation. The complete organic phase acts to diminish carryover between LC-MS/MS experiments due to peptides remaining bound to the 15 cm RP analytical column, which is used for multiple chromatographic separations.

Typical total ion current (TIC) and base peak chromatograms are depicted in Figure 2.2 for chromatography steps 1, 6, and 12. These steps were chosen as representatives of how the chromatograms should look for a LC separation. Note how the relative intensity disappears during the injection of salt across the chromatography column. The loss of intensity is a result of the greater conductivity of the salt raising the current of the nanospray tip causing cessation of electrospray. Also, there is a notable difference in peptide elution between steps 6 and 12. In step 12, elution of a majority of peptides occurs by 100 min into the chromatography step indicating complete elution of peptides from the analytical column, which leads to less carry over between sample analyses. Originally, step 12 was 120 min in length; however as noted above, the peptides primarily elute by 100 min and so the gradient was shortened accordingly (See Table 2.1).

Mass Spectrometry Experiments for the Detection of Peptides

During the entire chromatographic process, the three-dimensional ion trap (LCQ) or linear trapping quadrupole (LTQ) was operated in a data-dependent MS/MS mode detailed below. The chromatographic methods and HPLC columns were similar for all analyses. The LC-MS/MS system was fully automated and under direct control of the Xcalibur software system (Thermo Scientific, San Jose, CA). Operation of the mass

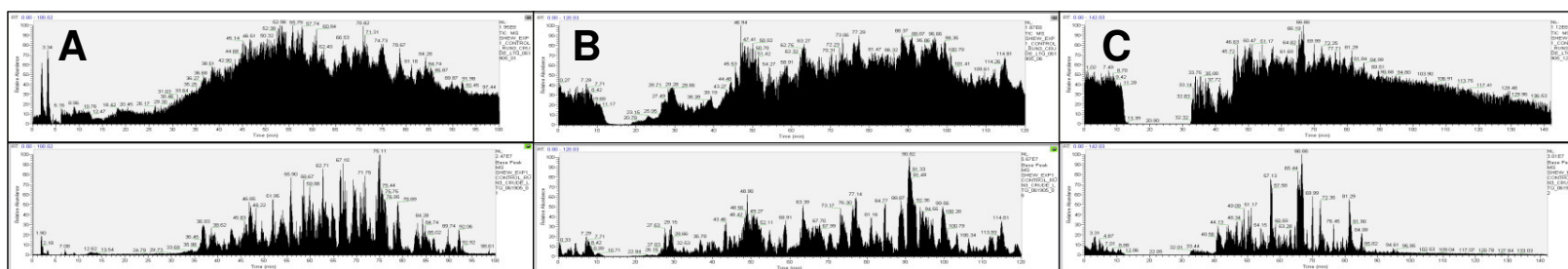


Figure 2.2. TIC and base peak chromatograms from selected chromatography steps.

The TIC chromatograms are on the top with the base peak chromatogram below for (A) chromatography step 1, (B) step 6, and (C) step 12 from Table 2.1. Even though there appears in the TIC chromatogram to be an overwhelming amount of peptides eluting at any given time, the base peak chromatogram illustrates that there is actually respectable separation of the peptides.

spectrometer in a data-dependent mode allows for increased dynamic range through the use of dynamic exclusion. Dynamic exclusion is used to reduce the sampling of abundant ions being triggered for MS/MS fragmentation; when an abundant ion is detected, it is subsequently placed on a list that prohibits that ion from being isolated for a set period of time (i.e. 3 min). The data-dependent mode of operation is independent of operator control, where the control software (Xcalibur) is programmed such that during a set period of time, a full MS scan is acquired followed by a specified number of MS/MS scans. This loop is repeated until the set period of time is completed (i.e. the liquid chromatographic separation). The MS/MS scans are dependent on ion intensity in the respect that following the MS scan, the n th most intense ion is isolated and fragmented where n is equal to 1, 2, 3, etc. Once the ion is chosen for fragmentation, the m/z value is placed on the dynamic exclusion list and is not isolated or fragmented until removed from the list. Discussed below are the details of how each mass spectrometer was operated and the process by which ions are detected and isolated by each instrument.

Operation of a three-dimensional ion trap (LCQ)

The LCQ is a three-dimensional ion trap composed of a ring electrode in the middle and two end-cap electrodes acting to trap ions in the center of the ring electrode. This instrument was first developed in 1960 by Paul and Steinwedel and known as the Paul trap [167]. Advancements to the design leading to successful commercialization of the instrument came in 1984 by Stafford *et al* [29]. Ions are injected into the trap via focusing multipoles transferring the ions as a coherent packet from the electrospray ionization source operated at atmospheric pressure through a heated capillary for desolvation of the ions and into the vacuum of the mass spectrometer. The ions become

energetically stable in the center of the trap according to the stability diagram represented in Figure 2.3 by applying DC (U) and AC (V) voltages as well as a frequency ($\cos\Omega t$) to the ring electrode, thereby creating a dynamic trapping field over a specific mass to charge (m/z) range [29]. The dynamic trapping field is depicted mathematically with the following equations. The DC voltage (usually kept at 0) is reflected by $a=4zU/mr_0^2\Omega^2$, where a is a unitless value comprising: U, DC voltage; z , charge of the analyte; m , mass of the analyte, r , radius of the ion trap; and Ω , rf frequency. The AC voltage is shown mathematically by $q=2zV/mr_0^2\Omega^2$, where q is a unitless value comprising: V, voltage, and all other components are the same as above. In addition, a dampening He gas is added to the trap to remove energy from the ions through collisions. In order to eject and thereby detect the trapped ions, the RF voltage is linearly increased to destabilize the trajectory of the ions inversely proportional to m/z according to $(m/z)_{\text{eject}}=4V/0.908 r_0^2\Omega^2$. Therefore, ions lighter in mass will be ejected from the trap prior to the heavier ions. Once an ion is ejected from the trap, it impinges on a conversion dynode, which dislodges many electrons that in turn impinge on an electron multiplier giving an intensity signal for a particular m/z value. The resulting mass spectrum displayed depicts the m/z values ejected from the ion trap and their resulting relative intensities.

This process of trapping ions is known as mass selective instability [29] in contrast to the original design of the Paul trap [168] using mass selective detection. The mass selective instability used in the Stafford ion trap [29] allows for faster scan speeds, which permits this instrument to function on liquid chromatographic separation time scales. In addition, Stafford *et al* [29] found that the addition of a low molecular weight gas (i.e. helium) improves the resolution, sensitivity, and dynamic range of the LCQ. By

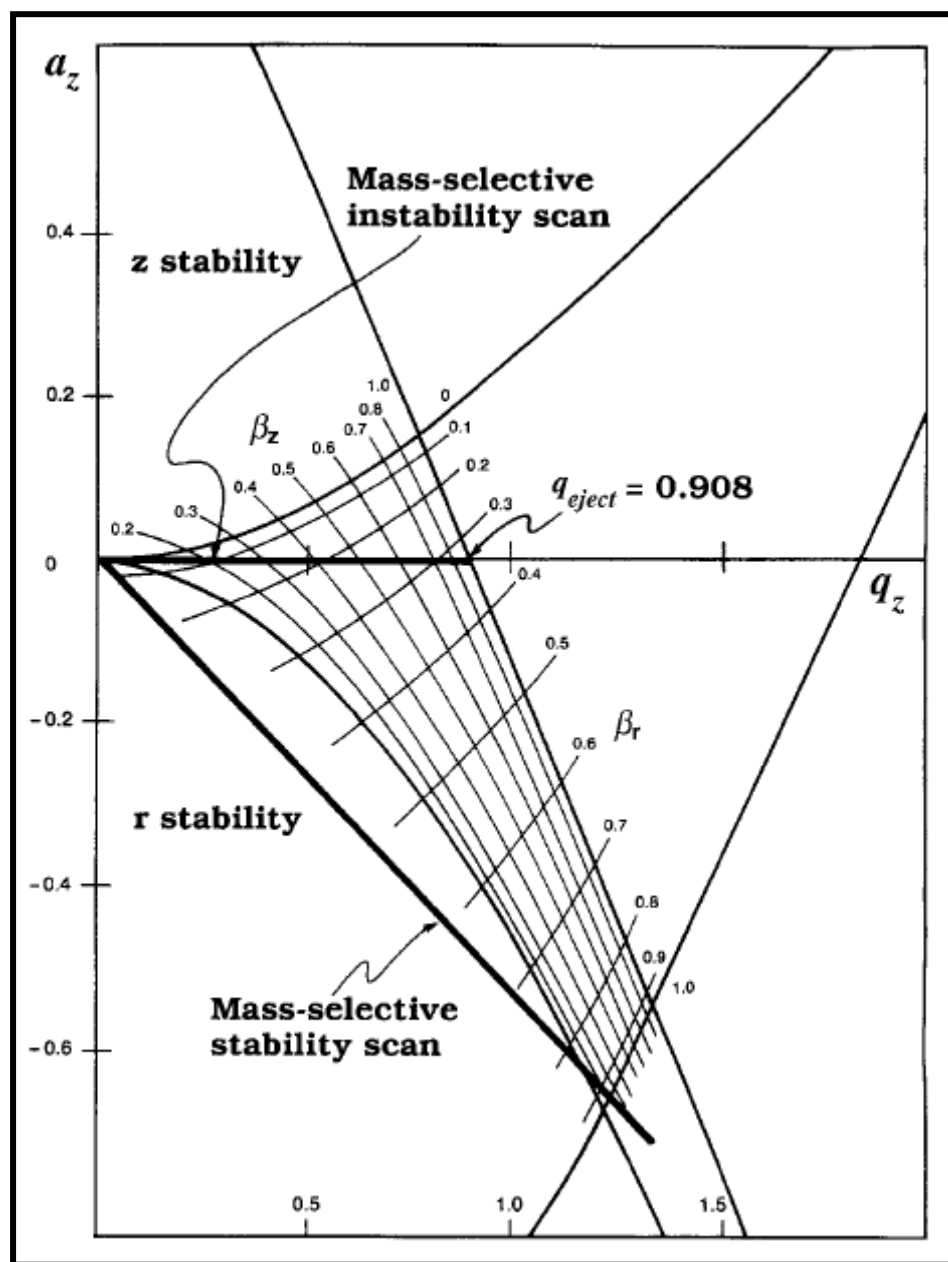


Figure 2.3. Instability diagram of the three-dimensional ion trap.

Reprinted Figure 3 from Analytical Biochemistry, Vol. 244, K. R. Jonscher and J. R.

Yates III, The quadrupole ion trap mass spectrometer--a small solution to a big challenge, pages 1-15, Copyright 1997, with permission from Elsevier.

the addition of He gas, the ions injected into the trap collapse towards the center minimizing field imperfections caused by structural errors of the ion trap. Tandem mass spectrometry operates in a similar manner as above, where the AC voltage is set as a window of m/z values that destabilizes the trajectory of all other m/z values of either lower or higher values except the m/z of interest. Fragmentation occurs through increasing the supplemental RF frequency causing the selected ions to be more energetic, colliding with the He gas molecules within the trap. This creates higher vibrational energy states for the selected ion, leading to dissociation of the relatively weaker covalent bonds within that ion, yielding fragments of the original ion detected as m/z peaks in the MS/MS [169].

The following parameters were applied to the LCQ analyses: nanospray voltage of 2.6 kV, heated capillary temperature of 200 °C, and a full mass scan range of 400-1700. MS/MS were acquired in a data-dependent mode as follows: 4 MS/MS were obtained following every full scan; 5 microscans were averaged for every full MS and MS/MS; a 5 m/z isolation width was employed; 35% collision energy was used for fragmentation, and the dynamic exclusion was set to 1 with the duration being 3 min in length.

Operation of a linear trapping quadrupole (LTQ)

The fundamental operation of the LTQ is very similar to the LCQ, especially considering both instruments are ion traps. This instrument was developed by Jae Schwartz at Thermo Finnigan (now Thermo Scientific) in 2002 [30]. The principal difference between the LCQ (a three-dimensional ion trap) and LTQ (a two-dimensional ion trap) is improvements that were made to the mechanical design of the trap itself. The

LTQ has a larger trapping volume for injected ions where the ring electrode has been extended in length and broken apart into 4 hyperbolic rods with slits in two for ion ejection and subsequent impingement on the conversion dynode. This is in contrast to the LCQ design where the trapping ring electrode is a single piece. The endcaps of the LCQ have been converted into smaller quadrupoles, in which RF and DC voltages are applied repelling the ions into the center quadrupole. The primary advantage to this instrument is the increased ion storage space provided by the lengthened trap. The design of the LCQ limited the storage capacity of the ion trap, thereby limiting the dynamic range of the instrument, as well as mass accuracy problems arising from space charging [30]. Space charging is defined as the effect of over-filling the ion trap with ions, causing a repulsive internal force on the ion packet. This repulsive force leads to ions on the outer edges of the packet to eject at a different resonance frequency than the m/z value predicts [170]. In other words, the m/z that is detected has a wider ion peak and the m/z is higher than the true m/z value for that particular ion leading to lower mass resolution. An example of the increased dynamic range of the LTQ is found in Figure 2.4, which depicts a low-abundant ion that could be misinterpreted as noise giving a m/z peak-rich MS/MS.

The LTQ was operated with a nanospray voltage of 2.6 kV, heated capillary temperature of 200 °C, and a full scan m/z range of 400–1700. The data-dependent MS/MS mode was operated as follows. Five MS/MS were acquired following every full scan and two microscans were averaged for every full MS and MS/MS. An isolation width of 3 m/z was used and 35% relative collision energy was used for fragmentation. The dynamic exclusion was set to 1 with an exclusion duration of 3 min.

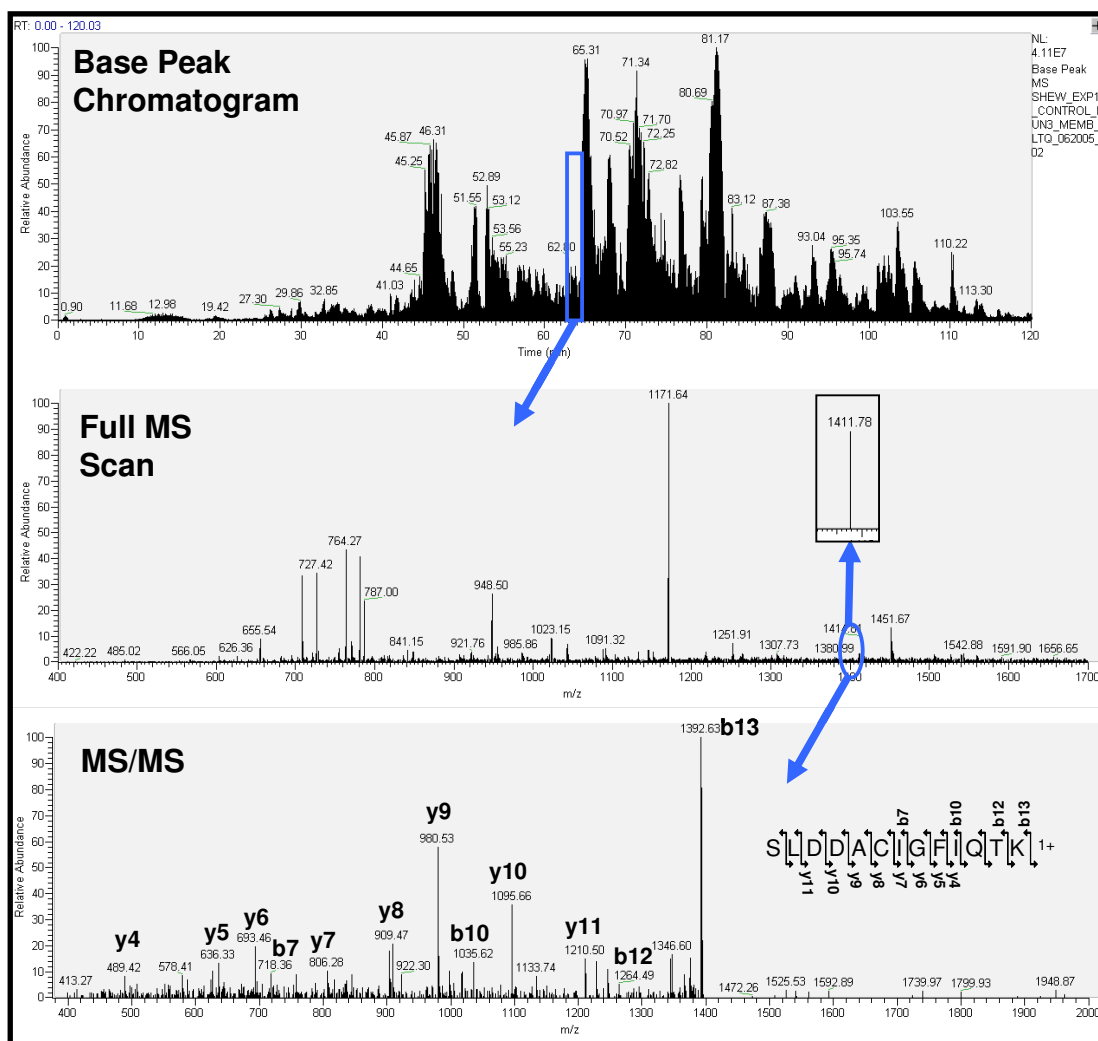


Figure 2.4. A MS/MS from a low-abundant peptide using the LTQ.

The peptide, SLDDACIGFIQTK, is from SO3587 a putative transmembrane domain hypothetical protein in *S. oneidensis*. This peptide was found as singly charged in the membrane fraction of a LC-MS/MS experiment. The top panel is the base peak chromatogram of chromatography step 2 from the experiment and the middle panel is the full MS spectrum with a zoomed-in region of the spectrum showing the corresponding intact peptide with an m/z value of 1411.78. The ion was subsequently isolated and fragmented yielding the MS/MS of the bottom panel with the respective fragment ions labeled.

Proteome Bioinformatics

Due to the hundreds of thousands of MS/MS acquired during the LC-MS/MS experiments performed, there is a paramount necessity for the development and optimization of bioinformatics platforms to distinguish the identities of the peptide ions fragmented, and filter the resulting datasets acquired by removing false identifications, also known as false positives. False identifications are the result of the misidentification of a MS/MS, which has a scored value that is greater than the threshold filters. A false negative identification is the result of a true peptide identification that has not scored high enough to pass the threshold filters. To this end, a number of search algorithms were assessed and filtering levels for identifications were optimized based on the characteristics of both the datasets (i.e. instrumentation platform) and the algorithm's performance for searching MS/MS data.

The Sequest algorithm

Sequest was the first algorithm written to identify peptides fragmented by MS/MS [39]. As the performance and speed of both mass spectrometers and liquid chromatographic separations increased, the bottleneck to be addressed was computational automation of MS/MS identification. To this end, Sequest was written and published in 1994 by Jimmy Eng at the University of Washington-Seattle. This now is part of the Bioworks software licensed by Thermo Scientific. First, Sequest “digests” the provided protein FASTA database *in silico* into peptides based on the enzyme specificity provided by the parameters file (i.e. fully tryptic, no enzyme specificity, etc.). This creates a list of possible peptides that are represented in the experimental MS/MS. Next, Sequest generates theoretical MS/MS using the provided digested peptides from the protein

database in order to determine identifications of the experimental spectra. The scoring process first determines the number of matching peaks between the two spectra and increases the resulting score if the experimental peak identifications comprise a consecutive sequence for the peptide. Next, a cross correlation score (Xcorr) is given based on a comparison of the top 500 scoring peptide identifications [39]. The highest Xcorr is then compared to the Xcorr of the second best identification and a DeltaCN value is given. The DeltaCN (Δ CN) value indicates a confidence in the identification of the MS/MS as belonging to the best scoring peptide from the database.

Sequest is widespread in proteomics; therefore results found in Chapters 3, 4, 5, 6, and 7 were all published with this algorithm. The database used in the searches performed in this dissertation can be found in the experimental section of the relevant chapter. The MS/MS spectra from individual RAW files were first converted to .mzXML format by using ReAdW software written at the Institute for Systems Biology in Seattle, WA (www.systemsbiology.org) and can be downloaded from the SourceForge repository (sashimi.sourceforge.net). Individual spectra were then converted to DTA files by mzXML2Other, also from the Institute for Systems Biology. DTA files are the required format for input into Sequest (see Ref. [2]). The parameters for searching the MS/MS data with Sequest are: enzyme type, trypsin; Parent Mass Tolerance, 3.0; Fragment Ion Tolerance, 0.5; up to 4 missed cleavages allowed; and fully tryptic peptides only. The following filter levels were applied to the Sequest search results using the algorithms DTASelect and Contrast [171]: tryptic peptides only, Δ CN value of at least 0.08, and Xcorr values of at least 1.8 (+1), 2.5 (+2), 3.5 (+3). These values were chosen and described in Chapters 3 and 4 due to the acceptable false discovery rate (FDR) of

~2% at the 2-peptide level of protein identification that result from this filter level. No chemical modifications were added to the Sequest searches for Chapters 3, 4, 6, and 7. As discussed in detail in Chapter 5, the addition of chemical modifications to a Sequest search is cumbersome.

The DBDigger algorithm

The search algorithm DBDigger [44] was written by David Tabb at Oak Ridge National Laboratory to help alleviate some of the inflexibilities present in the Sequest algorithm. In addition, the speed at which a search of MS/MS against a protein database can be performed using DBDigger on a desktop computer is greater than Sequest. DBDigger uses a similar method of scoring experimental MS/MS against a provided protein database to the algorithm Sequest. However, the method of searching by creating a theoretical spectrum once for a given set of experimental MS/MS yields the enhanced speed provided by this algorithm. DBDigger also allows for the additional flexibility of including an unlimited number of chemical modifications to the search parameters. This permits the ability to start searching for post-translational modifications embedded in the MS/MS datasets. However, there are a number of limitations to this algorithm that are discussed in detail in Chapter 5.

DBDigger was used as a search algorithm due to the advantages listed above for datasets presented in Chapters 5 and 7. The resulting raw MS/MS files were first converted to .ms2 files using the algorithm RAW2MS2 [172] with simple charge state assignment accomplished by MS2ZAssign. The resulting ms2 files were then searched against a provided protein database using DBDigger with the MASPIC scorer [173] with the following parameters: digestion sites after K and R; two digestion ends; Parent Mass

Tolerance, 3.0; Fragment Ion Tolerance, 0.5; and any PTMs that were specified as described in Chapter 5. DBDigger results files are in the form of .sqt files; which are imported into DTASelect for the following filtering rules for unmodified datasets: 2 peptides required for protein identification, 25 for +1 peptides, 30 for +2 peptides, and 45 for +3 peptides. Chapter 5 has a discussion on the optimization of the filtering rules when considering DBDigger searches including PTMs.

The InsPecT algorithm

InsPecT was specifically designed to search MS/MS datasets containing PTM information [40]. The Bafna group at University of California-San Diego developed this algorithm. This algorithm takes a different approach for searching MS/MS data against a provided search database. The first stage generates a set of three amino acids in length tags (25 were specified in the searches performed in this dissertation) using fragment ions in the experimental MS/MS and enables a relatively short list of peptides to be searched. A list of candidate peptides are scored based on seven different criteria: the number of predicted (1) b and (2) y ions that match to the MS/MS, how well the intensity of the identified (3) b and (4) y ions match the predicted intensity, (5) trypsin specificity, (6) the length of the candidate matching peptide where the presence of PTM(s) indicates a shorter peptide, and (7) the fragment ion profile of the spectrum (presence of an isotope, higher fragment ion intensity in the middle of the spectrum, and properties of the neighboring residue) [40]. The resulting top score (MQScore) is then compared to the distribution of the lower scores (DeltaScore) and a p-value is calculated. The p-value used by InsPecT is based on the p-value devised for the algorithm Peptide Prophet [174].

A p-value representing an ~2% FDR is chosen based on the p-value distribution for a particular MS/MS dataset as discussed in detail in Chapter 5.

An in-house perl script used to automate Sequest searches, `gitrseq.pl`, was adapted for automation of InsPecT searches and named `gitrinspect.pl`. The perl script `gitrinspect.pl` operates in a similar manner to `gitrseq.pl` with a few notable exceptions as follows. Figure 2.5 is a flow chart outlining the procedure of `gitrinspect.pl` from a Xcalibur raw file to a tab-delimited results file. The script automates the process from raw file to InsPecT results in four stages, creating a queue for each raw file to be searched sequentially. First, the conversion of the .raw file to the .mzXML format is performed using the ReAdW software (Institute for Systems Biology), which is the proper file format for InsPecT input. Next, the mzXML file is moved to a sub-folder named `temp_dir`. Once the mzXML file is in `temp_dir`, searching and scoring the MS/MS using InsPecT is completed. Finally, the mzXML and the .txt InsPecT results files are removed from `temp_dir` and placed in the directory above (`inspect_searches`). Once these files are removed, `temp_dir` is deleted and the loop starts over again and repeated for each raw file present in the directory. This process is necessary due to the limited memory availability of the InsPecT algorithm on a desktop computer. InsPecT attempts to load all MS/MS spectra in a given folder to be searched, thus leading to over 100,000 MS/MS being loaded into memory. Feasibly, only one raw file is searched at a time, leading to the above necessity of creating a sub-folder to perform the actual InsPecT search.

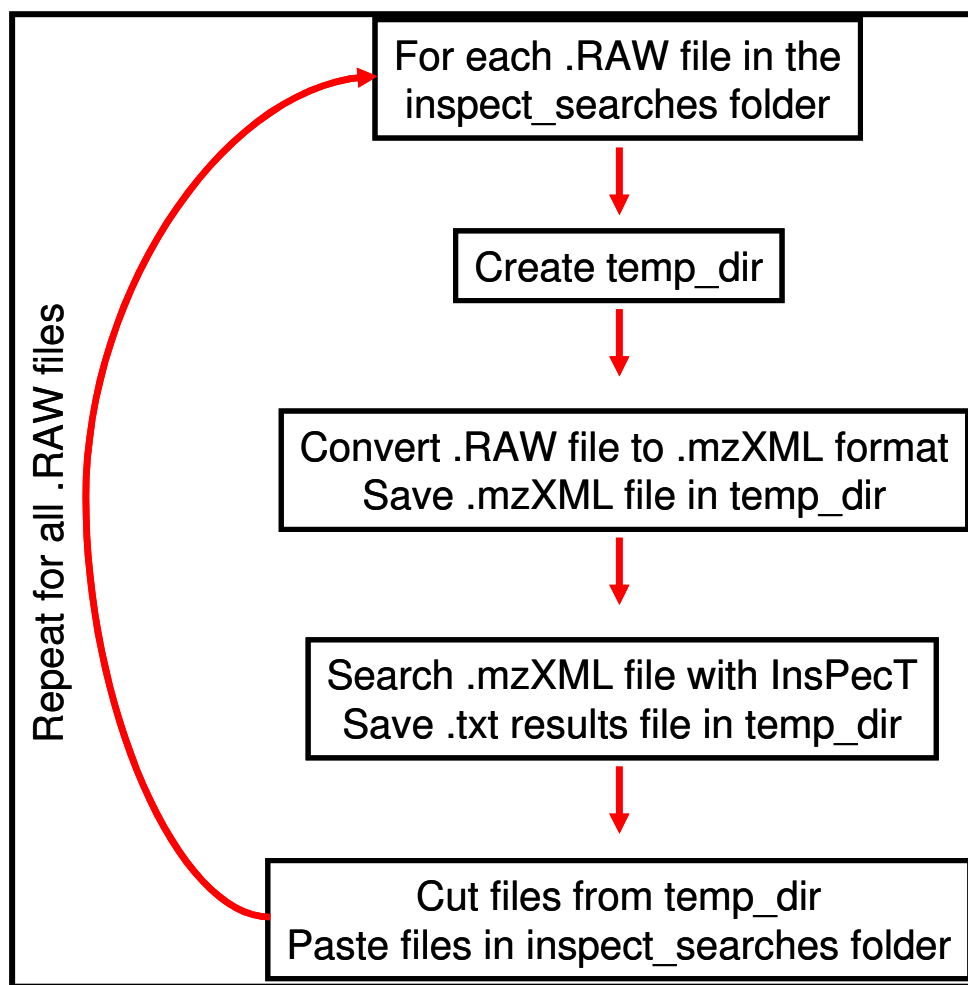


Figure 2.5. Flow diagram outlining the scheme of the `gitinspect.pl` perl script.

The .RAW files are located in the `inspect_searches` folder. Creating the `temp_dir` folder allows InsPecT to search one .mzXML file at a time without overwhelming computational capacity on a desktop computer.

Semiquantitation of protein abundance

There are many different methods of quantifying MS/MS data available; where stable isotope labeling [175, 176], isotope-coded affinity tags (ICAT) labeling cysteine residues [177, 178], and isobaric tagging for relative and absolute quantification (iTRAQ) [178-180] are some of the common examples of relative quantification by changing the mass of a peptide from one growth state to compare to a separate growth conditions. One method of absolute quantification is the use of AQUA peptides [181], which are synthetic peptides created with heavy isotopes that have the exact amino acid sequence as an endogenous peptide of interest. However, the microbial samples utilized in this dissertation were not amenable to the aforementioned methods as discussed in detail in Chapter 3. Thus, the semiquantitation method was used, which takes into account reproducible differences in spectra count, peptide count and sequence coverage. Spectral count is the total number of MS/MS identified as encompassing amino acid sequence from a particular protein and can be a measurement for relative quantification [182, 183]. The definition of peptide count is the total number peptides identified for a given protein and sequence coverage is the total percent of the protein sequence identified from the MS/MS data. The use of dynamic exclusion does not bias spectra count measurement, because all ions that are isolated are placed on the dynamic exclusion list.

Due to differences in dynamic range discussed in Chapter 4 of this dissertation, different quantification parameters are applied for the LCQ and LTQ datasets. LCQ datasets require the following parameters: $\geq 30\%$ change in sequence coverage, ≥ 4 unique peptides identified, and/or at least a 2x difference in spectra count between the treated and control samples (adapted from Refs. [184] and [97]). LTQ datasets require

the following semi-quantitation rules applied: $\geq 40\%$ change in sequence coverage, ≥ 5 unique peptides identified, and/or at least a 2x difference in spectra count [147, 158].

Peptide and protein false discovery rates

The peptide false discovery rate (FDR) can be calculated from using a distracter database (an unrelated proteome database), a reversed database (all protein sequences have been reversed) or a shuffled database (all protein sequences are scrambled). The most popular database types for calculating the peptide FDR are using a reversed database or a shuffled database. The argument for using either one of these two database types is both contain nonsense sequences to calculate the FDR. If the distracter database is used, caution must be taken that the homology of the sequences between the true database and the distracter database do not result in true identifications from sequences comprising the distracter database (i.e. ribosomal proteins, DNA polymerase, etc.). A study by Peng *et al* [185] describe the formula used to determine the peptide FDR for a MS/MS dataset using a reversed database. The formula is $\%FDR = 2 * (n_{rev}/n_{tot} * 100)$, where n_{rev} is the number of peptides identified that match the reversed database and n_{tot} is the sum of the peptides identified matching the reversed and forward databases [185]. The basis for multiplying the end value by 2 is the assumption that if a peptide sequence score from the reversed database is large enough to pass the filter thresholds then there is an incorrect peptide sequence score from the forward database that also was large enough to pass the filter threshold.

The resulting FDR at the protein level can be much higher (~10-fold) than the corresponding peptide FDR, resulting from the MS/MS identification confidence level. The protein FDR can be calculated from the peptide FDR as a function of the probability

of the possibilities. Illustrated in Figure 2.6 is the predicted FDR at the protein level based on a 2% FDR at the peptide level using the requirement of 2 and 3 peptides for a positive identification. Figure 2.6 displays the equation that determines the FDR for the resulting proteins. For example, the requirement of at least two peptides for protein identification leads to four different possibilities and eight total peptide possibilities. Applying a 2% peptide FDR corresponding to 98% true identifications, results in a protein FDR of 11.5%. This value agrees with the experimental FDR values found in Chapters 3-5. If a one-peptide requirement were applied to the Figure 2.6 equation, there would be two possibilities for both values x and z , yielding a FDR at the protein level to be 48%. This is in agreement with the protein FDRs found in Chapter 4. The ability to predict the protein FDR based on the value of the peptide FDR is helpful in determining proper threshold filters to be applied to a MS/MS dataset.

However, if for instance the cutoff was 5 or 6 peptides to be required for protein identification, the resulting FDR value at the protein level would be 0.9% and 0.64%, respectively. This decreases the resulting protein FDR as a consequence of requiring a larger number of true peptide identifications, with the protein FDR no longer of much consequence. These calculations only apply to results from one single MS experiment. If a protein is required to be identified from peptides from multiple MS experiments, the resulting FDR is even lower than as calculated above. As an example, the two-peptide requirement protein FDR is calculated to be 11.5%, however if the two peptides are required to be identified in two MS experiments the resulting FDR is 1.3%. If the one-peptide requirement were to be applied to this same scenario leading to one peptide in each MS experiment, the resulting protein FDR is now 23%. Therefore, using

$$\frac{(y)^x}{z} \times 100 = \text{protein FDR}$$

<p>2 peptides required TT, TF, FT, FF y = 0.98 x = 4 z = 8</p>	<p>3 peptides required TTT, TFT, TTF, TFF, FTT, FFT, FTF, FFF y = 0.98 x = 8 z = 24</p>
↓	↓
$\frac{(0.98)^4}{8} \times 100 = 11.5\%$	$\frac{(0.98)^8}{24} \times 100 = 3.5\%$

Figure 2.6. Predicted protein FDR based on the peptide FDR classification.

The values in the equation represent the peptide true discovery rate (y), the total number of true and false identification possibilities for the peptide requirement (x), and the total number of true and false identification possibilities for a given peptide (z).

a more stringent filter leads to a total protein FDR lower if the peptide requirements are from two MS experiments.

Conclusions

By improving MS sample preparation methods and data mining filter thresholds, we achieved a more in-depth proteome that would not have been possible otherwise. Through the incorporation of two-dimensional liquid chromatographic separation and the improved dynamic range capabilities of the LTQ, the global proteome studies presented in this dissertation would not have yielded as much depth into the microbial life processes. In addition, the increased dynamic range of the LTQ provided the ability to perform quantification comparisons between cultures of *S. oneidensis* MR-1 following acute and chronic Cr(VI) exposure yielding interesting information on differentially expressed proteins that otherwise would be overlooked using other technologies.

Chapter 3

Understanding Global Chromate Response of *Shewanella oneidensis* MR-1 under Acute and Chronic Exposure Using Shotgun Proteomics

All of the data presented below has been adapted from the following published journal articles' Results and Discussion text sections

Stephen D. Brown, Melissa R. Thompson, Nathan C. VerBerkmoes, Karuna Chourey, Manesh Shah, Jizhong Zhou, Robert L. Hettich, and Dorothea K. Thompson. Molecular Dynamics of the *Shewanella oneidensis* Response to Chromate Stress. *Molecular and Cellular Proteomics*, 2006; 5, 1054-1071. *Sample preparation, LTQ measurements, and data analysis for the proteomics portion of the manuscript were performed by Melissa R. Thompson with assistance from Nathan C. VerBerkmoes. Supplemental material can be found at http://compbio.ornl.gov/shewanella_metal_stress/stress.*

Karuna Chourey, Melissa R. Thompson, Jennifer Morrell-Falvey, Nathan C. VerBerkmoes, Stephen D. Brown, Manesh Shah, Robert L. Hettich, Jizhong Zhou, Mitchel Doktycz, and Dorothea K. Thompson. Global Molecular and Morphological Effects of 24-h Chromium Exposure on *Shewanella oneidensis* MR-1. *Applied and Environmental Microbiology*, 2006; 72, 6331-6344. *Sample preparation, LTQ measurements, and data analysis for the proteomics portion of the manuscript were performed by Melissa R. Thompson with assistance from Nathan C. VerBerkmoes on data analysis. Supplemental material can be found at http://compbio.ornl.gov/shewanella_metal_stress/chronic.*

Introduction

The global molecular response of *Shewanella oneidensis* MR-1 to chromate exposure was unexplored prior to this dissertation work. The need to understand both the initial response and prolonged exposure to hexavalent chromium [Cr(VI)] in the form of chromate (CrO_4^{2-}) for the purposes of using *S. oneidensis* as an agent for bioremediation has not been examined previously. The goal of the work presented in this chapter was to determine the global protein response in the form of a mass spectrometry based proteome dataset to reveal novel proteins that are indicative of Cr(VI) response. The proteome

studies described here impart a global insight into temporal alterations in protein content occurring in response to a toxic acute level (1mM) and following long term chronic exposure of a lower dosage of chromate (0.3 mM). The overall protein expression pattern of an organism will not change a great deal in response to a particular stimulus; however this chapter identifies novel proteins found to be differentially expressed during the bacterial response to a sub-lethal dosage of chromate. The responses identified will increase the understanding of possible protein expression mechanisms that allow Cr(VI) reduction, detoxification, and adaptation under aerobic growth conditions. Alterations in protein expression were complemented results from the microarray analysis. However, microarray analysis discussion is limited to only where it is relevant to the proteome results.

Materials and Methods

Preparation of Proteomes for HPLC-MS/MS Analysis

For the acute chromate shock large scale proteomic characterization, 500-ml cultures of *S. oneidensis* MR-1 in 4-liter flasks (a total of 1 liter of culture for treatment and control) were grown to midexponential phase (A_{600} , 0.5) under aerobic conditions and then either exposed to a final K_2CrO_4 concentration of 1 mM or allowed to continue growing in the absence of added chromate. At time points of 45 and 90 min after treatment with K_2CrO_4 , cells were harvested from each of the following conditions for HPLCMS/MS analysis: 1) Control 1 (untreated midlog phase cells after 45 min of further growth), 2) Treatment 1 (45 min post-Cr addition), 3) Control 2 (untreated midlog phase cells after 90 min of further growth), and 4) Treatment 2 (90 min post-Cr addition). For this, cells were pelleted by centrifugation (5,000 x g for 5 min), resuspended in ice-cold

LB medium, washed two times in 50 mM Tris, 10 mM EDTA (pH 7.6), and centrifuged at 5,000 x g for 10 min. For the chronic exposure large scale proteome characterization, *S. oneidensis* cells were first adapted for 24 h to chromate by growth in the presence of 0.3 mM K₂CrO₄ in a starter culture. An aliquot of the starter culture was used to inoculate fresh media with or without 0.3 mM K₂CrO₄. Cells were then incubated for 24 h and harvested by centrifugation for mass spectrometry analysis. The *S. oneidensis* cells were then placed on ice and lysed by sonication as detailed in Chapter 2. Approximately 2 mg of each proteome fraction (soluble and membrane) prepared from all of the growth conditions was denatured and reduced in 6 M guanidine and 10 mM DTT. Denaturation and reduction were followed by an overnight digestion (see Chapter 2).

LC/LC-MS/MS Analysis

The proteome fractions (soluble and membrane) prepared from control and chromate-treated samples were analyzed in duplicate via two-dimensional (2-D) LC-MS/MS experiments using an Ultimate HPLC system (LC Packings, a division of Dionex, San Francisco, CA) coupled to a linear trapping quadrupole (LTQ) mass spectrometer (ThermoFinnigan, San Jose, CA). See Chapter 2 for details of chromatographic separation of peptides. The multiphasic column system was positioned in front of the LTQ on a nanospray source (ThermoFinnigan). All samples were analyzed via a 24-h 12-step 2-D analysis consisting of increasing concentration (0–500 mM) salt pulses of ammonium acetate followed by 2-h reverse phase gradients (see Chapter 2 for details). During the entire chromatographic process, the LTQ was operated in a data-dependent MS/MS mode detailed in Chapter 2.

A protein database was created by combining the most recent version of the *S. oneidensis* MR-1 database (Version 8; www.tigr.org/) containing a total of 4,798 predicted proteins with 36 common contaminants (trypsin, keratin, etc.). The database can be downloaded from the website compbio.ornl.gov/shewanella_metal_stress/databases/. For all database searches, the MS/MS spectra were searched using Sequest (Ref. [39]; ThermoFinnigan) with the following parameters: enzyme type, trypsin; parent mass tolerance, 3.0; fragment ion tolerance, 0.5; up to four missed cleavages allowed; fully tryptic peptides only. The output data files were then filtered and sorted with the DTASelect algorithm [171] using the following parameters: fully tryptic peptides only with ΔCN of at least 0.08 and cross-correlation scores (Xcorr) of at least 1.8 (+1), 2.5 (+2), and 3.5 (+3). These threshold scores have been tested rigorously in our laboratory and provide a high confidence of identification (see Refs. [184] and [65] for more discussion) with a maximum false-positive rate of 1–2%. Post-translational modifications and other fixed modifications (*i.e.* due to addition of iodoacetamide) were not included in the search parameters. DTASelect files are available on the analysis page (compbio.ornl.gov/shewanella_metal_stress/) under the corresponding acute shock or chronic dataset and are filtered at one peptide and two peptides per protein. The files are presented in a text format or a viewable html version where every identified spectrum can be viewed by clicking on the spectral number (first column, labeled by filename). The DTASelect results from all control and chromate-treated samples were then compared with the Contrast program [171] for each time point. These results are located under the global contrast heading on the analysis page. A list was made of all proteins showing a

reproducible significant change of at least 40% sequence coverage, five or more unique peptides, and/or a reproducible spectral count difference of 2x between the control and chromate-treated samples at each time point (adapted from Refs. [184] and [97]). The analysis page also contains inter-run contrast files (compares duplicate runs on same sample) as well as fractionation comparisons (compares replicate runs of the same proteome broken down by fraction).

Results and Discussion

Acute Shock Proteome Dataset

Cellular fractions from each of the four *S. oneidensis* growth conditions (*i.e.* Control 1, Control 2, Treatment 1, and Treatment 2) were analyzed in duplicate using 2-D LC-ES-MS/MS with a linear trapping quadrupole mass spectrometer (see Chapter 2 for details). A total of 2,370 of the 4,931 total predicted genes in the *S. oneidensis* MR-1 genome were identified with at least two peptides (Table 3.1), representing 48% of the theoretical proteome. Due to the large number of false positives possible at the one-peptide filter level [65], we present a rigorous analysis of the two-peptide dataset only. High stringency filtering was used in this study, giving a maximum false-positive rate of 1–2%. The reproducibility between duplicate protein analyses on the LTQ was as follows: 78.6% (chromate-shocked) and 78.4% (control) for the 45-min poststress time point and 77.7% (chromate-shocked) and 73.5% (control) for the 90-min time point. This level of reproducibility is necessary for semiquantification. Variation is likely due to low abundance proteins identified with two peptides in one of the analyses and only one peptide in another, thereby being filtered out. Although previous studies using 2-D PAGE and LC-MS/MS have been used for global *S. oneidensis* proteome studies

Table 3.1. Proteome Analysis of Chromate-Shocked *S. oneidensis* MR-1

Condition	No. proteins identified 1 pep ^a	No. proteins identified 2 pep ^b	Av. Sequence coverage ^c
45 min Control	2610	1911	37.24%
45 min Shock	2644	1959	37.20%
90 min Control	2595	1892	36.38%
90 min Shock	2664	1992	36.45%
Total	2954	2370	

^aTotal proteins identified with at least 1 peptide per protein from duplicate runs. ^bTotal proteins identified with at least 2 peptides per protein from duplicate runs. ^cAverage sequence coverage per protein at the 2 peptide level.

[25, 97, 186] this study represents, to our knowledge, one of the largest measurement of the *S. oneidensis* proteome published to date. The entire list of identified proteins with total sequence coverage, functional categories, pI, and molecular weight information is given in Supplemental Table S2. No major biases were found between the pI and molecular weights of the predicted proteome from the genome and the observed proteome (Supplemental Table S2). The identified proteins with their peptide count (number of identified peptides), spectral count (number of MS/MS spectra identified per protein), and percent sequence coverage (total percentage of the protein sequence covered by tryptic peptides) for the different growth conditions and individual analyses can be found in Supplemental Table S3.

Proteins identified at the two-peptide level were grouped according to the functional categories assigned by the J. Craig Venter Institute annotation [formerly The Institute for Genomic Research (Ref. [69]; www.tigr.org, Comprehensive Microbial Resource)] (Table 3.2). Proteins with assigned functions in amino acid biosynthesis, cellular processes, protein fate, protein synthesis, nucleotide metabolism, and transcription were found with greater than 70% identified. More than 90% of the proteins comprising the functional classes of protein synthesis, nucleotide metabolism, and transcription were identified, representing an almost complete characterization of these categories at the proteome level. Proteins generally thought to be of lower abundance, such as those with assigned functions in signal transduction and transcriptional regulation, were identified at levels of 64 and 52%, respectively, of the total number of proteins per category. A total of 624 of the 2,039 predicted hypothetical proteins were identified. Of the 624 proteins in this functional category, 209 were

Table 3.2. Functional Categories of Identified Proteins with at Least Two Peptides

Number	Functional Category	Observed Proteome	Predicted Proteome	Percent Identified
1	Amino acid biosynthesis	70	91	76.92%
2	Biosynthesis of cofactors, prosthetic groups, and carriers	94	121	76.69%
3	Cell envelope	121	180	67.22%
4	Cellular processes	188	260	72.31%
5	Central intermediary metabolism	28	51	54.90%
6	DNA metabolism	97	144	67.36%
7	Energy metabolism	199	308	64.61%
8	Fatty acid and phospholipid metabolism	48	65	73.85%
9	Hypothetical proteins	624	2039	30.60%
10	Mobile and extrachromosomal element functions	34	317	10.73%
11	Protein fate	137	185	74.05%
12	Protein synthesis	131	141	92.91%
13	Purines, pyrimidines, nucleosides, and nucleotides	56	62	90.32%
14	Regulatory functions	104	199	52.26%
15	Signal transduction	39	61	63.93%
16	Transcription	49	54	90.74%
17	Transport and binding proteins	148	274	54.01%
18	Unknown function	203	379	53.56%
Total		2370	4931	48.06%

annotated as hypothetical proteins, and 415 were annotated as conserved hypothetical proteins. This represents one of the largest identifications of hypothetical protein expression for a microbial proteome to date.

Although absolute quantification at the global proteome level was not feasible, semiquantification of differentially expressed proteins between the chromate-treated and control samples could be accomplished by using a combination of percent sequence coverage, number of unique peptides, and spectral count from the mass spectra [20, 97, 184] (see Chapter 2 for details). Other methods for relative quantification, such as ICAT [177], were considered before the method used here was selected. ICAT labels the cysteine residues of a protein, and in *S. oneidensis* greater than 50% of the predicted proteins have two or fewer cysteine residues present. Moreover almost 20% of the predicted proteome does not contain any cysteine residues. This method would not detect almost 70% of the predicted proteome confidently; thus ICAT was not deemed appropriate for this study.

Comparisons were made between the transcriptome and proteome data to determine the relationship between gene and protein expression. However, in this dissertation, only the proteome data will be described in detail. Both up- and down-regulated proteins were measured by comparing the chromate-shocked cell samples to their respective control samples. Using the semiquantitative criteria discussed above, we identified 78 proteins (Supplemental Table S4) as being differentially expressed in response to chromate (Tables 3.3 and 3.4, Supplemental Table S4). Supplemental Table S4 divides the proteins identified at 45 min post-shock from the proteins identified at 90 min post-shock. We propose that reproducibility of at least 70% between replicate

Table 3.3. Up-Regulated Proteins Identified in the 90 min Chromate-Shocked Sample

Gene	Transcriptome	Control 1	Control 2	Chrom 1	Chrom 2	Category	Description
SO0343	No change ^a	20.8	18.3	43.3	45.7	7	aconitate hydratase 1 (<i>acnA</i>)
SO0423	Induced ^b	11.2	0.0	43.6	39.2	14	pyruvate dehydrogenase complex repressor (<i>pdhR</i>)
SO0798	Induced	0.0	0.0	24.7	21.7	9	conserved hypothetical protein
SO0934	No change	12.2	55.5	87.8	76.3	9	conserved hypothetical protein
SO1045	No change	0.0	0.0	22.3	24.5	9	hypothetical protein
SO1114 ^c	Induced	0.0	0.0	28.3	55.2	18	DNA-damage-inducible protein P (<i>dinP</i>)
SO1178	No change	11.7	11.3	45.7	41.6	17	magnesium and cobalt efflux (<i>corC</i>)
SO1190 ^c	Induced	39.0	20.2	55.5	51.8	9	conserved hypothetical protein
SO1482 ^c	Induced	30.2	28.8	82.7	80.5	17	TonB-dependent receptor, putative
SO1576	No change	20.7	0.0	39.2	44.6	4	glutathione S-transferase family protein
SO1580 ^c	Induced	5.0	14.0	29.0	45.3	17	TonB-dependent heme receptor
							phosphoglucosyltransferase/phosphomannomutase family protein
SO1755	Induced	22.3	10.6	34.6	49.6	7	protein
SO2290	No change	24.9	17.4	49.8	48.0	18	rhodanese domain protein
SO2426 ^c	Induced	0.0	0.0	37.1	48.1	15	DNA-binding response regulator
SO2577	No change	6.3	22.3	41.3	48.7	4	septum site-determining protein (<i>minD</i>)
SO2912 ^c	Induced	38.3	25.9	64.7	55.1	7	formate acetyltransferase (<i>pflB</i>)
SO2915	Induced	15.5	12.3	49.4	43.6	5	acetate kinase (<i>ackA</i>)
SO3030 ^c	Induced	12.9	0.0	62.4	66.1	17	siderophore biosynthesis protein (<i>alcA</i>)
SO3032 ^c	Induced	5.7	0.0	31.4	32.3	17	siderophore biosynthesis protein, putative
SO3033 ^c	Induced	12.0	6.7	57.6	57.3	17	ferric alcaligin siderophore receptor
SO3061	Induced	6.1	3.1	31.3	37.9	6	DNA topoisomerase III (<i>topB</i>)
SO3407	Induced	9.3	8.8	24.7	19.1	9	conserved hypothetical protein
SO3462 ^c	Induced	0.0	6.0	35.1	34.1	6	DNA repair protein RecN (<i>recN</i>)
SO3585 ^c	Induced	0.0	0.0	20.1	23.0	4	azoreductase, putative
SO3586 ^c	Induced	0.0	0.0	60.1	20.3	18	glyoxalase family protein
SO3599	Induced	12.8	18.5	68.7	64.8	17	sulfate ABC transporter, periplasmic protein (<i>cysP</i>)
SO3667 ^c	Induced	0.0	0.0	91.9	96.8	9	conserved hypothetical protein ^d
SO3669 ^c	Induced	9.3	11.6	71.6	77.9	17	heme transport protein (<i>hugA</i>)
SO3670 ^c	Induced	0.0	0.0	13.5	18.6	17	TonB1 protein (<i>tonB1</i>)
SO3671	Induced	0.0	0.0	20.4	26.5	17	TonB system transport protein (<i>exbB1</i>)
SO3673 ^c	Induced	0.0	0.0	63.1	61.2	17	hemin ABC transporter, periplasmic (<i>hmuT</i>)
SO3675 ^c	Induced	0.0	0.0	72.9	59.0	17	hemin ABC transporter, ATP-binding protein (<i>hmuV</i>)
SO3723	Induced	0.0	0.0	50.2	29.8	5	adenylylsulfate kinase (<i>cysC</i>)

Table 3.3. Continued

Gene	Transcriptome	Control 1	Control 2	Chrom 1	Chrom 2	Category	Description
SO3726	Induced	22.1	7.8	49.7	49.3	5	sulfate adenylyltransferase, subunit 1 (<i>cysN</i>)
SO3727	Induced	38.7	20.2	68.5	68.5	5	sulfate adenylyltransferase, subunit 2 (<i>cysD</i>)
SO3737	Induced	30.8	22.1	62.1	73.3	5	sulfite reductase (NADPH) hemoprotein (<i>cysI</i>)
SO3738	Induced	5.9	0.0	30.8	27.3	5	sulfite reductase (NADPH) flavoprotein (<i>cysJ</i>)
SO3907	No change	0.0	0.0	48.1	60.0	9	conserved hypothetical protein
SO3913 ^c	Induced	0.0	0.0	27.2	32.6	9	conserved hypothetical protein
SO3914 ^c	Induced	18.5	15.8	68.1	67.8	17	TonB-dependent receptor, putative
SO4077	Induced	14.5	14.0	36.7	37.1	17	TonB-dependent receptor, putative
SO4516	Induced	0.0	8.8	37.7	32.6	17	ferric vibriobactin receptor (<i>viuA</i>)
SO4523	Induced	39.4	50.5	70.8	74.4	17	iron-regulated outer membrane virulence (<i>irgA</i>)
SO4651 ^c	Induced	0.0	0.0	41.4	77.6	9	conserved hypothetical protein
SO4652 ^c	Induced	0.0	0.0	46.6	62.0	17	sulfate ABC transporter, periplasmic (<i>sbp</i>)
SO4655 ^c	Induced	0.0	0.0	54.5	55.1	17	sulfate ABC transporter, ATP-binding (<i>cysA-2</i>)
SO4743	Induced	50.9	49.9	71.7	67.7	17	TonB-dependent receptor, putative
SOA0042	No change	0.0	0.0	46.9	46.3	9	hypothetical protein

^aNo change in expression at the 90 min time point in the microarray analysis. No change defines a gene that was found to not have an induction or repression of expression at any time point on the microarray. ^bInduced defines a gene that exhibited at least two-fold induction at the 90 min time point. ^cProteins also found to be up-regulated in the 45 min chromate-exposure samples. ^dThe functional annotation of SO3667 was revised recently to a heme iron utilization protein, HugZ [187].

Table 3.4. Down-Regulated Proteins Identified in the 90 min Chromate-Shocked Samples

Gene	Transcriptome	Control 1	Control 2	Chrom 1	Chrom 2	Category	Description
SO0398	Repressed ^a	42.4	18.1	0.0	4.6	7	fumarate reductase flavoprotein subunit (<i>frdA</i>)
SO0404	Repressed	78.8	77.9	55.4	57.2	9	hypothetical protein
SO0548	Repressed	70.0	76.7	47.8	51.1	6	DNA-binding protein, HU family
SO0847	Induced	45.9	28.7	0.0	0.0	7	iron-sulfur cluster-binding protein (<i>napG</i>)
SO0848 ^b	Induced ^c	73.2	52.9	43.8	46.1	7	periplasmic nitrate reductase (<i>napA</i>)
SO0902	Repressed	49.8	37.5	26.5	18.4	7	NADH:ubiquinone oxidoreductase, (<i>nqrA-1</i>)
SO0970	Repressed	59.9	57.4	34.7	34.9	7	fumarate reductase flavoprotein subunit precursor
SO1111	Repressed	75.8	70.1	35.7	42.7	17	bacterioferritin subunit 2 (<i>bfr2</i>)
SO1405	No change ^d	40.1	31.4	11.1	0.0	18	transglutaminase family protein
SO1429	No change	42.8	26.8	0.0	0.0	7	anaerobic dimethyl sulfoxide reductase, A (<i>dmaA-1</i>)
SO1430	No change	31.2	36.2	0.0	0.0	7	anaerobic dimethyl sulfoxide reductase, B (<i>dmsB-1</i>)
SO1490	Repressed	67.3	70.2	27.2	39.8	7	alcohol dehydrogenase II (<i>adhB</i>)
SO1518	Repressed	80.4	81.5	48.1	52.4	9	conserved hypothetical protein
SO1776	Repressed	48.5	41.9	25.7	31.0	3	outer membrane protein precursor (<i>mtrB</i>)
SO1777	Repressed	8.7	6.9	0.0	0.0	7	decaheme cytochrome c MtrA (<i>mtrA</i>)
SO1778	Repressed	43.4	55.1	25.0	25.2	7	decaheme cytochrome c (<i>omcB</i>)
SO1779	Repressed	51.8	53.5	26.7	29.9	7	decaheme cytochrome c (<i>omcA</i>)
SO2469	Repressed	22.1	24.7	10.0	12.1	18	conserved hypothetical protein
SO2490	Repressed	51.8	66.9	33.5	28.9	14	transcriptional regulator, RpiR family
SO2929 ^b	Repressed	73.8	73.0	36.3	40.0	9	hypothetical protein
SO3538 ^b	Repressed	46.9	34.7	0.0	0.0	14	transcriptional regulator HlyU (<i>hlyU</i>)
SO3565	Repressed	72.0	59.9	36.8	39.6	13	2,3-cyclic-nucleotide 2-phosphodiesterase (<i>cpdB</i>)
SO3920	Repressed	21.7	27.6	0.0	0.0	7	periplasmic Fe hydrogenase, large subunit (<i>hydA</i>)
SO3967	No change	71.6	56.4	23.0	24.5	17	molybdenum ABC transporter, periplasmic protein
SO4513 ^b	No change	44.3	36.2	3.3	3.5	7	formate dehydrogenase, alpha subunit
SO4561	No change	37.7	47.4	0.0	0.0	9	conserved hypothetical protein

^aRepressed is a gene exhibiting at least two-fold repression at the 90 min time point. ^bProteins down-regulated in both the 45

and 90 min chromate-exposure experiments. ^cInduced is a gene exhibiting at least two-fold induction at the 90 min time point.

^dNo change in expression at the 90 min time point in the microarray analysis.

analyses at the protein level is necessary for a successful determination of differentially expressed proteins where a protein must be detected in both of the replicate analyses to be included as a candidate for semiquantification. For the 45-min chromate treatment analysis, a total of 24 proteins were found to be up-regulated with six additional proteins being down-regulated relative to the control sample (Supplemental Table S4). The genes for 23 of these 24 up-regulated proteins showed corresponding induction levels at the 30- and 60-min time points based on microarray hybridization. A putative formate acetyltransferase (encoded by *pflB*), which was identified as being up-regulated at the protein level, was found to be induced at the transcript level at the 30-min treatment time but repressed at the 60-min time point. The subset of proteins identified as up-regulated were dominated by species (12 total) assigned to the functional category of transport and binding proteins and included TonB-dependent receptors, siderophore biosynthesis proteins, heme transport proteins, and TonB1. Proteins classified as hypothetical were also dominant with a total of six conserved hypothetical proteins identified as up-regulated. For the six proteins down-regulated in the 45-min shocked sample relative to the control condition, five were found to be repressed at the mRNA level by microarray analysis, and the other protein, a hypothetical protein (SOA0141), revealed no change at the transcript level. Proteins that were measured as being down-regulated in the 45-min chromate-shocked samples consisted of three hypothetical proteins (SO1124, SO2929, and SOA0141), a periplasmic nitrate reductase (NapA), a transcriptional regulator (HlyU), and the α subunit of formate dehydrogenase (SO4513).

Proteomic analysis of the 90-min chromate treatment samples revealed 48 up-regulated proteins and 26 down-regulated proteins relative to the control sample

(Supplemental Table S4 and Tables 3.3 and 3.4). After 90 min of chromate exposure, 39 of the 48 proteins up-regulated under Cr(VI) conditions also were induced at the transcript level as identified by microarray analysis. Nine of the up-regulated proteins (AcnA, SO0934, SO1045, CorC, SO1576, SO2290, MinD, SO3907, and SOA0042) revealed no significant change ($p < 0.05$) in expression at the transcription level, and two of the proteins (AcnA and SO2290) expressed at higher abundance levels under chromate stress conditions did not exhibit a change in their mRNA expression levels at the 90-min time point but did at earlier time points (5, 30, and 60 min). Of the 48 up-regulated proteins, 19 proteins were from the transport and binding category, six proteins were from central intermediary metabolism, and 10 were annotated as hypothetical proteins. All of the transport and binding proteins identified as up-regulated in the 45-min chromate-shocked samples were also identified as up-regulated in the 90-min samples, whereas only four of the six conserved hypothetical proteins showed up-regulation at both postexposure time points.

Eighteen of 26 proteins down-regulated 90 min after chromate addition were also repressed at the transcript level. Of the remaining down-regulated proteins, five showed no change at the mRNA level, one protein of which was found to exhibit no mRNA change at the 90-min time point. Two down-regulated proteins (NapG and NapA) were found to be induced at the transcript level. Four of the six proteins down-regulated at the 45-min time point were also repressed at 90 min. The transcriptome data revealed an increase in the number of down-regulated energy metabolism genes over time in response to chromate. This trend was also reflected in the proteomic data in which 13 proteins

with functions in energy metabolism were identified as repressed at the 90-min time point relative to the 45-min interval.

Differences between the transcriptomic and proteomic responses of *S. oneidensis* to chromate shock are due to the stringency of filtering used in the proteome study and inherent measurement differences between microarray *versus* proteome technology. Supplemental Table S5 demonstrates the correlation of the identified and/or differentially expressed proteins to the top 100 mRNAs induced at each time point. The list is composed of a total of 194 mRNAs, which is a concatenated list representing the top 100 mRNAs at each time point (initial list was 400 genes in total before removal of redundant genes). A total of 67% of the genes in Supplemental Table S5 did not meet the differential criteria at the protein level where 45% were not identified by mass spectrometry and another 22% were not considered differentially expressed. The 67% of genes found not to meet differential expression criteria corresponds to 130 genes of 194, which is comparative in percentage to the total global analysis.

As revealed by transcriptome and proteome analyses, a major feature of the molecular response of *S. oneidensis* MR-1 to acute chromate challenge was the differential regulation of the TonB1-ExbB1-ExbD1 complex, an integral inner membrane system for iron transport, as well as other genes involved in exogenous iron acquisition. Genes that were highly induced based on time series microarray experiments and were identified as up-regulated proteins at the 45- and/or 90-min chromate treatment conditions (Table 3.3) included two putative siderophore biosynthesis proteins (AlcA and SO3032), a ferric alcaligin siderophore receptor (SO3033), HugA heme transport protein (SO3669), TonB1 (SO3670), a putative TonB-dependent receptor (SO3914), a TonB-

dependent heme receptor (SO1580), ViuA (SO4516), and HmuT (SO3673) and HmuV (SO3675) of the hemin ABC transporter. Wang and Newton [188] demonstrated that mutants harboring a deletion of the *tonB-trp* region of the *E. coli* chromosome were sensitive to chromic ion (Cr^{3+}) due to defective iron transport systems, and residual iron uptake by these strains was shown to be inhibited by chromic ion. Regulation of iron homeostasis is primarily carried out by the Fur protein (for a review, see Ref. [189]). It has been suggested previously that iron uptake regulation may not be the only function of Fur but that it may also serve to sequester iron to prevent the generation of highly reactive hydroxyl radicals via Fenton reactions [190]. The putative MR-1 ferritin genes, but not bacterioferritin genes, were induced in response to chromate, and these respective iron storage proteins have been suggested to have roles in short term iron flux and long term iron storage in *E. coli* [191].

In addition to iron transport genes, our global analyses demonstrated that CysP, CysC, CysD, CysN, CysI, CysJ, Sbp, and CysA-2 are up-regulated at both the mRNA and protein levels in response to chromate treatment (Table 3.3). The enhanced expression of genes encoding proteins involved in sulfate transport and assimilatory sulfate metabolism suggests the possibility of chromate-induced sulfur limitation in *S. oneidensis*, perhaps through competitive inhibition of sulfate uptake by chromate, as has been shown previously [149, 151]. Partial reduction of Cr(VI) to Cr(V) produces ROS [126, 140, 143], leading to chromate-mediated oxidative stress. Researchers working with a number of different bacteria have observed induction of genes involved in sulfur and iron homeostasis following different oxidative stresses [192-195]. A variety of explanations have been proposed including disruption of intracellular redox cycling

leading to insufficient sulfite reduction, a reduction in cysteine biosynthesis correlated with cell envelope damage and subsequent leakage of sulfide [196], and increased demand for low molecular weight protective thiol-containing compounds such as glutathione [197]. Alternatively induction of genes involved in sulfur metabolism and iron sequestration might represent an adaptive response to sulfur and iron limitation in MR-1 following chromate exposure.

One of the potentially interesting findings to emerge from this integrated global investigation was the co-regulated expression of a cluster of three genes (*so3585*, *so3586*, and *so3587*) at both the mRNA and protein levels. All three genes are transcribed in the same direction on the MR-1 chromosome and show a similar transcriptional profile in response to chromate with the peak in up-regulated expression occurring at the 30-min time point. The proteins encoded by two of these genes (*so3585* and *so3586*) were detected in the chromate-treated samples only (Table 3.3), suggesting that expression of SO3585 and SO3586 were differentially regulated in response to chromate stress conditions. By contrast, hypothetical protein SO3587 was found in both the control and chromate-shocked samples at the two-peptide level (Supplemental Table S3) even though the gene encoding this protein was shown to be up-regulated over the entire time course in response to chromate stress. In addition, SO3587 was found only in the membrane fractions, and a hydrophobicity plot analysis using the computer program SOSUI [198] identified a putative transmembrane domain (IGIALIFADVSLYLAYFFVGLGV) in SO3587. SO3585 and SO3586 were detected in both the soluble and membrane fractions. Based on their proximity in genome location and co-regulated expression profile within the context of chromate stress, we predict that SO3585, SO3586, and

SO3587 function together as a protein complex associated with the cell membrane and play an important role in the response of the cell to chromate toxicity.

S. oneidensis SO3585 and SO3586 are annotated as a putative azoreductase and glyoxalase family protein, respectively [69]. Glyoxalase systems are known to serve as key detoxification routes for preventing the intracellular accumulation of methylglyoxal, a natural metabolite with toxic electrophilic properties (for a review, see Ref. [199]). Azoreductases are responsible for the reductive cleavage of azo dyes, synthetic organic colorants used extensively in the textile, food, and cosmetics industries. Synthetic azo dyes are not readily reduced under aerobic conditions and are considered pollutants. Protein database searches using BLAST Version 2.2.12 [200] with the derived SO3585 primary sequence revealed ~28% sequence identity with *P. putida* ChrR and *E. coli* YieF, two soluble flavoproteins that have been demonstrated to exhibit chromate reductase activity [128, 138, 201]. Regions of conservation in the derived amino acid sequence of SO3585 included the characteristic signature, LFVTPEYNX ₆LKNAIDX ₂S (conserved residues in SO3585 are underlined), of the NADH_dh2 family of NAD(P)H oxidoreductases (Ref. [201]; results not shown). Recently further investigation demonstrated that the *P. putida* ChrR functions as a quinone reductase and minimizes oxidative stress induced by intracellular H₂O₂, which is generated during the course of chromate reduction [202]. An MR-1 strain carrying an in-frame deletion mutation in the *so3585* locus has been created, and future studies will characterize it to gain insight into the functional role of SO3585 and to assess the importance of azoreductase in the *S. oneidensis* response to chromate.

Nine proteins (SO0798, SO0934, SO1045, SO1190, SO3667, SO3907, SO3913, SO4651, and SOA0042) annotated as hypothetical or conserved hypothetical met our criteria of significance for differential expression and were identified as being up-regulated in response to chromate exposure at the 45- and/or 90-min time points (Table 3.3). For four of these unknown or conserved unknown proteins (SO0934, SO1045, SO3907, and SOA0042), we observed no significant change in expression at the mRNA level, suggesting post-transcriptional regulation of these proteins in response to chromate. Our integrated transcriptome and proteome study implicates these differentially regulated proteins of unknown function in the initial response of MR-1 to toxic chromate, thus revealing gene candidates for future functional analysis.

A recent study by Kolker *et al.* [187] analyzed expression for a subset of 538 hypothetical proteins that were confidently identified in *S. oneidensis* MR-1 as a result of large scale microarray and proteomic analyses of cell samples generated under different growth conditions. A total of 788 hypothetical proteins have been identified based on the study by Kolker *et al.* [187] and the present study: 368 of these functionally undefined proteins were found in both studies, 170 were found only by Kolker *et al.* [187], and 256 were found only in this study (Supplemental Table S6). The 368 hypothetical proteins identified independently by both studies should be considered as expressed proteins, and their annotations should be changed to unknown or conserved unknown [184]. Most of these proteins were found under all growth conditions and identified in most of the replicates. Differences between the datasets revealed by this proteomic study and the one reported by Kolker *et al.* [187] are likely due to differences in the growth conditions used.

Chronic Exposure Proteome Dataset

Proteome measurements using LC/LC-MS/MS were taken to characterize the response of *S. oneidensis* MR-1 at the 24-h time point following initial exposure to 0.3 mM chromate. At this time point of sampling the proteome for differentially expressed proteins, the bacterium is no longer in the presence of Cr(VI) and is now presumably resuming growth with cytoplasmic Cr(III). Gene and protein expression profiles of cells exposed to chromate were compared to those of untreated control cells grown in parallel (see Chapter 2 for experimental details). The microarray data will only be presented in this section if the dataset pertains to results obtained by the proteome measurements. At the protein level, a total of 2,313 gene products, representing 47% of the predicted MR-1 proteome, were identified at the two-peptide level in duplicate analyses of control samples and samples exposed to chromate for 24 h (Table 3.5). A total of 3,051 proteins were identified using the less stringent one-peptide filter level; however, a one-peptide filter level for the identification of proteins results in a dramatically higher false-positive discovery rate [65], so a thorough analysis of only the two-peptide data is presented here. The levels of reproducibility between replicate analyses of the control proteome and the experimental (chromate-treated) proteome on the LTQ instrument were 75.6% and 77.2%, respectively. For the observed proteome identified in this study, 109 protein species were found to be differentially expressed under prolonged Cr(VI) exposure, with 56 proteins displaying increased abundance and 53 showing decreased abundance (Table 3.5). Supplementary proteome data (i.e., a list of the complete raw and filtered proteome data and a list of differentially expressed proteins) can be accessed online at compbio.ornl.gov/shewanella_metal_stress/chronic/.

Table 3.5. Functional Distribution of the Observed and Predicted MR-1 Proteomes

Functional Category (no.)	Observed	Predicted	Percentage	Up-regulated	Down-regulated
Amino acid biosynthesis (1)	72	91	79.1%	4	0
Biosynthesis of cofactors, prosthetic groups, and carriers (2)	95	121	78.5%	0	1
Cell envelope (3)	115	180	63.9%	3	5
Cellular processes (4)	175	260	67.3%	0	7
Central intermediary metabolism (5)	28	51	54.9%	3	0
DNA metabolism (6)	84	144	58.3%	5	0
Energy metabolism (7)	205	308	66.6%	1	5
Fatty acid and phospholipid metabolism(8)	45	65	69.2%	0	0
Hypothetical proteins (9)	633	2039	31.0%	20	20
Mobile and extrachromosomal element functions (10)	45	317	14.2%	14	0
Protein fate (11)	131	185	70.8%	2	4
Protein synthesis (12)	128	141	90.8%	0	1
Purines, pyrimidines, nucleo-sides, and nucleotides (13)	58	62	93.5%	1	1
Regulatory functions (14)	104	199	52.3%	0	2
Signal transduction (15)	34	61	55.7%	0	0
Transcription (16)	45	54	83.3%	0	0
Transport and binding (17)	126	274	46.0%	0	5
Unknown function (18)	190	379	50.1%	3	2
Total	2313	4931	46.9%		

Proteins identified at the two-peptide level under the two different growth conditions were organized in Table 3.5 according to the functional categories assigned by the J. Craig Venter Institute [formerly The Institute for Genomic Research (see www.tigr.org; Comprehensive Microbial Resource)]. Using multidimensional HPLC-MS/MS, we identified more than 75% of the predicted MR-1 proteins for the following five functional categories: amino acid biosynthesis; biosynthesis of cofactors, prosthetic groups, and carriers; protein synthesis; purines, pyrimidines, nucleosides, and nucleotides; and transcription. Under 24-h Cr(VI) exposure, more proteins were identified in the functional categories of amino acid biosynthesis; biosynthesis of cofactors, prosthetic groups, and carriers; purines, pyrimidines, nucleosides, and nucleotides; and protein synthesis than were found under the corresponding control condition (Table 3.5).

Sequence analysis of the MR-1 genome revealed the presence of an integrated lambda-like phage (LambdaSo; 51,857 bp) and two phylogenetically distinct phages related to the *E. coli* mu (MuSo1 [34,551 bp] and MuSo2 [35,666 bp]) [69]. The lambdalike phage genome is also present in MR-1 in a nonintegrated form [69]. There are 75, 42, and 53 open reading frames (ORFs) annotated as LambdaSo, MuSo1, and MuSo2 genes, respectively [69]. A previous study focusing on *S. oneidensis* MR-1 demonstrated the induction of a large number of prophage-related genes in response to UV radiation, particularly those genes from the integrated LambdaSo genome, and the presence of phage particles in UV-irradiated MR-1 cultures [192]. Based on transcriptome analysis, the genomic response of MR-1 to ionizing radiation (40 Gy) was found to be very similar to its response to UV radiation [203]. Similarly, we observed the

strong induction of numerous prophage-related genes in MR-1 cells exposed to chromate for 24 h (see supplemental Table S1 at compbio.ornl.gov/shewanella_metal_stress/chronic/supplemental; Table 3.6), suggesting that prolonged Cr(VI) exposure and/or the accumulation of intracellular chromium may induce the lytic cycle of lysogenic bacteriophage in MR-1. Overall, 16 (21%), 2 (5%), and 10 (19%) ORFs annotated as LambdaSo, MuSo1, and MuSo2 genes, respectively, were significantly induced (more than twofold; $P < 0.05$) in response to prolonged Cr(VI) exposure. This molecular response was in striking contrast to the differentially expressed genes/proteins characterizing the cellular response to a 90-min acute 1 mM chromate challenge, during which a very small subset of predicted prophage genes (i.e., six) displayed a moderate two- to fourfold induction [147].

Gene products for 14 ORFs with annotations corresponding to mobile and extrachromosomal element functions were confidently identified as being up-regulated in response to prolonged Cr(VI) treatment based on both microarray analysis and multidimensional HPLC-MS/MS (Table 3.6). Ten of these 14 proteins were encoded in the LambdaSo genome, whereas 1 and 2 gene products were annotated as prophage MuSo1 and MuSo2 proteins, respectively. The majority of these genes encoded such prophage structural proteins as minor and major tail proteins, tail assembly components, and the major head subunit (Table 3.6). Six additional ORFs (SO2941, SO2969, SO2973, SO2978, SO2985, and SO3006) with prophage LambdaSo-related functions displayed significant increases (more than twofold; $P < 0.05$) in mRNA expression (see Supplemental Table S1 at compbio.ornl.gov/shewanella_metal_stress/chronic/). The corresponding proteins for those genes were detected only under Cr(VI) conditions by

Table 3.6. Relative Expression of Up-regulated mRNA and Corresponding Proteins in Response to 24-h Chromate Exposure

Gene	Gene product (functional category no. ^e)	Transcriptomics [Cr(VI)/ Con ratio] ^a	Control		24-h chromate exposure			
			% Coverage ^b	No. of unique peptides/ protein ^c	Avg no. of spectra ^d	% Coverage	No. of unique peptides/ protein	Avg no. of spectra
SO0401	Alcohol dehydrogenase, zinc containing (7)	1.2	0.0	0	0	45.1	9	11
SO0644	Prophage MuSo1 DNA transposition protein (10)	11.9	0.0	0	0	72.4	15	25
SO0795	Conserved hypothetical protein (9)	0.80	5.9	2	1	49.7	16	16.5
SO2654	Putative transposase (10)	1.5	0.0	0	0	36.9	19	16
SO2655	Prophage MuSo2 DNA transposition protein (10)	3.6	16.0	3	2	57.5	18	57.5
SO2660	Conserved hypothetical protein (9)	14.1	32.5	5	6	83.5	24	145
SO2663	Conserved hypothetical protein (9)	8.5	0.0	0	0	58.7	12	36
SO2667	Conserved hypothetical protein (9)	19.7	0.0	0	0	48.0	8	10
SO2673	Hypothetical protein (9)	10.8	0.0	0	0	55.4	8	7.5
SO2685	Putative prophage MuSo2 major head subunit (10)	24.5	22.7	3	2	51.8	12	17.5
SO2688	Hypothetical protein (9)	24.5	0.0	0	0	42.0	10	6.5
SO2834	Anaerobic ribonucleoside-triphosphate reductase, NrdD (13)	1.9	16.6	8	8	37.2	20	30
SO2940	Prophage LambdaSo host specificity protein J (10)	5.4	3.7	2	1	49.6	49	107
SO2942	Hypothetical protein (9)	42.4	0.0	0	0	59.6	11	19
SO2944	Hypothetical protein (9)	44.7	0.0	0	0	65.3	26	96.5
SO2945	Hypothetical protein (9)	129.8	26.6	4	6.5	67.8	15	78
SO2946	Hypothetical protein (9)	37.2	0.0	0	0	58.0	10	65.5
SO2948	Prophage LambdaSo tail assembly protein K (10)	23.7	0.0	0	0	51.9	8	7.5
SO2949	Prophage LambdaSo minor tail protein L (10)	5.6	0.0	0	0	50.6	10	23.5
SO2950	Hypothetical protein (9)	10.9	0.0	0	0	53.4	9	23.5

Table 3.6. Continued

Gene	Gene product (functional category no. ^e)	Transcriptomics [Cr(VI)/ Con ratio] ^a	Control		24-h chromate exposure			
			% Coverage ^b	No. of unique peptides/ protein ^c	Avg no. of spectra ^d	% Coverage	No. of unique peptides/ protein	Avg no. of spectra
SO2951	Hypothetical protein (9)	48.5	16.9	5	4	69.2	41	172.5
SO2952	Prophage LambdaSo minor tail protein M (10)	28.6	0.0	0	0	82.0	6	14.5
SO2953	Prophage LambdaSo tail length tape measure protein H (10)	33.4	4.2	2	2	58.5	51	74
SO2955	Conserved hypothetical protein (9)	74.9	14.0	1	1.5	46.3	7	20
SO2956	Prophage LambdaSo major tail protein V (10)	61.9	0.0	0	0	80.9	8	57.5
SO2963	Prophage LambdaSo major capsid protein, HK97 family (10)	168.0	36.6	12	13	80.8	32	183.5
SO2964	ClpP protease family protein (11)	57.7	0.0	0	0	23.6	7	11
SO2965	Prophage LambdaSo portal protein, HK97 family (10)	106.0	14.8	2	1	41.9	14	16
SO2979	Hypothetical protein (9)	11.7	0.0	0	0	45.0	7	8.5
SO2980	Hypothetical protein (9)	8.9	0.0	0	0	69.1	11	12.5
SO2988	Conserved hypothetical protein (9)	4.2	69.2	7	6.5	95.3	23	84.5
SO2993	Putative prophage LambdaSo type II DNA modification methyltransferase (10)	3.3	0.0	0	0	67.2	19	42.5
SO3001	Hypothetical protein (9)	8.4	0.0	0	0	80.6	9	28
SO3004	Putative prophage LambdaSo DNA modification methyltransferase (10)	2.4	0.0	0	0	68.2	21	51.5
SO3008	Hypothetical protein (9)	2.0	0.0	0	0	56.2	6	10.5
SO3013	Site-specific recombinase, phage integrase family (6)	1.4	0.0	0	0	24.3	11	10.5
SO3019	Anthranilate synthase component I, TrpE (1)	1.3	5.9	2	1	45.6	19	32
SO3020	Glutamine amidotransferase, TrpG (1)	2.5	0.0	0	0	51.0	6	8.5
SO3022	Isomerase, TrpC/F (1)	1.6	13.0	5	2.5	45.2	19	33.5
SO3061	DNA topoisomerase III, TopB (6)	1.3	8.0	3	3	37.9	18	16

Table 3.6. Continued

Gene	Gene product (functional category no. ^e)	Transcriptomics [Cr(VI)/ Con ratio] ^a	Control		24-h chromate exposure			
			% Coverage ^b	No. of unique peptides/ protein ^c	Avg no. of spectra ^d	% Coverage	No. of unique peptides/ protein	Avg no. of spectra
SO3183	Perosamine synthetase-related protein (18)	3.3	12.7	3	2.5	46.8	10	12.5
SO3185	Polysaccharide biosynthesis protein (3)	3.4	9.5	2	1	55.9	12	14.5
SO3189	Polysaccharide biosynthesis protein (3)	2.2	28.2	7	9	70.9	18	34.5
SO3315	Conserved hypothetical protein TIGR00048 (9)	0.80	0.0	0	0	36.5	10	9.5
SO3726	Sulfate adenylyltransferase, subunit I, CysN (5)	2.4	14.7	3	4	45.9	14	22.5
SO3727	Sulfate adenylyltransferase, subunit 2, CysD (5)	2.2	16.6	4	2.5	54.6	11	23.5
SO3737	Sulfite reductase (NADPH) hemoprotein beta component, CysI (5)	2.1	3.7	2	1	45.7	17	27
SO3797	Peptidase, U32 family (11)	1.0	0.0	0	0	28.1	10	10.5
SO4265	Type I restriction-modification system, M subunit, HSdM-2 (6)	1.1	22.9	6	6.5	52.9	17	20.5
SO4309	Diaminopimelate decarboxylase, LysA (1)	0.70	11.1	3	2	46.4	11	16.5
SO4343	Aminotransferase, class V (18)	1.7	0.0	0	0	59.3	14	24
SO4686	NAD-dependent epimerase/dehydratase family protein (3)	1.1	0.0	0	0	50.1	10	7
SOA0003	Putative type II restriction endonuclease (6)	0.70	16.7	3	1.5	50.9	17	23
SOA0004	Type II DNA modification methyltransferase (6)	0.90	13.0	4	4	54.9	24	44
SOA0160	Putative esterase (18)	0.70	30.5	6	7.5	63.4	11	21

^aRelative gene expression (induction) is presented as the mean ratio of the fluorescence intensity of Cr(VI)-exposed cells to

control cells. ^bTotal sequence coverage from replicate analyses. ^cTotal number of unique peptides identified per protein from

replicate analyses. ^dAverage number of spectra identified per protein from replicate analyses. ^eFrom Table 3.5.

HPLC-MS/MS analysis but failed to meet our filtering criteria for determining differential expression (see Chapter 2 and Supplemental Table S2):

SO2941 (~20% sequence coverage), SO2969 (protein not detected), SO2973 (~8.2%), SO2978 (~20%), SO2985 (~15%), and SO3006 (~15%). The genes encoded a putative LambdaSo-associated lysozyme (SO2973; 1,053.6-fold), tail assembly protein I (SO2941; 366.5-fold), a putative holin (SO2969; 49.2-fold), a sitespecific recombinase (SO2978; 23.8-fold), replication protein O (SO2985; 4.4-fold), and a type II DNA modification methyltransferase (SO3006; 3.8-fold). Other up-regulated prophage-related genes had predicted functions in virion morphogenesis (SO2690; 65.6-fold), DNA transposition (SO0644; 11.9-fold; SO2655; 3.6-fold) and circulation (SO2698; 4.1-fold), positive regulation of late transcription (SO2668; 16.7-fold), baseplate (SO2700; 4.3-fold) and tail assembly (SO2699, 10.3-fold; SO2704, 17.2-fold), and assembly of the major head subunit (SO0675; 5.9-fold; SO2685; 24.5-fold), as well as assembly of other structural components (SO2681, 6.2-fold; SO2684, 6.8-fold) (see supplemental Table S1).

Of the differentially expressed proteins determined as having increased abundance under Cr(VI) conditions, 36% corresponded to hypothetical or conserved hypothetical proteins (Table 3.6). Five of these proteins (SO2660, SO2663, SO2667, SO2673, and SO2688) are encoded by genes from the prophage MuSo2 genome, which implied their potential function in prophage activation and synthesis. The majority of the up-regulated hypothetical proteins (i.e., SO2942, SO2944 to -46, SO2950, SO2951, SO2955, SO2979, SO2980, SO2982, SO2988, SO3001, and SO3008) were derived from genes located in the LambdaSo genome, while no potentially MuSo1-related hypothetical

or conserved hypothetical proteins were measured as being differentially expressed under our experimental conditions (Table 3.6). The gene and protein expression data strongly suggest that, similar to UV irradiation [192], prolonged exposure to chromate and its derivatives may activate the lytic cycles of some or all three of the MR-1 prophages, leading to prophage-mediated cell lysis. At this point, it is not clear whether the induction of MR-1 prophage-related genes/structural proteins is a response to an extended Cr(VI) exposure per se or to the possible intracellular accumulation of chromium, particularly reduced Cr(III). *S. oneidensis* MR-1 cells exposed to Cr(VI) have been shown to precipitate reduced chromium both extracellularly on the cell surface and as electron-dense globules inside cells [135]. Qiu et al. [192] suggested that prophage activation was the major lethal factor in *S. oneidensis* MR-1 following UV C or UV B irradiation. Our results certainly point to prophage activation as a major contributor to the toxic effects of Cr under conditions of prolonged exposure and reduction. The conditions of Cr(III) toxicity and UV irradiation may be similar mechanistically due to both being DNA damage inducing agents.

The membrane response was characterized by changes in the expression of genes encoding outer membrane structural components and polysaccharide biosynthesis proteins. Induced genes included those encoding putative outer membrane porins (encoded by SO0312 and SO1821), OmpW (encoded by SO1673), and three proteins with functions related to polysaccharide biosynthesis (encoded by SO3158, SO3181, and SO3185). Proteomic analysis indicated increases in the synthesis of SO3185 and SO3189, both annotated as polysaccharide biosynthesis proteins, while four predicted lipoproteins (SO2570, NlpD, SOA0110, and SOA0112) and an OmpA family protein

(SO3969) belonging to the functional category of cell envelope proteins showed decreased abundance under Cr(VI) conditions (Tables 3.6 and 3.7). Located immediately upstream of *nlpD* (SO3433) in the MR-1 chromosome is the gene *pcm*, which is predicted to encode protein-L-isoaspartate *O*-methyltransferase, an enzyme involved in protein modification and repair. The ORF coding for the RNA polymerase sigma factor RpoS, which controls the expression of many stationary-phase-induced genes, is positioned just downstream of *nlpD* and is transcribed in the same direction as *nlpD* and *pcm*. Proteomic analysis revealed that, in addition to the lipoprotein NlpD, expression of protein-L-isoaspartate *O*-methyltransferase was down-regulated under conditions of 24-h Cr(VI) exposure (Table 3.7). This is of interest because, with age or under stress conditions, proteins are susceptible to various spontaneous or deleterious covalent modifications such as deamidation, the conversion of asparagines into aspartyls and isoaspartyls, which can result in loss of protein function. Pcm functions in repairing damaged proteins by selectively methylating atypical L-isoaspartyl sites and converting them back to L-aspartyls [204, 205]. The enzyme was shown to enhance the survival of stationary-phase *E. coli* subjected to a secondary environmental stress [206]. The physiological significance of decreased synthesis of *S. oneidensis* Pcm under the Cr(VI) conditions used here is unclear.

The vast majority of MR-1 proteins down-regulated under our experimental conditions are annotated as hypotheticals (Table 3.5). Besides poorly characterized proteins, other down-regulated proteins belonged to the functional categories of cellular process proteins, transport and binding proteins, cell envelope proteins, and energy metabolism proteins. The relative abundance levels of seven proteins were found to be

Table 3.7. Relative Expression of Down-regulated Proteins and Corresponding mRNA Levels after 24-h Exposure to Chromate

Gene	Gene product (functional category no. ^f)	Transcriptomics [Cr(VI)/Con ratio] ^a	Control		24-h chromate exposure			
			% Coverage ^b	No. of unique peptides/ protein ^c	Avg no. of spectra ^d	% Coverag e	No. of unique peptides/ protein	Avg no. of spectra
SO0433	Regulator of sigma D, Rsd (14)	0.70	67.7	12	19	36.0	5	2.5
SO0576	PhoH family protein (18)	0.80	58.6	19	22.5	0.0	0	0
SO0902	NADH:ubiquinone oxidoreductase, Na translocating, alpha subunit, NqrA-1 (7)	1.0	70.6	24	24	16.7	6	6
SO1144	Methyl-accepting chemotaxis protein (4)	0.60	86.5	33	71.5	31.8	9	12.5
SO1425	Hypothetical protein (9)	1.0	44.8	17	13	0.0	0	0
SO1518	Conserved hypothetical protein (9)	0.60	85.7	14	39	39.7	7	8
SO1689	Cation transport ATPase, E1-E2 family (4)	0.40	30.0	13	10	0.0	0	0
SO1700	Hypothetical protein (9)	0.90	61.2	21	23.5	0.0	0	0
SO2062	Conserved hypothetical protein (9)	0.50	63.8	12	29	44.0	3	5.5
SO2247	Hypothetical protein (9)	0.40	38.4	12	12	0.0	0	0
SO2304	Alanine dehydrogenase, authentic point mutation, Ald (7)	0.40	67.7	20	62.5	23.5	4	10
SO2469	Conserved hypothetical protein (9)	0.60	67.9	61	90.5	8.8	5	2.5
SO2570	Putative lipoprotein (3)	1.0	58.3	34	54.5	26.5	10	6
SO2682	Hypothetical protein (9)	2.5	54.5	3	7	0.0	0	0
SO2766	Conserved hypothetical protein (9)	1.0	63.6	27	25.5	34.3	7	6
SO2882	Conserved hypothetical protein (9)	0.80	75.2	51	91.5	43.8	21	23
SO2893	Conserved hypothetical protein (9)	1.9	72.3	16	57	25.1	3	4.5
SO2991	Conserved hypothetical protein (9)	0.70	55.0	5	10	0.0	0	0
SO3030	Siderophore biosynthesis protein, AlcA(17)	1.6	60.8	27	79.5	36.7	10	9.5
SO3069	Conserved hypothetical protein (9)	1.6	31.2	30	44.5	10.8	7	7
SO3103	AcrB/AcrD/AcrF family protein (4)	1.1	34.1	23	22.5	13.7	9	6.5
SO3145	Electron transfer flavoprotein, beta subunit, EtfB (7)	1.2	96.4	26	131.5	64.3	14	45.5

Table 3.7. Continued

Gene	Gene product (functional category no. ^f)	Transcriptomics [Cr(VI)/Con ratio] ^a	Control		24-h chromate exposure			
			% Coverage ^b	No. of unique peptides/ protein ^c	Avg no. of spectra ^d	% Coverage	No. of unique peptides/ protein	Avg no. of spectra
SO3207	Chemotaxis protein (4)	1.5	54.9	44	127	46.7	24	32
SO3235	Flagellar hook-associated protein FlhD (4)	0.80	71.3	30	39	34.6	7	5.5
SO3247	Flagellar hook protein FlgE (4)	0.90	66.0	14	36.5	31.1	6	10
SO3314	Putative fimbrial biogenesis and twitching motility protein(4)	1.0	53.1	10	10.5	0.0	0	0
SO3343	Conserved hypothetical protein (9)	0.80	81.2	20	97.5	61.3	11	28
SO3407	Conserved hypothetical protein (9)	0.80	28.6	16	16	0.0	0	0
SO3422	Ribosomal subunit interface protein, YfiA-2 (12)	1.0	89.8	8	28	17.8	2	1
SO3433	Lipoprotein NlpD (3)	1.2	46.3	10	9.5	0.0	0	0
SO3434	Protein-L-isoaspartate O-methyltransferase, Pcm (11)	0.80	64.0	9	7.5	0.0	0	0
SO3442	MazG family protein (18)	1.6	66.3	13	26	18.6	3	3.5
SO3468	Riboflavin synthase, alpha subunit, RibE-2 (2)	1.1	51.8	10	11	0.0	0	0
SO3483	HlyD family secretion protein (17)	1.0	68.6	19	18.5	25.5	5	3
SO3516	Transcriptional regulator, LacI family (14)	1.2	49.1	13	14	15.7	3	3
SO3539	Peptidase, M28D family (11)	0.50	72.7	26	40	30.7	9	5
SO3550	Hypothetical protein (9)	1.0	57.4	9	7	0.0	0	0
SO3560	Peptidase, M16 family (11)	0.30	65.0	45	50	33.7	20	19
SO3565	2,3-Cyclic-nucleotide 2-phosphodiesterase, CpdB (13)	0.70	79.7	53	74.5	28.8	12	8.5
SO3597	Conserved hypothetical protein (9)	1.0	78.7	13	48	0.0	0	0
SO3683	Coniferyl aldehyde dehydrogenase (7)	0.50	55.1	24	33	21.1	6	6.5
SO3720	Conserved hypothetical protein (9)	1.6	80.1	12	21.5	29.8	4	2.5
SO3800	Serine protease, subtilase family (11)	0.50	19.7	11	7	0.0	0	0

Table 3.7. Continued

Gene	Gene product (functional category no. ^f)	Transcriptomics [Cr(VI)/Con ratio] ^a	Control		24-h chromate exposure			
			% Coverage ^b	No. of unique peptides/ protein ^c	Avg no. of spectra ^d	% Coverag e	No. of unique peptides/ protein	Avg no. of spectra
SO3936	Sodium-type flagellar protein MotX (17)	0.90	47.6	8	6	0.0	0	0
SO3969	OmpA family protein (3)	1.5	61.8	14	19.5	20.6	2	1.5
SO3980	Cytochrome c552 nitrite reductase (7)	1.2	49.5	27	49.5	20.3	7	6.5
SO4319	HlyD family secretion protein (17)	1.3	46.7	20	23	25.0	7	6
SO4329	Conserved hypothetical protein (9)	1.4	94.0	15	47	66.7	6	13
SO4403	Hypothetical protein (9)	0.50	72.5	16	18	22.1	2	2
SO4505	Conserved hypothetical protein (9)	0.50	80.7	8	11.5	0.0	0	0
SO4523	Iron-regulated outer membrane virulence protein IrgA (17)	0.60	78.9	55	169	48.3	23	36.5
SOA0110	Putative lipoprotein (3)	0.50	43.3	10 (46)	147	16.4	1 (16)	32
SOA0112	Putative lipoprotein (3)	NA ^e	47.7	0 (52)	224.5	20.4	0 (17)	31.5

^aRelative gene expression (induction) is presented as the mean ratio of the fluorescence intensity of Cr(VI)-exposed cells

experimental) to control (nonexposed) cells. ^bTotal sequence coverage from replicate analyses. ^cTotal number of unique

peptides identified per protein from replicate analyses. ^dAverage number of spectra identified per protein from replicate

analyses. ^eNA, not applicable; gene was not represented on the microarray. ^fFrom Table 1.

decreased under 24-h Cr(VI) exposure compared to the control conditions: two chemotaxis proteins (SO1144 and SO3207), a cation transport ATPase (SO1689), an AcrB/AcrD/AcrF family protein (SO3103), and three proteins involved in motility (FliD, FlgE, and SO3314) (Table 3.7). Down-regulation of proteins involved in motility and chemotaxis was consistent with confocal laser scanning microscopy observations, which indicated a prevalence of nonmotile cells under prolonged Cr(VI) exposure (data not shown).

Conclusions

The proteome datasets presented here provide an in-depth analysis of the global response of *S. oneidensis* MR-1 to both acute toxic shock and chronic exposure to chromate. Using 2D LC-MS/MS for the proteome measurements, the proteome datasets provided protein expression information on previously unknown proteins and revealed possible post-transcriptional regulation that is not possible to predict by microarray analysis. Under the acute shock conditions, the proteins most commonly up-regulated were involved in iron uptake and assimilation as well as sulfate transport. Many hypothetical proteins were also found to be up-regulated in response to acute chromate exposure. In addition, a putative operon containing three genes (*so3585-so3587*) was detected up-regulated at the transcript and protein levels primarily under chromate exposure.

After growth in the presence of chromium for 24-h, the differentially expressed proteins identified from *S. oneidensis* were unique in comparison to the acute shock proteome dataset. Proteins corresponding to structural components and hypothetical proteins encoded within an integrated lambda-like phage (LamdaSo) were identified not

only highly up-regulated at the time of proteome sampling in the chromate-exposed culture, but was primarily detected in this sample as well. A similar response was found for this bacterium after exposure to UV radiation [192]. The activation of the lysogenic phage may be the lethal cause that results from prolonged exposure to chromate. Since the phage is activated after transformation of Cr(VI) to presumably Cr(III), understanding cellular response in the presence of Cr(III) may not be possible without first inactivating the lysogenic phage. The use of global whole-cell proteomics allowed the detection and characterization of these novel responses to chromate by *S. oneidensis*.

Since the purpose is to gain global understanding of the Cr(VI) response of *S. oneidensis* for the purposes of bioremediation, we chose to explore environmentally relevant scenarios of Cr(VI) exposure. Therefore, the two proteome studies discussed here provided insight into both initial and long-term Cr(VI) exposure. We found that after prolonged exposure, a high level of stress was demonstrated that may be detrimental to a long-term bioremediation strategy; however, without this work, the stress response would have remained unknown. Due to the large differences between the two proteomes, this resulted in the exploration of the Cr(VI) dosage response, another relevant scenario.

Chapter 4

Dosage-Dependent Proteome Response of *Shewanella oneidensis* MR-1 to Acute

Chromate Challenge

The work presented below has been published as the following journal article and adapted from the text

Melissa R. Thompson, Nathan C. VerBerkmoes, Karuna Chourey, Manesh Shah, Dorothea K. Thompson, and Robert L. Hettich. Dosage-Dependent Proteome Response of *Shewanella oneidensis* MR-1 to Acute Chromate Challenge. *Journal of Proteome Research*, 2007; 6, 1745-1757. *Sample preparation, LCQ and LTQ measurements, and data analysis were performed by Melissa R. Thompson. Supplemental material can be found at http://compbio.ornl.gov/shewanella_metal_stress/dosage.*

Introduction

Technological advances in the area of “shotgun” proteomics have substantially improved the quantity and quality of data that can be derived from diverse biological systems, including molecular descriptions of the growth states and environmental perturbation responses of various bacteria. Areas that have seen improvements include liquid chromatographic separation of peptides, new and improved mass spectrometers, and advanced computational approaches to search the resulting raw data files. In 2001, Washburn *et al* [33] first introduced multidimensional protein identification technology (MudPIT), in which a multiphasic column was used to separate peptides online for direct injection into a nanoelectrospray mass spectrometer. This design was enhanced by McDonald *et al* [166] in 2002 to incorporate a biphasic column that is connected upstream from the reverse-phase analytical column. These improvements in online peptide separation have greatly improved sample handling and have reduced the

complexity of ions injected into the mass spectrometer, thereby allowing more ions to be analyzed by MS/MS. Over the past 8 years, the quadrupole ion trap (QIT) has been the prevalent choice of instrumentation for this experimental approach [207-212]. However, advancements in instrumentation (i.e., the new linear trapping quadrupole LTQ [30] and LTQ-Orbitrap [23]) that can acquire full MS and MS/MS scans on greatly reduced time scales have become just as critical as improvements made in peptide separation. All of these improvements have led to a greater depth of proteome coverage, yielding confident identifications of greater than 2000 proteins on a routine basis for many microbes [63, 65, 147, 158].

These technological advances have enabled the elucidation of microbial proteomes at a remarkably deep level, now permitting the extensive examination of how a microbe adjusts its molecular machinery as a function of diverse growth conditions. The focus of this work was to exploit this technology to characterize for the first time the dosage-dependent changes in the proteome of the metal-reducing bacterium *Shewanella oneidensis* MR-1 in response to chromate insult. Hexavalent chromium [Cr(VI)], in the form of chromate (CrO_4^{2-}) or dichromate ($\text{Cr}_2\text{O}_7^{2-}$), is a widespread environmental contaminant due to its prevalent use in industrial and defense applications [121]. Microbially-catalyzed transformation of soluble Cr(VI) to less soluble Cr(III) hydroxides has been proposed as a potentially economical and environmentally friendly remediation strategy for Cr(VI)-contaminated subsurface environments [213]. Cr(III) hydroxides, for example, exhibit substantially reduced mobility, bioavailability, and toxicity. Species of the γ -proteobacterial genus *Shewanella* have been shown to mediate both direct

enzymatic [86, 133, 134] and indirect chemical reduction [131, 136, 137] of Cr(VI) to Cr(III), thus suggesting their potential utility for *in situ* bioremediation.

Under aerobic growth conditions, *S. oneidensis* preferentially uses oxygen as its terminal electron acceptor. Chromate reduction by this organism has been reported under both aerobic and anaerobic conditions [86, 133, 135, 146]. Although *S. oneidensis* can generate energy for growth via respiratory-linked reduction of certain metals such as Fe(III) and Mn(IV) [79], there have been no reports to date of this organism's growth on Cr(VI) as a sole terminal electron acceptor under anaerobic respiratory conditions [132]. Current evidence suggests that Cr(VI) reduction mechanisms are likely associated with bacterial electron transport systems [86, 214] and that Cr(VI) reduction is dependent on the physiological state of the culture [133], but the details describing these mechanisms and the molecular components themselves are not understood in *S. oneidensis*. Thus, the prediction and assessment of bioremediation performance is a difficult task, being compounded by the lack of fundamental knowledge on the molecular basis and regulation underlying bacterial metal reduction and cellular responses to metal toxicity.

This research builds upon and extends a previous study probing the temporal transcriptomic and proteomic changes in *S. oneidensis* MR-1 in response to a single exposure concentration of chromate [147] by investigating the Cr(VI) dosage-dependent proteome response. The lethal dosage for *S. oneidensis* was found to be around 2 mM; however, at dosages of 0.5 and 1 mM, a reduction in growth of 50 and 66%, respectively, was observed [147]. Given the likelihood that microorganisms are exposed to a gradient of chromate levels in contaminated local microenvironments, it is important to understand changes in the molecular response to metal toxicity that are dependent on

concentration and, thus, gain insight into the level of resistance exhibited by a bacterium. The objective of this study was to identify proteins involved in the general response of the bacterium to chromate insult, in particular those that demonstrate a dosage-dependent alteration in abundance level. The majority of proteins synthesized by this bacterium were expected to remain relatively constant, as this is the vital machinery that enables cell growth and survival maintenance. However, a subset of proteins that play important roles in the stress response to chromate and ultimately for cell survival in toxic metal environments should exhibit measurable changes in abundance as a function of growth conditions, and thus would provide key information about how this microbe copes with acute exposures to Cr(VI).

A component of this study was to evaluate the differences between the datasets obtained by the more conventional quadrupole ion trap technology as compared to the newer linear trapping quadrupole instrumentation. These technological advances have the potential to increase the correlation of transcriptome and proteome measurements due to improved dynamic range of the LTQ, thereby increasing proteome coverage and improving confidence in the interpretation of results derived from global high-throughput techniques.

Materials and Methods

Preparation of Proteomes for HPLC-MS/MS Analysis

Four independent cultures of wild-type *S. oneidensis* MR-1 were grown in Luria-Bertani (LB) medium (pH 7.2) at 30 °C under aerobic conditions. Aerobic conditions were maintained in batch cultures by growing both the control and treatment samples in the same-size Erlenmeyer flasks (with sufficient headspace) and continuously aerating

each culture by vigorous shaking at 200 rpm. Batch cultures were grown to mid-exponential phase (OD_{600} , 0.5), followed by the addition of potassium chromate (K_2CrO_4) to three of the four cultures at a final concentration of 0.3, 0.5, or 1.0 mM, respectively. The culture receiving no chromate served as the control and was grown in parallel with the treated cultures. Thirty minutes after chromate exposure, cells were harvested and lysed by sonication, as described in Chapter 2. On the basis of initial growth response studies of *S. oneidensis* [147], the decision for sampling the resulting proteome during the initial transitional period (i.e., 30 min post-shock) from logarithmic growth toward adaptation to chromate would reveal key regulatory and structural proteins that respond to the initial signs of chromate stress (see Supplemental Figure S1, Supporting Information). Each of the resulting four proteome samples (control and 0.3, 0.5, or 1.0 mM chromate) were separated into two fractions (crude/soluble and membrane) by high-speed centrifugation [147] and quantitated using BCA analysis (Pierce, Rockford, IL). Approximately 2 mg of each proteome fraction was then digested with trypsin, desalted and stored at $-80\text{ }^{\circ}\text{C}$ until HPLC-MS/MS analysis.

LC-MS/MS Analysis

Both the soluble and membrane-associated proteome fractions of the chromate-treated and control samples were analyzed in duplicate via two-dimensional LC-MS/MS on both an LCQ Deca XP three-dimensional ion trap mass spectrometer (Thermo Electron) and an LTQ linear trapping quadrupole mass spectrometer (Thermo Electron). Both instruments were coupled to identical Ultimate HPLC pumps (LC Packings; a division of Dionex, San Francisco, CA), each of which had an initial flow rate of $\sim 100\text{ }\mu\text{L/min}$ that was split precolumn to obtain a flow rate of $\sim 300\text{ nL/min}$ at the nanospray

tip. See Chapter 2 for details of chromatographic separation of peptides for both instrument platforms. The multiphasic column system was positioned in front of the LCQ or LTQ on a nanospray source (ThermoFinnigan). All samples were analyzed via a 24-h 12-step 2-D analysis consisting of increasing concentration (0–500 mM) salt pulses of ammonium acetate followed by 2-h reverse phase gradients (see Chapter 2 for details). During the entire chromatographic process, the LTQ was operated in a data-dependent MS/MS mode detailed in Chapter 2.

Proteome Bioinformatics

The *S. oneidensis* MR-1 protein database used in all MS/MS spectra searches consisted of 4798 open reading frames that were downloaded from the J. Craig Venter Institute (formerly TIGR) and concatenated with a list of common contaminants (trypsin, keratin, etc.); the entire database can be downloaded from compbio.ornl.gov/shewanella_metal_stress/dosage/databases/. All MS/MS spectra were searched with the Sequest Algorithm [39] as detailed in Chapter 2. The Xcorr values used here have been tested in a rigorous manner in the laboratory and typically give a maximum false positive rate of 1-2% for both bacterial isolates [184] and simple microbial communities [65]. All of the resulting DTASelect files from both the LCQ and LTQ datasets are available on the analysis page under the corresponding dataset and are filtered at 1 and 2 peptides per protein. Spectra identified for each peptide can be viewed by clicking on the spectral number (first column, labeled by filename) in the html version of the DTASelect files. The algorithm Contrast [171] was used to compare DTASelect files and all of the resulting files are also found on the page. Although there are a number of large-scale proteomics studies describing *S. oneidensis* MR-1 under various growth conditions, the

availability and accessibility of the entire datasets to the general scientific community is limited. This precludes direct comparisons of the large dataset across different laboratories. To assess the false identification rate of both the LTQ and LCQ, a database consisting of the protein sequences in reverse as well as the forward protein sequences was created. The 1 mM Cr(VI) dataset from each instrument was searched against this database to determine the false identification rate of the filtering levels used in this study and the results were calculated according to the equation presented in ref [185]. Results in the form of DTASelect files are found at compbio.ornl.gov/shewanella_metal_stress/dosage/.

Label free quantitation was employed to determine those proteins that were differentially expressed under the Cr(VI) dosage conditions with respect to the control sample. The criteria for label free quantitation are measurable differences in percent sequence coverage, peptide count, and spectral count, where two of the three criteria must be met for a protein to be identified as differentially expressed (see Chapter 2 for details). The use of more stringent criteria for the LTQ is due to the increase in the number of spectra acquired and identified. The increase in the amount of spectra acquired results in a plateauing effect in determination of differential expression for many moderately abundant proteins as discussed below.

Results and Discussion

Global Proteome Analysis

A total of 2406 out of 4931 predicted proteins from the annotation provided by TIGR were confidently identified with at least 2 peptides per protein using both the LCQ and the LTQ. This constitutes 49% of the predicted *S. oneidensis* MR-1 proteome and

represents the largest proteome characterization of this bacterium to date from this laboratory [147, 158]. The total number of proteins identified under each treatment condition for the two instruments is provided in Table 4.1. With the LTQ mass spectrometer, confident identification of 1883 proteins in the control sample was achieved, with a comparable amount detected in each of the dosage samples. By contrast, the LCQ instrument yielded 809 proteins for the control, with comparable amounts in each of the dosage samples.

The total number of proteins identified was organized into a list with the percent sequence coverage, functional category, isoelectric point (pI), and molecular weight information included (Supplemental Table S1, Supporting Information). With respect to these factors, there were no major biases between the observed proteome in this study and the predicted proteome. Proteins detected under the three chromate dosage conditions and the control condition are organized according to percent sequence coverage (the total percent of the protein sequence identified), peptide count (the number of peptides identified for a given protein), and spectral count (the number of spectra identified for a given protein) and can be accessed in Supplemental Table S2 (see Supporting Information) for both the LCQ and LTQ datasets.

Biological variability with respect to independently grown cultures of *S. oneidensis* was assessed to determine if perturbation of the environment reveals a culture-dependent proteome. Independently grown cultures that were sampled previously [147] for proteomics analysis were compared to the current datasets, and gave very similar results. These previous samples included a wild-type control culture grown in parallel with a 1 mM chromate-treated culture that was harvested 45 min after addition of the

Table 4.1. Global Proteome Analysis of Chromate Dose on *S. oneidensis*.

Condition	Instrument ^a	Proteins Identified 1 pep ^b	Proteins Identified 2 pep ^c	Average Sequence Coverage ^d	Reproducibility
Control	LCQ	1263	809	26.0%	78.6%
0.3 mM K ₂ CrO ₄	LCQ	1267	835	30.0%	72.8%
0.5 mM K ₂ CrO ₄	LCQ	1185	716	31.1%	81.8%
1.0 mM K ₂ CrO ₄	LCQ	1307	879	29.1%	74.5%
Control	LTQ	2574	1883	35.6%	79.4%
0.3 mM K ₂ CrO ₄	LTQ	2423	1752	38.9%	70.5%
0.5 mM K ₂ CrO ₄	LTQ	2425	1807	37.2%	81.3%
1.0 mM K ₂ CrO ₄	LTQ	2624	1953	37.5%	79.8%
Total Non-Redundant		3239	2406		

^aLCQ: Thermo Electron NanoES-quadrupole ion trap. LTQ: Thermo Electron NanoES-linear trapping quadrupole. ^bNon-redundant proteins identified with at least 1 peptide per protein. ^cNon-redundant proteins identified with at least 2 peptides per protein. ^dAverage sequence coverage with at least 2 peptides per protein.

metal. For these two datasets, the reproducibility at the protein level is 79% for the 30 min 1 mM chromate dosage versus the 45 min 1 mM acute shock sample and for the control samples is 78%. Therefore, even though there were differences in the chromate exposure times for these two separate experiments, there does not seem to be much measurable biological variation, even when chromate exposure is 15 min longer in the case of Brown *et al* [147].

Instrumentation Effects on Proteome Characterization

The LCQ and LTQ datasets were compared to determine differences in informational content. Under the control conditions (no added chromate), both instruments together identified a common list of 803 proteins at the two-peptide level. A total of 5 proteins were uniquely identified using the LCQ, whereas approximately 1100 proteins were only identified using the LTQ. The 5 unique LCQ proteins were identified with only 2 peptides per protein. For the 0.3 and 0.5 mM chromate-treated cells, 876 and 777 proteins identified were common between the two instruments, respectively; a total of 5 proteins were unique to the LCQ under these dosages, whereas almost 1000 proteins were unique to the LTQ. The unique LCQ proteins were investigated further and once again were found to consist of only 2 or 3 peptides identified for a given protein. A different trend was observed for the 1 mM chromate-treated samples compared to the other three conditions. All proteins identified using the LCQ were also identified using the LTQ mass spectrometer. Overall, 99% of the proteins identified using the LCQ were also identified when using the LTQ, indicating that the performance of these two instruments is similar; however, the LTQ offered enhanced performance in terms of dynamic range, as discussed below.

Because of its slower scanning speed, the LCQ mass spectrometer is not able to trigger and conduct MS/MS on as many ions as the LTQ during a chromatographic run, thus resulting in a lower number of total protein identifications (for the LCQ). The capability of the LTQ [30] instrument for not only higher duty cycle experiments but also a greater trapping efficiency of ions relative to the LCQ is already making LTQ technology the high-throughput instrumentation of choice for shotgun proteomics measurements. This improved ion trapping efficiency is evident by the triggering of MS/MS acquisitions on low abundance ions that would be missed by the LCQ measurements (see Figure 4.1). Due to the increased dynamic range offered by the LTQ linear trapping quadrupole, only the LTQ-derived datasets were analyzed in greater detail in the following discussion sections.

The increased scanning speed of the LTQ instrument results in a concomitant increase in the number of false positive identifications of peptides [32, 215]. Generation of more spectra with the LTQ leads to more possible matches to spectra that are considered “noise” and do not contain “true” peptide spectra. The 1 mM Cr(VI) dataset was used to test the false identification rate of both the LCQ and LTQ. These datasets were searched against a protein database containing the forward sequence of the protein database (see above) with the reverse sequences of the database concatenated to the end. The false identification rates for the duplicate analyses were averaged to give the following results for each instrumentation platform (Table 4.2). For the LCQ, a protein false identification rate of 10.5% was identified for the 1 peptide dataset and 0.1% for a 2 peptide requirement. For the LTQ, the protein false identification rate at the 1 peptide level was 33.3% and at the 2 peptide level 4.8%. As expected, the false identification

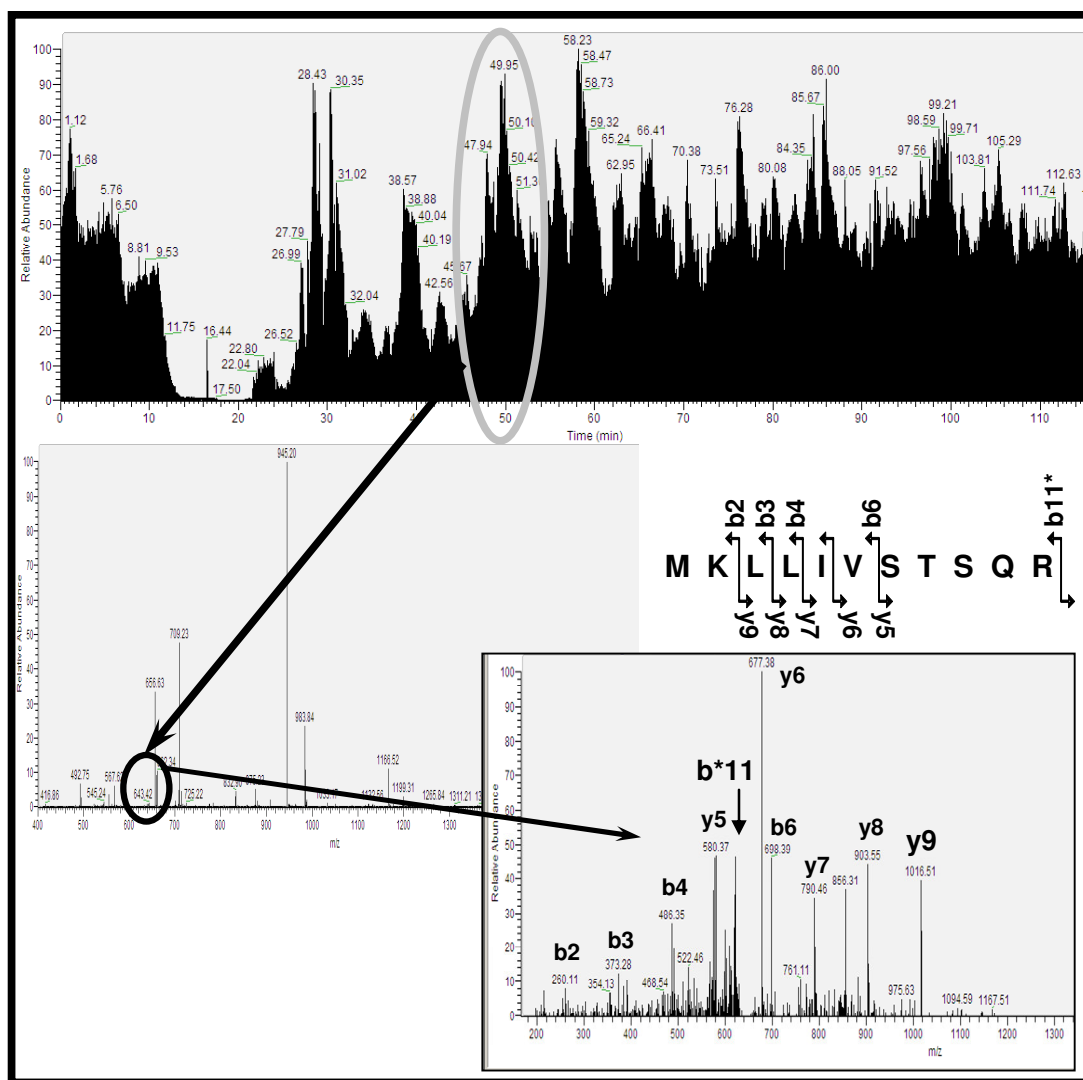


Figure 4.1. MS/MS from a peptide of SO3585 identified in the 0.3 mM dosage.

The base peak chromatogram (top figure) from the 0.3 mM chromate sample illustrates a full LTQ-MS scan that contains a peak of very low abundance at m/z 638.8 (middle figure). This peak was subsequently isolated and fragmented, giving the MS/MS spectrum (bottom figure), which contains the sequence of a peptide from the SO3585 protein that was identified as up-regulated at the 0.5 mM and 1 mM chromate levels.

Table 4.2. False Peptide and Protein Identifications with a LCQ and a LTQ

Instrument ^a	Requirement ^b	Peptide Identifications			Protein Identifications		
		False Unique ^c	Total Unique ^d	Rate	False Ids ^e	Total Ids ^f	Rate
LCQ Run 1	1 peptide	55	6041	1.8%	58	1157	10.0%
	2 peptide	0	5666	0.0%	0	736	0.0%
LCQ Run 2	1 peptide	65	6912	1.8%	73	1311	11.1%
	2 peptide	2	6492	0.0%	1	835	0.2%
LTQ Run 1	1 peptide	428	22014	3.8%	434	2735	31.7%
	2 peptide	68	21153	0.6%	34	1808	3.8%
LTQ Run 2	1 peptide	527	22476	4.6%	498	2854	34.8%
	2 peptide	108	21531	1.0%	53	1844	5.8%

^a1 mM Cr(VI) Dataset on both instrumentation platforms. ^bRequirement is whether

protein identification is based on at least 1 or 2 peptides for a given protein, respectively.

^cFalse Unique refers to the number of peptides identified using protein sequences from

the reversed protein database. ^dTotal Unique is the total number of unique peptides

identified using the forward and reverse protein databases. ^eFalse IDs are the proteins

identified from the reverse database. ^fTotal IDs are the total number of proteins identified

from the forward and reverse databases.

LTQ is higher, especially at the 1 peptide level; however, with the 2 peptide requirement, rate for the the rate is low enough that ~95% of the protein identifications are true. Therefore, using more stringent filtering criteria is necessary in order to minimize the false positive identifications for LTQ datasets.

In order to further understand the contribution of peptides to protein identification, the distribution of the number of peptides identified for a given protein was calculated using the Control dataset as an example. A protein identification is only made if at least two peptides are identified from one of the two MS analyses. The protein identifications made by two replicate MS experiments comprising two peptides were 260 (~14%) of the total proteins identified for the Control condition. A total of 75 (~4%) proteins were identified with three peptides, while 103 (~5%) proteins were found with four peptides. A majority of the protein identifications comprise at least five peptide identifications with 1443 (~77%) proteins. Therefore, the false identification rate is maintained at a reasonable level with less than 30% of the protein identifications arising from proteins identified with four or fewer peptides.

Semiquantitation was investigated on both the LCQ and LTQ datasets using the criteria described in Chapter 2. Results generated using both instrumentation platforms are provided in Supplemental Table S3 (see Supporting Information). Although there is reasonable agreement between the LCQ and LTQ datasets for the three chromatate dosage samples, the different depth of protein identification and the distinct semiquantification criteria for each MS platform made it difficult to directly compare the results. This is especially noticeable for the lower abundance proteins; they are likely to be missed in the LCQ analysis but found in the LTQ measurements. Thus, whereas the LCQ

measurements often reveal large semiquantitative differences, such as proteins completely absent in the control sample but present with a few peptides detected in a dosage sample, the deeper measurements possible with the LTQ often reveal the presence of the protein in both control and sample, with some differences in abundance. At the other end of the spectrum, the most abundant proteins also are somewhat difficult to quantify with the LTQ, because at least one of the semiquantitative metrics (percent sequence coverage) “saturates”, precluding determination of differences between samples. Thus, these factors must be taken into account in the determination of semiquantification criteria for LTQ measurements. Because of the increased depth of proteome coverage achieved by the LTQ measurements, all semiquantification determinations and discussions were focused on these datasets.

LTQ-Based Global Proteome Characterization

The proteins identified using the LTQ were organized according to the 18 functional category assignments given in TIGR’s Comprehensive Microbial Resource (www.tigr.org) and were grouped according to their annotated subcellular roles (Figure 4.2). The functional categories of amino acid biosynthesis; biosynthesis of cofactors, prosthetic groups, and carriers; cell envelope; cellular processes; DNA metabolism; energy metabolism; fatty acid and phospholipid metabolism; and protein fate were all represented with at least 50% of their protein members identified for the control and each Cr(VI) dosage sample. Furthermore, in the functional categories of protein synthesis, purines/pyrimidines/nucleosides/nucleotides, and transcription, identification of 80% of the members was achieved for each condition.

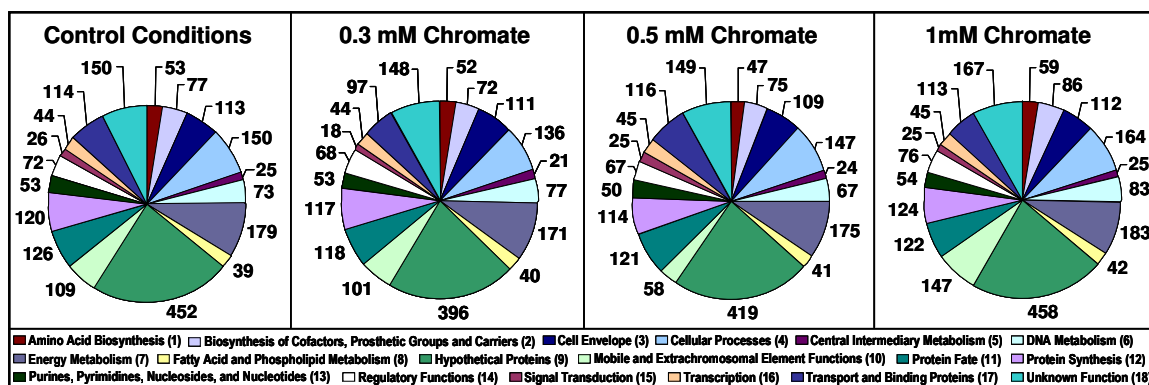


Figure 4.2 Functional category distribution for each dosage and the control condition. The total number of non-redundant proteins identified by LTQ-MS under each dosage condition organized according to the functional categories assigned by TIGR. The number of proteins identified under each functional category is labeled by the slice in which it is located for each dosage condition and the control condition.

The Venn diagrams in Figure 4.3 illustrate the relationship of the proteins identified under the three chromate dosage treatments: 1,535 proteins were identified under all three dosage conditions using the LTQ, while relatively few proteins (ranging from 86 to 231 proteins) were unique to a specific chromate dose, thus suggesting that the majority of the proteome was not measurably altered in response to acute chromate exposure. However, as detailed below, the actual proteins identified as putatively differentially expressed for each dosage treatment are for the most part unique for a given dose.

Dosage-Dependent Response of Differentially Expressed Proteins

The information in Supplemental Table S2 (see Supporting Information) (percent sequence coverage, peptide count, and spectral count) was used to identify those proteins from the three dosage treatments that were differentially expressed when compared to the control sample (as detailed in Chapter 2). Semiquantitation or label free quantitation is important in cases where other methods of quantitation like isotope coded affinity tags (ICAT) [177] or metabolic labeling [175] are not feasible for sample characterization. The semi-quantitation method relies on the average between the two sample runs of the same treatment, as compared to the average of the two runs of the control condition (Table 4.1). A previous study by our group [184] sampled technical replications from six growth conditions in *Rhodopseudomonas palustris* and established that a 70% measurement of reproducibility in replicated samples was readily and consistently achievable under optimal instrument conditions. This criterion has become the standard in our laboratories and has enabled more confident determination of proteins changing

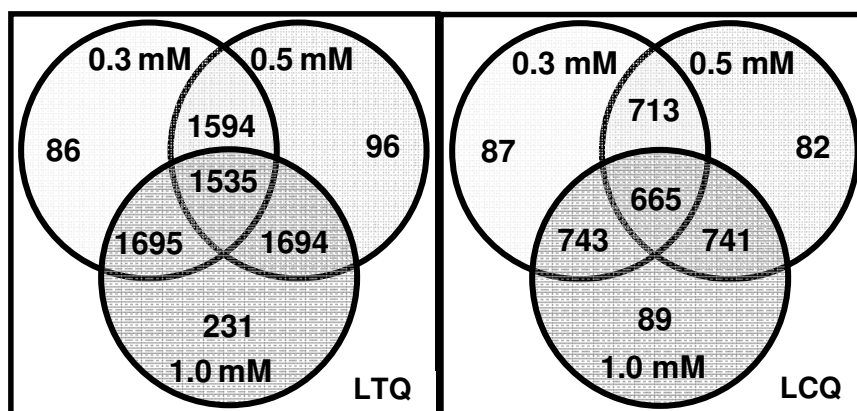


Figure 4.3. Venn diagrams of dosage response proteome samples for the LTQ and LCQ.

The Venn diagram on the left represents results using an LTQ mass spectrometer. The Venn diagram on the right depicts results using an LCQ mass spectrometer. The top left circle is the 0.3 mM K_2CrO_4 dosage sample, the top right circle is the 0.5 mM, and the bottom circle is the 1 mM. The numbers are the total number of proteins shared between the respective samples. For instance, 1535 proteins were identified in all three dosage conditions for the LTQ and 665 proteins were identified in all three doses with the LCQ.

abundance as a result of different biological growth conditions as opposed to varying sampling and instrumentation fluctuations.

A total of 14 proteins were up-regulated under all three Cr(VI) doses, with representatives in bold in Tables 4.3-4.5. In comparing the 0.3 mM chromate dosage with the other two higher doses, this dose appears to elicit a unique response in which only three up-regulated proteins are shared with the 0.5 mM dose. The datasets for the 0.5 and 1 mM chromate doses had 13 up-regulated proteins in common, suggesting that the toxicity of these two Cr(VI) concentrations may induce a similar molecular response. A greater variation was observed among the various chromate doses for proteins identified as down-regulated in contrast to up-regulated proteins, with only 10 proteins exhibiting decreased abundance levels across all three metal treatments. The 0.3 and 0.5 mM dosages were most similar with seven additional down-regulated proteins shared between the two; the down-regulated protein profiles for doses 0.3 and 1 mM shared a total of five proteins. No additional proteins were identified that were solely shared between the 0.5 and 1 mM doses, indicating that down-regulated protein expression in response to chromate was much more varied and showed more instances of dose-dependent patterns compared to the up-regulated expression profiles. Proteins with annotated functions in transport and binding consistently displayed up-regulation, with representatives over the treatments remaining constant as well. For down-regulated proteins, all three dosages displayed a large number of energy metabolism proteins with reduced expression. However, only a small subset of the proteins are conserved over the three treatment conditions. In addition, the representative functional categories varied

Table 4.3. Selected Differentially Expressed Proteins Identified after Treatment with 0.3 mM K₂CrO₄^a

Locus	0.3 mM Average			Control Condition Average			Functional Category ^b	Description
	% coverage	peptide	spectra	% coverage	peptide	spectra		
Up-regulated								
SO1190	69.3%	25	75.5	48.0%	11	19	9	conserved hypothetical protein
SO1482	78.2%	63.5	192.5	52.2%	26	35	17	TonB-dependent receptor, putative
SO2426	31.7%	6.5	11	0.0%	0	0	15	DNA-binding response regulator
SO3030	43.3%	20.5	37.5	4.0%	1	2	17	siderophore biosynthesis protein (alcA)
SO3033	50.6%	38	112	27.5%	15	23	17	ferric alcaligin siderophore receptor sulfate ABC transporter, periplasmic sulfate-binding protein (cysP)
SO3599	56.2%	16.5	49.5	42.0%	13	18	17	conserved hypothetical protein
SO3667	91.4%	24	88	25.2%	4	4	9	heme transport protein (hugA)
SO3669	76.1%	47	269	11.2%	4	4	17	TonB-dependent receptor, putative
SO3914	62.4%	56	199.5	44.5%	30	49	17	TonB-dependent receptor, putative
SO4077	42.9%	23.5	39.5	9.6%	4	5	17	iron-regulated outer membrane virulence protein (irgA)
SO4523	65.8%	42.5	146.5	51.4%	28	47	17	TonB-dependent receptor, putative
SO4743	74.6%	66	223	67.1%	46	100	17	conserved hypothetical protein
Down-regulated								
SO0004	24.6%	9	13.5	36.5%	23	42.5	3	inner membrane protein, 60 kDa
SO0848	45.2%	31.5	45.5	66.4%	68	186.5	7	periplasmic nitrate reductase (napA)
SO0947	28.0%	9.5	12.5	46.1%	19.5	32	16	ATP-dependent RNA helicase SrmB (srmB)
SO0970	52.5%	27.5	51.5	55.9%	38.5	99	7	fumarate reductase flavoprotein subunit precursor
SO1425	36.9%	9	12	45.2%	22	30.5	9	hypothetical protein
SO1490	30.7%	7.5	11.5	55.9%	21	43	7	alcohol dehydrogenase II (adhB)
SO1519	34.7%	18.5	23.5	54.9%	33.5	63	7	iron-sulfur cluster-binding protein
SO1677	68.6%	22	60.5	74.9%	32.5	112.5	8	acetyl-CoA acetyltransferase (atoB)
SO1679	36.6%	9.5	15.5	53.2%	18.5	28.5	8	acyl-CoA dehydrogenase family protein
SO1776	11.6%	4	4	40.0%	30.5	35.5	3	outer membrane protein precursor MtrB (mtrB)

Table 4.3. Continued

Locus	0.3 mM Average			Control Condition Average			Functional Category ^b	Description
	% coverage	peptide	spectra	% coverage	peptide	spectra		
SO1778	28.2%	15	25.5	43.3%	39	80	7	decaheme cytochrome c (omcB)
SO2606	19.0%	11	16	51.6%	36.5	55	18	PqiB family protein
SO2929	45.6%	15.5	22	69.6%	31	56	9	hypothetical protein
SO4053	9.5%	3.5	3.5	38.4%	18	25.5	4	methyl-accepting chemotaxis protein
SO4513	8.0%	6	8	42.3%	42	67.5	7	formate dehydrogenase, alpha subunit

^aProteins in bold are found differentially expressed under all three Cr(VI) dosage conditions. ^bFunctional Category number

refers to the designation in Figure 4.2 as an abbreviation for the category name.

Table 4.4. Selected Differentially Expressed Proteins Identified after Treatment with 0.5 mM K₂CrO₄^a

Locus	0.5 mM Average			Control Condition Average			Functional Category ^b	Description
	% coverage	peptide	spectra	% coverage	peptide	spectra		
Up-regulated								
SO0578	51.7%	36	68	29.6%	17	29	9	hypothetical protein
SO1190	84.0%	33	118	48.0%	11	19	9	conserved hypothetical protein
SO1482	71.0%	69	201	52.2%	26	35	17	TonB-dependent receptor, putative
SO2426	22.4%	5	18	0.0%	0	0	15	DNA-binding response regulator
SO2903	92.1%	59	617	82.3%	36	150	1	cysteine synthase A (cysK)
SO3030	48.7%	22	47	4.0%	1	2	17	siderophore biosynthesis protein (alcA)
SO3033	55.0%	38	100	27.5%	15	23	17	ferric alcaligin siderophore receptor
SO3420	75.8%	23	100	54.4%	9	30	7	cytochrome c
SO3509	40.5%	23	28	17.1%	10	12	7	beta-hexosaminidase b precursor (hex)
SO3585	28.0%	6	8	0.0%	0	0	4	azoreductase, putative
SO3599	80.0%	34	170	42.0%	13	18	17	sulfate ABC transporter, periplasmic sulfate-binding protein (cysP)
SO3667	91.4%	33	281	25.2%	4	4	9	conserved hypothetical protein
SO3669	69.6%	49	228	11.2%	4	4	17	heme transport protein (hugA)
SO3914	61.7%	52	126	44.5%	30	49	17	TonB-dependent receptor, putative
SO4743	74.1%	64	271	67.1%	46	100	17	TonB-dependent receptor, putative
Down-regulated								
SO0441	41.3%	13	27	49.8%	23	70.5	13	phosphoribosylamine--glycine ligase (purD)
SO1185	43.5%	10	28	38.2%	15	57	9	conserved hypothetical protein TIGR00092
SO1519	30.9%	19	27	54.9%	33.5	63	7	iron-sulfur cluster-binding protein
SO1776	17.0%	6	6	40.0%	30.5	35.5	3	outer membrane protein precursor MtrB (mtrB)
SO1853	16.5%	6	7	29.3%	16	25.5	17	ABC transporter, ATP-binding protein
SO2304	38.2%	10	27	47.6%	20.5	45	7	alanine dehydrogenase, authentic point mutation (ald)
SO2590	16.3%	3	3	44.6%	16	23.5	18	GTP-binding protein
SO2929	39.3%	10	14	69.6%	31	56	9	hypothetical protein

Table 4.4. Continued

Locus	0.5 mM Average			Control Condition Average			Functional Category	Description
	% coverage	peptide	spectra	% coverage	peptide	spectra		
SO3783	12.6%	5	7	36.7%	14	16	16	ATP-dependent RNA helicase, DEAD box family
SO3863	50.4%	11	22	68.6%	16.5	41	17	molybdenum ABC transporter, periplasmic
SO4053	13.5%	7	8	38.4%	18	25.5	4	molybdenum-binding protein (modA)
SO4066	20.3%	5	7	64.1%	25	36.5	13	methyl-accepting chemotaxis protein
SO4249	37.1%	6	11	47.1%	13.5	21.5	2	phosphoribosylaminoimidazole-succinocarboxamide synthase, putative
SO4513	19.8%	16	22	42.3%	42	67.5	7	DNA/pantothenate metabolism flavoprotein (dfp)
								formate dehydrogenase, alpha subunit

^aProteins in bold are found differentially expressed under all three Cr(VI) dosage conditions. ^bFunctional Category number

refers to the designation in Figure 4.2 as an abbreviation for the category name.

Table 4.5. Selected Differentially Expressed Proteins Identified after Treatment with 1 mM K₂CrO₄^a

Locus	1.0 mM Average			Control Condition Average			Functional Category ^b	Description
	% coverage	peptide	spectra	% coverage	peptide	spectra		
Up-regulated								
SO0343	48.0%	38	69	20.5%	14	14	7	aconitate hydratase 1 (acnA)
SO0578	49.2%	32	68	29.6%	17	29	9	hypothetical protein
SO1482	70.5%	60	160	52.2%	26	35	17	TonB-dependent receptor, putative
SO2426	32.3%	8	13	0.0%	0	0	15	DNA-binding response regulator
SO2903	90.7%	54	482	82.3%	36	150	1	cysteine synthase A (cysK)
SO2912	62.7%	54	115	36.8%	26	57	7	formate acetyltransferase (pflB)
SO3030	62.0%	30	77	4.0%	1	2	17	siderophore biosynthesis protein (alcA)
SO3033	57.0%	46	158	27.5%	15	23	17	ferric alcaligin siderophore receptor
SO3420	69.8%	20	66	54.4%	9	30	7	cytochrome c
SO3577	58.8%	66	167	34.0%	33	51	11	clpB protein (clpB)
SO3585	42.7%	10	32	0.0%	0	0	4	azoreductase, putative
SO3599	81.4%	35	107	42.0%	13	18	17	sulfate ABC transporter, periplasmic sulfate-binding protein (cysP)
SO3667	92.2%	34	241	25.2%	4	4	9	conserved hypothetical protein
SO3669	72.4%	54	199	11.2%	4	4	17	heme transport protein (hugA)
SO3737	67.0%	52	112	26.1%	14	20	5	sulfite reductase (NADPH) hemoprotein beta-component (cysI)
SO3914	56.5%	53	217	44.5%	30	49	17	TonB-dependent receptor, putative
SO4215	65.9%	31	90	45.9%	16	36	4	cell division protein FtsZ (ftsZ)
SO4743	69.6%	61	266	67.1%	46	100	17	TonB-dependent receptor, putative
SOA0048	45.6%	31	49	23.7%	12	15	11	prolyl oligopeptidase family protein
Down-regulated								
SO0029	20.8%	7	12.5	30.7%	15	29	17	potassium uptake protein TrkA (trkA)
SO0130	10.0%	4.5	5	29.6%	21	28	11	protease, putative
SO0398	6.1%	2	2	28.5%	13	19	7	fumarate reductase flavoprotein subunit (frdA)

Table 4.5. Continued

Locus	1.0 mM Average			Control Condition Average			Functional Category ^b	Description
	% coverage	peptide	spectra	% coverage	peptide	spectra		
SO0848	41.9%	34	60.5	66.4%	68	187	7	periplasmic nitrate reductase (napA)
SO0902	24.8%	6.5	8	39.0%	16	22	7	NADH:ubiquinone oxidoreductase, Na translocating, alpha subunit (nqrA-1)
SO0907	11.9%	5	7	32.3%	15	19	7	NADH:ubiquinone oxidoreductase, Na translocating, beta subunit (nqrF-1)
SO1066	14.6%	6.5	6.5	36.9%	20	24	6	extracellular nuclease
SO1424	23.0%	10	12.5	37.3%	25	29	9	hypothetical protein
SO1776	9.0%	4	6	40.0%	31	36	3	outer membrane protein precursor (mtrB)
SO1779	29.4%	17.5	25.5	47.9%	43	81	7	decaheme cytochrome c (omcA)
SO2929	47.8%	14.5	21.5	69.6%	31	56	9	hypothetical protein
								asparagine synthetase, glutamine-hydrolyzing (asnB-2)
SO3175	23.9%	13.5	15	40.3%	27	38	1	
SO4053	9.3%	6	19.5	38.4%	18	26	4	methyl-accepting chemotaxis protein
SO4513	11.7%	8	11	42.3%	42	68	7	formate dehydrogenase, alpha subunit
SOA0141	2.3%	1	1	51.4%	24	36	9	hypothetical protein

^aProteins in bold are found differentially expressed under all three Cr(VI) dosage conditions. ^bFunctional Category number

refers to the designation in Figure 4.2 as an abbreviation for the category name.

over the treatment conditions, with 9-13 categories represented in each dose (as outlined in detail below).

Differentially Expressed Proteins After Exposure to 0.3 mM Cr(VI)

Comparison of the 0.3 mM chromate-treated sample with the control sample revealed a total of 90 proteins that were differentially expressed in response to Cr(VI), with 26 proteins up-regulated and 64 proteins down-regulated. Overall, representatives of transport and binding proteins dominated this subset of up-regulated proteins, with 54% of the proteins annotated as such. Twelve of the proteins had increased abundance levels only in response to the 0.3 mM chromate dose (dose-dependent expression) and included a conserved hypothetical protein (SO0564), TopB (DNA topoisomerase III), and a sigma-54 dependent response regulator (SO4718) (Supplemental Table S3). The functional categories of hypothetical proteins with 12 members and cellular processes (in particular, chemotaxis and motility) with 8 members dominated the list of down-regulated proteins with a total of 12 hypothetical and conserved hypothetical proteins unique to this dose. The large proportion of repressed genes with unassigned cellular functions under this Cr(VI) dosage suggests that much remains to be explored in terms of the molecular response of MR-1 to chromate toxicity. Of the two predominant functional classes, only SO2929 (a hypothetical protein) and SO4053 (a methyl accepting chemotaxis protein) consistently displayed down-regulated expression across all three chromate doses (Tables 4.3-4.5), indicating the greater influence of chromate concentration on the down-regulated protein expression profiles. Interestingly, SO2929 was also identified in another study [216] investigating *S. oneidensis* growth under aerobic conditions.

In response to the 0.3 mM chromate dose, 14 annotated transport and binding proteins were up-regulated and comprised members of a hemin ABC transporter complex (HmuT, HmuV), a heme transport protein (HugA), a TonB-dependent heme receptor (SO1580), siderophore biosynthesis proteins (AlcA, SO3032), a member (CysP) of a sulfate ABC transporter system, four putative TonB-dependent receptors (SO1482, SO3914, SO4077, SO4743), a ferric alcaligin siderophore receptor (SO3033), a ferric vibriobactin receptor (ViuA), and an iron-regulated outer membrane virulence protein (IrgA) (Tables 4.3-4.5 and Supplemental Table S3, Supporting Information). The vast majority of these proteins have predicted functions in iron sequestration and transport, suggesting a possible linkage between chromate stress and iron transport and/or metabolism at the molecular level. Interestingly, 10 of these putative transport and binding proteins (SO1482, AlcA, SO3032, SO3033, CysP, HugA, HmuT, HmuV, SO3914, SO4743) were identified as being up-regulated in response to all three chromate doses (Tables 4.3-4.5 and Supplemental Table S3, Supporting Information), whereas 2 proteins (SO4077, IrgA) displayed a 0.3 mM chromate dose-dependent up-regulation (Table 4.3). These proteomic results suggest that the 10 shared transport and binding proteins constitute part of the initial core molecular response to chromate exposure that is induced irrespective of environmental metal concentration. Many of these initial responders are localized to the *S. oneidensis* outer membrane, periplasmic space, and the cytoplasmic membrane, all of which constitute cellular structures or compartments that are immediately impacted by metal stress and other environmental perturbations. SO1580 (a TonB-dependent heme receptor) and SO4516 (ViuA) were identified as being up-regulated upon challenge to 0.3 and 0.5 mM Cr(VI) but not to 1 mM, whereas,

SO3671 (TonB system transport protein ExbB1), SO4652 (sulfate ABC transporter Sbp), and SO4655 (sulfate ABC transporter CysA-2) were basically detected only in cells exposed to the higher Cr(VI) concentrations of 0.5 and 1 mM (Supplemental Table S3, Supporting Information).

Certain proteins with predicted functions in transport and binding demonstrated dose-dependent down-regulation in response to 0.3 mM chromate. For example, two proteins displaying decreased abundance in response to the 0.3 mM chromate dose were SO4598 and SOA0153, members of the CzcA family of heavy metal efflux pumps. However, these proteins were identified at low levels (2-4 peptides) under the other two Cr(VI) doses. In bacteria, efflux pumps are a commonly employed metal resistance mechanism, with both plasmid and chromosomal systems, and active efflux of chromate appears to be a resistance strategy used by some microorganisms [126, 217]. At this point, it is not known what role, if any, efflux pumps are playing in the resistance of *S. oneidensis* MR-1 to chromate stress. Perhaps these efflux pumps (SO4598 and SOA0153) are expressed only at higher (i.e., ≥ 0.3 mM) chromate concentrations or their expression is temporally controlled depending on the levels of accumulated intracellular chromate. More detailed studies are needed to explore this efflux pump system down-regulation, but are beyond the scope of this present study.

In addition, proteins with annotated functions in chemotaxis (SO3052, SO3282, SO4454) and in the assembly of the flagellum (PomB, FliS, FlgH) were down-regulated only in response to the 0.3 mM chromate dose based on our analysis. Two of these down-regulated proteins are the flagellar protein FliS, a chaperone, and the L-ring protein FlgH, a structural component of the flagellar apparatus. FliS is the molecular chaperone

that ensures the prevention of premature folding and polymerization of FliC in the cytosol of the cell [218]. Under low dosage conditions as exhibited here, this protein is down-regulated, but the two encoded flagellum proteins (SO3237 and SO3238), which are structural components of the helical filament that extends outward from the cell, are not differentially expressed under the dosage conditions investigated here. The down-regulation of FliS has implications with respect to cytosolic polymerization of flagellin upon exposure to low doses of chromate. Because assembly and rotation of the flagellum require an investment of energy by the cell, it seems reasonable that MR-1 might divert energy away from the production of flagella to cellular processes more directly involved in metal stress protection and detoxification.

Differentially Expressed Proteins After Exposure to 0.5 mM Cr(VI)

A total of 79 (40 up-regulated and 39 down-regulated) proteins were identified as being differentially expressed in cells challenged with 0.5 mM chromate for 30 min (Table 4.4 and Supplemental Table S3, Supporting Information) relative to the control culture. The up-regulated proteins were distributed over 10 of the 18 functional categories, where the most prevalent category was transport and binding proteins (category 17). Other notable functional categories represented in this dose response included hypothetical and conserved hypothetical proteins, with five members, and the unknown function category, with four members. Transport and binding proteins were represented by 17 members, constituting 44% of the up-regulated proteins in this dose response group, with 12 also showing up-regulated expression under the 0.3 mM dose. Particularly noteworthy was the observation from these global proteomic studies that proteins involved in sulfate transport and sulfur metabolism displayed dose-dependent

up-regulation. In *Pseudomonas fluorescens*, it was shown that chromate acts as a competitive inhibitor for sulfate uptake via sulfate active transport systems [149]. Similarly, it is likely that chromate enters *S. oneidensis* MR-1 cells by energy-dependent sulfate transport mechanisms because of chromate's structural similarity to sulfate [126, 149, 154]. We hypothesize that the increase in abundance of sulfate transporters observed following chromate exposure could be the result of a decrease in intracellular sulfur due to competitive inhibition by chromate.

Challenge with the 0.3 mM dose resulted in the up-regulation of only one protein involved in sulfate transport: SO3599 (sulfate ABC transporter CysP) (Table 4.3). However, in response to 0.5 mM Cr(VI), we observed a substantial expansion in the number of up-regulated proteins detected for the sulfate transport and sulfur metabolism categories, with five additional representatives identified under this higher dose (Table 4.4, Supplemental Table S3). With the exception of SO3602 (CysA-1), six proteins with annotated roles in transport and binding and central intermediary metabolism [SO3599 (CysP), SO3726 (CysN), SO3727 (CysD), SO3738 (CysJ), SO4652 (Sbp), and SO4655 (CysA-2)] were also found to be up-regulated in response to 1 mM Cr(VI) treatment (Tables 4.4, 4.5 and Supplemental Table S3). Three of these proteins are annotated as members of one of two sulfate ABC transporter systems found in the MR-1 genome and are located in gene clusters *so3599-3602* or *so4652-5*. With the reduction of Cr(VI) in the bacterium, the generation of an unstable Cr(V) intermediate produces reactive oxygen species and leads to an increase in oxidative stress[126, 140]. A possible explanation for the increased level of expression observed for certain sulfur metabolism proteins in this proteomic study may be due, in part, to an increased demand for protective thiol-

containing compounds needed for coping with the oxidative stress imposed by sub-toxic metal exposures.

In addition, proteins with predicted functions in stress responses (IbpA) and DNA repair (RecN) showed increased abundance under 0.5 mM Cr(VI), indicating that this dose creates increased oxidative stress in the bacterium. Two proteins, IbpA and RecN, were up-regulated at both the 0.5 and 1 mM Cr(VI) doses, while these same proteins were identified with a comparable number of peptides as the control under 0.3 mM Cr(VI) treatment, indicating no detectable differential expression. However, both proteins exhibited greater abundance levels in response to the 1 mM dose compared to the 0.5 mM dose demonstrating an increased response with dosage. With the 1 mM Cr(VI) dose, both the ATP-dependent ClpA and ClpB proteases were up-regulated. Clp proteases have been shown to be involved in the cellular response to thermal and other types of cellular stress by working in conjunction with the chaperone proteins in *Escherichia coli* [219]. In addition, the expression of a putative azoreductase (SO3585), which is predicted to play a role in cellular detoxification, was detected only under chromate treatment, with an average of ~28 and ~43 % sequence coverage identified under 0.5 and 1 mM Cr(VI), respectively. However, under the 0.3 mM dose treatment, SO3585 was not identified in the two analytical replicates, suggesting that this protein may be involved in metal detoxification mechanisms at higher chromate doses. The increased expression levels of general stress response proteins, DNA repair proteins, and SO3585 indicate an elevated response to the Cr(VI) stress in the growth medium.

Three members of the functional category energy metabolism were identified at a higher abundance level after exposing *S. oneidensis* to chromate. One member (PrpC, a

methylocitrate synthase) is up-regulated under all three dosage conditions. The second protein, Hex beta-hexosaminidase b precursor (SO3509), is only up-regulated in response to 0.5 mM chromate (Table 4.4), whereas SO3420 (cytochrome c) demonstrates increased abundance at higher levels of chromate (Tables 4.4 and 4.5). This cytochrome c does not change its abundance under the control condition or the 0.3 mM chromate dose, with approximately 10 peptides identified under both conditions. However, at a dosage of 0.5 and 1 mM chromate, the number of peptides identified increased to at least 20 on average for cytochrome c, suggesting the possible involvement of SO3420 in the MR-1 response to chromate stress. Previously, Myers *et al* [86] localized Cr(VI) reductase activity to the cytoplasmic membrane of anaerobically grown *S. oneidensis*. They concluded the possible involvement of cytochromes in the reductase activity, which is not inhibited by O₂. Also, Lovely and Phillips [214] identified the cytochrome c₃ of *Desulfovibrio vulgaris*, a member of the δ -proteobacteria, as a Cr(VI) reductase. Both studies either implicated or demonstrated the involvement of cytochromes in Cr(VI) reduction.

Proteins identified as down-regulated using our semi-quantitation method totaled 39 after cells were exposed to 0.5 mM chromate for 30 min, with the most dominant functional category being energy metabolism (category 7). Most of the 8 energy metabolism proteins showing differential expression were annotated as dehydrogenases and reductases (Table 4.4 and Supplemental Table S3, Supporting Information). With the exception of SO2304 and SO3546, all of the energy metabolism proteins down-regulated under the 0.5 mM chromate condition were also down-regulated under the 0.3

mM dose. There appears to be a similar response between the 0.3 mM and 0.5 mM doses; however, as detailed below, this is not the case with the 1 mM dose.

Differentially Expressed Proteins After Exposure to 1 mM Cr(VI)

The proteome response to 1 mM Cr(VI) was characterized by a total of 92 proteins showing differential expression, with 66 proteins up-regulated and 26 proteins down-regulated (Table 4.5 and Supplemental Table S3, Supporting Information). The functional category distribution among up-regulated proteins was similar to that elicited by the 0.3 mM dosage, where all but 5 of the functional categories were represented. There was a bias toward the following functional categories for up-regulated proteins: amino acid biosynthesis (7 proteins); cellular processes (4); central intermediary metabolism (6); energy metabolism (12); hypothetical and conserved hypothetical proteins (5); protein fate (7); and transport and binding proteins (14). The subsets of transport and binding proteins that were differentially expressed in response to the three different chromate doses were very similar. Exposure of cells to 1 mM Cr(VI) resulted in only one protein (SO1072, a putative chitin-binding protein) being unique to this dosage. The other two doses (0.3 and 0.5 mM) have a repertoire of more unique proteins in each category and share two other proteins not identified as up-regulated under the 1 mM chromate dosage (SO1580, a TonB-dependent heme receptor, and ViuA, ferric vibriobactin receptor). The category of amino acid biosynthesis is only represented by 1 member in the other two doses, whereas for the 1 mM Cr(VI)-treated sample there are 7 members identified as up-regulated. This same trend holds true for the functional classes of central intermediary metabolism, energy metabolism, and protein fate, which only

have up to 3 members in the other two Cr(VI) doses and 6-12 members with the 1 mM dose.

Four proteins were identified as being up-regulated under the 1 mM dose and annotated as involved in cellular processes. One of these proteins, a putative azoreductase (SO3585), demonstrates a dose-dependent response to Cr(VI) challenge and is up-regulated under the higher doses, as mentioned above. There are two other proteins (SO3586 and SO3587) located immediately downstream of SO3585 in the MR-1 chromosome that may be organized in an operon, as suggested previously [147]. SO3586 encodes a glyoxalase family protein and SO3587 encodes a hypothetical protein with a putative transmembrane domain [147]. SO3586-87 have a reduced level of detection with respect to SO3585, where SO3587 is identified with no more than 4 peptides. The predicted transmembrane-spanning domain of SO3587 comprises a 36 amino acid tryptic peptide (residues 38-73), which may contribute to the lack of identified peptides. SO3585-87 were identified solely under Cr(VI) challenge (Supplemental Table S2, Supporting Information). This is in contrast to a previous study [147] in which SO3587 was identified under both control and chromate treatments in response to temporally longer growth exposures (up to 90 min). It is important to note that the previous study involved control samples grown for 45 and 90 min. prior to harvesting, whereas the current study has a control sample grown for 30 min. After 90 min of exposure to Cr(VI), the growth rate of *S. oneidensis* decreased significantly with respect to control growth conditions (Supplemental Figure S1), whereas 30 and 45 min after introduction of Cr(VI) the difference is reduced. Also, in the previous study, only two peptides were identified for SO3587 in the 45 min control with the difference between them resulting

from a missed cleavage. However, since SO3587 is located at the terminus of the operon, the gene may not be translated to the same frequency perhaps due to the ribosome disengaging from the mRNA. This has been shown in *E. coli* using a fabricated betagalactosidase hexamer transcriptional unit, where the ribosome disengaged from the mRNA approximately half of the time when reaching the third copy of the gene [220].

An important class of proteins involved in signal transduction consists of relatively low-abundance proteins, with only about 50 members confidently identified at the two-peptide level under a given growth condition using the LTQ (Figure 4.2). Of these 50 proteins, two (SO2426, a DNA-binding response regulator, and SO4003, a response regulator) were up-regulated under doses 0.3 and 1 mM Cr(VI). Only one of these proteins (SO2426) was also up-regulated in response to the 0.5 mM dose (Tables 4.3-4.5). SO2426 was exclusively detected in the Cr(VI) treatment samples under all three doses relative to the control sample, and a MR-1 strain harboring an in-frame deletion of this gene showed impaired growth and Cr(VI) reduction activity under metal conditions (K. Chourey and D. K. Thompson, unpublished data), thus suggesting that this signal transduction component plays a regulatory role in the cellular response to chromate stress. Also, in a previous study [147], the transcript data for the *so2426* gene was consistent with the corresponding protein expression data.

As described above, proteins involved in general stress responses in the bacterium were up-regulated at a dosage of 0.5 mM Cr(VI). In addition to IbpA (16 kDa heat shock protein A) and RecN (a DNA repair protein), ClpB, PrlC, and a prolyl oligopeptidase family protein (SOA0048) were all up-regulated in response to 1 mM Cr(VI) exposure. Jiang *et al* concluded that PrlC in *E. coli* functions as a molecular chaperone [221]. The

greater degree of oxidative stress imposed by the higher 1 mM Cr(VI) dose correlates with the increased number of up-regulated proteins involved in stress protective response and protein fate determination.

A subset of 26 down-regulated proteins identified following acute exposure to 1 mM Cr(VI) displayed a trend similar to the other two dosages. The two dominant categories, energy metabolism and hypothetical/conserved hypothetical proteins, constituted almost 60% of the proteins down-regulated under 1 mM Cr(VI) challenge. Interestingly, a large number of energy metabolism proteins were also up-regulated under this dosage. Of the 308 energy metabolism proteins predicted from the MR-1 genome annotation, 183 were identified confidently at the two-peptide level representing almost 60% of the predicted total. Of these 183 proteins, 21 were differentially expressed under the 1 mM dose. Five of the down-regulated energy metabolism proteins are annotated as reductases, which might suggest a reconfiguration of energy metabolism by the cell in response to chromate stress.

Conclusions

The work presented here provides the first large-scale description (2406 proteins) of the proteome response of *S. oneidensis* to three different acute chromate concentration challenges. Approximately 90% of the proteins identified did not demonstrate a change in abundance in response to chromate treatment; however, the remaining 10% of proteins that demonstrated an abundance change in response to chromate (Tables 4.3-4.5 and Supplemental Table S3, Supporting Information) provided some important insights into the molecular response to chromate insult. Among the up-regulated proteins identified, it was clear that both general stress and specific chromate responses were elicited.

Primarily, the up-regulated sulfate transport system under higher chromate dosage (> 0.5 mM) suggested an increased demand for sulfate uptake and metabolism, possibly due to sulfate deficiency in the bacterium. Sulfate deficiency could lead to a decrease in the biosynthesis of certain amino acids (i.e., methionine and cysteine) and this may explain why there are many more down-regulated proteins under the lower dosage. Out of the 11 genes encoding members of the cysteine metabolism pathway, none were differentially expressed subsequent to 0.3 mM Cr(VI) exposure and one protein (SO2903, CysK) was up-regulated at a dosage of 0.5 mM. However, subsequent to the addition of a 1 mM Cr(VI) dosage, four proteins in the cysteine metabolism pathway were up-regulated: SO1095 (a putative O-acetylhomoserine (thiol)-lyase), SO2406 (AspC-2), SO2903 (cysK), and SO3598 (cysM). The methionine metabolism pathway is composed of 12 protein-encoding genes and demonstrated one up-regulated protein in the 1 mM dosage sample, SO1095. The 0.5 and 1 mM dosages may be compensating for sulfate deficiency with the apparent increased production of sulfate transport and metabolism protein complexes. Also, during Cr(VI) reduction, a one-electron transfer can occur producing the metastable, highly reactive Cr(V) species [140] leading to an increase in reactive oxygen species within the cytoplasm. Both of these response systems may lead to the observed proteome changes detected in this study. There were at least three general stress response proteins up-regulated as well under each dose, indicating a general stress response similar to other stress-response proteome studies [222].

The functional category of transport and binding proteins, particularly those with annotated functions in iron and sulfate transport, dominated the group of up-regulated proteins. Most of the TonB-dependent receptors and other iron acquisition proteins (e.g.,

siderophore biosynthesis proteins) showed increased abundance under all three Cr(VI) dose exposures, indicating that expression of these proteins is an important feature of the MR-1 response to chromate. In addition, proteins whose abundance levels behaved in a dose-dependent manner were identified by examining differences in peptide spectral counts between samples. Most of these transport and binding proteins were highly up-regulated under the 0.3 mM dosage and increased when challenged with 0.5 mM but remained the same between the 0.5 and 1 mM dosages (Figure 4.4). This was the general trend for most differentially expressed proteins, as illustrated by binning and comparing the relative abundances of the proteins between the 0.3 mM and 1.0 mM dosage conditions (Figure 4.5). Whereas more than 50 proteins that were up-regulated relative to the control showed no change between the 0.3 mM and 1.0 mM conditions, there were almost twice as many proteins up-regulated in the 1.0 mM condition relative to the 0.3 mM condition. Many fewer proteins were down-regulated in the 1.0 mM condition. Table S4 (see Supporting Information) lists the identities and spectral count ratios of all proteins shown in the bins of Figure 4.5.

Recently, an instrumentation comparison study between the linear trapping quadrupole and the three-dimensional ion trap for the proteome of the model organism *E. coli* OP50 was published [31], with similar results to the study discussed here. Our present study confirmed the substantially increased ability to identify proteins at the two peptide level in the LTQ datasets, with many proteins identified as being differentially expressed that were not even detected with the three-dimensional quadrupole ion trap. One objective of our present study was to conduct a direct comparison between the QIT and LTQ technology platforms to determine which would provide more extensive insight

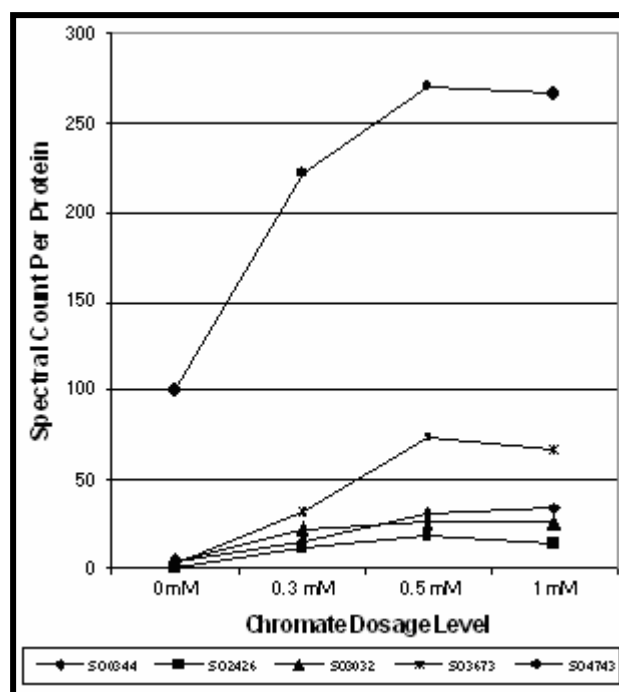


Figure 4.4. Proteins demonstrating dosage-dependent up-regulation.

Proteins up-regulated under all dosages tested, but were at similar levels of up-regulation under 0.5 and 1 mM dosages. SO0344: methylcitrate synthase (prpC), SO2426: a DNA-binding response regulator, SO3032: a putative siderophore biosynthesis protein, SO3673: the periplasmic hemin-binding protein of the hemin ABC transporter (hmuT), and SO4743: a putative TonB-dependent receptor.

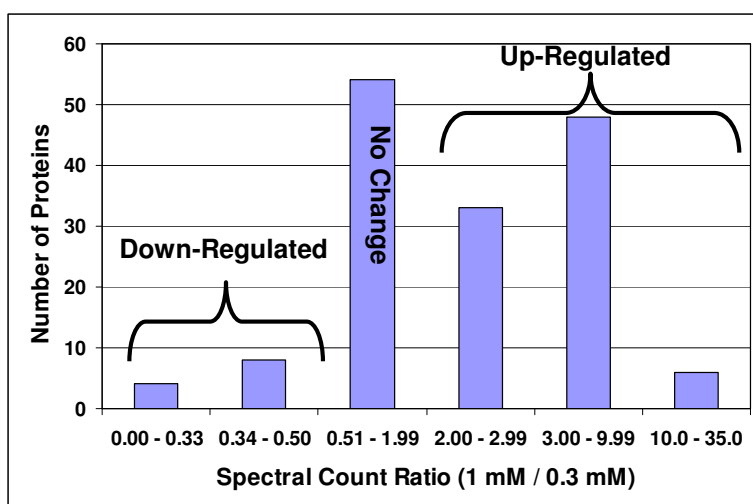


Figure 4.5. Dosage dependent abundance of proteins between 0.3 and 1 mM dosages.

A comparison of the relative abundances of proteins identified as differentially expressed between the 0.3 and 1 mM Cr(VI) dosage datasets (Supplemental Table S3). The x-axis represents the relative change in protein expression (1.0 mM / 0.3 mM), where the first two bins represent reduced abundance of proteins in the 1 mM dose, the third bin are the proteins that have the same concentration level in both dosages, and the last three bins represent proteins with increased abundance in the 1 mM dosage. The y-axis represents the number of proteins found in each bin out of a total of 153 differentially expressed proteins. Supplemental Table S4 contains the proteins identified under each bin.

into the molecular response of *S. oneidensis* to dosage-dependent chromate insult. In addition to a substantially deeper level of proteome characterization, the LTQ datasets should provide a much better degree of correlation with differentially expressed transcriptome data determined with microarray measurements. Furthermore, the LTQ datasets provided information about low-abundance proteins not identified by the three-dimensional ion trap. Proteins involved in transcription regulation are generally of low abundance, such as SO2426, a DNA-binding response regulator. With LTQ technology, the detection of SO2426 and other proteins with regulatory functions was achievable. In fact, SO2426 was identified only under chromate exposure and correlated with the results from a previous study [147], where the transcript levels were also up-regulated in response to acute chromate challenge.

Chapter 5

Systematic Assessment of the Benefits and Caveats in Mining Microbial Post-Translational Modifications from Shotgun Proteomic Data; Response of *Shewanella oneidensis* to Chromate Exposure

Text and data presented below has been accepted for publication

Melissa R. Thompson, Dorothea K. Thompson, and Robert L. Hettich. Systematic Assessment of the Benefits and Caveats in Mining Microbial Post-Translational Modifications from Shotgun Proteomic Data; Response of *Shewanella oneidensis* to Chromate Exposure. *Journal of Proteome Research*, Accepted, (2007). Melissa R. Thompson performed all data analysis. Supplemental material located at *Journal of Proteome Research* website.

Introduction

During the course of examining the global proteomic response of chromate exposure in *Shewanella oneidensis*, the need to obtain information on post-translational modifications (PTMs) involved in chromate response arose. PTMs are enzymatically-driven chemical changes to amino acids and constitute one mechanism used by microbes to regulate both protein synthesis and activity. Therefore, we expect that PTMs will contribute to the response of *S. oneidensis* to Cr(VI) exposure. This chapter outlines three algorithms evaluated for the purpose of providing a foundation for global PTM searches, which has to date been unexplored.

Protein activity can be modulated via the addition and/or removal of PTMs, which act to repress or stimulate target protein function [223]. Some common PTMs include phosphorylations, methylations, acetylations, and oxidations. Methylations and acetylations in bacteria typically occur on lysine and arginine residues [14, 223].

Methylation modifications have been implicated in regulation of gene expression as well as protein-protein and protein-DNA interactions (i.e. the histone code) [14]. In bacterial chemotaxis, which is the response to a chemical gradient of attractant or repellent molecules, methylation is involved in the adaptive mechanism and short-term memory abilities of methyl-accepting chemotaxis receptor proteins (chemoreceptors) [54, 224]. Two enzymes, a methyltransferase (CheR) and a methylesterase (CheB), function to covalently attach and remove a methyl group, respectively, from the chemoreceptor. Acetylations have also been shown to be involved in bacterial chemotaxis [53] and provide protein terminus stability in eukaryotes [50, 225] as well. For example, the ability of the chemotactic response regulator CheY to activate the flagellar switch is enhanced upon acetylation [53]. In contrast to the above PTMs, modification via the oxidation of a protein can be due to either chemical [46, 47, 226] or in some cases biological [227, 228] mechanisms. Free radicals formed during aerobic cellular metabolism are highly reactive and often damaging proteins abundant within the cytosol through oxidation [46, 47]. Detecting the level of chemically-induced oxidation of the proteome has been hypothesized as a way to determine oxidative stress levels in organisms [46]. In eukaryotes, a well studied enzymatically driven oxidation conversion of the protein ubiquinol to ubiquinone, a vital component of the electron transport chain in mitochondria, is mediated by the cytochrome bc1 complex [228].

To date, most studies detecting PTMs in both prokaryotes and eukaryotes have been accomplished using targeted approaches [48, 50, 229, 230] by purifying protein(s) or enrichment of a specific PTM. A study by MacCoss *et al* [51] was one of the first attempts at a more global approach by searching shotgun proteomic data for PTMs. In

this study, the authors purified the *Schizosaccharomyces pombe* Cdc2p complex as well as proteins from human lens tissue. Using a three-dimensional ion trap, they were able to characterize a number of PTMs, including phosphorylations, methylations, and acetylations. The tandem mass spectra (MS/MS) searches were accomplished with an initial search where no modifications were specified, followed by the creation of a sub-database to re-search the data for PTMs [51]. The sub-database was created taking identifications made by an initial search specifying no modifications and the -98 Da loss common to phosphorylated peptides using the collision induced dissociation (CID) fragmentation method. The building of a sub-database was necessary for this work in order to reduce the false discovery rate (FDR) of identified PTM-containing peptides due to the combinatorial increase in database search space generated by including PTMs.

In 2004, Strader *et al* [48] published a comprehensive characterization of the 70S ribosome from *Rhodospseudomonas palustris*. The 70S ribosome was characterized using the top-down bottom-up technique, wherein PTM information was acquired from both the intact protein mass spectral data and peptide MS/MS data. The term top-down refers to the measurement of the intact protein, while bottom-up corresponds to first digesting proteins followed by acquisition of fragmentation MS leading to sequencing information on the proteolytic peptides. The authors were able to confirm and identify novel PTMs present on the constituent proteins of the complex. One of the primary advantages of the top-down approach is the use of a high-resolution mass spectrometer (i.e. FT-ICR) to discern the difference between a trimethylation and an acetylation, which are isobaric on a lower resolution instrument (i.e. a 3-D or linear ion trap). Nielsen *et al* [231] further

demonstrated the utility of a high-resolution instrument (LTQ-FT hybrid instrument) for reducing the FDR of PTM peptides.

Phosphorylations are prevalent PTMs in both eukaryotes and prokaryotes. These PTMs play important roles in cell signaling cascades, specifically two-component signal transduction [232, 233], and in the regulation of cell cycle progression and cellular differentiation [223]. Phosphorylation sites play a critical role in both normal and diseased cell function, making them important targets for global studies. Phosphorylation in prokaryotes usually targets histidine and aspartic acid residues, producing modified species which are known to be acid labile and often do not survive the sample handling process for subsequent MS analysis. This usually precludes searching for phosphorylation in prokaryotic proteome studies. In contrast, phosphorylation in eukaryotes usually targets threonine and serine residues; these modified species are much more stable and survive the sample handling process. Unfortunately, most of these modified residues readily display phosphate neutral loss as the dominant fragmentation pathway when a low-energy, multiple collision fragmentation method is used [51, 233], thereby precluding information about the modification site. Nevertheless, Olsen *et al* [55] were able to identify and quantitate 6600 phosphorylation sites in HeLa cells using an LTQ-FTICR. To address the neutral loss problem, the authors performed MS/MS/MS to obtain more sequencing information on the modified peptide.

All of the aforementioned studies were targeted, whether that target was a protein complex (Cdc2p [51] or 70S ribosome [48]), a subset of proteins [230], or an enrichment due to the presence of a specific modification [55, 56, 58, 234]. As such, none of these targeted studies provides guidance on performing a truly non-biased global analysis of

PTMs in eukaryotes or prokaryotes. In addition, most PTM studies to date have focused on eukaryotic systems [46, 181, 223, 231, 234-236]. Since protein post-translational modifications also play a critical role in bacterial cellular processes, it is important to evaluate and optimize informatic methods which can accurately unravel this level of proteome detail. The goal of the present work is to identify a robust and accurate method for performing global PTM searches of shotgun proteomics data for microbial isolates. To this end, we searched a previously acquired shotgun proteomics dataset [147] derived from control (non-stressed) and chromate-stressed *S. oneidensis* cells in order to examine the potential roles of PTMs in the cellular response to acute metal challenge. Three search algorithms (DBDigger [44], InsPecT [40], and Sequest [39]) were employed to test the feasibility of performing a PTM search on a proteome and determine the feasibility of each method to provide detailed PTM information at an acceptable false discovery rate. Since the false discovery rate will increase with increasing search space, this work is a systematic attempt to compare different algorithmic tools on the same dataset for their efficacies in managing false positive rates. In addition, the search results for each algorithm were compared for overlap in PTM identifications as a method of validation, the ease of conducting searches using a standard desktop computer, and the flexibility in specifying PTMs in the search parameters. Note that this study was focused on data mining of peptide MS/MS data, and did not attempt to provide PTM heterogeneity at the protein level.

Materials and Methods

Experimental dataset

The shotgun proteomics dataset used in the PTM searches was acquired previously [147]. Briefly, four separate cultures of *S. oneidensis* MR-1 were grown aerobically to mid-log phase followed by addition of a sub-lethal dose (1 mM) of K_2CrO_4 to two of the cultures, which were exposed to chromate for 45 or 90 min and then harvested for proteome characterization. The other two cultures served as controls and were grown in parallel under identical conditions excluding metal addition. The goal of the previous work was to identify differentially expressed proteins implicated in the response to a sub-lethal, acute chromate exposure [147]. Cultures were lysed by sonication and fractionated into a crude/soluble and membrane-associated fraction by high-speed centrifugation. Lysates were then digested with trypsin and analyzed via online two-dimensional liquid chromatography (strong cation exchange and reverse phase) coupled to a LTQ mass spectrometer (Thermo Scientific, Waltham, MA). The LTQ was operated in a data-dependent mode for 24 h, and digested lysates were analyzed in duplicate.

Computational searches and algorithms

The above data (a total of 8 datasets) was searched using three separate search algorithms: DBDigger [44], InsPecT [40], and Sequest [39]. The database(s) used for all searches performed can be downloaded from the project website compbio.ornl.gov/shewanella_metal_stress/databases/. A reverse database was used for estimating the FDR in this study by applying the equation from Peng *et al* [185]. The use of a reverse database is one method to estimate the FDR, where peptide(s) and/or protein(s) matching

nonsense sequences from the reverse database are considered incorrect identifications. The false negative rate is a more difficult number to quantify in shotgun proteomics datasets, because the exact number and identity of all true peptide identifications are unknown. This number was qualitatively determined in the datasets presented here by comparing the total number of peptides or proteins identified in the unmodified searches to the searches specifying PTMs.

In our lab, DBDigger has been the algorithm of choice for PTM searches, because it allows simultaneous evaluation of sequentially modified forms of individual amino acid residues in the same peptide. DBDigger was used initially to develop proper filtering thresholds. The following PTMs were specified in separate DBDigger searches: (1)mono-, (2)di-, and (3)trimethylations on lysines and arginines; (4)monomethylations on glutamate; (5)mono- and (6)diacetylations on lysines and arginines; and (7)monooxidations on methionines, cysteines, tyrosines, and tryptophan; dioxidation on methionines and cysteines; and trioxidation on cysteine residues. Table 5.1 depicts the modifications and corresponding residue mass shifts that were targeted in the present study. Due to the use of an LTQ mass spectrometer in this study, phosphorylations were not searched in the resulting datasets. Results from DBDigger were stored in the form of .sqt files that were then filtered and sorted using DTASelect [171] with the following options: -m 0 (extracts only modified peptides) and --DB (exports results in database format). The resulting DTASelect output files were imported into Microsoft Access for storage and data analysis.

Sequest searches were performed on a subset of mass spectra initially identified as PTM-containing by DBDigger as follows: selected DTA files were extracted from one

Table 5.1. Amino Acid Residues and Corresponding Post-translational Modifications

Amino Acid	PTM ^a	Amino Acid Mass	Amino Acid + PTM mass (Da)
Lysine	+CH ₂	128.09	142.11
Lysine	+C ₂ H ₄	128.09	156.12
Lysine	+C ₃ H ₆	128.09	170.14
Lysine	+COCH ₂	128.09	170.10
Lysine	+C ₂ O ₂ C ₂ H ₄	128.09	210.11
Arginine	+CH ₂	156.10	170.12
Arginine	+C ₂ H ₄	156.10	184.13
Arginine	+C ₃ H ₆	156.10	198.15
Arginine	+COCH ₂	156.10	198.11
Arginine	+C ₂ O ₂ C ₂ H ₄	156.10	238.12
Glutamic Acid	+CH ₂	129.04	143.06
Methionine	+O	131.04	147.03
Methionine	+O ₂	131.04	163.02
Cysteine	+O	103.01	119.00
Cysteine	+O ₂	103.01	134.99
Cysteine	+O ₃	103.01	150.99
Tryptophan	+O	186.08	202.07
Tyrosine	+O	163.06	179.05

^aEmpirical formula for post-translational modification

directory and placed into another directory using DTACopy (Vilmos Kertesz, Oak Ridge National Laboratory) and results were filtered and sorted using DTASelect as described above. Since Sequest is only able to search three modifications at a time, the above DTA files were searched repeatedly until all of the above modifications had been specified in the sequest.params file (total of 8 searches for each dataset). InsPecT searches were performed in one search where all 8 modification events on 7 amino acids were specified (Table 5.1). A total of 3 modification events were allowed for each peptide. The following filter levels were used for the InsPecT dataset: a minimum of 2 peptides identified per protein and a p-value score that gives a FDR of 2% for the total peptide dataset (see *InsPecT scoring optimization for post-translationally modified peptides* for details). The results were then imported into Access in order to compare the PTM identifications with the DBDigger results.

Results and Discussion

DBDigger scoring optimization for post-translationally modified peptides

Initially, searches were performed using the DBDigger algorithm on the 45 min Control dataset in order to determine the correct filter thresholds for minimizing the FDR and false negative rate. The 45 min Control Run1 dataset was searched using two methods: (1) raising the scoring threshold levels and (2) creating a sub-database prior to PTM searches applying loose filtering criteria and no modifications. As a comparison, all searches were performed either with no modifications specified or with monomethylations on lysines and arginines. This particular PTM was chosen first due to the small mass shift in the amino acid residue by the addition of a methyl group, and preliminary searches demonstrated a high FDR through the use of a reverse database with

this modification. Table 5.2 depicts the FDRs for a number of filter threshold levels tested and demonstrates a basic premise of data filtering in shotgun proteomics at present. This premise is that care must be taken in order to maximize the number of resulting peptide identifications made while minimizing the FDR of the filter threshold levels chosen. As a control, the dataset was searched with no modifications using “normal” filtering levels that give a FDR of 2.6% at the two peptide threshold level corresponding to the minimum peptide score of 25 for +1 peptides, 30 for +2 peptides, and 45 for +3 peptides using DBDigger. Using these same scoring minima, the addition of a differential modification (monomethylation) to lysines and arginines raises the FDR to 7.6%. The increased FDR is expected and is caused by the combinatorial increase in database search space due to the modification. Increasing the minimum peptide level for protein identification to four decreased the FDR to 1.7%; however, this also led to a dramatic decrease in the number of proteins identified. Therefore, the decision was made to pursue increasing the minimum peptide score while retaining the minimum two peptides for protein identification. Increasing the minimum scores to 29 (+1), 34 (+2), and 49 (+3) leads to a FDR of 1.9%, while maintaining a protein identification level similar to the non-modification search. There was less of a reduction in protein identifications using stringent peptide scoring filters (283 proteins) than by increasing the minimum peptide count to four (585 proteins), demonstrating a relatively lower false negative rate for the stringent peptide scoring filters.

The other option explored for retaining a FDR of 2%, while identifying at least a similar number of proteins compared to a non-modification search, is to construct a sub-database for subsequent PTM searching. This was performed by MacCoss *et al* [51] on a

Table 5.2. False Discovery Rates for 45min Control Run1 Dataset at Various Filter Threshold Levels

		2 peptide filter level						4 peptide filter level					
No PTM		Protein		Peptide				Protein		Peptide			
25, 30, 45 ^a	156 ^b	2111 ^c	14.8% ^d	333 ^c	25943 ^f	2.6% ^g	9	1443	1.2%	17	24390	0.1%	
27, 32, 47	68	1933	7.0%	136	24111	1.1%	7	1383	1.0%	8	22817	0.1%	
29, 34, 49	20	1816	2.2%	37	22643	0.3%	3	1326	0.5%	3	21482	0.0%	

		2 peptide filter level						4 peptide filter level					
Monomethylation		Protein		Peptide				Protein		Peptide			
25, 30, 45	427	2560	33.4%	1069	28112	7.6%	51	1526	6.7%	224	25690	1.7%	
27, 32, 47	215	2146	20.0%	503	25388	4.0%	21	1420	3.0%	75	23685	0.6%	
29, 34, 49	96	1924	10.0%	217	23330	1.9%	9	1343	1.3%	25	21952	0.2%	
31, 36, 51	50	1818	5.5%	106	21764	1.0%							
35, 40, 55	15	1689	1.8%	32	19089	0.3%							

^aMinimum peptide scores for +1, +2, and +3 charged peptides, respectively. Number of proteins^b or peptides^e identified

matching to reverse database sequences. Total number of proteins^c or peptides^f identified from both the forward and reverse

databases. ^{d,g}False discovery rate value calculated as described in Peng *et al* [185].

yeast protein complex and human lens tissue. The sub-database in this study was constructed by using loose filtering criteria in an initial non-modification search. The filtering criteria were as follows: 1 peptide minimum for protein identification and peptide scores of 25 (+1), 30 (+2), and 45 (+3). These criteria were chosen since the minimum score will filter out 92.4% of the false peptide identifications, but retain a reasonable database size so that when the modification search is done, the identification of a protein with one modified and one unmodified peptide is possible. The sub-database consists of 2,751 forward protein sequences plus their corresponding reversed sequences, thus yielding a total database size of 5,502 protein sequence entries. The normal *S. oneidensis* proteome database size is 4,798 forward protein sequences; therefore, the sub-database reduced the number of protein entries by approximately half. After the sub-database was created, a modification search for monomethylations on lysines and arginines was performed with the following threshold filters: “normal” [2 peptides per protein, 25 (+1), 30 (+2), and 45 (+3)] and “stringent” [2 peptides per protein, 29 (+1), 34 (+2), and 49 (+3)]. The “normal” filters yielded a FDR of 7.1% and the “stringent” filters 1.8%. These FDRs are similar to those above for the full-size database, and comparing the peptides identified with both strategies leads to an overlap in identification of 90% (Figure 5.1). The use of a sub-database for PTM searches on bacterial species does not appear to be necessary based on the results obtained here. The caveats of first creating a sub-database include the added complexity of performing two searches for each dataset, creating a separate database for each dataset, and a relatively insignificant decrease in overall search time. Therefore, the decision was made for the remaining searches to use a

Monomethylation Peptide IDs of 45 min Control Run1

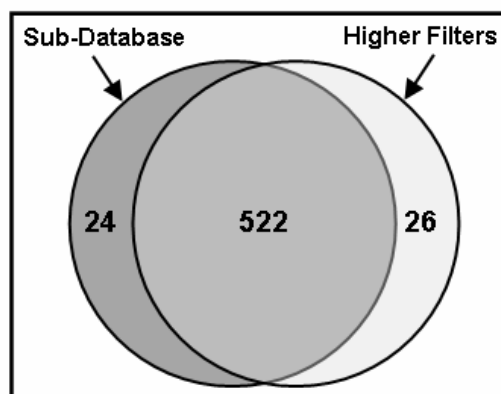


Figure 5.1. A Venn diagram comparing peptide identifications.

The results are from a search for monomethylations on lysines and arginines by two different search methods. The circle on the left represents the modification search with the sub-database and the circle on the right represents the modification search with the full-size database and stringent filters. The value in the middle (522) is the number of modified peptide identifications shared between the two methods and corresponds to a 90% overlap between the two methods.

full-size database with the stringent filters [2 peptides per protein, 29 (+1), 34 (+2), and 49 (+3)].

Using the above threshold filters, many peptides with putative PTMs were identified with the search algorithm DBDigger [44]. DBDigger allows more flexibility in searching for differential PTMs than the search algorithm Sequest, because it generates a candidate sequence once for the collection of spectra rather than once for every spectrum and is much faster in searching complex datasets [44]. Therefore, initial searches with DBDigger were conducted in order to obtain a preliminary list of putative modified peptides. There were a total of 8494, 7203, 9358, and 6588 non-redundant peptides, respectively, containing at least one post-translationally modified amino acid residue for the 45 min Control, 45 min Cr, 90 min Control, and 90 min Cr datasets. Table 5.3 displays the number of peptides identified in each dataset for the PTMs specified, and all modified peptides are listed in Supplemental Tables S1 and S2 (Supporting Information). However, as also depicted in Table 5.3, the FDR for modified searches is high (~50%) compared to the overall FDR described in Table 5.2. This high FDR led to the testing of two other algorithms (InsPecT [40] and Sequest [39]) to determine if the FDR of a PTM search could be improved.

Sequest scoring optimization for post-translationally modified peptides

MS/MS in the form of DTA files (tab-delimited flat-files for each spectrum) identified as PTM-containing peptides from the above DBDigger searches were extracted using DTACopy (Vilmos Kertesz, ORNL) and interrogated with the algorithm Sequest. This algorithm was chosen in order to help validate the DBDigger results since Sequest is a widespread algorithm for searching shotgun proteomics data. Only selected MS/MS

Table 5.3. Number of Post-Translationally Modified Peptides Identified in Each Dataset Searched using DBDigger

Modification Type	45 min Control	FDR^a	45 min Cr	FDR	90 min Control	FDR	90 min Cr	FDR
Monomethylation	1147 ^b	53.9%	1167	62.4%	1356	45.7%	902	53.8%
Dimethylation	1058	N/A ^c	852	N/A	951	N/A	890	N/A
Trimethylation	889	N/A	769	N/A	798	N/A	720	N/A
Monoacetylation	709	62.1%	594	65.3%	619	59.0%	557	65.5%
Diacetylation	779	N/A	669	N/A	667	N/A	620	N/A
Oxidation	5567	8.0%	3940	8.6%	7068	4.2%	3209	9.3%

^aFDR: false discovery rate. ^bNumber of PTM peptides identified. ^cN/A: not available

first identified by DBDigger were searched due to the slower speed of Sequest on desktop computers. The resulting OUT files were filtered and sorted with DTASelect [171]. The filtering thresholds used in the Sequest searches were a one-peptide requirement for protein identification and 1.8 for +1 charged peptides, 2.5 (+2), and 3.5 (+3). Table 5.4 gives the number of peptides identified using Sequest as well as the number of MS/MS searched (DTA files extracted).

As apparent in Table 5.4, the number of MS/MS identified in the Sequest searches compared to the total number searched is much lower for all PTMs considered. There are two possible reasons for this low identification rate using Sequest: one is due to the high FDR of PTM-containing peptides obtained with DBDigger, and the other may be the result of the search algorithm itself. Concerning the high FDR, the average for monomethylated peptides was 54% using DBDigger. In addition, the Sequest searches were performed on all MS/MS spectra identified by DBDigger as containing a PTM including MS/MS identified from relevant reverse database searches and matching protein contaminant sequences. Therefore, the MS/MS count is somewhat inflated with erroneous identifications (false-positives from the reverse database) and protein contaminant identifications. The inflated MS/MS count may be an underlying cause of the low identification rate from Sequest.

The second possible reason for the resulting low identification rate may lie in the fact that Sequest was not originally designed to search for differential PTMs. The original design of the algorithm required that the PTM mass (i.e. 14 Da for monomethylation) be added to the amino acid mass [i.e. 14 Da + lysine (128.09 Da)] with the modification considered static or always present [39]. This search method is limiting,

Table 5.4. Sequest Peptide Identifications from a Subset of MS/MS Spectra First Identified by DBDigger

Dataset	Monomethylation		Dimethylation		Trimethylation		Monoacetylation		Diacetylation		Oxidation	
	Spectra	Identified	Spectra	Identified	Spectra	Identified	Spectra	Identified	Spectra	Identified	Spectra	Identified
45 min Control	1363	314	967	172	776	123	887	123	749	73	6044	3480
45 min Cr	1357	406	790	136	669	116	719	95	647	73	4371	2352
90 min Control	1558	456	885	159	682	111	716	78	628	74	7388	4770
90 min Cr	1059	248	808	140	628	89	680	74	580	70	3549	1896

resulting in both a decrease in peptide identifications and an increase in incorrect identifications. A subsequent version of Sequest will only allow 3 differential modifications to be specified, while DBDigger allows an unlimited number of PTMs to be specified in the search parameters. This limitation leads to reduced identifications, since different modifications can occur on the same peptide and result in a total of 32 separate searches performed on the datasets. This is a significant issue with the oxidation dataset (total of 7 modifications on 4 amino acids), where DBDigger completed the search in one round while Sequest required 3 separate rounds. Therefore, the Sequest results were noted and can be found in Supplemental Tables S3-S6 but were not used for validation.

InsPecT scoring optimization for post-translationally modified peptides

Due to difficulties with Sequest and the high FDR of DBDigger when considering PTM-containing peptides only, the decision was made to search the datasets using the algorithm InsPecT [40]. Compared to DBDigger and Sequest, InsPecT uses a different approach to searching MS/MS for PTMs. The first stage in filtering for InsPecT is to create a set of tags (25 were specified in the searches performed here) three amino acids in length using fragment ions in the experimental MS/MS. This enables a relatively short list of peptides to be searched from the forward and reverse sequence database used here. The resulting candidate peptides are scored based on seven different criteria: the number of predicted (1) b and (2) y ions that match to the MS/MS, how well the intensity of the identified (3) b and (4) y ions match the predicted intensity, (5) trypsin specificity, (6) the length of the candidate matching peptide where the presence of PTM(s) indicates a shorter peptide, and (7) the fragment ion profile of the spectrum (presence of an isotope,

higher fragment ion intensity in the middle of the spectrum, and properties of the neighboring residue) [40]. The resulting top score (MQScore) is then compared to the distribution of the lower scores (DeltaScore) and a p-value is calculated. The p-value used by InsPecT is based on the p-value devised for the algorithm Peptide Prophet [174]. A lower p-value and higher match score are indicative of a better match, which is in contrast to the limited evaluative parameters employed by the other two algorithms used in this study.

To determine filtering parameters that would give at least an equivalent if not lower FDR for modified peptides, various filtering options were applied to the 45 min Control Run1 dataset. The default parameters for InsPecT are a p-value of 0.1 and the requirement of at least one peptide for protein identification. Using the default parameters yields a FDR of 0.7% (125 reverse peptides and 37,120 forward peptides). Therefore, the p-value was raised to 0.35, giving a FDR of 2.0% (428 reverse peptides and 42,200 forward peptides). We then evaluated a p-value giving a 2% FDR and requiring two peptides for positive protein identification. A p-value of 0.75 was chosen for the two-peptide dataset since this gave a FDR of 2.1% (499 reverse peptides and 46,943 forward peptides). A total of 97% of the proteins identified in the two-peptide dataset were identified in the one-peptide dataset as well. However, the one-peptide dataset had only 77% overlap with an additional 472 proteins identified with only one peptide. This observation raises an important issue of proteins identified solely by one peptide with the possibility of the identification coming from a modified peptide. The FDRs when considering only peptides containing a putative PTM was 11.9% (420 reverse peptides and 6668 forward peptides) for the one-peptide dataset and 10.8% (492

reverse peptides and 8634 forward peptides) for the two-peptide dataset. When comparing the reverse peptide identifications for the PTM peptides and the total reverse peptide identifications for the datasets, ~99% of the reverse identifications came from a PTM peptide. Therefore, all InsPecT datasets presented below had the following filtering criteria: two peptides required for protein identification and a p-value cutoff that provides a $2\pm 0.1\%$ FDR for the total peptide dataset. These criteria are more conservative and reduce the FDR of modified peptides by an average of 30% when compared to DBDigger's modified peptide FDR.

The result files from the InsPecT search were filtered differently according to the p-value distribution for that dataset. For the 45 min Control dataset, p-values of 0.75 (Run1) and 0.73 (Run2) were used as cutoff scores, because this value gave a FDR of 2.1% and 2.0%, respectively, for the total peptide dataset (both unmodified and modified peptide identifications) with 10.8% (Run1) and 9.1% (Run2) FDRs when considering only modified peptide identifications. Table 5.5 depicts the FDRs and number of peptides (total and modified only) identified for the remaining datasets evaluated in this study. All PTM peptides identified by InsPecT are located in Supplemental Tables S7 and S8. The reason for choosing a p-value that reflects a FDR value instead of one p-value to be applied across all the datasets is due to the large variance in FDRs across the datasets for a given p-value. For instance, if a p-value of 0.75 were chosen as the cutoff for all datasets, FDRs would range from 1.8-4.0% with an average of 2.3%. This wide range skews the identifications between datasets and leads to some having a great deal more false or true identifications than others. This variance was only pronounced in one dataset from the DBDigger searches (90 min Control oxidation versus 90 min Cr

Table 5.5. FDRs for Total and PTM Peptide Identifications with InsPecT

Dataset	p-value	FDR^a Total Peptide Identifications			FDR PTM Peptide Identifications		
		Reverse IDs	Total IDs	% FDR	Reverse IDs	Total IDs	% FDR
45 min Control Run 1	0.75	499	47442	2.1	492	9126	10.8
45 min Control Run 2	0.73	921	91769	2.0	857	18888	9.1
45 min Cr Run 1	0.75	458	48057	1.9	449	8928	10.0
45 min Cr Run 2	0.75	444	46475	1.9	378	8771	8.6
90 min Control Run 1	0.75	482	48375	2.0	476	8671	10.4
90 min Control Run 2	0.55	585	56904	2.1	530	18040	5.7
90 min Cr Run 1	0.70	454	44784	2.0	444	9053	9.4
90 min Cr Run 2	0.80	440	45736	1.9	381	7466	9.7

^aFDR: false discovery rate

oxidation); and in general, DBDigger and Sequest do not have the FDR variation between datasets that was observed with InsPecT. This variance is most likely due to differences in the p-value distribution in each dataset, which is in contrast to the charge-state dependant scoring of the other two algorithms.

Post-translational modification results with DBDigger and InsPecT

To illustrate the benefit of performing a search for PTMs, all modified proteins identified were compared according to their functional category. Annotated genes of the *S. oneidensis* MR-1 genome were assigned to one of 18 functional categories by The Institute for Genomic Research (now the J. Craig Venter Institute). Figure 5.2 depicts the functional distribution of the modified peptides identified using DBDigger and InsPecT according to the role categories. As a comparison to the previously reported unmodified dataset [147], the categories of hypothetical proteins, energy metabolism, unknown function, cellular processes, and protein fate were the top five functional categories representing at least 55% of the unmodified protein identifications. By contrast, the top five modified categories based on DBDigger analysis (Figure 5.2A) consisted of hypothetical proteins, energy metabolism, protein synthesis, protein fate, and cellular processes. The category of protein synthesis is composed primarily of genes encoding components of the ribosome, which has been shown previously to contain a large number of modifications on the constituent proteins [48]. The cellular processes category also comprises a large number of proteins with putative PTMs (average of 570 PTM peptides) and some of these proteins are involved in the chemotactic response of *S. oneidensis* to environmental cues. The identification of a number of modified proteins involved in chemotaxis is discussed below. The functional category distribution of PTM peptides

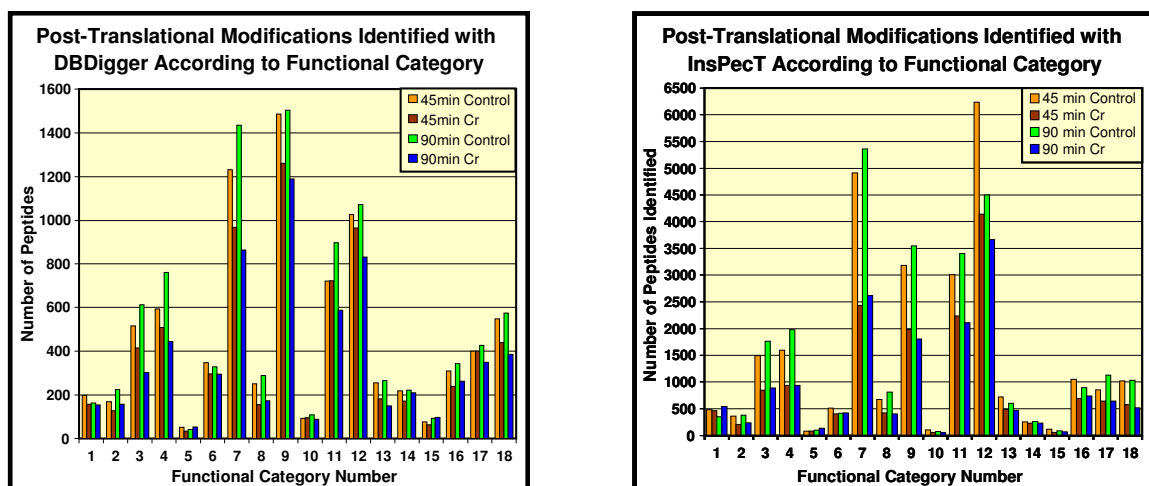


Figure 5.2. Identification of PTM peptides using (A) DBDigger and (B) InsPecT.

Assignment of a peptide into a category was according to the parent protein's membership. The functional category assignments are as follows: (1) Amino acid biosynthesis; (2) Biosynthesis of cofactors, prosthetic groups, and carriers; (3) Cell envelope; (4) Cellular processes; (5) Central intermediary metabolism; (6) DNA metabolism; (7) Energy metabolism; (8) Fatty acid and phospholipid metabolism; (9) Hypothetical proteins; (10) Mobile and extrachromosomal element functions; (11) Protein fate; (12) Protein synthesis; (13) Purines, pyrimidines, nucleosides, and nucleotides; (14) Regulatory functions; (15) Signal transduction; (16) Transcription; (17) Transport and binding proteins; and (18) Unknown function.

based upon InsPecT analysis was similar to that observed with DBDigger. The predominant categories containing PTM peptides were protein synthesis (~4600), energy metabolism (~3800), protein fate (~2700), hypothetical proteins (~2600), and cellular processes with ~1300 peptides on average (Figure 5.2B). Some functional categories demonstrate a putative bias in modifications in the control versus chromate-shocked datasets (energy metabolism and hypothetical proteins). At this time, however, the detailed understanding of this putative difference in control versus chromate-shocked PTM peptides is not known and is beyond the scope of the current work.

A majority of the proteins comprising the functional categories of cellular processes and signal transduction are annotated as part of signaling cascades first activated by a PTM on the initiating protein, which responds to various environmental stimuli. Signal transduction proteins are generally of low abundance, and identifications are usually confirmed by observing approximately two peptides per protein. In a search that specifies no modifications on the proteins, less than 0.2% of the total spectra count are attributed to signal transduction proteins; where spectral count was used as a measure of protein abundance previously [182, 183, 237]. Out of the 61 proteins predicted to be involved in signal transduction in the *S. oneidensis* proteome, 53 of the proteins are annotated as members of two-component regulatory systems. Two-component systems contain a sensor histidine kinase, which autophosphorylates in response to a specific environmental cue and then transfers the high energy phosphate group to a cognate response regulator, which effects a change in gene expression upon phosphorylation [232, 238, 239]. In our previous study [147], 39 members of two-component systems were identified without specifying PTMs in the search. By including the option of

methylation, acetylation, or oxidation to seven different amino acids, there was an increase in the rate of identification for some members of this category using identifications from both DBDigger and InsPecT. DBDigger was able to identify a total of 269 peptides containing at least one PTM from 41 proteins. The signal transduction functional category yielded 47 protein identifications with at least two peptides using InsPecT. A total of 253 unique PTM peptides annotated as involved in signal transduction were identified in the InsPecT dataset, with 101 of these peptides containing at least one methyl group. Both algorithms identified more proteins than in our previous study solely by including PTMs in the search parameters. All but two of the proteins identified previously [147] were identified by either DBDigger or InsPecT. Both algorithms identified 13 proteins as being post-translationally modified in this study. Interestingly, the control datasets yielded these shared peptides, while the chromatexposed cultures did not yield any shared modified peptides.

Methylation has been implicated previously in changing DNA-protein interactions [238, 239]. The signal transduction group of proteins in bacteria may be phosphorylated in the activation domain, while DNA interaction occurs in the other domain [52]. The methylation could either perturb the domain preventing interaction with the phosphate backbone of the DNA or the phosphorylation event could cause a conformational change that leads to the methylation event. The signal transduction proteins identified above were cross-referenced between DBDigger and InsPecT. SO2541, a response regulator, was identified with various PTMs including methylation of various degrees up to trimethylation on multiple residues by both algorithms, but was identified in the Control dataset with InsPecT whereas DBDigger identified this protein in the Cr dataset for the

45 min time-point. While DBDigger identified SO3196 and SO3688 in the 90 min dataset, InsPecT identified them in the 45 min Control dataset. Both algorithms confirmed only one protein, SO2544, from the 90 min dataset. However, each algorithm identified a different MS/MS and peptide. This is not unexpected in complex proteome datasets, and illustrates the need to validate MS/MS from PTM identifications (especially since many modified peptides are of low abundance).

Chemotaxis, part of the cellular processes functional category, plays an important role in enabling bacteria to identify and respond to small molecules (nutrients or toxins) in the surrounding environment. The end result is a mechanical response that moves the organism either toward or away from the molecule concentration gradient. Bacterial chemotaxis has been well-studied and largely elucidated mechanistically in the model bacterium *E. coli* [53, 54, 224, 240, 241]. In *E. coli*, methyl-accepting chemotaxis protein receptors (chemoreceptors) are encoded by five genes that detect amino acids such as serine (*tsr*) and aspartate (*tar*); dipeptides (*tap*); ribose and galactose (*trg*); and the redox potential (*aer*) [224] of the surrounding environment. The level of stimulation of a particular chemoreceptor is controlled by two proteins CheR, a methyltransferase, and CheB, a methylesterase. Therefore, the presence of a methyl group on the chemoreceptor is indicative of stimulation due to the binding of a specific molecule, this initiates a signaling cascade through the autophosphorylation of CheA and results in the activation of FlhM (the protein subunit comprising the flagellar motor). Activation of FlhM results in the bacterium swimming in a tumbling motion either toward or away from the chemical gradient. Methylation of the chemoreceptors is important in controlling the level of stimulation so that the bacterium is not constantly tumbling [54, 224].

Chemotaxis is not only indicative of stress (i.e. from chromate shock as described here), but rather is a response to the surrounding environment, so the presence of methylation on chemoreceptors from both the control and chromate-shocked datasets [88, 92, 242-244] is not surprising.

The chemotaxis system of *S. oneidensis* is more complicated and includes pathways responding to a number of anaerobic electron acceptors [88, 92], three separate signal cascades initiated by CheA, and 29 chemoreceptors. The *E. coli* and *S. oneidensis* chemoreceptors were aligned and a dendrogram (or sequence tree) was constructed to assess sequence similarity between *S. oneidensis* and *E. coli* chemoreceptors. Figure 5.3 depicts the relationship between the five chemoreceptors from *E. coli* along with 29 from *S. oneidensis*. As shown, four of the *E. coli* chemoreceptors cluster tightly together in the middle of the tree and do not demonstrate sequence similarity with chemoreceptors from *S. oneidensis*. Aer, which responds to redox potential, shows sequence similarity with three *S. oneidensis* chemoreceptors (SO1385, SO0584, and SO3404). The lack of sequence similarity between the chemoreceptors in the two organisms is expected due to the differences of the natural habitats in which the bacteria are found. *S. oneidensis* is a fresh water microbe, which must be ready to adapt to rapidly changing concentrations in nutrients and metals [88, 92, 242, 243]. A large number of chemoreceptors were identified with and without PTM peptides in the 45 and 90 min datasets both under control and chromate-shocked growth conditions (Table 5.6). DBDigger was able to identify all but one (SO3510) of the chemoreceptors predicted. While InsPecT identified SO3510 in the 90 min Control dataset, this algorithm did not identify a couple of low abundant receptors identified by DBDigger (SO1434 and SO2117).

Table 5.6: Identification of Chemoreceptors using DBDigger and InsPecT from the 45 and 90 min Datasets

Locus	DBDigger Identifications				InsPecT Identifications			
	45 min Control	45 min Cr	90 min Control	90 min Cr	45 min Control	45 min Cr	90 min Control	90 min Cr
SO0500	2 ^a	4	2	3	3	4	2	3
SO0584	2	3	4 (2) ^b	2	4 (1)	2 (1)	5 (1)	0
SO0987	32	24 (2)	39 (2)	28 (1)	29 (2)	20 (2)	36 (1)	25 (2)
SO1056	44 (1)	37 (1)	45 (5)	37 (1)	57	35 (1)	74 (2)	26
SO1144	31 (2)	29	24 (2)	24	19	18	19 (2)	15
SO1278	5	10	11 (1)	9	2	6	3	3
SO1385	11	13 (2)	8	12	9 (1)	7	5	8
SO1434	4	3	4	4	0	0	0	0
SO2083	7	8	7	8	6	2	3	2
SO2117	4	3	4	4	0	0	0	0
SO2123	0	3	2	0	6 (1)	4 (1)	4 (1)	2
SO2240	17 (2)	20 (2)	25 (1)	17	19 (1)	17	27	9
SO2317	2	2	3	3	0	2 (1)	3 (1)	5 (2)
SO2323	11	11	6	6	8	13	7	5
SO3052	13 (1)	14	13	21	8	8	7	16
SO3207	38	36	40 (1)	39	43 (3)	27	27	33
SO3282	16	8	25	14	14 (1)	0	24	6
SO3396	4	4	4	5 (2)	2 (2)	3 (1)	2 (1)	0
SO3404	4	2	5	3	0	3	2	0
SO3510	0	0	0	0	0	0	2	0
SO3582	17 (1)	15 (1)	14	20 (2)	9	8 (2)	8	6
SO3642	43 (1)	38 (2)	38 (2)	42 (3)	45 (3)	34 (2)	41 (2)	35 (2)
SO3838	21 (1)	32 (1)	24 (1)	25 (2)	19	25 (1)	31 (1)	15 (1)
SO3890	7 (1)	7	7	9	8	7	4	9 (1)
SO4053	20	11	24	12	12	6	25	9
SO4454	22 (2)	24 (1)	24	24 (1)	12	15 (1)	22 (1)	14

Table 5.6. Continued.

Locus	DBDigger Identifications				InsPecT Identifications			
	45 min Control	45 min Cr	90 min Control	90 min Cr	45 min Control	45 min Cr	90 min Control	90 min Cr
SO4466	5 (1)	2	3	4	2	0	4	0
SO4557	30	37	30	33	40 (1)	37 (1)	52 (4)	31 (2)
SO4635	4	5	4	4	0	0	2	2
SOA0106	36 (2)	39 (2)	37 (3)	34	42 (2)	48 (3)	61 (1)	33 (2)

^aNumber of unique peptides both unmodified and containing a PTM identified for a given chemoreceptor. ^bNumber of monomethylated glutamate residues found for a given chemoreceptor.

The *S. oneidensis* chemoreceptor SO3642 was identified consistently as having a methylated glutamate residue at the C-terminus of the protein. A total of 9 MS/MS were identified using InsPecT and 16 were identified using DBDigger (Table 5.6). An example MS/MS found in common between the two algorithms is depicted in Figure 5.4. The mass shift due to the addition of 14 Da is readily present and causes the fragment ions with the glutamate residue to be 14 Da heavier. Using InsPecT, two spectra were identified and scored very well (p-values of $< 4e^{-5}$) in the 45 min Control dataset. DBDigger did not score these MS/MS high enough to pass the filter thresholds. In addition, InsPecT did not identify any modified MS/MS in the 45 min Cr datasets, but DBDigger found 3 spectra. The 90 min Control Run 2 dataset was more consistent with 4 MS/MS found by InsPecT and 9 by DBDigger. Overall, the 90 min Cr dataset was the most consistent as both algorithms identified the MS/MS depicted in Figure 5.4. As mentioned, chemoreceptors are a well-studied class of proteins, and information in the literature [54, 224, 246] was used to help confirm the physiological significance of this modification. The SO3642 peptide was identified solely in the membrane fraction of cell lysates, which is consistent with a cytoplasmic membrane location of known chemoreceptors [224, 240]. Chemoreceptors have also been shown to be methylated on conserved C-terminal glutamate residues, as is the case with SO3642 demonstrated here [224, 240]. Therefore, based on our MS data and the extant literature, we conclude that SO3642 is methylated on residue E515. However, the implication of this modification in terms of a response to chromate is not known at this time and was not evaluated in detail within the scope of this work. While the present study delineates the computational data mining approach for identifying the range of protein post-translational modifications at

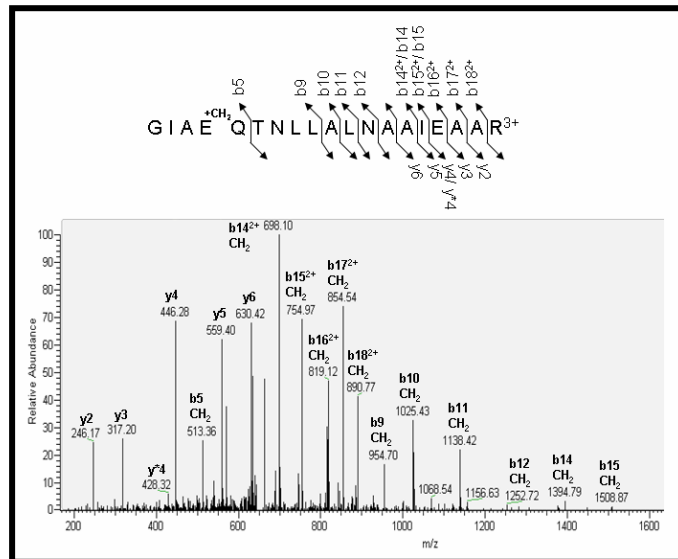


Figure 5.4. A MS/MS for SO3642, a chemoreceptor, confirms a C-terminal peptide. The C-terminal peptide contains a monomethylated glutamate residue. All major peaks of the MS/MS are labeled, and 12 fragment ions demonstrate a mass shift of 14 Da corresponding to the addition of a methyl group. The MS/MS scored high for both algorithms: DBDigger score of 75.73, DelCN of 0.46 and InsPecT MQScore 3.268, DeltaScore 0.65, p-value 0.151.

the global level, thereby providing detailed information about the types of proteins modified and the range of modifications, future detailed studies will be required to fully unravel the biological details of PTM correlation with chromate exposure for *S. oneidensis*.

Conclusions

InsPecT and DBDigger are complementary algorithms that both identified a large number of putative post-translationally modified peptides. However, the FDR for DBDigger was more than twice that for PTM peptides, and its search capabilities for large datasets was reduced, thereby limiting combinatorial PTMs. Therefore, InsPecT was tested and resulted in a much lower FDR for PTM peptides. If an identification resulting from the chemical addition of a methyl, acetyl, or hydroxyl group was made by both DBDigger and InsPecT for a particular peptide, this was taken as a positive confirmation of that modification. The PTM peptide identifications between DBDigger and InsPecT were compared in this study. For the 45 min Control Run1 dataset, a total of 3219 modified peptides were shared between the two algorithms (Figure 5.5). This corresponds to 69% of the peptides identified using DBDigger (a total of 4651 PTM peptides) and 37% from InsPecT. The InsPecT overlap is much smaller due to the scoring scheme of the algorithm: InsPecT allows high scoring MS/MS from non-tryptic and semi-tryptic peptides to pass the filtering thresholds. The option of specifying a non-tryptic cleavage was not used with DBDigger due to the increased time and search space, and thus higher FDRs. Removing the non-tryptic and semi-tryptic identifications from the InsPecT dataset yields 4005 fewer peptides; this brings the overlap between

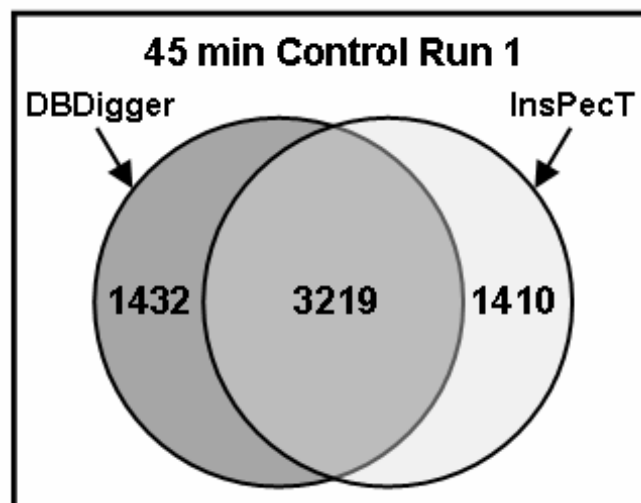


Figure 5.5. A Venn diagram comparing DBDigger and InsPecT PTM peptides.

The results represent the 45min Control Run1 dataset. A total of 3219 peptide identifications were shared between the two algorithms. DBDigger identified a further 1432 unique tryptic peptides. InsPecT identified 3996 semi-tryptic, 9 non-tryptic, and a further 1410 unique tryptic peptide identifications.

DBDigger and InsPecT to 70%. Comparable results were found for the remaining datasets (Supplemental Figures S1-S7, pubs.acs.org/journals/jprobs/index.html).

Even though an average of 3000 post-translationally modified peptides for each dataset were shared between the two algorithms, there is still room for improvement in performing PTM searches. DBDigger and InsPecT search the MS/MS very differently. DBDigger uses the MASPIC [173] scoring algorithm to determine peptide identifications for the MS/MS. MASPIC separates the MS/MS spectra into different intensity classes where the most intense class is restricted to a few fragment ions. The score is weighted based on identification of intense peaks. InsPecT is similar to MASPIC in the respect that there is a scoring factor for intensity. However, InsPecT first discriminates whether an intense peak is identified as a b or y ion and then weights that intensity into the score, where the y ions derived from the lower energy CID as used in this study are more intense than their counterpart b ions. This is more discriminatory than MASPIC and leads to more stringent filtering of false identifications. The more stringent scoring of InsPecT is the reason for the 30% reduction in false identifications of modified peptides. Another advantage to using InsPecT is the incredible speed with which the algorithm searches shotgun proteomic data. InsPecT was able to search over 240,000 MS/MS in approximately 84 hours specifying all PTMs in one search on a desktop computer for each dataset, while DBDigger took twice as long with seven different searches for each dataset. The authors initially attempted to specify all methylations in one search, but due to the combinatorial increase in search space the computational memory was overwhelmed. The ability to search for all modifications at one time is physiologically relevant, since a peptide can be methylated and oxidized at the same time. However,

using both algorithms together increases the confidence and accuracy of identifications with the overlap between them composed of the top-scoring PTM peptides, which was a major goal of this work.

As evident from other studies, the use of a higher performance mass spectrometer will undoubtedly provide more confident identifications of peptide PTMs, since improved mass accuracy will reduce ambiguities. However, at present, many readily available algorithms, such as the three tested in this study, do not contain a scoring element which exploits mass accuracy of the parent peptide or resulting fragment ions as an additional metric. Since medium resolution mass spectrometers are common in many research laboratories, and since many existing bioinformatic approaches do not utilize higher mass accuracies, we chose to focus on evaluating methodologies which would be readily available to the current field. There are certainly efforts underway in many laboratories to incorporate high performance mass spectral datasets from Orbitrap, FTICRMS, and QTOF platforms into data mining schema. This is already providing increased confidence in identification of peptide modifications, including the ability to discriminate between phosphorylation (79.980) and sulfonation (80.064) as well as trimethylation (42.03 Da) versus monoacetylation (42.01 Da).

Chapter 6

Proteomic Comparison of *Shewanella oneidensis* MR-1 Wild-Type and a Response

Regulator Deletion Strain under Conditions of Chromate Transformation

Data presented below is in preparation for submission for publication

Melissa R. Thompson, Karuna Chourey, Dorothea K. Thompson, and Robert L. Hettich. Proteomic Comparison of *Shewanella oneidensis* MR-1 Wild-Type and a Response Regulator Deletion Strain under Conditions of Chromate Transformation. *In preparation for submission to Applied and Environmental Microbiology*, 2007. *Melissa R. Thompson performed all sample preparation, LTQ measurements, and data analysis for the proteomics portion of the manuscript. Melissa R. Thompson was assisted by Karuna Chourey in growth of S. oneidensis cultures. Supplemental material can be found at http://compbio.ornl.gov/shewanella_metal_stress/reduction.*

Introduction

Our previous work with Cr(VI) exposure and *S. oneidensis* MR-1 identified over 2400 proteins expressed from the MR-1 genome [147, 156, 158], with a subset demonstrating differential expression in response to Cr(VI). Many of the differentially expressed proteins had annotated functions in metal ion transport and sulfate transport/metabolism. Interestingly, a putative response regulator, SO2426, was also identified as being up-regulated under Cr(VI) conditions (5, 39). Response regulators are part of two-component signal transduction systems that serve as a basic stimulus-response coupling mechanism, allowing organisms to sense and respond to changes in many different environmental conditions [238]. For example, the redox sensing system pathway involves the ArcAB complex in *Escherichia coli* [247]. In fact, due to the extensive respiratory versatility in *S. oneidensis*, Gralnick *et al* [247] hypothesized that this bacterium must have an extensive regulatory system.

In our acute shock study [147], *S. oneidensis* was exposed to a sub-lethal concentration of 1 mM Cr(VI) for 45 and 90 min. When compared to the control cultures (no Cr(VI) added), SO2426 was highly up-regulated. The corresponding transcript was found to follow a trend of increasing expression level with increased exposure time [147]. A Cr(VI) dosage study [156] also found SO2426 to be up-regulated under three different sub-lethal concentrations (0.3, 0.5, and 1 mM) of Cr(VI) exposure for 30 min. Therefore, SO2426 appears to be activated under growth conditions where Cr(VI) is present, irrespective of the dosage. In another study, *so2426* was found to also be up-regulated after exposure to acute Strontium stress [248]. These observations led to the conclusion that SO2426 may be a response regulator for transition metal redox state. This prompted further investigation of the role SO2426 may be playing in response to sub-lethal concentrations of Cr(VI) by “knocking out” the gene through an in-frame deletion, as described by Chourey *et al* [157]. The $\Delta 2426$ mutant strain demonstrates sensitivity to other transition metals besides Cr(VI) (Chourey *et al*, unpublished results).

The use of shotgun proteomics of biological replicates to probe the functionality of global regulator proteins provides information not found with other methodologies. Also, the resulting variability between cultures consisting of a gene deletion mutant has not been explored in great detail. Information about gene function can be probed utilizing shotgun proteomics, thus allowing for increased understanding of the global response [249] and possible compensatory pathways encoded in the bacterium’s genome. Most shotgun proteomics studies have been performed using technical replicates [19, 20, 147, 211, 250] instead of biological replicates. A technical replicate is defined as multiple LC-MS experiments on one sample (i.e. a cell culture, tissue sample, etc.) [251].

However, recently there has been a number of shotgun proteomics studies [210, 252, 253] and a review article [251] on both the informational value and necessity of biological replicates for quantitation of the measured proteins. Most of the focus for the discussion between the use of technical replicates or biological replicates has been on the resulting statistical treatment of the dataset [182, 183, 251, 253]. The primary argument for the use of biological replicates is to reduce the background biological noise of the sample [251]. Available nutrients, temperature fluctuations, and light availability (relevant for phototropic bacteria) are factors considered biological noise and may play a significant role in the growth variability of a culture. The resulting protein complement of the culture may vary based on these factors.

The possible role of SO2426 as a global regulator of Cr(VI) response pathways is explored further through the comparison of a $\Delta 2426$ mutant to the wild-type strain of MR-1. In this study, differentially expressed proteins solely from biological replicates of wild-type and a $\Delta 2426$ mutant in response to a sub-lethal concentration of Cr(VI) are identified. Differential regulation of protein function through the identification of post-translational modification sites on proteins present in the global dataset is also investigated.

Materials and Methods

Chemical reagents and culture growth

Luria-Bertani (LB) medium, Guanidine HCl, Tris, EDTA, Ammonium Acetate, and CaCl_2 were purchased from Sigma Chemical Co. (St. Louis, MO) and were used without further purification. Modified sequencing grade trypsin was purchased from Promega (Madison, WI) and used for all protein digestions. The 99% formic acid was

obtained from EM Science (Darmstadt, Germany) and HPLC-grade water and acetonitrile from Burdick & Jackson (Muskegon, MI).

Three independent cultures of wild-type *S. oneidensis* MR-1 and three independent cultures of strain $\Delta 2426$ (obtained from D. Thompson, Purdue University) were grown in a 250 mL flask with 100 mL of LB medium (pH 7.2) at 30°C under aerobic conditions with constant agitation at 200 rpm. When the OD at 600 nm reached 0.5 (mid-log phase), a 10-ml aliquot of each culture was taken as the 0 h time point and processed as described in Brown *et al* [147]. Afterwards, Cr(VI) in the form of K_2CrO_4 was added to yield a final concentration of 0.3 mM in all six cultures. Cr(VI) concentration in the media was monitored using the 1,5-diphenylcarbazide (DPC) method as described previously [138]. When the approximate concentration of Cr(VI) in the media of the control cultures (wild-type MR-1 strain) reached 0.25 (1 h), 0.15 (3 h), and 0 (4 h) mM, 10 mL aliquots of culture were harvested. *Cell lysis and digestion*

The resulting frozen cell pellets from the 10 mL aliquots were weighed and then further distributed into 5 mg wet cell pellets for lysis. The lysis protocol used is essentially as described in Thompson *et al* [160]. Briefly, 6 M Guanidine with 10 mM DTT were added to each sample and incubated at 37°C overnight after which the guanidine was diluted 6-fold with 50 mM Tris/ 10 mM $CaCl_2$. Then, 5 μ g of trypsin was added, followed by a 6 h incubation period after which another aliquot of trypsin was added with an overnight incubation at 37°C. A final reduction step for 2 h was performed with 20 mM DTT. Protein digests were then spun at 10,000 x g for 10 min to remove cellular debris and then stored at -80 °C until the LC/LC-MS/MS experiment.

Global proteome LC/LC-MS/MS analysis

The LC/LC-MS/MS experiments were performed as described in Brown *et al* [147]. Each lysis/digestion from each culture was a separate 24 h LC/LC-MS/MS experiment. Samples were loaded onto a split phase column consisting of reverse phase (C18) and strong cation exchange (SCX) separation materials. This column was placed behind a 15 cm C18 analytical column located directly in front of the mass spectrometer (LTQ, Thermo Scientific, San Jose, CA). The LTQ was coupled with an Ultimate HPLC pump (LC Packings, a division of Dionex, San Francisco, CA). The samples were analyzed with a 12-step 2D HPLC analysis by adding increasing concentrations (0 to 500 mM) of ammonium acetate salt pulses followed by an aqueous (95% H₂O, 5% ACN, 0.1% formic acid) to organic (30% H₂O, 70% ACN, 0.1% formic acid) gradient. The LTQ was operated in the data-dependent mode during the chromatographic separations as detailed in Brown *et al* [147].

Proteome bioinformatics

The protein database used for all MS searches consisted of Version 8 (www.tigr.org) of the *S. oneidensis* MR-1 proteome (4,798 proteins) as well as 36 common contaminant sequences (trypsin, keratin, etc.). The database is available for download at the project website compbio.ornl.gov/shewanella_metal_stress/databases/. Initially, Sequest was used to search the resulting MS raw files for peptide/protein identifications. Sequest searches were performed as detailed in Brown *et al* [147] with the following scoring cutoffs. A minimum of 2 peptides were required for a positive identification of a protein with peptide charge state score minimums of 1.8 (+1), 2.5 (+2), and 3.5 (+3). A delCN value of 0.08 was required for peptide identifications. Sequest

results were then filtered and sorted according to the above criteria with DTASelect and Contrast [171], and all resulting data is available on the project website (compbio.ornl.gov/shewanella_metal_stress/reduction).

For performing searches for post-translational modifications, the search algorithm InsPecT [40] was used. For optimization of PTM searches with InsPecT on shotgun proteomics data, see reference [59]. The proteome database used in these searches consisted of the forward database (mentioned above) with the reversed sequences of all proteins concatenated to the end. This database was used in order to estimate the false discovery rate of each individual search. MS/MS spectra were extracted from the raw files using ReAdW.exe to create a .mzXML file. The mzXML files were then searched with InsPecT [40] specifying the following PTMs. An optional mass of 14 Da (monomethylation) was added to lysines, arginines, and glutamates; optional masses of 28 (dimethylation), 42 (trimethylation/monoacetylation), 84 (diacetylation) Da were added to lysines and arginines; 16 Da (monooxidation) to methionines, cysteines, tyrosines, and tryptophans; 32 Da (dioxidation) to methionines and cysteines; and 48 Da (trioxidation) on cysteines. The scripts Summary.py and Pvalue.py were used to filter the resulting output tab-delimited text files by p-value and peptide count. A peptide count of two was required for all proteins, and the p-value was adjusted to give a false discovery rate of $2 \pm 0.2\%$ for the total peptide dataset.

Results and Discussion

The gene *so2426* encodes a putative DNA-binding response regulator and may regulate the transcriptional activation of genes involved in response to Cr(VI) in the bacterium. *so2426* contains two putative domains, a CheY-like domain and a putative

DNA-binding domain. The CheY-like domain is ~50% similar to the other three CheY proteins predicted in the *S. oneidensis* genome. However, the similarity extends only to residue 131, leaving 106 residues not aligning to CheY. The 106 remaining residues are on the C-terminal end and constitute a putative DNA-binding domain. SO2426 is also highly conserved at the amino acid level to a putative ortholog from fifteen other *Shewanella* genomes sequenced to date. The C-terminal DNA-binding domain portion of the protein is annotated as a member of the Trans_reg_C family (PF00486) as described using the Pfam database [254]. The top-aligning proteins from the other *Shewanella* genomes are also annotated as part of the Trans_reg_c family. Figure 6.1 is a dendrogram (or sequence tree) tree depicting SO2426 clustering with a protein from the Sargasso Sea *Shewanella* genome [74]. CheY from *S. oneidensis* and *Escherichia coli* were used as an outgroup, further demonstrating SO2426 is not CheY, but rather a fusion protein with a CheY-like domain, that is conserved across the genus *Shewanella*. Even though the top blast hit from *Geobacter metallireducens* GS-15 did not cluster with these *Shewanella* proteins, this protein is also identified in the same family with SO2426.

Microbial growth during Cr(VI) transformation

S. oneidensis strains MR-1 and $\Delta 2426$ were cultivated aerobically in LB medium (see Materials and Methods for details). The strains were cultured for 4 h in the presence of Cr(VI) in the form of 0.3 mM K₂CrO₄. Figure 6.2 depicts the transformation of Cr(VI) over the exposure period. The arrows point to the time points of harvest for global proteome analysis. The standard error bars for the strains are shown for triplicate cultures and the abiotic control, which demonstrated undetectable transformation of Cr(VI) during the 4-h period. The standard deviation for the abiotic control ranged from

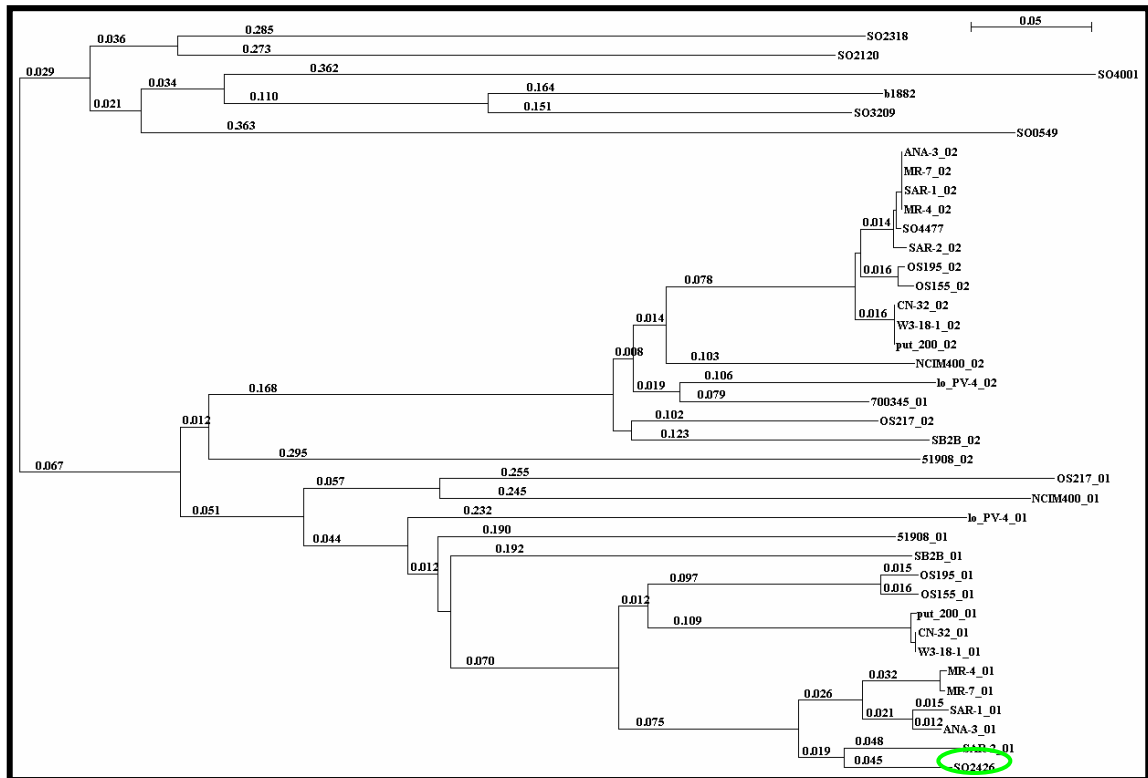


Figure 6.1. A sequence tree aligning the protein sequences of SO2426 and SO4477. SO2426 and SO4477 (CpxR transcriptional regulator) are aligned against the top Blast hit for each species/strain of *Shewanella* for genomes sequenced to date. SO2426 is at the bottom of the tree and most closely aligns with a protein sequence from a *Shewanella* strain from the Sargasso Sea[74]. The following proteins were used as an outgroup: from *S. oneidensis* MR-1 SO2318 (CheY-2); SO2120 (CheY-1); SO3209 (CheY-3); and SO0549 and SO4001 (chemotaxis protein CheY/response regulator receiver domain proteins) and b1882 (CheY) from *E. coli*. The species/strains of *Shewanella* are as follows: *S. oneidensis* MR-1 (SO4477), *S. putrefaciens* 200 (put_200_01 and put_200_02), *Shewanella* W3-18-1 (W3-18-1_01 and W3-18-1_02), *Shewanella* ANA-3 (ANA-3_01 and ANA-3_02), *S. woodyi* ATCC 51908 (51908_01 and 51908_02),

Figure 6.1. Continued.

S. frigidimarina NCIMB400 (NCIM400_01 and NCIM400_02), *Shewanella* MR-4 (MR-4_01 and MR-4_02), *Shewanella* MR-7 (MR-7_01 and MR-7_02), *S. baltica* OS195 (OS195_01 and OS195_02), *S. denitrificans* OS217 (OS217_01 and OS217_02), *S. putrefaciens* CN-32 (CN-32_01 and CN-32_02), *Shewanella* SAR-1 environmental sequence (SAR-1_01 and SAR-1_02), *Shewanella* SAR-2 environmental sequence (SAR-2_01 and SAR-2_02), *S. loihica* PV-4 (lo_PV-4_01 and lo_PV-4_02), *S. baltica* OS155 (OS155_01 and OS155_02), *S. amazonensis* SB2B (SB2B_01 and SB2B_02), and *S. pealeana* ATCC 700345 (700345_01). There was no significant conservation found between proteins from *Geobacter sulfurreducens* GS-15 and *S. oneidensis* MR-1 (data not shown). Alignment and Neighbor-Joining tree (bootstrap value of 1000) was created by ClustalX [version 1.8, [245]]. The dendrogram was visualized with njplot (pbil.univ-lyon1.fr/software/njplot.html).

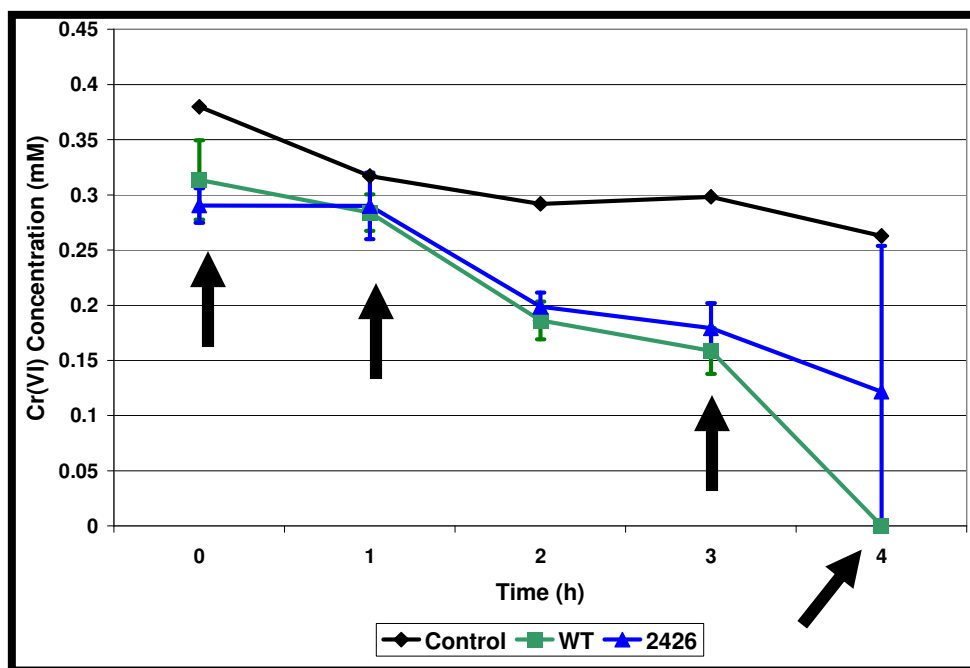


Figure 6.2. Transformation of 0.3 mM Cr(VI) in the form of K_2CrO_4 .

The Cr(VI) transformation is depicted for strains MR-1 and $\Delta 2426$ of *S. oneidensis*.

There was no detectable reduction of Cr(VI) by an abiotic control (sterile LB medium) shown as black diamonds and the standard deviation of the triplicate measurements

ranged between 9×10^{-5} to 0.02 mM. This standard deviation is too small to be

visualized in the figure. Strain MR-1 (WT and squares in the figure) completely reduced

the Cr(VI) during the 4 hour time period and only 1 culture of strain $\Delta 2426$ (2426 and

triangles in the figure) completely reduced Cr(VI). Error bars represent triplicate cultures

for stains MR-1 and $\Delta 2426$.

9×10^{-5} to 0.02 mM. Strain MR-1 was able to completely transform the 0.3 mM Cr(VI) by the fourth hour, with 0.15 mM left by the third hour of exposure. Strain $\Delta 2426$ demonstrated comparable reduction as MR-1 during the first 3 hours of exposure. In contrast, between 3 and 4 hours of Cr(VI) exposure, strain $\Delta 2426$ transformed the Cr(VI) incompletely for two of the three cultures. The incompletely reduced cultures had 0.10 and 0.26 mM Cr(VI) remaining after 4 hours of cultivation. The incomplete transformation of Cr(VI) by $\Delta 2426$ for two of the three cultures indicates the possibility that SO₂ may be involved in response to Cr(VI) toxicity. The reason as to why one culture from strain $\Delta 2426$ was able to transform Cr(VI) completely is not understood at this time and is beyond the scope of this work.

Global proteomics profile of strains MR-1 and $\Delta 2426$

A total of 5 mg of cell pellet were lysed, and the resulting protein content was digested with trypsin and analyzed by 2D-HPLC-MS/MS. The resulting MS/MS spectra were searched with Sequest [39] for each culture during the 4 harvested time points. A total of 2,121 proteins comprising 44% of the predicted proteome were confidently identified at the two peptide level for strains MR-1 and $\Delta 2426$. Table 6.1 depicts the total proteins identified for strains MR-1 and $\Delta 2426$ for each time point harvested. The molecular weight and isoelectric point distribution for the total dataset from each time point was plotted and demonstrated no discrepancy when compared to the predicted distribution of the proteome (data not shown). The reproducibility at the protein level for each biological replicate was at least 60%. Previously, the aim was to obtain a reproducibility of 70% for technical replicates [65, 147, 158, 184]. Achieving a

Table 6.1. Total Proteins Identified by Strains MR-1 and $\Delta 2426$ at Each Time Point

Time of harvest	Amount of Cr(VI) present	Strain MR-1 ^a	Strain $\Delta 2426$ ^a
0 hr	0.3 mM	1537	1398
1 hr	0.3 mM	1583	1540
3 hr	~0.2 mM	1535	1599
4 hr	0.0 – 0.2 mM	1468	1687

^aTotal number of proteins identified by the three biological replicates.

reproducibility of at least 60% as demonstrated here is comparable since there is the added complexity of an additional proteome dataset represented by the third culture.

All three replicates of each strain during each time point were grouped according to their functional category distribution annotated by the J. Craig Venter Institute (formerly The Institute for Genomic Research) and the results are presented in Figure 6.3. Overall, most of the functional categories did not fluctuate significantly between the first time point and the last or between the two strains. However, proteins annotated in the functional categories biosynthesis of cofactors, prosthetic groups, and carriers; hypothetical proteins; transport and binding proteins; and proteins of unknown function demonstrated large fluctuations in protein expression between the two strains or over time within a particular strain. Strain $\Delta 2426$ exhibited the most variation during the time-course. The number of proteins identified in a particular category was lower for the sample obtained at the 0 time point versus the last sample that was harvested at 4 h. This may be due to the strain in general demonstrating deficient growth, where the starter culture required a longer time of incubation prior to inoculation for strain $\Delta 2426$ (data not shown). The effects of removing a transcriptional regulator are known to cause growth deficiencies in bacteria [94, 255, 256].

The large fluctuations of biosynthesis of cofactors, prosthetic groups, and carriers; hypothetical proteins; central intermediary metabolism; transport and binding proteins; and proteins of unknown function may be the result of perturbing regulation of the expressed genome through the knockout of *so2426*. However, the hypothetical proteins category appears to fluctuate due to the presence of Cr(VI) in the growth media. Prior to the addition to Cr(VI), there are comparable numbers of proteins identified by each

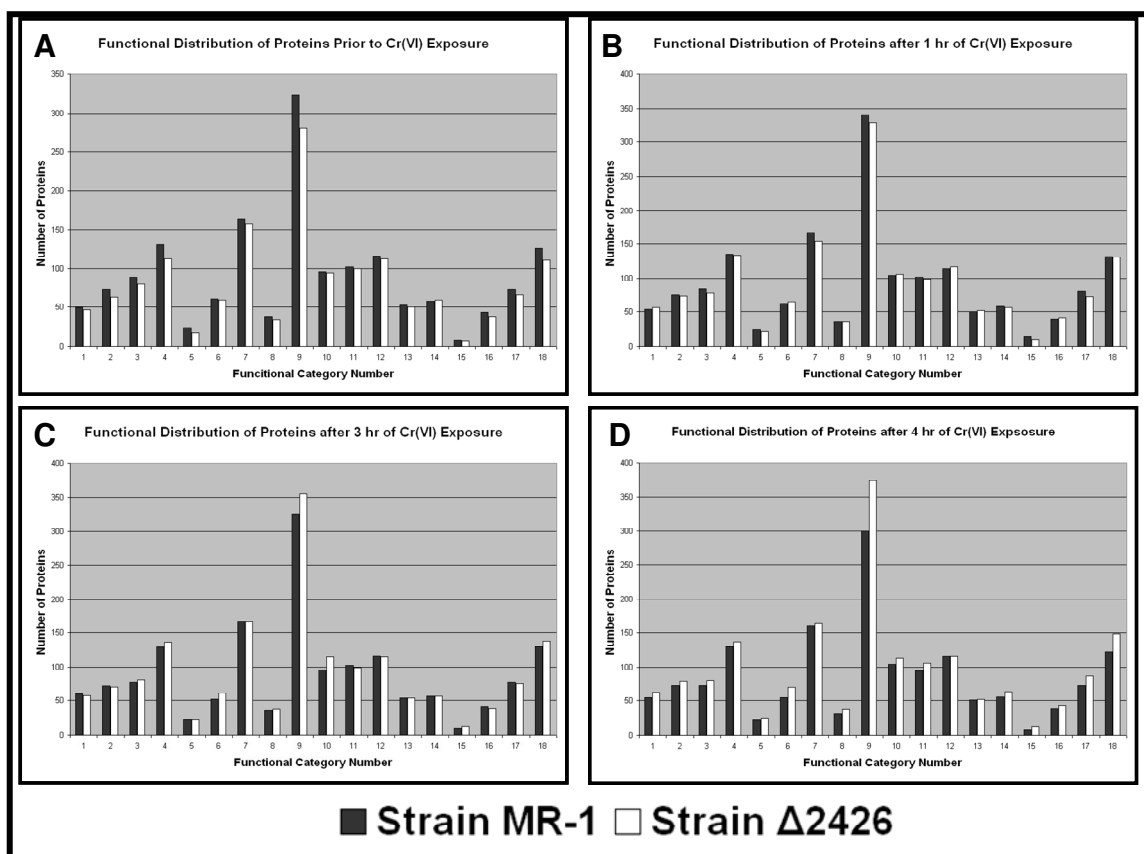


Figure 6.3. Functional category distribution of proteins from strains MR-1 and Δ2426. Distribution for each strain (A) prior to Cr(VI) exposure, (B) after 1 hr of exposure, (C) 3 hr exposure, and (D) 4 hr exposure. The functional category numbers along the x axis are: (1) Amino acid biosynthesis; (2) Biosynthesis of cofactors, prosthetic groups, and carriers; (3) Cell envelope; (4) Cellular processes; (5) Central intermediary metabolism; (6) DNA metabolism; (7) Energy metabolism; (8) Fatty acid and phospholipid metabolism; (9) Hypothetical proteins; (10) Mobile and extrachromosomal element functions; (11) Protein fate; (12) Protein synthesis; (13) Purines, pyrimidines, nucleosides, and nucleotides; (14) Regulatory functions; (15) Signal transduction; (16) Transcription; (17) Transport and binding proteins; and (18) Unknown function.

strain. However, at the 1 h time point (equivalent to acute shock) where no significant Cr(VI) transformation has been detected, there is an increase by at least 20 proteins between the two strains. The effect is much greater in strain $\Delta 2426$, with 48 proteins. In strain MR-1, the resulting number counts for hypothetical proteins declines during the 3 and 4 h time points. In contrast, strain $\Delta 2426$ consistently continues to increase the number of hypothetical proteins detected to the 4 h time point. The protein expression level implications of a number of hypothetical proteins are discussed further below.

Protein expression effects due to deletion of so2426

Within the *S. oneidensis* genome, *so2426* is organized into a cluster with five other genes (*so2422-2425* and *so2427*), which constitutes an approximately 5 kb region of the genome [69]. The gene cluster organization with respect to localization and transcriptional regulation is described in detail in Chourey *et al* [157]. Prior to Cr(VI) introduction into both strains, SO2424 and SO2427 were identified with the same number of peptides indicating there was no polar effect on expression of these proteins (Supplemental Table S1). Following 1 and 3 h of Cr(VI) exposure, SO2424 and SO2427 did not demonstrate a difference in protein expression level (Supplemental Table S2-S3). However, SO2422 was identified with 2 peptides in the mutant strain and not identified in the wild-type strain following Cr(VI) exposure for 1 h. After 3 h of Cr(VI) exposure, SO2422 was identified in both the wild-type and mutant $\Delta 2426$ strains. Following complete reduction of Cr(VI) in strain MR-1 at 4 h post-exposure, SO2422 was not identified as expressed, while SO2424 and SO2427 maintained the same relative protein expression level as prior to Cr(VI) introduction in both strains. SO2423 and SO2425 were not found in the MS/MS data presented here, however they were identified at

baseline levels (2-5 peptides) in previous work [147, 156]. Therefore, the expression of these two proteins may be repressed due to the deletion of *so2426*.

Proteins differentially expressed between strains MR-1 and $\Delta 2426$

Semiquantitation was employed as the method for determining proteins differentially expressed between the two strains. This method takes into account reproducible differences of percent sequence coverage, peptide count, and spectral count between the knockout mutant strain $\Delta 2426$ and the wild-type strain MR-1. Usually, semiquantitation compares the differences between technical replicates of a HPLC-MS/MS experiment having a reproducibility of at least 70% between them. In this study, the use of biological triplicates has reduced the reproducibility between the cultures to 60%, so attempting the semiquantitation method is more difficult and the number of proteins differentially expressed is reduced compared to previous studies on *S. oneidensis* [147, 156, 158].

In light of this criteria, a number of proteins were identified as differentially expressed reproducibly across the cultures between each strain. Table 6.2 comprises the differentially expressed proteins identified as down-regulated in the $\Delta 2426$ cultures. A total of 22 proteins were found down-regulated in $\Delta 2426$ cultures at any given time point, with six of these proteins down-regulated under all of the time points. Out of the total 22 proteins down-regulated in $\Delta 2426$ cultures, 73% were annotated in the functional categories of hypothetical, transport and binding, and energy metabolism during the time-course explored. In addition, 23 proteins were identified as up-regulated in strain the $\Delta 2426$ in comparison to strain MR-1, with only one protein (HugA, a heme transport protein) up-regulated prior to the addition of Cr(VI) to the cultures (Table 6.3). The

Table 6.2. Up-Regulated Proteins from MR-1 Cultures Versus Δ 2426 Cultures

Locus	Time	Average Δ 2426			Average MR-1			Description (Number)
		Peptide Count	Spectra Count	% Coverage	Peptide Count	Spectra Count	% Coverage	
SO0970	0 hr	25.3	55.0	46.8	39.0	105.3	61.4	fumarate reductase flavoprotein subunit precursor (7)
SO1072	1 hr	4.0	5.3	18.2	9.3	14.3	24.9	chitin-binding protein, putative (17)
SO1180	0 hr	5.0	5.0	18.4	10.7	11.7	34.1	PhoH family protein (18)
SO1190	0 hr	0.0	0.0	0.0	11.0	13.0	43.0	conserved hypothetical protein (9)
SO1190	1 hr	0.0	0.0	0.0	12.0	25.0	46.0	conserved hypothetical protein (9)
SO1190	3 hr	0.0	0.0	0.0	18.7	40.7	58.3	conserved hypothetical protein (9)
SO1190	4 hr	0.0	0.0	0.0	14.3	26.3	57.3	conserved hypothetical protein (9)
SO1405	4 hr	0.7	0.7	3.5	5.7	8.0	23.2	transglutaminase family protein (18)
SO1779	4 hr	6.0	7.7	13.2	12.0	18.3	19.3	decaheme cytochrome c (omcA) (7)
SO1784	1 hr	2.7	3.7	7.2	7.7	14.0	14.6	ferrous iron transport protein B (feoB) (17)
SO2492	1 hr	5.7	7.7	10.3	11.0	18.7	21.7	oxidoreductase, acyl-CoA dehydrogenase family (18)
SO2796	1 hr	7.3	9.3	13.4	16.0	24.0	24.2	conserved hypothetical protein (9)
SO2912	0 hr	13.3	18.7	21.3	21.7	38.0	36.9	formate acetyltransferase (pflB) (7)
SO2916	0 hr	22.3	38.0	33.3	31.0	76.0	57.8	phosphate acetyltransferase (pta) (7)
SO3030	1 hr	3.3	4.7	9.9	14.0	22.7	35.4	siderophore biosynthesis protein (alcA) (17)
SO3030	3 hr	2.7	2.7	7.7	8.0	11.3	20.1	siderophore biosynthesis protein (alcA) (17)
SO3032	1 hr	4.3	5.3	9.2	13.7	28.7	27.9	siderophore biosynthesis protein, putative (17)
SO3032	3 hr	5.3	9.0	12.1	9.0	25.3	18.2	siderophore biosynthesis protein, putative (17)
SO3032	4 hr	7.3	12.3	15.0	11.3	27.7	22.5	siderophore biosynthesis protein, putative (17)
SO3033	1 hr	4.3	6.3	10.6	12.7	29.3	26.1	ferric alcaligin siderophore receptor (17)
SO3637	1 hr	9.0	40.0	33.9	15.3	85.3	46.4	survival protein surA (surA) (11)
SO3833	0 hr	5.7	7.7	26.3	11.7	17.0	44.5	peptide chain release factor 1 (prfA) (12)
SO3863	0 hr	3.7	4.3	26.1	15.7	41.0	65.8	molybdenum ABC transporter (modA) (17)

Table 6.2. Continued

Locus	Time	Average $\Delta 2426$			Average MR-1			Description (Number)
		Peptide Count	Spectra Count	% Coverage	Peptide Count	Spectra Count	% Coverage	
SO3863	3 hr	8.7	14.3	39.9	15.3	44.7	63.4	molybdenum ABC transporter (modA) (17)
SO3863	4 hr	7.0	8.3	42.2	16.7	51.7	69.3	molybdenum ABC transporter (modA) (17)
SO3967	0 hr	0.7	0.7	7.4	8.3	12.3	64.4	molybdenum ABC transporter, putative (17)
SO3967	1 hr	1.3	2.0	7.3	12.3	20.3	64.2	molybdenum ABC transporter, putative (17)
SO3967	3 hr	0.7	0.7	2.3	11.0	23.7	59.4	molybdenum ABC transporter, putative (17)
SO3967	4 hr	1.7	1.7	6.5	13.0	29.7	55.0	molybdenum ABC transporter, putative (17)
SO4509	0 hr	0.0	0.0	0.0	16.7	23.7	25.6	formate dehydrogenase, alpha subunit (7)
SO4509	1 hr	0.0	0.0	0.0	12.3	15.7	19.3	formate dehydrogenase, alpha subunit (7)
SO4509	3 hr	0.0	0.0	0.0	8.7	14.3	13.0	formate dehydrogenase, alpha subunit (7)
SO4509	4 hr	0.0	0.0	0.0	9.7	14.7	15.8	formate dehydrogenase, alpha subunit (7)
SO4513	0 hr	3.7	4.0	7.1	15.0	20.0	22.6	formate dehydrogenase, alpha subunit (7)
SO4513	1 hr	0.0	0.0	0.0	6.0	7.3	9.2	formate dehydrogenase, alpha subunit (7)
SO4513	3 hr	0.0	0.0	0.0	6.7	10.3	11.0	formate dehydrogenase, alpha subunit (7)
SO4513	4 hr	0.0	0.0	0.0	6.3	8.7	8.8	formate dehydrogenase, alpha subunit (7)
SO4719	0 hr	18.3	25.0	65.8	31.0	66.7	75.6	conserved hypothetical protein (9)
SO4719	1 hr	22.3	35.3	74.1	32.3	89.0	78.7	conserved hypothetical protein (9)
SO4719	3 hr	24.0	60.7	75.2	38.7	198.7	79.7	conserved hypothetical protein (9)
SO4719	4 hr	22.0	35.3	71.6	38.3	118.3	78.2	conserved hypothetical protein (9)
SO4743	0 hr	0.0	0.0	0.0	9.7	10.3	22.0	TonB-dependent receptor, putative (17)
SO4743	1 hr	0.0	0.0	0.0	16.0	22.7	35.7	TonB-dependent receptor, putative (17)
SO4743	3 hr	3.0	3.0	8.9	14.3	22.0	29.1	TonB-dependent receptor, putative (17)
SO4743	4 hr	2.0	2.0	4.3	9.7	17.3	21.7	TonB-dependent receptor, putative (17)

functional category distribution for up-regulated proteins was more diverse compared to the down-regulated proteins, with 11 different categories represented and no proteins reproducibly up-regulated across the time course. In addition, 14 of the up-regulated proteins were found at the 4 h time point, indicating that differential expression may be due to Cr response and not necessarily the role of SO2426 as a transcriptional regulator.

Proteins annotated under the functional role of hypothetical proteins were identified as being repressed in the Δ 2426 mutant cultures. Two conserved hypothetical proteins (SO1190 and SO4719) were consistently down-regulated during the entire time course. SO1190 was not identified as being expressed in any of the Δ 2426 cultures, while SO4719 was found with an average of $\sim 21 \pm 3$ peptides corresponding to a steady expression level over the time course. In addition, SO4719 behaved similarly in the MR-1 cultures with an average peptide count of 70 ± 5 as well corresponding to a steady expression level during the time course. The corresponding mRNA levels corroborated these results demonstrating an elevated induction of these genes during the Cr(VI) transformation period for strain MR-1 [157]. The predicted protein sequence of SO4719 was aligned to the top blast hits from 16 other sequenced genomes of the genus *Shewanella* (Supplemental Figure S1). SO4719 demonstrated good alignment with a predicted extracellular solute-binding protein (family 1) from eight of the species/strains. This group of proteins are members of the LysR substrate binding protein family, which is part of a larger clan of periplasmic binding proteins. However, SO4719 is not annotated in the clan of periplasmic binding proteins, but rather the protein is located within the protein family of PfamB PB011652 according to the Pfam database [pfam.sanger.ac.uk, [254]]. This family was generated automatically from an alignment

Table 6.3. Down-Regulated Proteins in MR-1 Cultures Versus Δ 2426 Cultures

Locus	Time	Average Δ 2426			Average MR-1			Description (number)
		Peptide Count	Spectra Count	% Coverage	Peptide Count	Spectra Count	% Coverage	
SO0343	1 hr	36.0	78.0	53.3	21.0	38.3	32.3	aconitate hydratase 1 (acnA) (7)
SO0343	4 hr	45.3	116.7	62.4	26.7	53.0	40.3	aconitate hydratase 1 (acnA) (7)
SO0344	4 hr	23.0	48.7	54.0	7.7	10.7	26.2	methylcitrate synthase (prpC) (7)
SO0345	1 hr	18.0	98.3	58.8	13.0	46.0	48.7	methylisocitrate lyase (prpB) (7)
SO0346	4 hr	9.3	14.3	37.7	1.3	1.7	8.5	transcriptional regulator. GntR family (14)
SO0575	4 hr	10.0	13.7	18.7	3.0	6.3	5.3	RNA polymerase-associated protein (hepA) (16)
SO0798	3 hr	6.0	6.3	12.1	0.7	0.7	1.3	conserved hypothetical protein (9)
SO0840	4 hr	45.0	72.0	40.6	19.0	34.0	19.8	acetyl-CoA carboxylase multifunctional enzyme accADC (8)
SO0934	3 hr	6.0	8.3	27.2	0.0	0.0	0.0	conserved hypothetical protein (9)
SO0958	4 hr	11.3	17.0	63.7	6.0	7.0	37.8	alkyl hydroperoxide reductase, C subunit (ahpC) (4)
SO1484	4 hr	8.3	11.3	24.9	1.3	2.3	4.9	isocitrate lyase (aceA) (7)
SO1551	1 hr	13.0	18.0	31.5	4.7	5.7	14.2	GGDEF domain protein (18)
SO1551	4 hr	16.3	33.7	31.8	5.0	7.3	14.4	GGDEF domain protein (18)
SO1898	4 hr	11.3	14.3	62.2	5.3	7.0	42.8	transcriptional regulator, putative (14)
SO1930	4 hr	39.0	69.7	46.3	20.3	34.3	26.9	2-oxoglutarate dehydrogenase, E1 component (sucA) (7)
SO2415	4 hr	16.7	24.7	28.5	7.7	12.3	14.0	ribonucleoside-diphosphate reductase, alpha subunit (nrdA) (8)
SO3089	4 hr	5.7	8.3	23.9	0.0	0.0	0.0	fatty oxidation complex, beta subunit (8)
SO3545	3 hr	25.3	99.3	49.1	14.7	39.0	28.6	OmpA family protein (3)
SO3585	4 hr	8.3	14.0	39.1	0.7	0.7	1.8	azoreductase, putative (4)
SO3669	0 hr	10.7	19.7	21.9	5.3	7.3	13.4	heme transport protein (hugA) (17)
SO3669	3 hr	40.3	155.0	57.3	21.3	57.7	37.2	heme transport protein (hugA) (17)
SO3669	4 hr	42.7	158.7	60.1	24.7	74.0	39.4	heme transport protein (hugA) (17)
SO3681	1 hr	10.7	19.7	79.0	4.0	7.0	46.8	universal stress protein family (4)
SO3914	3 hr	20.7	35.3	28.3	8.0	14.0	10.6	TonB-dependent receptor, putative (17)

Table 6.3. Continued

Locus	Time	Average $\Delta 2426$			Average MR-1			Description (number)
		Peptide Count	Spectra Count	% Coverage	Peptide Count	Spectra Count	% Coverage	
SO3914	4 hr	22.0	30.7	31.8	7.3	10.3	12.3	TonB-dependent receptor, putative (17)
SO4523	1 hr	27.3	58.7	49.7	9.0	16.0	21.5	iron-regulated outer membrane virulence protein (irgA) (17)
SO4523	3 hr	29.0	67.0	45.9	7.0	14.3	18.1	iron-regulated outer membrane virulence protein (irgA) (17)
SO4523	4 hr	34.3	84.3	58.7	11.7	19.0	27.7	iron-regulated outer membrane virulence protein (irgA) (17)
SO4652	3 hr	14.0	32.3	35.4	8.0	19.0	20.8	sulfate ABC transporter, periplasmic sulfate-binding protein (sbp) (17)
SOA0048	1 hr	24.7	31.3	38.5	13.0	16.0	25.5	prolyl oligopeptidase family protein (11)
SOA0048	3 hr	30.0	48.3	44.0	15.3	29.7	29.1	prolyl oligopeptidase family protein (11)

created by Prodom (prodom.prabi.fr) having the annotation of being a tungsten extracellular binding protein. The protein sequence also aligned well with a sulfate substrate binding protein from five of the species/strains. Therefore, SO4719 may be under transcriptional control of SO2426, but does not appear to demonstrate a Cr(VI) exposure-dependent regulation.

SO1190 is located in a putative operon with two other genes (*so1188* and *so1189*), which were identified as highly induced in the microarray work [157]. SO1190 was found with an average of 14 peptides over the time course and demonstrates the highest expression level at the 3 h time point during Cr(VI) transformation. SO1189 was identified solely in the MR-1 cultures during the 0, 1, and 3 h time points, with an average of 2 peptides, and SO1188 was not identified in this study. Our previous study testing acute chromate shock in *S. oneidensis* [147] identified both SO1188 and SO1189 expressed after 45 min of growth in the presence of 1 mM Cr(VI). Both proteins were identified with 2-4 peptides, which is the minimum for positive protein identification according to the criteria in the study. SO1188 was solely identified in the membrane fraction, where 2 peptides from SO1189 were identified in the crude fraction and the rest of the peptides in the membrane fraction. Based on these observations, SO1188-SO1190 may be under the transcriptional control of SO2426.

Due to SO1188 and SO1189 appearing to associate with the membrane fraction of *S. oneidensis* cell lysates previously [147]; this may be the reason the shotgun proteomics results presented here identify SO1189 with the minimum peptide count. The development of mass spectrometry proteome technology is not as mature with respect to sensitivity as microarray technology. In addition, the lysis method utilized here does not

obtain the level of membrane protein coverage found previously through fractionation [147, 156, 158]. Factors such as protein solubility and, in the case of this study, trypsin specificity, reduce the peptide count of membrane embedded proteins. These factors account for some of the discrepancy between microarray and proteomics technologies. For example, each protein contains 12 (SO1188) and 21 (SO1189) tryptic cleavage sites (lysines and arginines). Using biological replicates instead of technical replicates reduces the biological background and increases the confidence level that a protein found up-regulated reproducibly is actually responding to the condition presented to the culture. SO1189 is an example of a protein that was borderline up-regulated during the 3 h time point. Each LC-MS experiment comprised a unique culture of either strain MR-1 or $\Delta 2426$ (indicative of Culture 1, 2, and 3, respectively). Cultures 2 and 3 identified the protein with 3 and 5 tandem mass spectra, respectively, which Culture 3 passes the criteria of spectral count in the semiquantitation method. However, due to the absence of detection of SO1189 in Culture 1, this protein is not reproducibly up-regulated during the time point. If only Culture 3 had been sampled for proteome analysis, this protein would have been identified as differentially expressed for that particular time point.

The most prevalent category to demonstrate down-regulation of proteins was transport and binding. Two transport and binding proteins were repressed during the entire time course in the $\Delta 2426$ cultures. SO3967 encodes a putative molybdenum ABC transporter and was identified predominately in the MR-1 cultures (average of 18.5 peptides) with an increased induction at the 3 and 4 h time points. SO4743 encodes a putative TonB-dependent receptor and was predominantly found in the MR-1 cultures as well, with an average of 12.4 peptides during the time course. SO4743 demonstrated a

different trend with an increased peptide count identified at the 1 and 3 h time points. The 4 h time point demonstrated a similar abundance to that found prior to the addition of Cr(VI) in the media. The Cr(VI)-dependent regulation of this protein is implicated in the results presented here and may be one pathway in which Cr(VI) gains access into the cell. Previously, SO4743 was also found to be highly up-regulated following acute chromate shock [147] and appears to be induced irrespective of Cr(VI) concentration [156]. The repression of transport and binding proteins in strain $\Delta 2426$ during Cr(VI) transformation indicates that SO2426 may be a transcriptional regulator of these particular proteins and may operate in conjunction with Fur to regulate iron homeostasis.

A total of six proteins were found to be repressed in strain $\Delta 2426$ cultures belonging to the functional category energy metabolism. Included in the repressed proteins are two separate alpha subunits of a formate dehydrogenase complex (SO4509 and SO4513). There are a total of three formate dehydrogenase operons encoded in the *S. oneidensis* genome, *so0102-so0104*, *so4509-so4511*, *so4513-so4515*. *so0102-so0104* encode a nitrate inducible formate dehydrogenase with the alpha subunit, *so0102*, containing a selenocysteine residue. SO0102 was identified in both the wildtype MR-1 strain and the mutant $\Delta 2426$ strain with two or three unique peptides, respectively. The presence of SO0102 was identified solely prior to the introduction of Cr(VI) in the cultures. Interestingly, this nitrate-inducible operon appears to demonstrate a low-level constitutive expression in the absence of Cr(VI). One of the subunits of this operon possibly encodes a molybdenum center (SO0103) that coordinates with the selenocysteine containing alpha subunit (SO0102). Therefore, Cr(VI) may be interfering

with molybdenum uptake, which is causing up-regulation of the molybdenum ABC transporter under Cr(VI) stress thereby allowing more molybdenum uptake into the cell.

so4509-so4511 and *so4513-so4515* are organized in tandem and appear to be constitutively expressed under wildtype conditions. Formate dehydrogenase is a multi-protein enzyme complex, which uses the electron donor formate for respiration and utilizes transition metals in the redox center [257]. Prior to the alpha subunit genes in both operons, there are small genes annotated within the genome, *so4508* and *so4512*. There is no evidence found in the proteome datasets to suggest these proteins are expressed. They may represent regulatory sequences, which have characteristics indicative of a protein-coding gene. SO4509, alpha subunit of formate dehydrogenase, was solely identified in the MR-1 cultures over the entire time course. The alpha subunit identified here is the only soluble member of the complex, which explains the ease of identification of this protein [257]. Formate dehydrogenase in MR-1 has been shown to be an important member of the electron transport chain to the terminal ferric reductase in anaerobically grown MR-1 using Fe(III) citrate [102]. Cr(VI) may be inhibiting the activity of formate dehydrogenase under the conditions tested here.

Other energy metabolism proteins identified included a fumarate reductase flavoprotein subunit precursor (SO0970), PflB (formate acetyltransferase), and Pta (phosphate acetyltransferase), which were all found repressed in the $\Delta 2426$ cultures prior to chromate introduction. The decaheme cytochrome c, OmcA, was found to be repressed in $\Delta 2426$ cultures after 4 h of exposure to Cr(VI). This protein is known to play an important role in the reduction of Fe(III) and Mn(IV) in *S. oneidensis* MR-1 [107,

113, 258]. During the other time points sampled for proteome analysis, there is no change in the level of expression between strain MR-1 and $\Delta 2426$ cultures for OmcA.

As mentioned, 11 of the functional categories were represented as up-regulated in $\Delta 2426$ cultures over the time points sampled for proteome analysis. These categories included proteins involved in energy metabolism and iron transport. For the most part, the proteins repressed in $\Delta 2426$ cultures were members of two molybdenum ABC transporters. The proteins up-regulated in $\Delta 2426$ were involved in transport of iron (HugA and IrgA). IrgA was up-regulated during Cr(VI) exposure and transformation in $\Delta 2426$ cultures and was borderline up-regulated prior to Cr(VI) introduction. HugA was up-regulated in the control (0 h) and during active transformation, but borderline up-regulated during the 1 h time point. The up-regulation of these proteins during active Cr(VI) transformation indicates a possible intracellular iron deficiency more pronounced in the $\Delta 2426$ cultures versus wild-type cultures.

A putative operon involved in energy metabolism and comprising genes *so0344-so0346* was identified as up-regulated in strain $\Delta 2426$ (Table 6.3). *so0346* encodes a transcriptional regulator from the GntR family and is at the beginning of the operon. *so0344* (*prpC*) and *so0345* (*prpB*) are located directly downstream of *so0346*. *prpBC* encode methylisocitrate lyase and methylcitrate synthase, respectively, which are required for growth on propionate in *Salmonella enterica* [259]. SO0346 does share over 90% sequence similarity to other members of the genus *Shewanella*, indicating this is a conserved putative transcriptional regulator (data not shown). In addition, the operon structure also appears to be conserved with other *Shewanella* species as well. The GntR family of transcriptional regulators contain a N-terminal helix-turn-helix DNA-binding

domain with one of four subtypes of a C-terminal signaling domain [260, 261]. For SO0346, the C-terminal domain belongs to the FadR subtype, featuring an all alpha-helical structure [260], which are usually involved in regulating activity of proteins involved with amino acid metabolism pathways. This is in contrast to the structural organization of SO2426 and may indicate interaction between these two proteins. The GntR family of transcriptional regulators are known to dimerize with one another [260], the up-regulation of SO0346 may be a consequence of the protein dimerizing with itself in the absence of SO2426.

SO0346 was only detected in strains MR-1 and Δ 2426 upon Cr(VI) introduction to the growth media (Supplemental Tables S1-S4). The level of expression for the other two members of the operon did not demonstrate any change in regulation prior to chromate introduction, indicating that SO0346 is not necessary for transcriptional activation of *so0344* and *so0345*. After 1 h in the presence of Cr(VI), SO0346 was identified in both strains, with only one of the triplicate cultures of strain MR-1 detecting this protein and all three cultures of strain Δ 2426 having a similar detection level for this protein. After 3 h of Cr(VI) exposure, three peptides from SO0346 were found in two of the replicates from strain MR-1 cultures. SO0346 in strain Δ 2426 cultures was borderline up-regulated at this time point with 5, 10, and 12 peptides, respectively identified in the replicate cultures. When approximately half of the Cr(VI) had been transformed in strain Δ 2426, SO0346 was detected up-regulated and only one of the replicate cultures of strain MR-1 detected any peptides at this point corresponding to complete transformation of Cr(VI) (Table 6.3). The transcriptomic data indicates that the gene is up-regulated only after 24 h of exposure in strain Δ 2426 [157]. Based on results

from previous studies [147, 156, 158, 248], SO0346 has not been found to be up-regulated in wild-type cultures exposed to various concentrations and intervals of chromate exposure. At this time, the exact mode of regulation of SO0346 with respect to the proposed function of SO2426 is not clear. Further investigation will be needed in order to decipher the relationship between SO2426 and SO0346 if indeed a relationship exists.

Proteins differentially expressed during Cr(VI) transformation in strain MR-1

Wild-type cultures of strain MR-1 prior to and following exposure to Cr(VI) were compared to identify proteins that are differentially expressed during acute shock and transformation of Cr(VI) (Tables 6.4 and 6.5). A total of 42 proteins were found to be up-regulated following addition of Cr(VI) with two primary functional categories represented (energy metabolism and transport and binding proteins). In contrast, 13 proteins were down-regulated following exposure to Cr(VI) in MR-1 cultures. There was a greater variety of functional categories represented in the down-regulated proteins; however energy metabolism dominated with five members down-regulated. Relatively few proteins identified as down-regulated indicated that the MR-1 cultures had not begun to be stressed by the transformation of Cr(VI) [158].

A number of the proteins found differentially expressed in MR-1 compared to Δ 2426 were also found to demonstrate a Cr(VI) dependent response. For instance, AcnA, aconitate hydratase 1, was found to be up-regulated in response to Cr(VI) exposure in MR-1 cultures, but up-regulated in the Δ 2426 cultures. AcnA and AcnB are well characterized in *E. coli* [262] with a role in the TCA cycle by catalyzing the isomerization of citrate to isocitrate. This important step in the TCA cycle is one reason

Table 6.4. Proteins Identified as Up-Regulated upon Cr(VI) Exposure in MR-1 Cultures

Locus	Average 0hr MR-1 culture			Average Cr(VI) exposed MR-1 culture			Time point	Description (Number)
	Peptide Count	Spectra Count	% Coverage	Peptide Count	Spectra Count	% Coverage		
SO0343	8.7	14.7	12.9	21.0	38.3	32.3	1	aconitate hydratase 1 (acnA) (7)
SO0343	8.7	14.7	12.9	26.0	53.3	39.5	3	aconitate hydratase 1 (acnA) (7)
SO0343	8.7	14.7	12.9	26.7	53.0	40.3	4	aconitate hydratase 1 (acnA) (7)
SO0345	6.7	18.3	37.0	13.0	46.0	48.7	1	methylisocitrate lyase (prpB) (7)
SO0345	6.7	18.3	37.0	16.0	45.0	53.1	3	methylisocitrate lyase (prpB) (7)
SO0429	15.3	19.3	31.5	20.7	41.7	41.0	1	peptidase, M13 family (3)
SO0429	15.3	19.3	31.5	24.3	55.3	45.2	4	peptidase, M13 family (3)
SO0518	1.7	1.7	5.6	6.7	9.7	23.3	4	outer membrane efflux family protein, putative (17)
SO0519	4.0	4.0	15.3	9.0	18.7	31.9	3	cation efflux protein, putative (4)
SO0519	4.0	4.0	15.3	9.7	20.3	34.0	4	cation efflux protein, putative (4)
SO0554	4.0	5.3	26.6	9.3	17.3	50.4	3	hypothetical protein (9)
SO0554	4.0	5.3	26.6	10.3	16.0	45.8	4	hypothetical protein (9)
SO1072	2.7	4.7	11.2	9.3	14.3	24.9	1	chitin-binding protein, putative (17)
SO1072	2.7	4.7	11.2	8.7	10.3	27.8	3	chitin-binding protein, putative (17)
SO1075	11.3	12.0	18.3	17.3	24.3	29.5	1	conserved hypothetical protein (9)
SO1482	5.0	5.3	10.7	10.7	18.0	23.2	1	TonB-dependent receptor, putative (17)
SO1490	23.0	46.7	59.2	29.7	107.3	65.2	4	alcohol dehydrogenase II (adhB) (7)
SO1677	24.3	57.7	64.5	31.0	138.3	73.8	1	acetyl-CoA acetyltransferase (atoB) (8)
SO1678	1.3	2.0	3.1	8.0	19.0	22.6	4	methylmalonate-semialdehyde dehydrogenase (mmsA) (7)
SO1679	11.3	20.7	34.6	18.0	44.0	54.8	3	acyl-CoA dehydrogenase family protein (8)
SO1679	11.3	20.7	34.6	20.0	49.3	52.6	4	acyl-CoA dehydrogenase family protein (8)
SO1755	10.0	15.3	23.7	15.7	34.3	36.7	4	phosphoglucomutase/phosphomannomutase family (7)
SO1816	6.0	7.7	28.6	12.7	30.0	45.9	3	conserved hypothetical protein (9)

Table 6.4. Continued

Locus	Average 0hr MR-1 culture			Average Cr(VI) exposed MR-1 culture				Description (Number)
	Peptide Count	Spectra Count	% Coverage	Peptide Count	Spectra Count	% Coverage	Time point	
SO1894	13.0	18.0	29.5	22.7	42.3	40.4	4	acetyl-CoA carboxylase, biotin carboxylase, putative (8)
SO2903	33.3	214.0	86.6	45.0	482.7	91.9	1	cysteine synthase A (cysK) (1)
SO2903	33.3	214.0	86.6	47.7	474.0	93.5	3	cysteine synthase A (cysK) (1)
SO2903	33.3	214.0	86.6	46.3	526.7	91.2	4	cysteine synthase A (cysK) (1)
SO3030	0.7	0.7	2.2	14.0	22.7	35.4	1	siderophore biosynthesis protein (alcA) (17)
SO3030	0.7	0.7	2.2	8.0	11.3	20.1	3	siderophore biosynthesis protein (alcA) (17)
SO3032	4.3	6.0	8.5	13.7	28.7	27.9	1	siderophore biosynthesis protein, putative (17)
SO3032	4.3	6.0	8.5	11.3	27.7	22.5	4	siderophore biosynthesis protein, putative (17)
SO3033	4.0	7.7	8.1	12.7	29.3	26.1	1	ferric alcaligin siderophore receptor (17)
SO3033	4.0	7.7	8.1	13.3	33.3	24.6	3	ferric alcaligin siderophore receptor (17)
SO3033	4.0	7.7	8.1	9.3	22.0	17.7	4	ferric alcaligin siderophore receptor (17)
SO3145	8.3	22.7	43.7	13.3	46.3	61.2	4	electron transfer flavoprotein, beta subunit (etfB) (7)
SO3237	6.7	13.7	38.2	11.7	43.0	48.3	3	flagellin (4)
SO3238	5.3	12.0	35.0	10.7	37.3	53.7	4	flagellin (4)
SO3430	16.3	23.3	47.4	35.3	133.7	77.1	1	recA protein (recA) (6)
SO3430	16.3	23.3	47.4	37.3	129.3	75.2	3	recA protein (recA) (6)
SO3430	16.3	23.3	47.4	36.7	122.0	85.3	4	recA protein (recA) (6)
SO3462	0.0	0.0	0.0	7.7	10.7	17.1	1	DNA repair protein RecN (recN) (6)
SO3462	0.0	0.0	0.0	11.0	14.0	28.6	3	DNA repair protein RecN (recN) (6)
SO3462	0.0	0.0	0.0	8.0	12.0	19.4	4	DNA repair protein RecN (recN) (6)
SO3599	14.0	28.3	56.5	24.0	88.7	71.9	1	sulfate ABC transporter, periplasmic sulfate-binding (cysP) (17)
SO3599	14.0	28.3	56.5	22.7	90.7	67.1	4	sulfate ABC transporter, periplasmic sulfate-binding (cysP) (17)
SO3667	4.0	4.3	40.6	20.0	87.7	85.8	1	conserved hypothetical protein (9)
SO3667	4.0	4.3	40.6	16.0	69.3	74.6	3	conserved hypothetical protein (9)

Table 6.4. Continued

Locus	Average 0hr MR-1 culture			Average Cr(VI) exposed MR-1 culture				Time point	Description (Number)
	Peptide Count	Spectra Count	% Coverage	Peptide Count	Spectra Count	% Coverage			
SO3667	4.0	4.3	40.6	17.3	64.7	76.6	4		conserved hypothetical protein (9)
SO3669	5.3	7.3	13.4	27.0	78.3	46.9	1		heme transport protein (hugA) (17)
SO3669	5.3	7.3	13.4	21.3	57.7	37.2	3		heme transport protein (hugA) (17)
SO3669	5.3	7.3	13.4	24.7	74.0	39.4	4		heme transport protein (hugA) (17)
SO3673	1.7	3.0	9.1	15.3	35.0	54.1	1		hemin ABC transporter, periplasmic hemin-binding (hmuT) (17)
SO3673	1.7	3.0	9.1	15.7	43.0	52.6	3		hemin ABC transporter, periplasmic hemin-binding (hmuT) (17)
SO3673	1.7	3.0	9.1	16.3	37.3	55.3	4		hemin ABC transporter, periplasmic hemin-binding (hmuT) (17)
SO3726	1.7	2.3	6.3	8.0	13.7	31.6	1		sulfate adenylyltransferase, subunit 1 (cysN) (5)
SO3727	3.7	4.7	18.8	13.0	19.0	43.4	1		sulfate adenylyltransferase, subunit 2 (cysD) (5)
SO3727	3.7	4.7	18.8	12.0	22.7	45.6	3		sulfate adenylyltransferase, subunit 2 (cysD) (5)
SO3737	10.0	11.7	22.5	20.7	39.7	35.7	1		sulfite reductase (NADPH) hemoprotein beta-component (cysI) (5)
SO3737	10.0	11.7	22.5	23.3	47.3	42.3	3		sulfite reductase (NADPH) hemoprotein beta-component (cysI) (5)
SO3914	5.3	9.0	11.1	12.3	17.0	19.2	1		TonB-dependent receptor, putative (17)
SO4134	1.3	1.7	18.6	8.0	13.3	50.0	4		conserved hypothetical protein (9)
SO4215	13.7	20.0	41.3	23.7	46.0	52.9	4		cell division protein FtsZ (ftsZ) (4)
SO4476	0.7	0.7	3.7	7.7	14.3	27.2	4		spheroplast protein y precursor, putative (18)
SO4480	0.0	0.0	0.0	7.3	10.3	14.2	3		aldehyde dehydrogenase (aldA) (18)
SO4652	1.3	2.7	6.3	10.0	32.7	28.8	4		sulfate ABC transporter, periplasmic sulfate-binding (sbp) (17)
SO4655	0.7	0.7	1.9	5.0	11.7	26.2	4		sulfate ABC transporter, ATP-binding protein (cysA-2) (17)
SO4692	9.0	11.3	11.9	14.0	25.3	19.9	1		AcrB/AcrD/AcrF family protein (4)
SO4743	9.7	10.3	23.1	16.0	22.7	35.7	1		TonB-dependent receptor, putative (17)
SOA0100	9.7	15.0	21.4	18.7	35.0	40.9	4		conserved hypothetical protein (9)

Table 6.5. Proteins Identified as Down-Regulated upon Cr(VI) Exposure in MR-1 Cultures

Locus	Average 0hr MR-1 culture			Average Cr(VI) exposed MR-1 culture				Time point	Description (Number)
	Peptide Count	Spectra Count	% Coverage	Peptide Count	Spectra Count	Coverage %			
SO0575	10.0	25.7	15.7	3.0	6.3	5.3		4	RNA polymerase-associated protein (hepA) (16)
SO0848	27.3	41.7	38.0	8.0	13.3	15.2		1	periplasmic nitrate reductase (napA) (7)
SO0848	27.3	41.7	38.0	4.3	5.0	9.8		3	periplasmic nitrate reductase (napA) (7)
SO0848	27.3	41.7	38.0	5.0	7.7	9.7		4	periplasmic nitrate reductase (napA) (7)
SO1519	9.0	10.3	21.1	3.3	3.7	9.1		4	iron-sulfur cluster-binding protein (7)
SO1602	20.0	26.7	14.5	10.0	13.3	7.9		3	multi-domain beta-ketoacyl synthase (18)
SO1602	20.0	26.7	14.5	11.3	16.0	8.3		4	multi-domain beta-ketoacyl synthase (18)
SO1631	10.0	23.0	49.2	4.3	8.3	21.9		4	uridylate kinase (pyrH) (13)
SO2218	14.0	21.0	31.2	8.3	19.7	24.5		4	asparaginyl-tRNA synthetase (asnS) (12)
SO2248	8.0	12.0	17.4	3.7	5.7	12.1		3	L-serine dehydratase 1 (sdaA) (7)
SO2427	26.7	54.0	39.0	20.3	35.0	30.3		4	TonB-dependent receptor, putative (17)
SO2705	20.7	26.0	30.6	9.0	12.0	12.4		3	DNA topoisomerase I (topA) (6)
SO3565	10.7	11.7	19.5	3.0	3.3	6.7		1	2,3-cyclic-nucleotide 2-phosphodiesterase (cpdB) (13)
SO3565	10.7	11.7	19.5	2.3	3.0	5.3		4	2,3-cyclic-nucleotide 2-phosphodiesterase (cpdB) (13)
SO3980	20.7	42.3	36.1	9.0	12.7	20.0		1	cytochrome c552 nitrite reductase (7)
SO3980	20.7	42.3	36.1	5.0	7.3	12.4		3	cytochrome c552 nitrite reductase (7)
SO3980	20.7	42.3	36.1	6.7	7.7	15.4		4	cytochrome c552 nitrite reductase (7)
SO4513	15.0	20.0	20.6	6.0	7.3	9.2		1	formate dehydrogenase, alpha subunit (7)
SO4513	15.0	20.0	20.6	6.7	10.3	11.0		3	formate dehydrogenase, alpha subunit (7)
SO4513	15.0	20.0	20.6	6.3	8.7	8.8		4	formate dehydrogenase, alpha subunit (7)
SO4659	6.0	8.7	21.2	0.0	0.0	0.0		3	conserved hypothetical protein (9)
SO4659	6.0	8.7	21.2	0.0	0.0	0.0		4	conserved hypothetical protein (9)

why the isozyme AcnB has a compensatory pathway. AcnB has been found to be constitutively expressed, but easily inactivated due to demetallation [262]. AcnA is characterized as a compensatory counterpart to AcnB and is resistant to oxidative stress. This resistance is unusual for this type of [4Fe-4S] cluster enzyme. The presence of AcnA is generally as a minor component (i.e. no Cr(VI) added equals ~13 spectra identified); however, during Cr(VI) transformation the prevalence of AcnA increases up to 50 MS/MS spectra identified at the 4 h time point. This result is expected due to the transformation of Cr(VI) to Cr(III), which can proceed through the unstable redox active species Cr(V) [86, 126, 140, 146]. The fact that AcnA demonstrated increased expression in the $\Delta 2426$ cultures compared to MR-1 provides further evidence of the increased oxidative stress in strain $\Delta 2426$ cultures. In addition, the AcnB product was found not to (1) change expression level following Cr(VI) exposure and (2) was not down-regulated in the $\Delta 2426$ cultures. This is expected based on the known role of AcnB in *E. coli* as a house-keeping protein [262].

The alpha subunit of formate dehydrogenase (SO4513) demonstrated a contrasting expression pattern to AcnA. As described above, SO4513 was found to be highly up-regulated in MR-1 cultures and to be expressed in $\Delta 2426$ cultures only in the absence of Cr(VI). This protein was further found to be down-regulated following exposure to Cr(VI) in the MR-1 cultures. All three time points sampled following Cr(VI) introduction revealed approximately the same level of expression (~6 peptides on average identified) in contrast to prior to Cr(VI) introduction (15 peptides on average identified). This result indicates a perhaps complex control mechanism for expression of SO4513.

A number of proteins involved in sulfate uptake and metabolism were also identified as up-regulated upon exposure to Cr(VI) in the MR-1 cultures. CysK, CysP, CysN, CysD, CysI, Sbp, and CysA-2 were all found to be up-regulated post Cr(VI) introduction to MR-1 cultures. In fact, a majority of these proteins were identified as up-regulated during the initial shock time point (1 h post Cr(VI) introduction), indicating an initial up-take of Cr(VI) perhaps through the sulfate system thereby creating an intracellular sulphate deficiency, as has been implicated elsewhere [141]. CysK encodes the enzyme cysteine synthase A, which catalyzes the final synthesis step by condensing sulfide with *O*-acetyl-L-serine to yield cysteine [263]. In *Bacillus subtilis*, CysK was shown to negatively regulate the sulfur metabolism genes similar to the nitrogen metabolism regulatory system [263]. Therefore, the up-regulation of CysK under the conditions presented here implicates a possible deficiency of intracellular sulfur in response to the presence of Cr(VI) or oxidative stress. The possible regulatory role of CysK in *S. oneidensis* is not clear at this time. Two sulfate ABC transporters are encoded in the MR-1 genome (*so3599-so3602* and *so4652-4655*) with three members from these operons up-regulated following exposure to Cr(VI). CysP, the periplasmic sulfate-binding protein, is a member of the first operon and was found up-regulated during the 1 and 4 h time points, but demonstrated an equal expression level at the 3 h time point. Sbp is the periplasmic protein of the second operon and was found up-regulated following complete Cr(VI) transformation at the 4 h time point in addition to member CysA-2, the ATP-binding protein. Since Cr(VI) has been demonstrated as an inhibitor of sulfate uptake [141], there may be a deficiency within the cytoplasm of sulfide leading to the activation of genes necessary for sulfur acquisition and metabolism.

Post-translational modifications of strain MR-1 during Cr(VI) transformation

The 0, 1, 3, and 4 h MR-1 datasets were searched using InsPecT to determine MS/MS containing post-translational modifications (PTMs) overlooked during the initial Sequest search. Thompson *et al* [59] discusses the optimization of the scoring scheme used here, where the p-value threshold chosen for each dataset demonstrates a false discovery rate (FDR) of $2.0 \pm 0.2\%$. Therefore, each dataset will have a unique p-value cutoff due to the scoring distribution of that dataset. Table 6.6 contains the p-value cutoff chosen for each dataset with the corresponding FDRs observed. The p-value distribution was from 0.45 to 0.83 for the four time points of the MR-1 cultures sampled. The resulting FDR when considering PTM-containing peptides only was 12.0-19.0%. For example, the MR-1 culture harvested prior to Cr(VI) addition had a FDR of 2.1% with the p-value cutoff score of 0.45 and a total of 10,871 PTM peptides identified. All PTM peptide identifications can be accessed in Supplemental Table S5. Prior to Cr(VI) introduction into the cultures (0 h), many more PTM peptides were identified. This is in contrast to the non-modifications searches, where a comparable number of total proteins and peptides were identified under all of the time points (Table 6.1). The resulting optimization of the filtering threshold for identification of PTM peptides to a specific FDR leads to a more accurate comparison across the information in the datasets.

The most prevalent PTM in the 0 h dataset was oxidation of methionines, cysteines, tryosines, and tryptophan residues, followed by diacetylation of lysines and arginines. In contrast, there was approximately the same amount of monomethylations as diacetylations in the 4 h dataset and much fewer dimethylations identified. Relative to the total number of PTM peptides identified for the two respective datasets (Table 6.6),

Table 6.6. InsPecT p-value Thresholds and Corresponding FDRs for Strain MR-1 PTMs

Culture Time point	p-value	Total Peptide Identifications			PTM Peptide Identifications		
		Reverse IDs	Total IDs	% FDR	Reverse IDs	Total IDs	% FDR
0 hr	0.45	733	68640	2.1	694	11565	12.0
1 hr	0.70	670	74244	1.8	621	8166	15.2
3 hr	0.83	759	71248	2.1	745	8736	17.1
4 hr	0.75	712	65193	2.2	706	7415	19.0

there were more oxidized peptides found at the 4 h time point relative to the 0 h control. The oxidation identifications for both datasets primarily consisted of monooxidations. In addition, the other two Cr(VI) exposure time points, 1 and 3 h, exhibited the same overall distribution of PTMs characteristic of the 4 h time point. Even though phosphorylations are common signaling PTMs, this modification was not searched in the resulting datasets. In bacteria, most phosphorylations occur on histidine or aspartic acid residues consisting of temporally rapid events that are difficult to detect [52, 236, 264]. In addition, the method of fragmentation utilized in this study (collision induced dissociation) is not amenable for retaining the location of the phosphorylation site on the peptide resulting in a neutral loss of 98 Da as the primary fragment ion [59].

Due to the global differences in PTM characteristics for the time course, the PTM-containing peptides identified for each time point were organized according to the functional category role of the parent protein. Figure 6.4 depicts the category distribution of the peptides from each time point. The protein synthesis role category predominates across all time points as containing the greatest number of post-translationally modified peptides. This is expected due to the proteins encoding the ribosome comprising this role category, which have been shown previously to be highly modified [48]. Peptides with a role in amino acid biosynthesis demonstrated increased modifications indicative of increased control over this process (Figure 6.4). In addition, as exposure to Cr(VI) progresses, proteins involved in cellular processes become gradually more modified indicating a change in the level of regulation. However, a majority of the categories do not change over Cr(VI) transformation time, but rather the constituents that are modified vary.

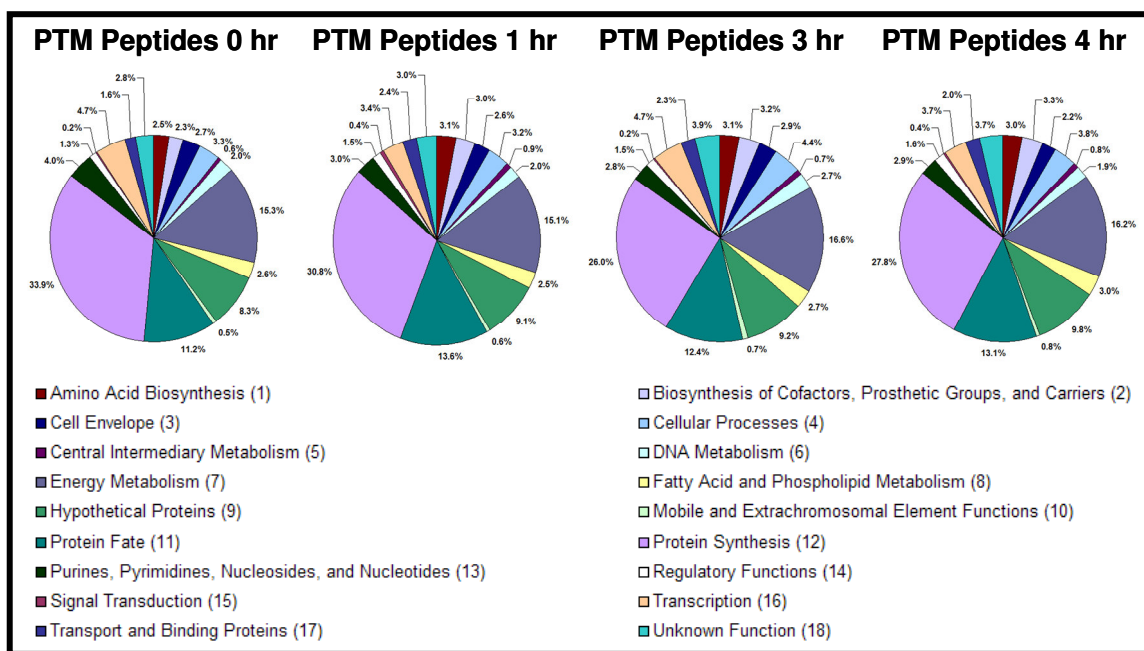


Figure 6.4. Post-translationally modified peptides identified by InsPecT for strain MR-1. Each slice represents a functional category and comprises the percent of peptides for the category identified out of the total PTM peptides for each time point (i.e. 0 hr, 1 hr, 3 hr, and 4 hr).

The functional category of signal transduction comprises proteins involved in gene expression regulation, namely the 53 two-component response regulators annotated in this group. SO2426, which has been knocked out in this study, is an orphan response regulator in this category demonstrating a number of PTMs over time. Over the time course presented here, signal transduction proteins identified as unmodified comprised 8-14 protein identifications. This is expected due to these members having a low copy number within a bacterial cell. By including differential chemical modifications for the InsPecT search, the identification rate of signal transduction proteins increased to at least 11-18 proteins identified over the time course.

A number of signal transduction proteins demonstrated Cr(VI)-dependent modifications during the time course evaluated here. Three proteins demonstrated differential modification states over the time course: SO2426, SO2742, and SO4472. SO2426 is a putative Cr(VI) transcriptional regulator shown here to be involved in controlling gene expression of a number of proteins. SO2742 is an orphan sensor histidine kinase/response regulator similar to SO2426, while NtrC (SO4472) is a nitrogen regulatory protein. Supplemental Figures S2-S4 are the annotated MS/MS of all the modified peptides documented for SO2742. There were a total of seven amino acids found to be chemically modified after 1 and 4 h of exposure to Cr(VI). An oxidized methionine was identified after Cr(VI) exposure for 1 h. After 4 h, two dioxidized methionines, a triply oxidized cysteine, a monomethylated lysine residue, and two arginines were dimethylated and diacetylated, respectively. Interestingly, one of these peptides included the monomethylated lysine, dioxidized methionine, and the dimethylated arginine would not have been identified with previous methods of PTM

search methods [51, 59], due to restrictions in both the computational requirements of algorithms and the flexibility in specifying PTMs in the algorithm parameters. However, the PTMs present on SO2742 are interesting and may point to a level of control for this protein after Cr(VI) transformation has occurred.

SO2426 is a response regulator that has been implicated to specifically respond to Cr(VI) exposure previously [147, 156]. Due to the importance of this protein in response to chromate exposure, understanding possible regulation by PTMs is necessary to decipher both regulation and function within the bacterium. Prior to Cr(VI) addition to the strain MR-1 cultures, the presence of SO2426 was not detected with PTMs and without any proteomic evidence from the non-modifications searches to suggest that the protein had even been translated at that time. Following addition of Cr(VI) to strain MR-1 cultures, SO2426 was identified in the proteome samples acquired, present with and without modified peptides. According to the identifications made by the algorithm InsPecT, a total of five putative spectra were identified as comprising a PTM peptide with two spectra found to be incorrect identifications after manual inspection. SO2426 was identified with 2-3 peptides for all three MR-1 cultures after exposure to Cr(VI) for 1 h. Following 3 h of exposure to Cr(VI), a total of six peptides passed the filter thresholds used for InsPecT. The 4 h time point yielded a total of 3 peptides for cultures 2 and 3 only. The identification of one modified peptide was found in culture 3 as well as the unmodified counterpart. The modification consisted of a methionine oxidation that may or may not be due to the sample preparation procedures used in this study. This same methionine residue was found to be oxidized after culture 2 was exposed to Cr(VI) for 4 h. The identification of a diacetylated arginine was found in culture 2 at the 3 h

timepoint. At this time, there is active transformation of Cr(VI) to presumably Cr(III) (Figure 6.2). The dicetylation was confidently identified by four fragment ions in the MS/MS and corresponds to R13 of SO2426 (Figure 6.5). This peptide also contains a triply oxidized cysteine and a doubly oxidized methionine. The acetylation may be regulatory in nature; however, the significance of this modification is unknown at this time. The regulation is possibly due to the relative proximity of the diacetylated arginine (R13) to an aspartic acid that is putatively phosphorylated aspartic acid (D57) [232].

Conclusions

Although this global proteomic study has provided a great deal of valuable information as to the response of *S. oneidensis* to chromate exposure during the transformation period, much more effort is needed in order to fully appreciate the physiological response to Cr(VI) exposure and stress. The deletion mutant strain Δ 2426 demonstrated a deficiency in Cr(VI) transformation during the time course examined in this study. The deficiency may be due to genes that are involved in chromate transformation being under the control of SO2426. In regards to possible gene control of SO2426, a number of proteins were found to be heavily down-regulated in strain Δ 2426 when compared to the wild-type strain MR-1 during parallel time points. Out of the differentially expressed proteins identified, the presence of a chromate reductase protein was not clear. However, as suggested by Viamajala *et al* [265], there may not be a dedicated chromate reductase encoded in the genome of *S. oneidensis*, but rather a number of reductase enzymes may recognize chromate as a substrate.

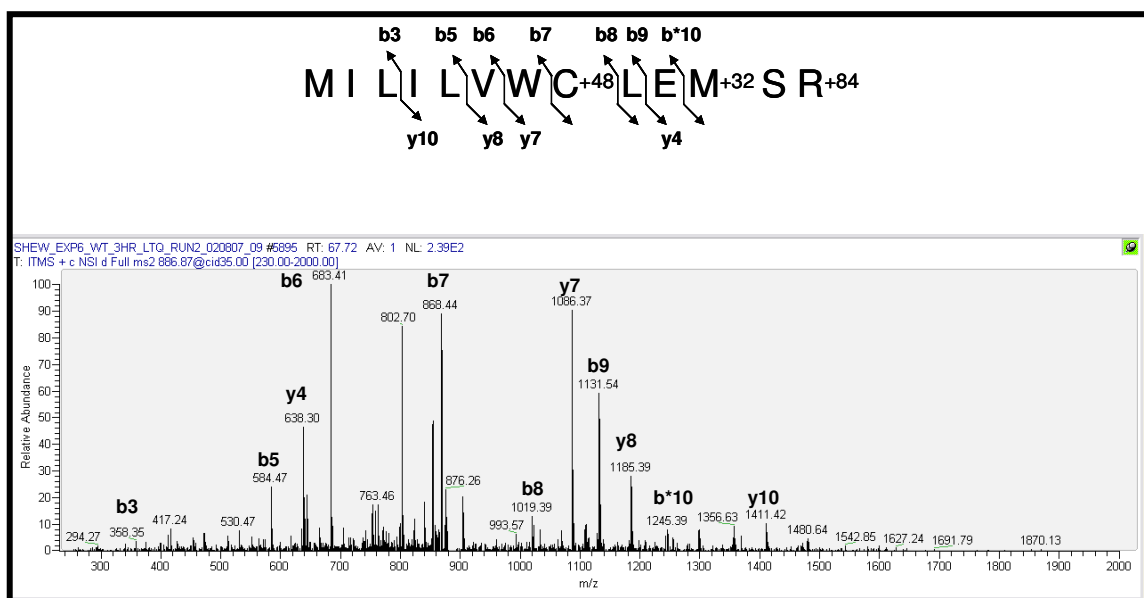


Figure 6.5. A peptide MS/MS from SO2426 with confirmed modifications.

The N-terminal peptide from SO2426 (MILILVWC⁺⁴⁸LEM⁺³²SR⁺⁸⁴) has two oxidation events and a diacetylation event. Fragment ions y4, y7, y8, and y10 confirm the diacetylated arginine residue, while fragment ions b8, b9, and b*10 confirm the triply oxidized methionine. All three modifications are present in fragment ions y7, y8, and y10.

Chapter 7

An Experimental Approach for Large-Scale Proteome Measurements from Small-Scale Amounts of Microbial Cultures and Communities

Portions of the data presented is in preparation for submission for publication

Melissa R. Thompson, Jennifer M. Froelich, Brian Erickson, Nathan C. VerBerkmoes, and Robert L. Hettich. Experimental Approach For Large-Scale Proteome Measurements From Small Amounts (low mg) Of Microbial Cultures. *In preparation for submission to Analytical Chemistry*, 2007. *Melissa Thompson performed sample preparation and LTQ measurements with the assistance of Jennifer M. Froelich, Brian Erickson, and Nathan C. VerBerkmoes. All data analysis was performed by Melissa R. Thompson. Supplemental material located at journal website.*

Introduction

A foremost consideration in shotgun proteomics experiments has been the amount of biomass needed for deep proteome characterization by LC-MS. With many different methods of lysing microorganisms available to choose from, the most common methods utilize a manual disruption of the membrane to release the protein complement of the cell. Research in mass spectrometry-based proteomics has focused both method development and application efforts on microorganisms that are readily cultured in a laboratory. The limited range of organisms that can be cultured and studied with this technique is one of the many disadvantages to limiting the scope of investigation with these approaches. In addition, many tissue samples available from more complex organisms may be limiting as well [266].

In general, the amount of starting microbial cellular material has been a limiting factor in shotgun proteomics experiments. A relatively large quantity of biomass has

been the standard for an in-depth analysis of the protein complement in a given organism. Investigations published as recently as 2006 demonstrate the large amounts of cellular biomass (greater than 1 g) needed for an evaluation of the resulting proteome [63, 97, 267-269]. In 2003, Corbin *et al* [267] investigated the relationship between the transcriptome and the proteome of *Escherichia coli* MG1655. In order to obtain enough material for the proteome analysis, cultivation of $\sim 3 \times 10^9$ cells in a 100 mL culture was necessary. Furthermore, a recently published study by Ding *et al* [63] on various growth conditions of the dissimilatory metal-reducing bacterium *Geobacter sulfurreducens* also exploited large culturing conditions (a 1.5 L culture volume) to obtain a suitable quantity of starting cellular material. The significant quantity of starting material needed is also due to the considerable losses inherent to the sample processing steps, which involve lysis, fractionation, digestion, and cleanup. In addition to lysis, proteome experiments usually involve the fractionation of protein into a membrane-associated and a soluble fraction [63, 147, 156, 270]. Fractionation of cellular lysate requires greater amounts of starting material (at least 750 mg) due to the inherent losses caused by centrifugal separation and splitting the sample. However, fractionation was necessary previously, in order to routinely identify low-abundant proteins. The use of technical replicates also requires an increase in the amount of starting biomass. Developing a method where lysis and digestion occur in the same tube reduces the number of surfaces proteins/peptides come in contact with, thereby reducing sample losses, while maintaining a level of proteome coverage similar to the traditional lysis method.

The ability to efficiently rupture the cellular membrane of an organism, whether it is of macro- (mammalian tissue) or micro-size (bacteria) has been at the forefront of

biological research. In 1970, Coleman *et al* first described the enzyme lysozyme as an efficient agent to disrupt the cellular membrane of bacteria exposing the nucleic acid inside [271]. However, this technique is unsuitable for gram-positive bacteria, which have a different membrane composition [272]. Van Huynh *et al* described a method of lysing gram-positive bacteria using DMSO instead of a lytic enzyme [272]. Both of these methods are not suitable for shotgun proteomics experiments due to the use of excessive amounts of an enzyme for the lysozyme method [271] and employment of SDS detergent for the DMSO method [272]. The lysozyme protein would suppress the signal of endogenous proteins and SDS interferes with the activity of the commonly used protease trypsin [273] as well as the resulting LC-MS/MS analysis [274] in a shotgun proteomics experiment. Therefore, a new method of lysis had to be developed to alleviate these inherent problems associated with shotgun proteomics. Two methods of manual disruption, sonication and French press, of microbial cells have been used extensively [275, 276], and have been shown to be efficient in lysing bacterial cells [276]. The disadvantage of these lysis methods is their requirement for milliliter volumes of sample. As discussed below for microbial ecology studies, there will most likely not be that much starting material available. Designing a method of lysis that does not require a large volume for the suspended cells is critical in order to fully utilize the capabilities offered by shotgun proteomics experiments. To address this issue, Wang *et al* in 2005 developed a method of lysis that utilizes trifluoroethylene (TFE) as a lysing agent followed by urea as the protein denaturant [266]. The disadvantage of this method is the increased dilution needed after the denaturing step to minimize trypsin inhibition in urea [277]. The method

described in this study uses Guanidine HCl as both a lysis agent and denaturant yielding in-depth proteome coverage.

To date, the number of microbial species that are cultivable has been estimated to be less than 1% [278-280]. In fact, the estimate for genome complexity in soil is equivalent to ~6000-10,000 *E. coli* genomes, but the complexity that is actually recovered through cultivation is equivalent to 40 *E. coli* genomes [281]. This creates a bias in the characterization and understanding of microbes with respect to both their evolutionary role and their metabolic role in the natural world [280]. Many ecologists and population geneticists understand the need for utilizing a proteomics approach for classifying metapopulation structures and the adaptive processes at work in the natural environment [282]. Microorganisms play key metabolic roles in natural settings like degradation and transformation of metal and organic pollutants in the soil [71, 121, 129, 283] and are utilized in the treatment of sewage wastewater [284, 285]. A few studies on the proteome characterization of natural microbial communities have been published to date. Wilmes and Bond [284, 285] utilized two-dimensional polyacrylamide gel electrophoresis (2D-PAGE) to characterize proteins present in a laboratory-scale activated sludge system. Powell *et al* [286] in 2005 used a similar yet distinct approach to characterize the dissolved organic matter (DOM) of marine environments utilizing SDS-PAGE LC-MS and MudPIT [33]. Recent work in our laboratory has demonstrated the comprehensive characterization of a natural microbial community found in acid mine drainage [65]. This microbial community thrives in the mine drainage, and was characterized by LC/LC-MS/MS. All of these studies discuss the critical need for better sample preparation methods, in particular for processing small samples for characterizing

natural microbial communities. A comprehensive approach to the lysis of the microbes, chromatographic separation of the digested peptides, and analysis of shotgun proteomics data from microbial communities will greatly expand knowledge in microbial ecology.

Materials and Methods

Reagents, Sample Acquisition, and Sample Preparation

Chemical reagents (i.e. Guanidine HCl) were acquired from Sigma Chemical Co. (St. Louis, MO) and were used as supplied without further purification. Modified sequencing grade trypsin (Promega, Madison, WI) was used for all protein digestions. Trifluoroethylene (TFE) was purchased from Fluka (Buchs, Switzerland). HPLC-grade water and acetonitrile were obtained from Burdick & Jackson (Muskegon, MI), and 99% formic acid was purchased from EM Science (Darmstadt, Germany). Wild-type *Shewanella oneidensis* MR-1 was cultivated under aerobic conditions as described in Brown *et al* [147] and was a gift from Dr. D. Thompson. Wild-type *Rhodopseudomonas palustris* CGA0010 was cultured under photoheterotrophic conditions and was a gift from Dr. D. Pelletier of Oak Ridge National Laboratory. The AMD biofilm was sampled from the Richmond Mine as described [65] and was a gift from Dr. J. Banfield of the University of California at Berkley.

Five separate lysis techniques were tested during the course of this study: sonication, Guanidine HCl, TFE, freeze-grinding, and bead-beating. Figure 7.1 depicts a flow diagram of the experimental differences (sample size, preparation steps) between the lysis techniques of sonication and the two single tube (Guanidine HCL and TFE) methods described here. Sonication was performed on *S. oneidensis* and *R. palustris* as a control lysis technique and is described in detail in [147] for *S. oneidensis*, with the only

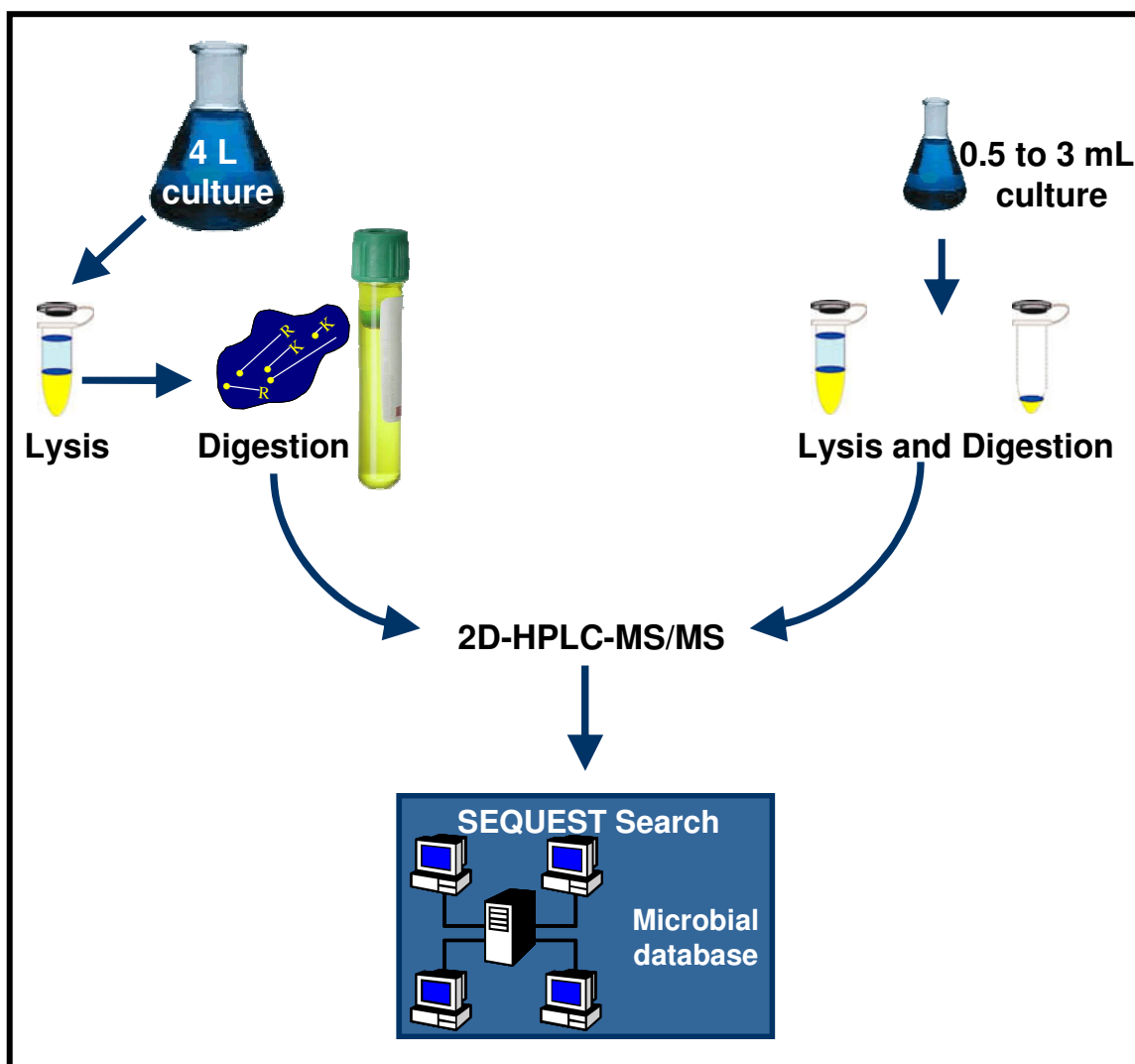


Figure 7.1. Schematic of the traditional sonication versus the single tube lysis method. In a traditional sonication lysis, this requires approximately 4 L of culture to obtain ~4 g of wet cell pellet. While, the single tube lysis method requires much less ~0.3 to 5.0 mL of culture for down to 1 mg of wet cell pellet.

modification for *R. palustris* being 10-30 s sonication pulses. The Guanidine HCl lysis method was performed by lysing and simultaneously denaturing the resulting protein content with 6 M Guanidine/10 mM DTT dissolved in 50 mM Tris/ 10 mM CaCl₂ pH 7.6 (Tris Buffer) overnight at 37 °C with details described in Chapter 2. Lysis using TFE was performed in the same manner as the Guanidine HCl method except TFE was added initially at a concentration of 50:50 TFE:Tris Buffer/10mM DTT. For the AMD biofilm, two other methods were attempted in addition to guanidine-lysis and TFE. The freeze-grinding method was performed by first flash-freezing the biofilm with liquid N₂ followed by pulverization of the biofilm for subsequent cellular lysis and digestion as described in Chapter 2. A bead-beating method was also attempted for the AMD biofilm to determine if this method would destroy the biofilm structure and is also described in Chapter 2. Details of the tryptic digestion following lysis can be found in Chapter 2.

Protein Yield Quantification

Wet cell pellets of 1, 5, and 10 mg from *R. palustris*; 1, 5, and 10 mg from *S. oneidensis* were lysed overnight in 6 M Guanidine HCl/ Tris Buffer. Lysates were then centrifuged to pellet cellular debris and BCA analysis (Pierce, Rockford, IL) was performed according to the manufacturer's instructions. A total of eight replicate cell lysates were analyzed for the 1 & 5 mg *R. palustris* and 1, 5, & 10 mg *S. oneidensis* samples, with the Biofilm samples and 10 mg *R. palustris* sample having two replicates. The average protein yield with standard deviation error bars was plotted in Excel (Microsoft, Redmond, WA). The working absorbance range for the samples was 0.2 to 2.0. Due to interfering chromophores present in the AMD biofilm, the BCA quantification was not performed.

LC/LC-MS/MS Analysis

All resulting lysis samples were analyzed via two-dimensional on-line liquid chromatography using identical Ultimate pumps (LC Packings; a Division of Dionex, San Francisco, CA) coupled to a LCQ ion trap (Thermo Electron, Waltham, MA) or a LTQ linear trapping quadrupole (Thermo Electron). The flow rate of the Ultimate pump at ~100 μ L/min was split pre-column to achieve a final flow rate at the nanospray tip of ~300 nL/min. The samples were loaded onto a split-phase column (packed in-house with C₁₈ reverse phase and SCX chromatographic resin) as described in [147]. The split-phase column was placed behind a 15 cm C₁₈ analytical column (packed in-house [147]) and both were situated in front on a Thermo Electron nanospray source for the LCQ and a Proxeon nanospray source (Odense, Denmark) for the LTQ. The liquid chromatographic method used here for analyses with the LCQ and LTQ consisted of increasing step pulses of (0-500 mM) ammonium acetate salt, followed by a 2 hr 100% aqueous (95% H₂O, 5% ACN, 0.1% formic acid) to 50% organic (30% H₂O, 70% ACN, 0.1% formic acid) gradient. During the liquid chromatographic separation both the LCQ and LTQ were operated in a data-dependent mode [147, 156] and under the control of the Xcalibur software (Thermo Electron).

Proteome Bioinformatics

The following databases were used to search resulting MS/MS spectra with the algorithm Sequest [39] or DBDigger [44]. For the *S. oneidensis* dataset, the database (4,798 open reading frames) was downloaded from TIGR (www.tigr.org, Comprehensive Microbial Resource) and concatenated with a list of common contaminants (trypsin, keratin, etc.). The *R. palustris* dataset used the database annotated at Oak Ridge National

Laboratory and can be accessed at compbio.ornl.gov/rpal_proteome/databases. The AMD biofilm database used was from Tyson *et al* [67]. The following parameters were used for all searches: enzyme type, trypsin; Parent Mass Tolerance, 3.0; Fragment Ion Tolerance, 0.5; up to 4 missed cleavages allowed, and fully tryptic peptides only. Output files were then sorted with DTASelect [171] with the following filtering criteria for the Sequest searches: tryptic peptides only, delCN value of at least 0.08, and Xcorr values of at least 1.8 (+1), 2.5 (+2), 3.5 (+3). For the DBDigger searches the following criteria were applied using DTASelect [171]: tryptic peptides only, delCN of 0.08, and MASPIC [173] scores of at least 25 (+1), 30 (+2), and 45 (+3). The criteria used here have been tested in our laboratory [59, 65, 156, 184, 287] and give a false positive identification rate between 1-2% for bacterial isolates as well as simple microbial mixtures and communities. A comprehensive list of all proteins identified for a given sample size was created using the algorithm Contrast [171].

Results and Discussion

Lysis Efficiency

In order to determine the efficiency of Guanidine HCl as a lysing agent with respect to bacterial cells, control lysing experiments (sonication) of *R. palustris* and *S. oneidensis* were performed (Figure 7.2), and protein was quantified using the BCA analysis. The results for a *R. palustris* cell pellet of 1 mg yielded 85.6 ± 18.9 $\mu\text{g/mL}$ protein (equates to 94.16 μg of total protein) and the 5 mg pellet 286 ± 45.6 $\mu\text{g/mL}$ protein (equates to 343.2 μg of total protein). The *S. oneidensis* 1 mg cell pellets yielded 276 ± 52.4 $\mu\text{g/mL}$ protein and the 5 and 10 mg protein yields were initially above the working absorbance range, so a second set of replicates were diluted 2-fold and yielded

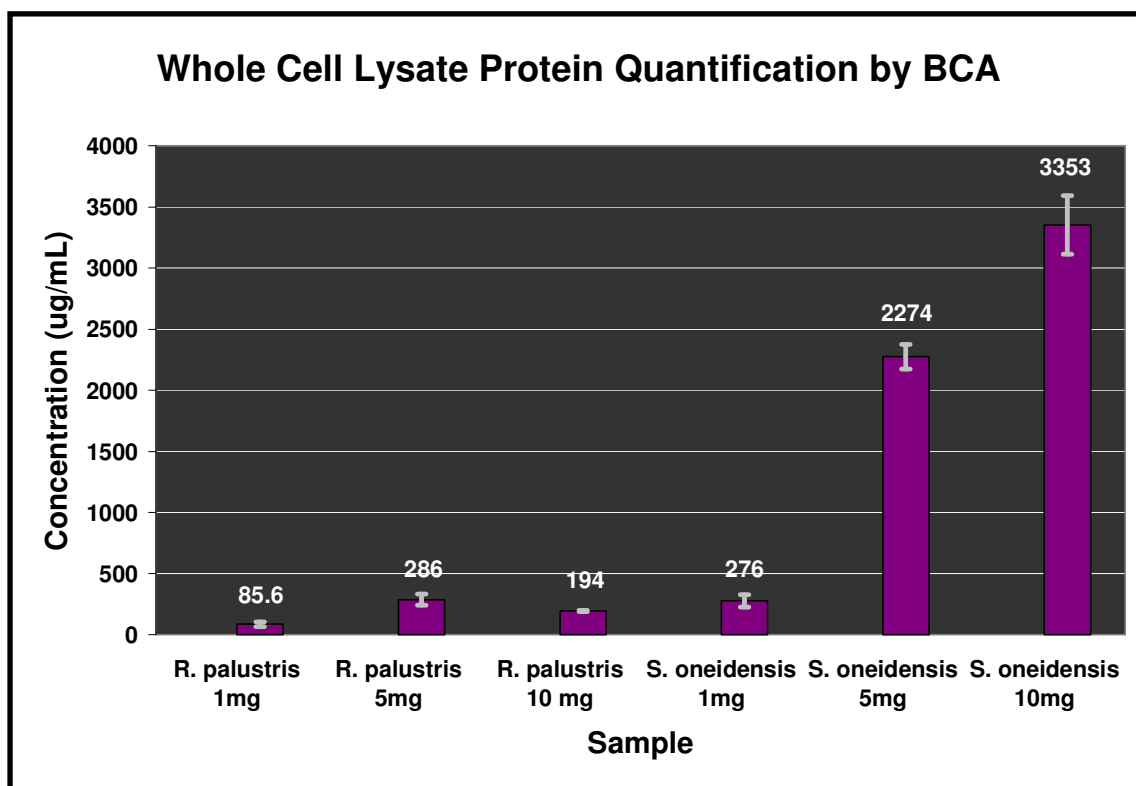


Figure 7.2. BCA protein quantification assay for different amounts of wet cell pellets. Protein quantification was performed with 1, 5 or 10 mg of *R. palustris* lysed by adding 6 M Guanidine or 1, 5, or 10 mg of *S. oneidensis* by the addition of 6 M Guanidine. Error bars represent triplicate measurements and values within the bar graph are the average protein measured for each cell pellet mass for the respective bacterial species.

2274 \pm 102 and 3353 \pm 241 μ g/mL protein, respectively. As apparent from above, this method lyses *S. oneidensis* more efficiently than *R. palustris*, which is due to their respective membrane compositions. The membrane of *R. palustris* grown photoheterotrophically contains many infoldings [288] that are not present in *S. oneidensis*; which makes penetrating the membrane for lysis more difficult. Therefore, a way to improve the lysing efficiency of *R. palustris* is to add more denaturant (Guanidine HCl) to the cell pellets.

Bacterial Isolates Characterization

S. oneidensis wet cell pellets were lysed using sonication and Guanidine HCl in order to assess the proteome coverage identified with both methods of lysis. From a total of ~6 g of wet cell pellet harvested, ~4 g was lysed by sonication to yield ~82.5 mg of crude protein. The other 2 g of wet cell pellet was resuspended at a concentration of 1 g/mL, and then aliquoted into the smaller samples accordingly. Using a LCQ ion trap mass spectrometer, the number of proteins identified for each of the different cell pellet sizes was similar to the 4 g sonication lysis sample, when the samples were desalted offline by solid phase extraction (Table 7.1). There is a marked decrease in identification from samples desalted online, suggesting interference of the samples with the chromatography system. The Comprehensive Microbial Resource at TIGR (www.tigr.org) organizes the *S. oneidensis* MR-1 predicted proteome into 18 functional category assignments. By examining the proteins identified in each category, the distribution of the observed proteome is inferred. According to this metric, lysing 1 and 5 mg of wet cell pellet provides a more comprehensive identification rate (more proteins identified) versus sonication in eight of the 18 functional categories including the signal

Table 7.1. Protein Identifications Made Using the LCQ Ion Trap

Organism	Biomass Size	Number of Proteins
<i>S. oneidensis</i>	4 g	754
<i>S. oneidensis</i>	50 mg	700
<i>S. oneidensis</i>	25 mg	782
<i>S. oneidensis</i>	10 mg	698
<i>S. oneidensis</i>	10 mg	502*
<i>S. oneidensis</i>	5 mg	791
<i>S. oneidensis</i>	5 mg	567*
<i>S. oneidensis</i>	1 mg	820
<i>S. oneidensis</i>	1 mg	515*

* Online desalting of peptide mixture.

transduction category (Supplemental Table S1). Proteins involved in signal transduction are of low abundance normally and in the sonication lysis sample, no proteins were identified at the two-peptide level belonging to this category. However, from a cell pellet of 1 mg, a response regulator (SO4003) was identified with two peptides and the 5 mg cell pellet sample yielded the identification of a sensor histidine kinase (SO4173) with two peptides as well. These proteins are of low abundance, as evident by their level of detection here, but they are of great importance to cellular function. Identification of low abundance proteins is vital to understanding cellular responses to growth perturbations.

In order to determine if the resulting identifications were biased against membrane fraction proteins, the following samples were compared against identifications found in membrane fraction proteomes [147, 158]. For the control sonication sample, 60% of the membrane fraction proteins identified in previous studies was identified. The 1 and 5 mg samples did better, with 65-67% of the membrane fraction proteins being identified. However, using the LCQ ion trap without fractionating the samples into soluble and membrane fractions results in a loss of around 40% of the protein identifications. This method of lysis is not well suited for the LCQ ion trap instrumentation platform.

The LTQ linear trapping quadrupole has been described extensively as a more high-throughput instrument [31, 32, 156, 215]. Therefore, the *S. oneidensis* samples were also analyzed by this instrumentation platform (Table 7.2 and Supplemental Table S2). For the control sonication samples, a total of five sample analyses were conducted, yielding from 1229-1333 proteins identified under a single sample analysis and the total number of proteins identified was 1,831. Table 7.2 depicts the combined list from the top

Table 7.2. Functional Category Distribution for *S. oneidensis* MR-1 LTQ Dataset

Number	Functional Category	4 g	5 mg	1 mg
1	Amino Acid Biosynthesis	58	52	40
2	Biosynthesis of Cofactors, Prosthetic Groups, and Carriers	86	82	63
3	Cell Envelope	94	94	73
4	Cellular Processes	148	143	122
5	Central Intermediary Metabolism	26	27	21
6	DNA Metabolism	64	67	47
7	Energy Metabolism	189	182	161
8	Fatty Acid and Phospholipid Metabolism	38	37	35
9	Hypothetical Proteins	375	373	250
10	Mobile and Extrachromosomal Element Functions	106	100	93
11	Protein Fate	119	115	92
12	Protein Synthesis	124	116	106
13	Purines, Pyrimidines, Nucleosides, and Nucleotides	55	55	52
14	Regulatory Functions	65	71	47
15	Signal Transduction	16	16	5
16	Transcription	41	41	35
17	Transport and Binding Proteins	70	79	43
18	Unknown Function	151	155	115
Total		1825	1805	1400

three MS experiments. The 5 mg lysis was analyzed in triplicate and yielded protein identifications from 1282-1472, with a total of 1,805 proteins identified from the three analyses. The 1 mg lysis was analyzed once and detected 1308 proteins. Note that the number of proteins identified by the LTQ is more than twice that of the LCQ, therefore it is reasonable to assume there would be less bias with this instrumentation platform.

Indeed, when analyzing the functional category distribution between the 5 mg lysis and the control sonication samples (Supplemental Table S2), nine of the eighteen functional category assignments for the 5 mg sample are represented by equal or greater number of proteins when compared to the control sonication sample. In fact, the category of signal transduction contains 16 members for the LTQ dataset. Thirteen of the protein members are shared between the two lysis techniques, indicating a similar performance between the two analyses. Proteins localizing to membrane fractions in the previous studies described above were also analyzed with the LTQ dataset. The results indicate for the 5 mg lysis sample an overlap of 82% of membrane fraction proteins identified from previous experiments were found. For the control sonication sample, between 45 and 47% of proteins were identified in the control sonication that localized to the membrane fraction in previous experiments. The 1 mg lysis sample was intermediate, with 66-68% of the membrane fraction proteins identified. Therefore, the smaller biomass (1 and 5 mg) samples performed better with the LTQ than the LCQ with respect to membrane fraction protein identification, but also performed better than the control sonication sample for both instrumentation platforms.

The metabolically diverse bacterium *R. palustris* was also utilized to test the ability of Guanidine HCl as both a lysis and reducing agent. As above, one aliquot was

sonicated while the other was used to test Guanidine HCl and TFE (results below). The LTQ mass spectrometer was utilized in assessing the *R. palustris* sample with a total of three control sonication samples and three 1 mg Guanidine HCl lysates to be compared. A total of 1,897 proteins were identified in the 2 g sonicated *R. palustris* cell pellet, and the 1 mg Guanidine HCl cell lysate yielded 1,797 proteins (Supplemental Table S3). As above with *S. oneidensis*, there is not a significant difference in protein identifications with sonication versus Guanidine HCl. However, the significant advantage of Guanidine HCl appears to be the chemical's ability to efficiently lyse cells and simultaneously denature the protein complement in a single tube experiment for tryptic digestion and subsequent mass spectrometry analysis. The *R. palustris* predicted proteome is divided into 16 functional category assignments, and these are used to compare the bias in sampling between the two methods. First, the sonicated sample identified 39.4% of the total predicted proteins in the genome, with unknowns and unclassified, lipid metabolism, translation, amino acid metabolism, metabolism of cofactors and vitamins, and purine and pyrimidine metabolism dominating with over 60% of the constituent members being confidently identified. The 1 mg Guanidine HCl lysates performed similarly, with 37.3% of the predicted proteins identified and the same functional categories dominated the identifications.

Therefore, lysing 1-5 mg bacterial isolates with Guanidine HCl gives comparable and less biased coverage of the resulting proteome, as compared to a 2-4 g control sonication lysate. The results presented here suggest a new era in “shotgun” proteomics experiments, where small < 10 mL of culture can be sampled and the subsequent proteome analyzed. Sampling of a cell culture with a lower cell density leads to

understanding microbial processes and relationships in the environment. Plus, this leads to the ability to analyze environmental samples where the limiting factor will most likely be the amount of starting material present. In order to assess Guanidine HCl as a method for lysing environmental samples, the following acid mine drainage biofilm was tested.

Comparison of Guanidine HCl versus Trifluoroethylene

Recently, a similar small-scale approach has been published, highlighting the use of trifluoroethylene (TFE) as a lysing agent for mammalian tissue preparations [266]. TFE has been used in the past for stabilizing bacterial membrane proteins [289]; therefore its use as a lysing agent would be compatible with the system presented in this study. Instead of further denaturing the resulting proteins present in the cell lysates, TFE was added in a higher concentration initially and then diluted 6-fold to minimize interference with trypsin. In our study, *R. palustris* was lysed by sonication, Guanidine HCl, or TFE. A 1 mg wet cell pellet was used in the small sample lysing studies. These samples were analyzed in triplicate on the LTQ mass spectrometer, and the following results were obtained. For the Guanidine HCl lysate, 1334-1467 proteins were identified by mass spectrometry, with a total of 1797 found in the three replicate experiments. The TFE lysate identified between 1566-1635 proteins, with a total of 1992 found in three replicates.

These results were further analyzed in order to determine whether or not a bias in protein identification was present. The experimental reproducibility for these samples was determined; however, due to the nature of the lysing methods (both as lysing agent and denaturant), bias should not be present. Experimental reproducibility is defined as the percentage of proteins from the total list (i.e. 1797) that are identified in each

replicate experiment. Here, the replicate experiment is a technical replicate, since only one data-dependent LC/LC-MS/MS experiment can be performed for each lysate. For the Guanidine HCl lysate, the reproducibility was 58.2% and for the TFE lysate, 60.2%. This demonstrates that reproducible lysing, digestion, and mass spectrometric analysis of the resulting peptides occurs at a similar level between the two lysing methods. Furthermore, as depicted in Table 7.3, comparable identification across all 16 functional categories in the predicted proteome was achieved with these lysing techniques. Using either Guanidine HCl or TFE results in a similar proteome dataset for bacterial isolates.

Proteome analysis of the AMD biofilm with the single-tube methods

The Guanidine HCl, TFE, and freeze-grinding single-tube lysis methods as well as the bead-beating method were tested for the AMD biofilm. The community consists of five dominant members from both the bacterial and archeal domains found in a rigid matrix [65]. Table 7.4 illustrates the proteome measurement from various cell pellet sizes with all lysis methods using the algorithm DBDigger for searching. DBDigger was chosen for searching this dataset due to the increased speed of the algorithm for searching MS/MS data against large predicted protein databases [44]. A total of 527 proteins were identified from less than 20 mg of biofilm using the Guanidine HCl method and 391 from a comparable biofilm size with TFE. When a subsequent biofilm (C75) was tested with Guanidine HCl, freeze-grinding, and bead-beating with sample sizes from ~60-250 mg as well as a sonication control of 7.5 g, this resulted in even fewer protein identifications. The average identification rate for the Guanidine HCl method was 14 proteins for the two samples analyzed. The bead-beating was even worse with only up to 9 proteins identified. Freeze-grinding with liquid nitrogen seemed the most promising with an

Table 7.3. Functional Category Distribution for *R. palustris* LTQ Dataset

Number	Functional Category	2 g Sonication	1 mg Guanidine	1 mg TFE
1	Hypothetical	30	44	45
2	Unknowns and Unclassified	269	284	278
3	Replication and Repair	53	30	40
4	Energy Metabolism	130	122	148
5	Carbon and Carbohydrate Metabolism	81	64	78
6	Lipid Metabolism	110	95	115
7	Transcription	76	65	70
8	Translation	140	133	131
9	Cellular Processes	250	236	279
10	Amino Acid Metabolism	125	110	122
11	General Function Prediction	206	172	184
12	Metabolism of Cofactors and	110	87	100
13	Conserved Hypothetical	77	62	71
14	Transport	121	176	193
15	Signal Transduction	76	77	95
16	Purine and Pyrimidine Metabolism	43	40	43
Total		1897	1797	1992

Table 7.4. AMD Biofilm Proteome Measurements using DBDigger with the LTQ

Biofilm Mass	Biofilm	Lysis Method	Protein IDs	Peptide IDs	Spectra
29.1 mg	AB	TFE	391	6767	10477
401.2 mg	AB	TFE	158	1292	2197
16.5 mg	AB	Guanidine	527	8681	21113
97.9 mg	AB	Guanidine	551	7950	20886
386.2 mg	AB	Guanidine	95	2514	9995
69.3 mg	C75	Guanidine	column clogged no information available		
176.67 mg*	C75	Guanidine	15	26	87
248.54 mg*	C75	Guanidine	13	23	91
59.5 mg	C75	Freeze-grinding	21	34	50
178.43 mg*	C75	Freeze-grinding	29	55	145
249.88 mg*	C75	Freeze-grinding	29	55	162
59.7 mg	C75	Bead-beating	1	2	4
172.49 mg*	C75	Bead-beating	2	3	34
256.72 mg*	C75	Bead-beating	9	9	160
7.5 g Run 1	C75	Sonication	2328	13197	25985
7.5 g Run 2	C75	Sonication	2097	11372	22769
7.5 g Run 3	C75	Sonication	2038	10945	19695

*Used SCX material on the back column only.

average of 26 proteins detected. Initially, the LC column was found to completely clog with the C75 biofilm. A modified method was used where only SCX was loaded on the back column. The goal was to obtain ~2000 proteins out of the approximately 14,000 predicted from the genome annotation [67], which had been identified in previous proteome measurements with larger starting sample [65, 290] as well as for the 7.5 g sonication lysis of the C75 biofilm (Table 7.4). A possible explanation as to why this microbial community did not yield a comprehensive proteome measurement similar to the bacterial isolates for the small scale method is due to the strong cellulose composition of the surrounding matrix (P. Wilmes, personal communication). The rigidity of the biofilm matrix creates a formidable challenge for the lysis procedure, which will require further investigation. One solution would be to enzymatically digest the matrix, thereby releasing the microbial cells. The disadvantage to this method is that the resulting proteome may be different after the incubation period is completed. In addition, by removing the scaffold during this incubation period, the microbial cells may go into shock due to the loss of the supporting structure. This would not allow for identification of low-abundant proteins of metabolic significance.

Conclusions

The need to sample complex environmental or biomedical samples with limited biomass has prompted the development of lysis methodologies that are unbiased and can be easily coupled with mass spectrometry-based proteomics as described here and elsewhere [266]. The method described here differs from other lysis techniques as being a true single-tube lysis method. From wet cell pellet to tryptically digested proteins, all steps are performed in the same eppendorf tube. In addition, there is no deleterious effect

on the tryptic digestion step with, as long as the Guanidine HCl is diluted to 1 M or less. The work presented here demonstrates both the ease and utility of performing a novel single-tube lysis method for the proteome-level characterization of bacterial isolates. An advantage to this lysis method is the unbiased means by which an equal coverage of transmembrane-domain and soluble cytosolic proteins can be achieved in the resulting LC-MS experiment. In addition, there is very little difference in the number of proteins identified utilizing 5 mg or less of wet cell pellet, in comparison to 2 g by a traditional sonication lysis technique. The single-tube lysis method must now be optimized further for the AMD biofilm, which illustrates the challenges of the transition from bacterial isolates to complex microbial communities within proteomics. Recently, a study by Wang *et al* [266] described the TFE single-tube lysis method for mouse brain samples in the range of 4.5-5.0 mg in size. Using the accurate mass and time (AMT) tag approach, the authors were able to confidently identify 491 proteins from three replicate lysates [266]. Our results show similar total proteins identified with one of the AMD microbial communities, indicating a possible stoichiometric limitation for single-tube lysis. Stoichiometric limitation as indicated here is specific for complex mixtures, where only the most abundant proteins will be identified from the sample leaving the low-abundant proteins undetectable with current methodologies. For example, far less than the mass weighed for the microbial community is actual biomass, but rather the bulk of the material is the supporting matrix.

Chapter 8

Conclusions

Proteomics serves as one of the key lynch-pins for systems biology studies, and has progressed dramatically from its humble beginnings with 2D-PAGE gels. Many labs around the world are employing MS-based proteomic measurements to study biological problems ranging from simple bacteria to complicated human systems. Even with these remarkable advancements and applications of proteomics, there are still many challenges for enhancing this approach to comprehensively characterize biological systems. For example, consider the simple bacteria *S. oneidensis*, which is the focus of this dissertation work. This bacterium has a genome consisting of ~5000 annotated open-reading frames that could be translated into proteins. Our proteome measurements have revealed the presence of ~1800 non-redundant proteins under any single growth condition. The question then arises as to how many proteins are actually translated under a single growth condition, and whether these proteins can be comprehensively detected by the MS technology employed here. Clearly, the dynamic range of protein expression is large, possibly reaching 10^5 in bacterial systems, reflecting the range from highly abundant house-keeping proteins (such as ribosomal proteins) to low abundance (< 10 copies per cell) transcription factors. The complexity and dynamic range of the proteome samples provide an enormous analytical challenge to the shotgun MS technique. However, the advancements of on-line multidimensional LC-MS/MS based approaches have almost kept up with these challenges. Returning to our example with *S. oneidensis*, other

evidence indicates that this organism may only express about 40% of its proteome under a single growth condition, thereby maintaining a reserve of untapped proteins for other environmental scenarios. This would imply that of the ~2000-2500 proteins expressed under a single condition, our MS-based technology can detect roughly 75-90% of the proteins. This clearly demonstrates that this approach is not merely skimming the surface of the most abundant (and possibly uninteresting) house-keeping proteins, but rather is digging quite deep into the proteome. This provides strong hope for reconstructing detailed pathways and networks of the protein machinery that is operational for a bacteria's life processes.

One interesting aspect of these shotgun proteomics experiments is the detection of a large number of unknown proteins resulting from expression of hypothetical genes. This direct measurement of definitive proteins strongly validates the validity of the genome annotation and aids in helping resolve the realities of gene expression. Without these non-targeted MS-based proteomics experiments, the realities and possible functional roles of these unknown proteins would be completely absent.

Within a shotgun proteomics experiment, many proteins are found to be expressed constitutively; albeit at varying levels under various growth or stress conditions. Therefore, quantitative proteomics allows for the determination of either relative or absolute abundance levels for proteins identified from a whole-cell lysate experiment. These differentially expressed proteins are typically used to compare two different growth conditions for the organism. Quantification allows for the identification of proteins which may be induced or repressed in response to a specific stimulus. For example, a central objective of this dissertation was to explore wild-type *S. oneidensis*

versus chromate-exposed cultures, to identify differentially expressed proteins that would provide insight into how this organism deals with metal stress. The measured protein abundances using shotgun proteomics is challenging due to the amino acid distribution within the peptides, the confidence in the calculated abundance value for a given protein, and the labeling method used for a peptide/protein. For this bacterium, most proteins will not vary significantly in abundance, since they are necessary for critical life functions and may not be influenced by the presence of chromate. However, the more interesting proteins will be sensitive to this metal shock, which will impact their abundances. The confidence in abundance measurements is challenging for proteins having a 2-3 fold change in expression level in response to growth changes.

For bacterial systems, there are three standard methods of protein quantification: iTRAQ [1], isotopic labeling, and semiquantitation (or unlabeled quantification). iTRAQ labels the N-terminal amine and the ϵ -amino group of lysines with one of four tags of the same mass, which works well for bacteria. The resulting MS/MS will contain sequencing information identifying the peptide as well as quantification information from the reporter group giving relative abundances. However, at the time of the studies described here, iTRAQ was not available for general use. Isotopic labeling requires providing an isotopically “heavy” nutrient during growth in order for subsequent quantification of the intact peptide. This method is not amenable for growth conditions chosen for *S. oneidensis* here due to the requirement in using a minimal medium for isotopic labeling of proteins. Therefore, semiquantitation was chosen as the method of quantification here. Its benefits include: no additional sample preparation or special media growth considerations, no requirement for a dedicated mass spectrometry method, and a clear

identification of those proteins that have dramatic changes in expression level. As discussed below, the FDR for these proteins is below 1%, which allows for a confident conclusion that the protein is actually differentially expressed. Ultimately, additional improvements must be made in order to extract meaningful information from smaller changes in protein abundance.

The most important consideration of any aspect of a shotgun proteomic dataset is how the resulting FDR will affect the conclusions drawn. The FDR for the work presented here was set to ~2.0% for peptides, which reflects a calculated protein FDR of ~11.5% at the two-peptide level. However, only ~14% of the total protein identifications in a given proteomics dataset arise from a two-peptide identification. A majority (~77%) of proteins are identified from five or more peptides, which have a calculated FDR of 0.9% for the protein identification. These conservative filter levels increase the confidence of the resulting dataset for proteins identified and the resulting quantification performed. However, more attention must be drawn to the issue of false identifications in shotgun proteomics datasets, because there are a large number of proteins that are subsequently identified and in many cases quantified.

Understanding the role of PTMs in cell cycle control and signaling pathways is critical for providing a complete representation of the Cr(VI) stress response in *S. oneidensis*. In order to predict the presence and location of a PTM, there are a number of principles that must first be understood. In light of the previous drawbacks for investigating PTMs in shotgun proteomics datasets (detailed in Chapter 5), one of the aims in the research performed in the dissertation was the assessment of three separate algorithms which provide the option of searching for PTMs. The FDR for PTM-

containing peptides was found to be ~10% when searching the dataset with InsPecT, which is in contrast to the 50% found utilizing DBDigger. In addition, InsPecT was found to search the shotgun proteomics dataset in approximately half the time required by DBDigger using a desktop computer. Another metric to gauge the success of a PTM search is identifying an increased number of proteins. However, there is not an increase in the total number of proteins identified by adding the option of including PTMs. There is a slight decrease in the total number of peptides and spectra that are identified by specifying PTMs corresponding to an elevated false negative rate. The increased thresholds necessary to compensate for the increased FDR in the PTM searches cause an elevation in the false negative rate (a decrease in peptide and spectral count). A better metric may be to determine if information on the relative modification level of a protein is changed based on the growth condition. However, much more work is needed in order to better understand how to search and interpret the resulting datasets.

All of the methods development performed in this dissertation played a role in understanding chromium exposure in *S. oneidensis* at the molecular level. A total of four large-scale proteome studies were performed to assess at the molecular level the response of *S. oneidensis* to chromium exposure during various times and dosages of exposure. Both technical and biological replicate measurements were made. The first study performed involved acute chromate exposure in *S. oneidensis* to a sub-lethal concentration for a brief period of time (up to 90 min). This study was followed by the molecular level characterization of the response of *S. oneidensis* to chromium exposure after complete transformation of Cr(VI) (at the 24 h time point). Based on proteins found differentially expressed following acute and chronic exposure at fixed Cr(VI)

concentrations, a dosage-response study was undertaken. The final study involved characterizing both wild type strain MR-1 and a gene knockout mutant strain ($\Delta 2426$) during transformation of Cr(VI) to presumably Cr(III). *so2426* was chosen for deletion due to the protein and transcript identified as up-regulated following acute shock exposure under various Cr(VI) dosages.

The first study performed involved understanding acute chromate exposure in *S. oneidensis* to a sub-lethal concentration. Prior to this study, very little was known about how *S. oneidensis* responded to chromate exposure in culture. Previous work focused on extremely low concentrations of chromate, which neither caused a stress response nor were an accurate representation of Cr(VI) concentration in contaminated sites [2-8]. The first study examined the response of *S. oneidensis* MR-1 to 1 mM of Cr(VI) for 45 or 90 min. A concentration of 1 mM Cr(VI) was chosen based on the growth response curves of *S. oneidensis* as a function of chromate concentration [9]. No Cr(VI) was reduced in the acute study; rather the goal of the study was to identify the initial transcriptome and proteome response of *S. oneidensis*. Semi-quantification was performed on the resulting proteome dataset, taking into account reproducible differences in sequence coverage, peptide count, and spectral count. The sulfur metabolism pathway predicted from the genome sequence of *S. oneidensis* is depicted as a KEGG map in Figure 8.1, where the protein components highlighted in blue within the pathway were found up-regulated and the green pathway components were not differentially expressed. However, semi-quantification is instrument-dependent, where the increased dynamic range of the LTQ requires a more stringent level of filtering for quantification of proteins detected with this instrumentation. The benefit of the increased dynamic range of the LTQ allowed for the

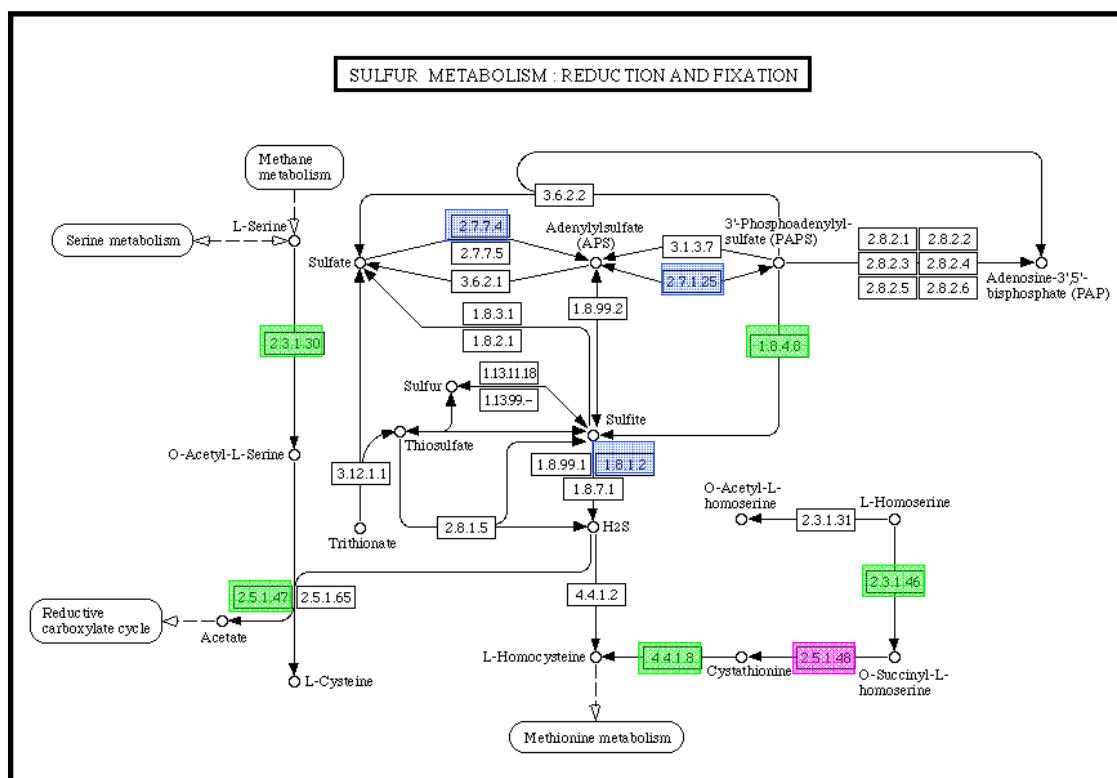


Figure 8.1. The sulfur metabolism pathway of *S. oneidensis* MR-1.

Depicted is the KEGG (Kyoto Encyclopedia of Genes and Genomes) pathway of sulfur metabolism (www.genome.jp/kegg/pathway.html). Proteins shaded in blue were found up-regulated during Cr(VI) shock, shaded in green were not differentially expressed, and shaded in pink was not identified in the proteome dataset.

detection and quantification of a putative transcriptional regulator (SO2426) that appeared to respond overwhelmingly to Cr(VI) in the transcriptome data. Previously, this level of detection was not possible with the older instrumentation (LCQ). Now, detection and quantification of low abundance proteins, such as transcriptional regulators, is possible. The more sensitive detection level leads to a greater corroboration with the transcriptome data, which in general has a much more sensitive level of detection. If *S. oneidensis* is to be utilized for bioremediation purposes, then understanding the effects of long-term exposure to environmental factors such as chromate is necessary prior to implementation of *S. oneidensis* as an agent of bioremediation in contaminated sites. Therefore, a proteome study was undertaken where *S. oneidensis* was exposed to 0.3 mM Cr(VI) for 24 h correlating to a chronic exposure. This concentration was chosen based on the growth results of the acute exposure study [9]. The concentration of 1 mM demonstrated a biphasic growth pattern, where there was a long lag period of ~40 h before growth resumed. Whereas a 0.3 mM Cr(VI) concentration would allow the bacterial cells to recover and resume growth after a lag period between 20-30 h, thus allowing enough biomass to be produced for the proteome experiments. The proteome results from the chronic exposure study were very surprising. The assumption prior to data analysis was that a similar proteome profile to the acute exposure study would be observed. However, when data analysis was complete, a unique proteome profile was obtained. The results indicated a high level of stress response in *S. oneidensis* in addition to the presumable activation of a lytic phage based on up-regulated phage related proteins. Out of the 76 proteins identified up-regulated after chronic Cr(VI) exposure in *S. oneidensis*, 36 proteins up-regulated corresponded to regions of the genome known to

harbor phage insertion sites. The chronic exposure work was the first integrated transcriptomic and proteomic study to comprehensively evaluate chronic Cr(V) exposure in *S. oneidensis*.

S. oneidensis was exposed to Cr(VI) concentrations of 0, 0.3, 0.5, and 1 mM for 30 min. These doses were also chosen based on growth response curves found in the acute exposure study [9]. In addition, Cr(VI) contaminated sites are known to comprise many different concentrations of Cr(VI), with a gradient ranging from low to highly contaminated regions within a particular site. Understanding whether or not *S. oneidensis* will respond to and reduce Cr(VI) at various concentrations is critical before use of the bacterium as an agent for bioremediation. The use of *S. oneidensis* at sites where the Cr(VI) contamination is minimal would not be useful if the bacterium does not respond to lower concentrations. The time period of exposure response for the dosage-response study and the acute exposure study were comparable, creating the assumption that the proteome profiles for the two studies should be comparable (at least for the shared dosage). This indeed was the case when the profiles were compared. In addition, the overall response for each dosage demonstrated a number of similarities as well. The overall profile indicated that a number of transport and binding proteins, as well as a putative transcriptional regulator (SO2426), were highly up-regulated for all dosages tested. However, a number of proteins were found to demonstrate a dosage-dependent response to Cr(VI) as well. These proteins were found to increase in their relative abundance with increasing dosage and included examples such as transporter proteins and the putative transcriptional regulator (SO2426). The results of the dosage-response

study indicated a dosage dependent activation for SO2426, which was chosen for evaluation further as a positive regulator of Cr(VI) gene activation.

Due to results from previous studies involving acute Cr(VI) exposure and the dosage-dependent response of *S. oneidensis*, a proteome study of Cr(VI) transformation was performed. This study sampled time periods during Cr(VI) transformation of both wild-type strain MR-1 and a deletion mutant derived from strain MR-1. The SO2426 putative transcriptional regulator was knocked out in order to test how *S. oneidensis* would respond to Cr(VI) exposure during the transformation period of 4 h in length. SO2426 was chosen for deletion based on the previous studies, which indicated a clear activation of this gene in response to Cr(VI) exposure. SO2426 previously was found to either not be expressed prior to Cr(VI) introduction or displayed a minimal level of expression (~2 peptides identified). Therefore, we knew that SO2426 must play a key role in regulation of protein activation in response to Cr(VI) if this protein is indeed a transcriptional regulator as the genome annotation provided states. Another aspect to this study was the use of biological triplicate cultures for proteome analysis. Very few proteome studies published to date have utilized biological replicates for measurements or for quantification of protein abundance. There is more difficulty in determining protein abundance from biological replicates versus technical replicates. However, the differentially expressed proteins found in a biological replicate are more significant. One caveat of using biological replicates is the overall decrease in reproducibility of proteins identified in comparison to using technical replicates. However, the Cr(VI) transformation study confirmed the hypothesis of the importance of SO2426 in response to Cr(VI) exposure. The Δ 2426 cultures demonstrated an impaired ability to transform

Cr(VI) and a number of proteins were identified that indicate importance in Cr(VI) transport across the *S. oneidensis* outer and inner membranes. Conclusions drawn from these proteome experiments indicate (1) that Cr(VI) may be a competitive inhibitor of sulfate, (2) Cr(III) may be more toxic to *S. oneidensis* than Cr(VI), (3) proteome results demonstrated a dosage-dependent stress response to Cr(VI), and (4) the characterization of a putative metal response regulator (SO2426), which appears to be a global regulator of not only Cr(VI), but a number of other transition metals.

The evidence for competitive inhibition of sulfate by chromate arises from the induction of proteins annotated as involved in sulfate uptake and metabolism. In the acute shock study, three of the nine sulfur metabolism pathway components were identified up-regulated (Figure 8.1). The functions of the up-regulated components within in the pathway are enzymes that catalyze production of sulfate from other sulfur-containing compounds, which indicates an intracellular sulfate deficiency. In addition, there are two sulfate ABC transporters annotated in the *S. oneidensis* genome (*so3599-so3602* and *so4652-so4655*) and members of both transporters are found up-regulated during exposure to Cr(VI). Finally, four members of the cysteine biosynthesis pathway were found up-regulated following exposure to 1 mM Cr(VI). If sulfate deficiency were not an issue, *S. oneidensis* would not need to increase the production of these proteins. There may also be similarities between the hydration radius of chromate and sulfate, which leads to the chromate interacting with the sulfate transporters. Competitive inhibition of sulfate could be caused by more Cr(VI) present in the media, which outcompetes sulfate for binding at the ABC transporters. By increasing the sulfate concentration, one may be able to rescue *S. oneidensis* from chromate shock.

Prior to the studies presented here, the consensus in the field of microbiology was that the Cr(VI) species led to the toxicity phenotype observed when microbes are exposed to chromium [6, 10-18]. After *S. oneidensis* was grown in the presence of Cr for 24, all Cr(VI) was presumably transformed to Cr(III). Cr(VI) and Cr(III) are the two stable forms of chromium commonly found in the environment [12]. The conclusion drawn from the chronic study is that Cr(III) may in fact be more toxic than Cr(VI). In this study, the proteome profile observed was unique in comparison to the other Cr(VI) exposure proteome studies reported. The activation of two lytic prophages appeared to be the signature response of *S. oneidensis* after the transformation of Cr(VI) to presumably Cr(III). The presence of Cr(III) was not tested; as well as there was not a noticeable precipitate reported in the media. The proteome dataset allowed for the confirmation of the lytic phage cycle by providing confirmation of translation of these genes by seizing the host cell's translation apparatus. The results of this chronic exposure study were similar to the transcriptome results reported for *S. oneidensis* exposure to both ionizing radiation and artificial UV radiation [19, 20]. The actual response of *S. oneidensis* towards long-term exposure to Cr could be deciphered by inactivation of the integrated phages or the use of a strain that does not have an integrated phage. Also, one could test the mutagenesis rate of intracellular Cr(III) by a whole genome microarray as shown for *E. coli* [21]. This could detect the mutation rate of the *S. oneidensis* chromosome, thereby determining if critical house-keeping genes have nucleotide sequence changes following long-term exposure to Cr(III)-containing products. In addition, O'Brian *et al* [22] demonstrated that Cr interacts with the phosphate backbone of double-stranded DNA molecules. This interaction will cause the

DNA replication machinery to stall, with DNA replication arrest in cells that are actively reducing Cr(VI). The stalled replication machinery may be one of the reasons as to the observed phenotype of elongated, filamentous bacterial cells at the 24 h sampling point.

In addition to the physiological responses just described, we found that upon Cr(VI) exposure there was evidence of stress response from the expressed proteome datasets. Characteristic proteins found activated in response to Cr(VI) intracellular stress include RecN, TopB, SO1648 (cold shock domain family protein), IbpA, and ClpB. There was a dosage-dependent response found for stress response proteins (see Chapter 4 for details). The dosage-dependence of stress response-related proteins indicates a possible tolerance level to Cr(VI), which upon increased concentrations of Cr(VI) there is a trigger that indicates increased intracellular stress. However, at this time there is not an indication as to the identity of the protein(s) responsible for activating the stress response demonstrated in the acute shock or dosage response studies.

Finally, the characterization of a putative DNA-binding response regulator, SO2426, as a metal response regulator was the culmination of the proteome studies on Cr exposure. Prior to the acute Cr(VI) shock study, there was no evidence that SO2426 was translated into protein or was induced at the transcriptome and proteome level under Cr(VI) conditions. Further work determined that SO2426 putatively controlled gene expression at the transcript level of genes involved with sulfate metabolism and iron homeostasis after creation of a knockout of *so2426* [23]. The same proteins identified as down-regulated in the mutant cultures both prior to and following Cr(VI) addition were found up-regulated during acute Cr(VI) shock; indicating that the gene expression is controlled by an actively expressed and translated *so2426*. This work demonstrates the

utility and value of performing global non-targeted proteome studies to identify putative roles for proteins expressed under given growth conditions. In addition, the expectation is that information gleaned from the Cr(VI) proteome studies will provide fodder for future proteome studies in environmental microbiology to better understand the complex role of Cr(VI) biogeochemical cycling in the environment.

Measurements using mass spectrometry based proteomics have enhanced the scientific knowledge on microbial and eukaryotic systems. Research in the areas of microbial ecology and human disease would not have progressed as quickly without global proteome studies. First, comprehensive proteome studies provide novel non-targeted biochemical information on protein presence and abundance. In addition, the area of shotgun proteomics is helping to validate genome annotation. The large number of hypothetical genes annotated led many individuals to question the validity of genome annotation. Therefore, with the advent of shotgun proteomics, the identification and in some cases tentative functional assignments can be given to hypothetical proteins.

The research to date is very helpful, but also can be overwhelming. Repositories for MS/MS data must be created to organize, standardize, and increase the availability of information obtained from the large-scale proteome studies. HUPO, the human proteome project, has begun the process of providing guidelines for proteome datasets [24]. The organizers were visionary, because they realized both the value of the proteome data and the need for community wide availability of the information. In the future, other areas must following the HUPO example, otherwise the field of proteomics will suffer the same problems as faced when nucleotide sequencing of the human genome was

completed [25-28]. Some of these issues include organizing the large amount of sequencing information and dissemination of the genome sequence.

Since the induction of routine proteome measurements, the scientific questions posed have become more complex. Previously, measurements on pure microbial cultures and human cell lines were considered to be significant studies. However, as shotgun proteomics experiments have become more routine, there is an increasing interest in investigating microbial environmental communities [29-31] and complex mammalian tissues [32-35]. The current platform is limited to relatively abundant members within a particular community; therefore there is an increased concern of the overall dynamic range capabilities of the experimental platform. In order to compensate for the current dynamic range limitations, improvements in chromatographic separation and the mass spectrometry instruments will be needed. The mass spectrometer duty cycle is more efficient now than five years ago; however, many peptides/proteins are still not sampled during the experiments. Low abundant peptides/proteins sampling will improve by adding a third dimension of separation. Without dramatic advancements to the instrumentation, the goal of detecting proteins found at reduced expression levels is not possible. In the end, an enrichment of low-abundant community members will be necessary to understand their contribution.

List of References

1. Ideker, T., et al., *Integrated genomic and proteomic analyses of a systematically perturbed metabolic network*. Science, 2001. **292**: p. 929-934.
2. O'Farrell, P.H., *High resolution two-dimensional electrophoresis of proteins*. J Biol Chem, 1975. **250**(10): p. 4007-21.
3. Lovell-Badge, R.H. and M.J. Evans, *Changes in protein synthesis during differentiation of embryonal carcinoma cells, and a comparison with embryo cells*. J Embryol Exp Morphol, 1980. **59**: p. 187-206.
4. Krakauer, T., et al., *Analysis of the heterogeneity of the mouse H-2K, D, and L gene products*. J Immunol, 1980. **124**(5): p. 2149-56.
5. Niall, H.D. and P. Edman, *Two structurally distinct classes of kappa-chains in human immunoglobulins*. Nature, 1967. **216**(5112): p. 262-3.
6. Edman, P. and G. Begg, *A protein sequenator*. European Journal of Biochemistry, 1967. **1**(1): p. 80-91.
7. Fales, H.M., G.W. Milne, and M.L. Vestal, *Chemical ionization mass spectrometry of complex molecules*. Journal of the American Chemical Society, 1969. **91**(13): p. 3682-5.
8. de Hoffman, E. and V. Stroobant, *1. Ion Sources*, in *Mass Spectrometry: Principles and Applications*. 2002, John Wiley & Sons, LTD: New York. p. 11-61.
9. Hillenkamp, F., et al., *Matrix-assisted laser desorption/ionization mass spectrometry of biopolymers*. Analytical Chemistry, 1991. **63**(24): p. 1193A-1203A.

10. Berndt, P., U. Hobohm, and H. Langen, *Reliable automatic protein identification from matrix-assisted laser desorption/ionization mass spectrometric peptide fingerprints*. Electrophoresis, 1999. **20**(18): p. 3521-6.
11. Laiko, V.V., M.A. Baldwin, and A.L. Burlingame, *Atmospheric pressure matrix-assisted laser desorption/ionization mass spectrometry*. Analytical Chemistry, 2000. **72**(4): p. 652-7.
12. Fenn, J.B., et al., *Electrospray ionization for mass spectrometry of large biomolecules*. Science, 1989. **246**(4926): p. 64-71.
13. Siuzdak, G., *The emergence of mass spectrometry in biochemical research*. PNAS, 1994. **91**(24): p. 11290-7.
14. Canas, B., et al., *Mass spectrometry technologies for proteomics*. Briefings in Functional Genomics and Proteomics, 2006. **4**(4): p. 295-320.
15. Peng, J. and S.P. Gygi, *Proteomics: the move to mixtures*. Journal of Mass Spectrometry, 2001. **36**: p. 1083-1091.
16. Tyers, M. and M. Mann, *From genomics to proteomics*. Nature, 2003. **422**: p. 193-197.
17. Rompp, A., et al., *Examples of Fourier transform ion cyclotron resonance mass spectrometry developments: from ion physics to remote access biochemical mass spectrometry*. Eur J Mass Spectrom (Chichester, Eng), 2005. **11**(5): p. 443-56.
18. Guan, S., A.G. Marshall, and M.C. Wahl, *MS/MS with high detection efficiency and mass resolving power for product ions in Fourier transform ion cyclotron resonance mass spectrometry*. Anal Chem, 1994. **66**(8): p. 1363-7.

19. Wolters, D.A., M.P. Washburn, and J.R. Yates III, *An automated multidimensional protein identification technology for shotgun proteomics*. Analytical Chemistry, 2001. **73**: p. 5683-5690.
20. Liu, H., R.G. Sadygov, and J.R. Yates, 3rd, *A model for random sampling and estimation of relative protein abundance in shotgun proteomics*. Analytical Chemistry, 2004. **76**(14): p. 4193-201.
21. Marshall, A., *Fourier transform ion cyclotron resonance mass spectrometry*. Acc. Chem. Res., 1985. **18**: p. 316-322.
22. Syka, J.E.P., et al., *Novel linear quadrupole ion trap/FT mass spectrometer: performance characterization and use in the comparative analysis of histone H3 post-translational modifications*. Journal of Proteome Research, 2004. **3**: p. 621-626.
23. Hu, Q., et al., *The Orbitrap: a new mass spectrometer*. Journal of Mass Spectrometry, 2005. **40**: p. 430-443.
24. Sundqvist, B., et al., *Californium-252 plasma desorption time of flight mass spectroscopy of proteins*. Biomed Mass Spectrom, 1984. **11**(5): p. 242-57.
25. VerBerkmoes, N.C., et al., *Integrating "Top-Down" and "Bottom-Up" mass spectrometric approaches for proteomic analysis of Shewanella oneidensis*. Journal of Proteome Research, 2002. **1**: p. 239-252.
26. Pandey, A. and M. Mann, *Proteomics to study genes and genomes*. Nature, 2000. **405**: p. 837-846.

27. Chernushevich, I.V., A.V. Loboda, and B.A. Thomson, *An introduction to quadrupole-time-of-flight mass spectrometry*. J Mass Spectrom, 2001. **36**(8): p. 849-65.
28. Hopfgartner, G., et al., *Triple quadrupole linear ion trap mass spectrometer for the analysis of small molecules and macromolecules*. J Mass Spectrom, 2004. **39**(8): p. 845-55.
29. Stafford Jr., G.C., et al., *Recent improvements in and analytical applications of advanced ion trap technology*. International Journal of Mass Spectrometry and Ion Processes, 1984. **60**: p. 85-98.
30. Schwartz, J.C., M. Senko, and J.E.P. Syka, *A two-dimensional quadrupole ion trap mass spectrometer*. Journal of the American Society for Mass Spectrometry, 2002. **13**: p. 659-669.
31. Blackler, A.R., et al., *Quantitative comparison of proteomic data quality between a 2D and 3D quadrupole ion trap*. Analytical Chemistry, 2006. **78**(4): p. 1337-44.
32. Riter, L.S., et al., *Comparison of the Paul ion trap to the linear ion trap for use in global proteomics*. Proteomics, 2006. **6**: p. 1735-1740.
33. Washburn, M.P., D.A. Wolters, and J.R. Yates III, *Large-scale analysis of the yeast proteome by multidimensional protein identification technology*. Nature Biotechnology, 2001. **19**: p. 242-247.
34. Cargile, B.J., et al., *Gel based isoelectric focusing of peptides and the utility of isoelectric point in protein identification*. Journal of Proteome Research, 2004. **3**(1): p. 112-9.

35. Essader, A.S., et al., *A comparison of immobilized pH gradient isoelectric focusing and strong-cation-exchange chromatography as a first dimension in shotgun proteomics*. Proteomics, 2005. **5**(1): p. 24-34.
36. Courchesne, P.L., et al., *Optimization of capillary chromatography ion trap-mass spectrometry for identification of gel-separated proteins*. Electrophoresis, 1998. **19**(6): p. 956-67.
37. Figeys, D., et al., *Data-dependent modulation of solid-phase extraction capillary electrophoresis for the analysis of complex peptide and phosphopeptide mixtures by tandem mass spectrometry: application to endothelial nitric oxide synthase*. Anal Chem, 1999. **71**(13): p. 2279-87.
38. Lipton, M.S., et al., *AMT tag approach to proteomic characterization of *Deinococcus radiodurans* and *Shewanella oneidensis**. Methods of Biochemical Analysis, 2006. **49**: p. 113-34.
39. Eng, J.K., A.L. McCormack, and J.R. Yates III, *An approach to correlate tandem mass spectral data of peptides with amino acid sequences in a protein database*. Journal of the American Society for Mass Spectrometry, 1994. **5**: p. 976-989.
40. Tanner, S., et al., *InsPecT: identification of posttranslationally modified peptides from tandem mass spectra*. Analytical Chemistry, 2005. **77**(14): p. 4626-39.
41. Perkins, D.N., et al., *Probability-based protein identification by searching sequence databases using mass spectrometry data*. Electrophoresis, 1999. **20**(18): p. 3551-67.

42. Tabb, D.L., C.G. Fernando, and M.C. Chambers, *MyriMatch: Highly accurate tandem mass spectral peptide identification by multivariate hypergeometric analysis*. Journal of Proteome Research, 2007: p. [8].
43. Geer, L.Y., et al., *Open mass spectrometry search algorithm*. Journal of Proteome Research, 2004. **3**(5): p. 958-64.
44. Tabb, D.L., et al., *DBDigger: reorganized proteomic database identification that improves flexibility and speed*. Analytical Chemistry, 2005. **77**(8): p. 2464-74.
45. VerBerkmoes, N.C., et al., *Mass spectrometric approaches for characterizing bacterial proteomes*. Expert Rev Proteomics, 2004. **1**(4): p. 433-47.
46. Mirzaei, H. and F. Regnier, *Identification of yeast oxidized proteins: chromatographic top-down approach for identification of carbonylated, fragmented, and cross-linked proteins in yeast*. Journal of Chromatography A, 2007. **1141**: p. 22-31.
47. Gianazza, E., J. Crawford, and I. Miller, *Detecting oxidative post-translational modifications in proteins*. Amino Acids, 2006.
48. Strader, M.B., et al., *Characterization of the 70S ribosome from Rhodopseudomonas palustris using an integrated "top-down" and "bottom-up" mass spectrometric approach*. Journal of Proteome Research, 2004. **3**: p. 965-978.
49. Forbes, A.J., et al., *Targeted analysis and discovery of posttranslational modifications in proteins from methanogenic archaea by top-down MS*. PNAS, 2004. **101**: p. 2678-2683.
50. Mann, M. and O.N. Jensen, *Proteomic analysis of post-translational modifications*. Nature Biotechnology, 2003. **21**: p. 255-261.

51. MacCoss, M.J., et al., *Shotgun identification of protein modifications from protein complexes and lens tissue*. PNAS, 2002. **99**(12): p. 7900-5.
52. Stock, J.B., A.M. Stock, and J.M. Mottonen, *Signal transduction in bacteria*. Nature, 1990. **344**(6265): p. 395-400.
53. Eisenbach, M., *Control of bacterial chemotaxis*. Molecular Microbiology, 1996. **20**(5): p. 903-10.
54. Baker, M.D., P.M. Wolanin, and J.B. Stock, *Systems biology of bacterial chemotaxis*. Current Opinion in Microbiology, 2006. **9**(2): p. 187-92.
55. Olsen, J.V., et al., *Global, in vivo, and site-specific phosphorylation dynamics in signaling networks*. Cell, 2006. **127**(3): p. 635-48.
56. Cantin, G.T. and J.R. Yates, 3rd, *Strategies for shotgun identification of post-translational modifications by mass spectrometry*. Journal of Chromatography A, 2004. **1053**(1-2): p. 7-14.
57. Blagoev, B., et al., *Temporal analysis of phosphotyrosine-dependent signaling networks by quantitative proteomics*. Nature Biotechnology, 2004. **22**(9): p. 1139-45.
58. Garcia, B.A., J. Shabanowitz, and D.F. Hunt, *Analysis of protein phosphorylation by mass spectrometry*. Methods, 2005. **35**(3): p. 256-64.
59. Thompson, M.R., D.K. Thompson, and R.L. Hettich, *Systematic Assessment of the Benefits and Caveats in Mining Microbial Post-Translational Modifications from Shotgun Proteomic Data; Response of Shewanella oneidensis to Chromate Exposure*. Journal of Proteome Research, 2007. **Accepted**.

60. Gupta, N., et al., *Whole proteome analysis of post-translational modifications: Applications of mass-spectrometry for proteogenomic annotation*. Genome Research, 2007.
61. Myers, C.R. and K.H. Nealson, *Bacterial manganese reduction and growth with manganese oxide as the sole electron acceptor*. Science, 1988. **240**: p. 1319-1320.
62. Nealson, K.H. and D. Saffarini, *Iron and manganese in anaerobic respiration: environmental significance, physiology, and regulation*. Annu Rev Microbiol, 1994. **48**: p. 311-43.
63. Ding, Y.H., et al., *The proteome of dissimilatory metal-reducing microorganism Geobacter sulfurreducens under various growth conditions*. Biochimica et Biophysica Acta, 2006. **1764**(7): p. 1198-206.
64. Nealson, K.H. and C.R. Myers, *Iron reduction by bacteria: A potential role in the genesis of banded iron formations*. American Journal of Science, 1990. **290-A**: p. 35-45.
65. Ram, R.J., et al., *Community proteomics of a natural microbial biofilm*. Science, 2005. **308**: p. 1915-1920.
66. Arnold, R.G., et al., *Regulation of Dissimilatory Fe(III) Reduction Activity in Shewanella putrefaciens*. Applied and Environmental Microbiology, 1990. **56**(9): p. 2811-2817.
67. Tyson, G.W., et al., *Community structure and metabolism through reconstruction of microbial genomes from the environment*. Nature, 2004. **428**: p. 37-43.

68. Larimer, F., et al., *Complete genome sequence of the metabolically versatile photosynthetic bacterium Rhodospseudomonas palustris*. Nature Biotechnology, 2004. **22**: p. 55-61.
69. Heidelberg, J.F., et al., *Genome sequence of the dissimilatory metal ion-reducing bacterium Shewanella oneidensis*. Nature Biotechnology, 2002. **20**: p. 1118-1123.
70. Frazier, M.E., et al., *Realizing the potential of the genome revolution: the genomes to life program*. Science, 2003. **300**: p. 290-293.
71. Seshadri, R., et al., *Genome sequence of the PCE-dechlorinating bacterium Dehalococcoides ethenogenes*. Science, 2005. **307**(5706): p. 105-8.
72. Parkhill, J., et al., *Genome sequence of Yersinia pestis, the causative agent of plague*. Nature, 2001. **413**(6855): p. 523-7.
73. Rondon, M.R., et al., *Cloning the soil metagenome: a strategy for accessing the genetic and functional diversity of uncultured microorganisms*. Applied and Environmental Microbiology, 2000. **66**(6): p. 2541-7.
74. Venter, J.C., et al., *Environmental genome shotgun sequencing of the Sargasso Sea*. Science, 2004. **304**(5667): p. 66-74.
75. Mongodin, E.F., J.B. Emerson, and K.E. Nelson, *Microbial metagenomics*. Genome Biol, 2005. **6**(10): p. 347.
76. Martin, H.G., et al., *Metagenomic analysis of two enhanced biological phosphorus removal (EBPR) sludge communities*. Nature Biotechnology, 2006.
77. Tringe, S.G., et al., *Comparative metagenomics of microbial communities*. Science, 2005. **308**(5721): p. 554-7.

78. Gill, S.R., et al., *Metagenomic analysis of the human distal gut microbiome*. Science, 2006. **312**(5778): p. 1355-9.
79. Myers, C.R. and K.H. Nealson, *Respiration-linked proton translocation coupled to anaerobic reduction of manganese(IV) and iron(III) in Shewanella putrefaciens MR-1*. Journal of Bacteriology, 1990. **172**(11): p. 6232-8.
80. Venkateswaren, K., et al., *Polyphasic taxonomy of the genus Shewanella and description of Shewanella oneidensis sp. nov.* International Journal of Systematic Bacteriology, 1999. **49**: p. 705-724.
81. Myers, C.R. and J.M. Myers, *Role of menaquinone in the reduction of fumarate, nitrate, iron (III) and manganese (IV) by Shewanella putrefaciens MR-1*. FEMS Microbiology Letters, 1993. **114**: p. 215-222.
82. Petrovskis, E.A., T.M. Vogel, and P. Adriaens, *Effects of electron acceptors and donors on transformation of tetrachloromethane by Shewanella putrefaciens MR-1*. FEMS Microbiology Letters, 1994. **121**(3): p. 357-63.
83. Saffarini, D.A., et al., *Anaerobic respiration of Shewanella putrefaciens requires both chromosomal and plasmid-borne genes*. FEMS Microbiology Letters, 1994. **119**: p. 271-278.
84. Scott, J.H. and K.H. Nealson, *A biochemical study of the intermediary carbon metabolism of Shewanella putrefaciens*. Journal of Bacteriology, 1994. **176**(11): p. 3408-11.
85. Moser, D.P. and K.H. Nealson, *Growth of the facultative anaerobe Shewanella putrefaciens by elemental sulfur reduction*. Applied and Environmental Microbiology, 1996. **62**(6): p. 2100-5.

86. Myers, C.R., et al., *Chromium(VI) reductase activity is associated with the cytoplasmic membrane of anaerobically grown Shewanella putrefaciens MR-1*. Journal of Applied Microbiology, 2000. **88**: p. 98-106.
87. Krause, B. and K.H. Nealson, *Physiology and enzymology involved in denitrification by Shewanella putrefaciens*. Applied and Environmental Microbiology, 1997. **63**(7): p. 2613-8.
88. Nealson, K.H., D.P. Moser, and D.A. Saffarini, *Anaerobic electron acceptor chemotaxis in Shewanella putrefaciens*. Applied and Environmental Microbiology, 1995. **61**(4): p. 1551-4.
89. Myers, C.R. and K.H. Nealson. *Iron mineralization by bacteria: metabolic coupling of iron reduction to cell metabolism in Alteromonas putrefaciens strain MR-1*. in *Conference on Iron Biominerals*. 1990. University of New Hampshire: New York: Plenum Press.
90. Nealson, K.H. and C.R. Myers, *Microbial reduction of manganese and iron: new approaches to carbon cycling*. Applied and Environmental Microbiology, 1992. **58**(2): p. 439-43.
91. Serres, M.H. and M. Riley, *Structural domains, protein modules, and sequence similarities enrich our understanding of the Shewanella oneidensis MR-1 proteome*. Omics, 2004. **8**(4): p. 306-21.
92. Bencharit, S. and M.J. Ward, *Chemotactic responses to metals and anaerobic electron acceptors in Shewanella oneidensis MR-1*. Journal of Bacteriology, 2005. **187**(14): p. 5049-53.

93. Saffarini, D.A. and K.H. Nealson, *Sequence and genetic characterization of etrA, an fnr analog that regulates anaerobic respiration in Shewanella putrefaciens MR-1*. Journal of Bacteriology, 1993. **175**(24): p. 7938-44.
94. Maier, T.M. and C.R. Myers, *Isolation and characterization of a Shewanella putrefaciens MR-1 electron transport regulator etrA mutant: reassessment of the role of EtrA*. Journal of Bacteriology, 2001. **183**(16): p. 4918-26.
95. Beliaev, A.S., et al., *Microarray transcription profiling of a Shewanella oneidensis etrA mutant*. Journal of Bacteriology, 2002. **184**(16): p. 4612-6.
96. Thompson, D.K., et al., *Transcriptional and proteomic analysis of a ferric uptake regulator (Fur) mutant of Shewanella oneidensis: possible involvement of fur in energy metabolism, transcriptional regulation, oxidative stress*. Applied and Environmental Microbiology, 2002. **68**: p. 881-892.
97. Wan, X.F., et al., *Transcriptomic and proteomic characterization of the Fur modulon in the metal-reducing bacterium Shewanella oneidensis*. Journal of Bacteriology, 2004. **186**(24): p. 8385-400.
98. Myers, C.R. and K.H. Nealson, *Microbial reduction of manganese oxides: Interactions with iron and sulfur*. Geochimica et Cosmochimica Acta, 1988. **52**: p. 2727-2732.
99. Lovley, D.R., E.J. Phillips, and D.J. Lonergan, *Hydrogen and Formate Oxidation Coupled to Dissimilatory Reduction of Iron or Manganese by Alteromonas putrefaciens*. Applied and Environmental Microbiology, 1989. **55**(3): p. 700-706.

100. Myers, C.R. and J.M. Myers, *Localization of cytochromes to the outer membrane of anaerobically grown Shewanella putrefaciens MR-1*. Journal of Bacteriology, 1992. **174**(11): p. 3429-38.
101. Myers, C.R. and J.M. Myers, *Fumarate reductase is a soluble enzyme in anaerobically grown Shewanella putrefaciens MR-1*. FEMS Microbiology Letters, 1992. **98**: p. 13-20.
102. Myers, C.R. and J.M. Myers, *Ferric reductase is associated with the membranes of anaerobically grown Shewanella putrefaciens MR-1*. FEMS Microbiology Letters, 1993. **108**: p. 15-22.
103. Myers, C.R. and J.M. Myers, *Ferric iron reduction-linked growth yields of Shewanella putrefaciens MR-1*. The Journal of Applied Bacteriology, 1994. **76**(3): p. 253-8.
104. Myers, C.R. and J.M. Myers, *Cloning and sequence of cymA, a gene encoding a tetraheme cytochrome c required for reduction of iron(III), fumarate, and nitrate by Shewanella putrefaciens MR-1*. Journal of Bacteriology, 1997. **179**(4): p. 1143-52.
105. Myers, C.R. and J.M. Myers, *Outer membrane cytochromes of Shewanella putrefaciens MR-1: spectral analysis, and purification of the 83-kDa c-type cytochrome*. Biochimica et Biophysica Acta, 1997. **1326**(2): p. 307-18.
106. Beliaev, A.S. and D.A. Saffarini, *Shewanella putrefaciens mtrB encodes an outer membrane protein required for Fe(III) and Mn(IV) reduction*. Journal of Bacteriology, 1998. **180**(23): p. 6292-6297.

107. Myers, J.M. and C.R. Myers, *Isolation and sequence of omcA, a gene encoding a decaheme outer membrane cytochrome c of Shewanella putrefaciens MR-1, and detection of omcA homologs in other strains of S. putrefaciens*. Biochimica et Biophysica Acta, 1998. **1373**(1): p. 237-51.
108. Leys, D., et al., *Structure and mechanism of the flavocytochrome c fumarate reductase of Shewanella putrefaciens MR-1*. Nature Structural Biology, 1999. **6**(12): p. 1113-7.
109. Myers, J.M. and C.R. Myers, *Role of the tetraheme cytochrome CymA in anaerobic electron transport in cells of Shewanella putrefaciens MR-1 with normal levels of menaquinone*. Journal of Bacteriology, 2000. **182**(1): p. 67-75.
110. Beliaev, A.S., et al., *MtrC, an outer membrane decahaem c cytochrome required for metal reduction in Shewanella putrefaciens MR-1*. Molecular Microbiology, 2001. **39**(3): p. 722-30.
111. Tsapin, A.I., et al., *Purification and properties of a low-redox-potential tetraheme cytochrome c3 from Shewanella putrefaciens*. Journal of Bacteriology, 1996. **178**(21): p. 6386-8.
112. Myers, C.R. and J.M. Myers, *Isolation and characterization of a transposon mutant of Shewanella putrefaciens MR-1 deficient in fumarate reductase*. Letters in Applied Microbiology, 1997. **25**(3): p. 162-8.
113. Myers, J. and C. Myers, *Role for outer membrane cytochromes OmcA and OmcB of Shewanella putrefaciens MR-1 in reduction of manganese dioxide*. Applied and Environmental Microbiology, 2001. **67**: p. 260-269.

114. Tsapin, A.I., et al., *Identification of a small tetraheme cytochrome c and a flavocytochrome c as two of the principal soluble cytochromes c in Shewanella oneidensis strain MR1*. Applied and Environmental Microbiology, 2001. **67**(7): p. 3236-44.
115. Saffarini, D.A., S.L. Blumberman, and K.J. Mansoorabadi, *Role of menaquinones in Fe(III) reduction by membrane fractions of Shewanella putrefaciens*. Journal of Bacteriology, 2002. **184**(3): p. 846-8.
116. Maier, T.M. and C.R. Myers, *The outer membrane protein Omp35 affects the reduction of Fe(III), nitrate, and fumarate by Shewanella oneidensis MR-1*. BMC Microbiology, 2004. **4**: p. 23.
117. Meyer, T.E., et al., *Identification of 42 possible cytochrome C genes in the Shewanella oneidensis genome and characterization of six soluble cytochromes*. Omics, 2004. **8**(1): p. 57-77.
118. Bouhenni, R., A. Gehrke, and D. Saffarini, *Identification of genes involved in cytochrome c biogenesis in Shewanella oneidensis, using a modified mariner transposon*. Applied and Environmental Microbiology, 2005. **71**: p. 4935-4937.
119. Yang, F., et al., *Characterization of purified c-type heme-containing peptides and identification of c-type heme-attachment sites in Shewanella oneidensis cytochromes using mass spectrometry*. Journal of Proteome Research, 2005. **4**: p. 846-854.
120. Lower, S.K., M.F. Hochella Jr., and T.J. Beveridge, *Bacterial recognition of mineral surfaces: nanoscale interactions between Shewanella and α -FeOOH*. Science, 2001. **292**: p. 1360-1363.

121. James, B.R., *The challenge of remediating chromium-contaminated soil*. Environmental Science & Technology, 1996. **30**: p. A248-A251.
122. Langard, S., *Metals in the Environment*. 1980, Academy Press Inc.: New York. p. 111-132.
123. Riley, R.G., J.M. Zachara, and F.J. Wobber. Report DOE/ER-0547T, Chemical Contaminants on DOE Lands and Selection of Contaminant Mixtures for Subsurface Science Research. 1992, Washington, D.C.: United States Department of Energy.
124. Palmer, C.D. and P.R. Wittbrodt, *Processes affecting the remediation of chromium-contaminated sites*. Environmental Health Perspectives, 1991. **92**: p. 25-40.
125. Shupack, S.I., *The chemistry of chromium and some resulting analytical problems*. Environ Health Perspect, 1991. **92**: p. 7-11.
126. Cervantes, C., et al., *Interactions of chromium with microorganisms and plants*. FEMS Microbiology Reviews, 2001. **25**: p. 335-347.
127. Dubiel, M., et al., *Microbial iron respiration can protect steel from corrosion*. Applied and Environmental Microbiology, 2002. **68**: p. 1440-1445.
128. Park, C.H., et al., *Remediation and Beneficial Reuse of Contaminated Sediments*, in *Batelle Press*. 2002: Columbus, OH. p. 103-111.
129. Brakstad, O.G. and A.G. Lodeng, *Microbial diversity during biodegradation of crude oil in seawater from the North Sea*. Microbial Ecology, 2005. **49**(1): p. 94-103.

130. de Lorenzo, V., *Blueprint of an oil-eating bacterium*. Nature Biotechnology, 2006. **24**(8): p. 952-3.
131. Nyman, J.L., et al., *Biogeochemical elimination of chromium(VI) from contaminated water*. Biorem. J., 2002. **6**: p. 39-55.
132. Bencheikh-Latmani, R., et al., *Global transcriptional profiling of Shewanella oneidensis MR-1 during Cr(VI) and U(VI) reduction*. Applied and Environmental Microbiology, 2005. **71**: p. 7453-7460.
133. Viamajala, S., et al., *Chromate/nitrite interactions in Shewanella oneidensis MR-1: Evidence for multiple hexavalent chromium [Cr(VI)] reduction mechanisms dependent on physiological growth conditions*. Biotechnology and Bioengineering, 2002. **78**: p. 770-778.
134. Daulton, T.L., et al., *Electron energy loss spectroscopy techniques for the study of microbial chromium(VI) reduction*. Journal of Microbiological Methods, 2002. **50**: p. 39-54.
135. Middleton, S.S., et al., *Cometabolism of Cr(VI) by Shewanella oneidensis MR-1 produces cell-associated reduced chromium and inhibits growth*. Biotechnology and Bioengineering, 2003. **83**(6): p. 627-37.
136. Wielinga, B., et al., *Iron promoted reduction of chromate by dissimilatory iron-reducing bacteria*. Environmental Science & Technology, 2001. **35**: p. 522-527.
137. Caccavo, F., N.B. Ramsing, and J.W. Costerton, *Morphological and metabolic responses to starvation by the dissimilatory metal-reducing bacterium Shewanella alga BrY*. Applied and Environmental Microbiology, 1996. **62**: p. 4678-4682.

138. Park, C.H., et al., *Purification to homogeneity and characterization of a novel Pseudomonas putida chromate reductase*. Applied and Environmental Microbiology, 2000. **66**: p. 1788-1795.
139. Ishibashi, Y., C. Cervantes, and S. Silver, *Chromium reduction in Pseudomonas putida*. Applied and Environmental Microbiology, 1990. **56**: p. 2268-2270.
140. Suzuki, T., et al., *NAD(P)H-dependent chromium (VI) reductase of Pseudomonas ambigua G-1: a Cr(V) intermediate is formed during the reduction of Cr(VI) to Cr(III)*. Journal of Bacteriology, 1992. **174**(16): p. 5340-5.
141. Riedel, G.F., *The relationship between chromium (VI) uptake, sulfate uptake, and chromium toxicity in the estuarine diatom Thalassiosira pseudonana*. Aquatic Toxicology, 1985. **7**: p. 191-204.
142. Katz, S.A. and H. Salem, *The toxicology of chromium with respect to its chemical speciation: a review*. Journal of Applied Toxicology, 1993. **13**: p. 217-224.
143. Singh, J., et al., *Chromium-induced genotoxicity and apoptosis: relationship to chromium carcinogenesis*. Oncol. Rep., 1998. **5**: p. 1307-1318.
144. Hossain, M.A., M. Alam, and D.R. Yonge, *Estimating the dual-enzyme kinetic parameters for Cr (VI) reduction by Shewanella oneidensis MR-1 from soil column experiments*. Water Research, 2005. **39**(14): p. 3342-8.
145. Hossain, M.A., et al., *Finite element modeling of Cr(VI) reduction by Shewanella oneidensis MR-1 employing the dual-enzyme kinetic model*. Computers & Geosciences, 2005. **31**: p. 1286-1292.
146. Viamajala, S., et al., *Toxic effects of Chromium(VI) on anaerobic and aerobic growth of Shewanella oneidensis MR-1*. Biotechnol. Prog., 2004. **20**: p. 87-95.

147. Brown, S.D., et al., *Molecular Dynamics of the Shewanella oneidensis Response to Chromate Stress*. Molecular & Cellular Proteomics, 2006. **5**: p. 1054-1071.
148. Summers, A.O. and G.A. Jacoby, *Plasmid-determined resistance to boron and chromium compounds in Pseudomonas aeruginosa*. Antimicrob. Agents Chemother., 1978. **13**: p. 637-640.
149. Ohtake, H., C. Cervantes, and S. Silver, *Decreased chromate uptake in Pseudomonas fluorescens carrying a chromate resistance plasmid*. Journal of Bacteriology, 1987. **169**: p. 3853-3556.
150. Cervantes, C. and H. Ohtake, *Plasmid-determined resistance to chromate in Pseudomonas aeruginosa*. FEMS Microbiology Letters, 1988. **56**: p. 173-176.
151. Cervantes, C., et al., *Cloning, nucleotide sequence, and expression of the chromate resistance determinant of Pseudomonas aeruginosa plasmid pUM505*. . Journal of Bacteriology, 1990. **172**: p. 287-291.
152. Bopp, L.H., A.M. Chakrabarty, and H.L. Ehrlich, *Chromate resistance plasmid in Pseudomonas fluorescens*. Journal of Bacteriology, 1983. **155**: p. 1105-1109.
153. Bopp, L.H. and H.L. Erlich, *Chromate resistance and reduction in Pseudomonas fluorescens strain LB300*. Arch. Microbiol., 1988. **150**: p. 426-431.
154. Nies, A., D.H. Nies, and S. Silver, *Cloning and expression of plasmid genes encoding resistances to chromate and cobalt in Alcaligenes eutrophus*. Journal of Bacteriology, 1989. **171**: p. 5065-5070.
155. Nies, A., D.H. Nies, and S. Silver, *Nucleotide sequence and expression of a plasmid-encoded chromate resistance determinant from Alcaligenes eutrophus*. Journal of Biological Chemistry, 1990. **265**: p. 5648-5653.

156. Thompson, M.R., et al., *Dosage-Dependent Proteome Response of Shewanella oneidensis MR-1 to Acute Chromate Challenge*. Journal of Proteome Research, 2007. **6**(5): p. 1745-1757.
157. Chourey, K., et al., *The orphan response regulator SO2426 of Shewanella oneidensis MR-1 is involved in the cellular response to metal stress*. 2007. **In preparation for submission to Journal of Bacteriology.**
158. Chourey, K., et al., *Global Molecular and Morphological Effects of 24-h Chromium Exposure on Shewanella oneidensis MR-1*. Applied and Environmental Microbiology, 2006. **72**: p. 6331-6344.
159. Thompson, M.R., et al., *Proteomic Comparison of Shewanella oneidensis MR-1 Wild-Type and a Response Regulator Deletion Strain under Conditions of Chromate Transformation*. 2007. **In preparation for submission to Applied and Environmental Microbiology.**
160. Thompson, M.R., et al., *Experimental Approach For Large-Scale Proteome Measurements From Small Amounts (low mg) Of Microbial Cultures*. 2007. **In preparation for submission to Analytical Chemistry.**
161. Rice, R.H., G.E. Means, and W.D. Brown, *Stabilization of bovine trypsin by reductive methylation*. Biochimica et Biophysica Acta, 1977. **492**(2): p. 316-21.
162. Smith, P.K., et al., *Measurement of protein using bicinchoninic acid*. Analytical Biochemistry, 1985. **150**(1): p. 76-85.
163. Chao, L. and I.E. Liener, *Autoactivation of Porcine Trypsinogen in the Presence and Absence of Calcium*. Biochim Biophys Acta, 1965. **96**: p. 508-16.

164. Wollum, A.G., *Cultural methods for soil microorganisms*, in *Methods of Soil Analysis. Part 2-Chemical and Microbiological Properties*, A.L. Page, R.H. Miller, and D.R. Keency, Editors. 1982, Soil Science Society of America: Madison, WI. p. 781-802.
165. Qian, W.J., et al., *Comparative proteome analyses of human plasma following in vivo lipopolysaccharide administration using multidimensional separations coupled with tandem mass spectrometry*. *Proteomics*, 2005. **5**(2): p. 572-84.
166. McDonald, W.H., et al., *Comparison of three directly coupled HPLC MS/MS strategies for identification of proteins from complex mixtures: single-dimension LC-MS/MS, 2-phase MudPIT, and 3-phase MudPIT*. *International Journal of Mass Spectrometry*, 2002. **219**: p. 245-251.
167. de Hoffman, E. and V. Stroobant, 2. *Mass Analyzers*, in *Mass Spectrometry: Principles and Applications*. 2002, John Wiley & Sons, LTD.: New York. p. 63-132.
168. Paul, W. and H. Steinwedel, *Patent No. 2.939,952*. 1960: United States Patent.
169. de Hoffman, E. and V. Stroobant, 3. *Tandem Mass Spectrometry (MS/MS)*, in *Mass Spectrometry: Principles and Applications*. 2002, John Wiley & Sons, LTD: New York. p. 133-181.
170. Schwartz, J.C. and I. Jardine, *Quadrupole ion trap mass spectrometry*. *Methods in Enzymology*, 1996. **270**: p. 552-86.
171. Tabb, D.L., W.H. McDonald, and J.R. Yates III, *DTASelect and Contrast: Tools for assembling and comparing protein identifications from shotgun proteomics*. *Journal of Proteome Research*, 2002. **1**: p. 21-26.

172. Tabb, D.L., et al., *Determination of peptide and protein ion charge states by Fourier transformation of isotope-resolved mass spectra*. Journal of the American Society for Mass Spectrometry, 2006. **17**(7): p. 903-15.
173. Narasimhan, C., et al., *MASPIC: intensity-based tandem mass spectrometry scoring scheme that improves peptide identification at high confidence*. Anal Chem, 2005. **77**(23): p. 7581-93.
174. Keller, A., et al., *Empirical statistical model to estimate the accuracy of peptide identifications made by MS/MS and database search*. Analytical Chemistry, 2002. **74**(20): p. 5383-92.
175. Washburn, M.P., et al., *Analysis of quantitative proteomic data generated via multidimensional protein identification technology*. Analytical Chemistry, 2002. **74**: p. 1650-1657.
176. Wu, C.C., et al., *Metabolic labeling of mammalian organisms with stable isotopes for quantitative proteomic analysis*. Analytical Chemistry, 2004. **76**(17): p. 4951-9.
177. Gygi, S.P., et al., *Quantitative analysis of complex protein mixtures using isotope-coded affinity tags*. Nature Biotechnology, 1999. **17**(10): p. 994-9.
178. Wu, W.W., et al., *Comparative study of three proteomic quantitative methods, DIGE, cICAT, and iTRAQ, using 2D Gel- or LC-MALDI TOF/TOF*. Journal of Proteome Research, 2006. **5**: p. 651-658.
179. Shadforth, I.P., et al., *i-Tracker: For quantitative proteomics using iTRAQ (TM)*. BMC Genomics, 2005. **6**: p. 145-150.

180. Zieske, L.R., *A perspective on the use of iTRAQ (TM) reagent technology for protein complex and profiling studies*. Journal of Experimental Botany, 2006. **57**: p. 1501-1508.
181. Kirkpatrick, D.S., S.A. Gerber, and S.P. Gygi, *The absolute quantification strategy: a general procedure for the quantification of proteins and post-translational modifications*. Methods, 2005. **35**(3): p. 265-73.
182. Zybailov, B.L., L. Florens, and M.P. Washburn, *Quantitative shotgun proteomics using a protease with broad specificity and normalized spectral abundance factors*. Molecular Biosystems, 2007. **3**(5): p. 354-60.
183. Zhang, B., et al., *Detecting differential and correlated protein expression in label-free shotgun proteomics*. Journal of Proteome Research, 2006. **5**: p. 2909-2918.
184. VerBerkmoes, N.C., et al., *Determination and comparison of the baseline proteomes of the versatile microbe Rhodospseudomonas palustris under its major metabolic states*. Journal of Proteome Research, 2006. **5**: p. 287-298.
185. Peng, J., et al., *Evaluation of multidimensional chromatography coupled with tandem mass spectrometry (LC/LC-MS/MS) for large-scale protein analysis: the yeast proteome*. Journal of Proteome Research, 2003. **2**(1): p. 43-50.
186. Giometti, C.S., et al., *Analysis of the Shewanella oneidensis proteome by two-dimensional gel electrophoresis under nondenaturing conditions*. Proteomics, 2003. **3**: p. 777-785.
187. Kolker, E., et al., *Global profiling of Shewanella oneidensis MR-1: Expression of hypothetical genes and improved functional annotations*. PNAS, 2005. **102**: p. 2099-2104.

188. Wang, C.C., and Newton, A. (1969) *Iron transport in Escherichia coli: relationship between chromium sensitivity and high iron requirement in mutants of Escherichia coli*. Journal of Bacteriology, 1969. **98**: p. 1135-1141.
189. Andrews, S.C., A.K. Robinson, and F. Rodriguez-Quinones, *Bacterial iron homeostasis*. FEMS Microbiology Reviews, 2003. **27**: p. 215-237.
190. de Lorenzo, V., et al. *Iron transport in bacteria*. in *American Society for Microbiology*. 2004. Washington, D.C.
191. Andrews, S.C., et al., *Overproduction, purification and characterization of the bacterioferritin of Escherichia coli and a C-terminally extended variant*. European Journal of Biochemistry, 1993. **213**: p. 329-338.
192. Qiu, X., et al., *Comparative analysis of differentially expressed genes in Shewanella oneidensis MR-1 following exposure to UVC, UVB, and UVA radiation*. Journal of Bacteriology, 2005. **187**: p. 3556-3564.
193. Palma, M., et al., *Transcriptome analysis of the response of Pseudomonas aeruginosa to hydrogen peroxide*. Journal of Bacteriology, 2004. **186**: p. 248-252.
194. Salunkhe, P., et al., *Genome-wide transcriptional profiling of the steady-state response of Pseudomonas aeruginosa to hydrogen peroxide*. Journal of Bacteriology, 2005. **187**: p. 2565-2572.
195. Zheng, M., et al., *OxyR and SoxRS regulation of fur*. Journal of Bacteriology, 1999. **181**: p. 4639-4643.
196. Benov, L., Kredich, N. M., and Fridovich, I. (1996) *The mechanism of the auxotrophy for sulfur-containing amino acids imposed upon Escherichia coli by superoxide*. Journal of Biological Chemistry, 1996. **271**: p. 21037-21040.

197. Newton, G.L., et al., *Distribution of thiols in microorganisms: mycothiol is a major thiol in most actinomycetes*. Journal of Bacteriology, 1996. **178**: p. 1990-1995.
198. Mitaku, S., T. Hirokawa, and T. Tsuji, *Amphiphilicity index of polar amino acids as an aid in the characterization of amino acid preference at membrane-water interfaces*. Bioinformatics, 2002. **18**: p. 608-616.
199. Ferguson, G.P., et al., *Methylglyoxal production in bacteria: suicide or survival?* Arch. Microbiol., 1998. **170**: p. 209-219.
200. McGinnis, S. and T.L. Madden, *BLAST: at the core of a powerful and diverse set of sequence analysis tools*. Nucleic Acids Research, 2004. **32**: p. W20-W25.
201. Ackerley, D.F., et al., *Chromate-reducing properties of soluble flavoproteins from Pseudomonas putida and Escherichia coli*. Applied and Environmental Microbiology, 2004. **70**: p. 873-882.
202. Gonzalez, C.F., et al., *ChrR, a soluble quinone reductase of Pseudomonas putida that defends against H₂O₂*. Journal of Biological Chemistry, 2005. **280**: p. 22590-22595.
203. Qiu, X., et al., *Transcriptome analysis applied to survival of Shewanella oneidensis MR-1 exposed to ionizing radiation*. Journal of Bacteriology, 2006. **188**: p. 1199-1204.
204. Aswad, D.W., *Stoichiometric methylation of porcine adrenocorticotropin by protein carboxyl methyltransferase requires deamidation of asparagine 25. Evidence for methylation at the alpha-carboxyl group of atypical L-isoaspartyl residues*. Journal of Biological Chemistry, 1984. **259**: p. 10714-10721.

205. Murray, E.D., Jr. and S. Clarke, *Synthetic peptide substrates for the erythrocyte protein carboxyl methyltransferase. Detection of a new site of methylation at isomerized L-aspartyl residues*. Journal of Biological Chemistry, 1984. **259**: p. 10722-10732.
206. Visick, J.E., H. Cai, and S. Clarke. 1998. , *The L-isoaspartyl protein repair methyltransferase enhances survival of aging Escherichia coli subjected to secondary environmental stresses*. Journal of Bacteriology, 1998. **180**: p. 2623-2629.
207. Elias, D.A., et al., *Confirmation of the expression of a large set of conserved hypothetical proteins in Shewanella oneidensis MR-1*. Journal of Microbiological Methods, 2006. **66**(2): p. 223-33.
208. Jonscher, K.R. and J.R. Yates III, *The quadrupole ion trap mass spectrometer--a small solution to a big challenge*. Analytical Biochemistry, 1997. **244**: p. 1-15.
209. Kolker, E., et al., *Initial proteome analysis of model microorganism Haemophilus influenzae strain Rd KW20*. Journal of Bacteriology, 2003. **185**: p. 4593-4602.
210. Florens, L., et al., *A proteomic view of the Plasmodium falciparum life cycle*. Nature, 2002. **419**: p. 520-526.
211. Romine, M.F., et al., *Validation of Shewanella oneidensis MR-1 small proteins by AMT tag-based proteome analysis*. OMICS, 2004. **8**: p. 239-254.
212. Elias, D.A., et al., *Global detection and characterization of hypothetical proteins in Shewanella oneidensis MR-1 using LC-MS based proteomics*. Proteomics, 2005. **5**: p. 3120-3130.

213. Gadd, G.M., *Bioremedial potential of microbial mechanisms of metal mobilization and immobilization*. Curr Opin Biotechnol, 2000. **11**: p. 271-9.
214. Lovley, D.R. and E.J. Phillips, *Reduction of Chromate by Desulfovibrio vulgaris and Its c(3) Cytochrome*. Applied and Environmental Microbiology, 1994. **60**(2): p. 726-728.
215. Xie, H. and T.J. Griffin, *Trade-off between high sensitivity and increased potential for false positive peptide sequence matches using a two-dimensional linear ion trap for tandem mass spectrometry-based proteomics*. Journal of Proteome Research, 2006. **5**(4): p. 1003-9.
216. Luo, Q., et al., *Preparation of 20- μ m-i.d. silica-based monolithic columns and their performance for proteomics analyses*. Analytical Chemistry, 2005. **77**: p. 5028-5035.
217. Alvarez, A.H., R. Moreno-Sánchez, and C. Cervantes, *Chromate efflux by means of the ChrA chromate resistance protein from Pseudomonas aeruginosa*. Journal of Bacteriology, 1999. **181**: p. 7398-7400.
218. Muskotal, A., et al., *Interaction of FliS flagellar chaperone with flagellin*. FEBS Letters, 2006. **580**(16): p. 3916-20.
219. Thomas, J.G. and F. Baneyx, *Roles of the Escherichia coli small heat shock proteins IbpA and IbpB in thermal stress management: comparison with ClpA, ClpB, and HtpG in vivo*. Journal of Bacteriology, 1998. **180**: p. 5165-5172.
220. Tsung, K., S. Inouye, and M. Inouye, *Factors affecting the efficiency of protein synthesis in Escherichia coli. Production of a polypeptide of more than 6000 amino acid residues*. J Biol Chem, 1989. **264**(8): p. 4428-33.

221. Jiang, X., et al., *Escherichia coli prlC gene encodes a trypsin-like proteinase regulating the cell cycle*. J Biochem (Tokyo), 1998. **124**(5): p. 980-5.
222. Weber, A., S.A. Kogl, and K. Jung, *Time-dependent proteome alterations under osmotic stress during aerobic and anaerobic growth in Escherichia coli*. Journal of Bacteriology, 2006. **188**(20): p. 7165-75.
223. Han, K.K. and A. Martinage, *Post-translational chemical modification(s) of proteins*. The International Journal of Biochemistry, 1992. **24**(1): p. 19-28.
224. Sourjik, V., *Receptor clustering and signal processing in E. coli chemotaxis*. Trends in Microbiology, 2004. **12**(12): p. 569-76.
225. Humbard, M.A., S.M. Stevens, Jr., and J.A. Maupin-Furlow, *Posttranslational modification of the 20S proteasomal proteins of the archaeon Haloferax volcanii*. Journal of Bacteriology, 2006. **188**(21): p. 7521-30.
226. Guan, J. and M.R. Chance, *Structural proteomics of macromolecular assemblies using oxidative footprinting and mass spectrometry*. Trends in Biochemical Sciences, 2005. **30**: p. 583-592.
227. Jaakkola, P., et al., *Targeting of HIF- α to the von Hippel-Lindau Ubiquitylation Complex by O₂-Regulated Prolyl Hydroxylation*. Science, 2001. **292**(5516): p. 468-472.
228. Mulkidjanian, A.Y., *Ubiquinol oxidation in the cytochrome bc1 complex: reaction mechanism and prevention of short-circuiting*. Biochim Biophys Acta, 2005. **1709**(1): p. 5-34.

229. Roth, M.J., et al., *Precise and parallel characterization of coding polymorphisms, alternative splicing and modifications in human proteins by mass spectrometry*. Molecular & Cellular Proteomics, 2005. **4**(1002-1008).
230. Garcia, B.A., J. Shabanowitz, and D.F. Hunt, *Characterization of histones and their post-translational modifications by mass spectrometry*. Current Opinion in Chemical Biology, 2007. **11**(1): p. 66-73.
231. Nielsen, M.L., M.M. Savitski, and R.A. Zubarev, *Extent of modifications in human proteome samples and their effect on dynamic range of analysis in shotgun proteomics*. Molecular & Cellular Proteomics, 2006. **5**(12): p. 2384-91.
232. Lewis, R.J., et al., *Phosphorylated aspartate in the structure of a response regulator protein*. Journal of Molecular Biology, 1999. **294**: p. 9-15.
233. Kleinnijenhuis, A.J., et al., *Analysis of Histidine Phosphorylation Using Tandem MS and Ion-Electron Reactions*. Analytical Chemistry, 2007.
234. Vasilescu, J., et al., *Proteomic analysis of ubiquitinated proteins from human MCF-7 breast cancer cells by immunoaffinity purification and mass spectrometry*. Journal of Proteome Research, 2005. **4**(6): p. 2192-200.
235. Havilio, M. and A. Wool, *Large-scale unrestricted identification of post-translational modifications using tandem mass spectrometry*. Analytical Chemistry, 2007: p. (7).
236. Annan, R.S. and S.A. Carr, *The essential role of mass spectrometry in characterizing protein structure: mapping posttranslational modifications*. Journal of Protein Chemistry, 1997. **16**(5): p. 391-402.

237. Florens, L., et al., *Analyzing chromatin remodeling complexes using shotgun proteomics and normalized spectral abundance factors*. Methods, 2006. **40**: p. 303-311.
238. Allen, J.F., *Redox control of transcription: sensors, response regulators, activators and repressors*. FEBS Letters, 1993. **332**: p. 203-207.
239. Kato, A. and E.A. Groisman, *Connecting two-component regulatory systems by a protein that protects a response regulator from dephosphorylation by its cognate sensor*. Genes Dev, 2004. **18**(18): p. 2302-13.
240. Stock, J.B., M.N. Levit, and P.M. Wolanin, *Information processing in bacterial chemotaxis*. Science's STKE, 2002.
241. Djordjevic, S. and A.M. Stock, *Structural analysis of bacterial chemotaxis proteins: components of a dynamic signaling system*. J Struct Biol, 1998. **124**(2-3): p. 189-200.
242. Groh, J.L., et al., *A method adapting microarray technology for signature-tagged mutagenesis of *Desulfovibrio desulfuricans* G20 and *Shewanella oneidensis* MR-1 in anaerobic sediment survival experiment*. Applied and Environmental Microbiology, 2005. **71**: p. 7064-7074.
243. Liu, Y., et al., *Transcriptome analysis of *Shewanella oneidensis* MR-1 in response to elevated salt conditions*. Journal of Bacteriology, 2005. **187**: p. 2501-2507.
244. Shioi, J., C.V. Dang, and B.L. Taylor, *Oxygen as attractant and repellent in bacterial chemotaxis*. Journal of Bacteriology, 1987. **169**(7): p. 3118-23.
245. Jeanmougin, F., et al., *Multiple sequence alignment with Clustal X*. Trends in Biochemical Sciences, 1998. **23**: p. 403-405.

246. Kleene, S.J., M.L. Toews, and J. Adler, *Isolation of glutamic acid methyl ester from an Escherichia coli membrane protein involved in chemotaxis*. The Journal of Biological Chemistry, 1977. **252**(10): p. 3214-8.
247. Gralnick, J.A., C.T. Brown, and D.K. Newman, *Anaerobic regulation by an atypical Arc system in Shewanella oneidensis*. Molecular Microbiology, 2005. **56**(5): p. 1347-57.
248. Brown, S.D., et al., *Cellular response of Shewanella oneidensis to strontium stress*. Applied and Environmental Microbiology, 2006. **72**(1): p. 890-900.
249. Mizoguchi, H., H. Mori, and T. Fujio, *Escherichia coli minimum genome factory*. Biotechnology and Applied Biochemistry, 2007. **46**: p. 157-167.
250. Lipton, M.S., et al., *Global analysis of the Deinococcus radiodurans proteome by using accurate mass tags*. PNAS, 2002. **99**: p. 11049-11054.
251. Karp, N.A., et al., *Impact of replicate types on proteomic expression analysis*. Journal of Proteome Research, 2005. **4**(5): p. 1867-71.
252. Schmid, A.K., et al., *Global whole-cell FTICR mass spectrometric proteomics analysis of the heat shock response in the radioresistant bacterium Deinococcus radiodurans*. Journal of Proteome Research, 2005. **4**: p. 709-718.
253. Zybaylov, B., et al., *Statistical analysis of membrane proteome expression changes in Saccharomyces cerevisiae*. Journal of Proteome Research, 2006. **5**(9): p. 2339-47.
254. Finn, R.D., et al., *Pfam: clans, web tools and services*. Nucleic Acids Res, 2006. **34**(Database issue): p. D247-51.

255. Bigas, A., et al., *Non-viability of Haemophilus parasuis fur-defective mutants*. Vet Microbiol, 2006. **118**(1-2): p. 107-16.
256. Idone, V., et al., *Effect of an orphan response regulator on Streptococcus mutans sucrose-dependent adherence and cariogenesis*. Infect Immun, 2003. **71**(8): p. 4351-60.
257. Jormakka, M., B. Byrne, and S. Iwata, *Formate dehydrogenase--a versatile enzyme in changing environments*. Curr Opin Struct Biol, 2003. **13**(4): p. 418-23.
258. Myers, C.R. and J.M. Myers, *MtrB is required for proper incorporation of the cytochromes OmcA and OmcB into the outer membrane of Shewanella putrefaciens MR-1*. Applied and Environmental Microbiology, 2002. **68**(11): p. 5585-94.
259. Palacios, S. and J.C. Escalante-Semerena, *prpR, ntrA, and ihf functions are required for expression of the prpBCDE operon, encoding enzymes that catabolize propionate in Salmonella enterica serovar typhimurium LT2*. J Bacteriol, 2000. **182**(4): p. 905-10.
260. Rigali, S., et al., *Subdivision of the helix-turn-helix GntR family of bacterial regulators in the FadR, HutC, MocR, and YtrA subfamilies*. Journal of Biological Chemistry, 2002. **277**(15): p. 12507-15.
261. Gorelik, M., et al., *Structural characterization of GntR/HutC family signaling domain*. Protein Science, 2006. **15**(6): p. 1506-11.
262. Varghese, S., Y. Tang, and J.A. Imlay, *Contrasting sensitivities of Escherichia coli aconitases A and B to oxidation and iron depletion*. J Bacteriol, 2003. **185**(1): p. 221-30.

263. Albanesi, D., et al., *Bacillus subtilis* cysteine synthetase is a global regulator of the expression of genes involved in sulfur assimilation. *J Bacteriol*, 2005. **187**(22): p. 7631-8.
264. Hess, J.F., R.B. Bourret, and M.I. Simon, *Phosphorylation assays for proteins of the two-component regulatory system controlling chemotaxis in Escherichia coli*. *Methods in Enzymology*, 1991. **200**: p. 188-204.
265. Viamajala, S., et al., *Chromate reduction in Shewanella oneidensis MR-1 is an inducible process associated with anaerobic growth*. *Biotechnology Progress*, 2002. **18**(2): p. 290-5.
266. Wang, H., et al., *Development and evaluation of a micro- and nanoscale proteomic sample preparation method*. *Journal of Proteome Research*, 2005. **4**: p. 2397-2403.
267. Corbin, R.W., et al., *Toward a protein profile of Escherichia coli: comparison to its transcription profile*. *PNAS*, 2003. **100**: p. 9232-9237.
268. Ross, P.L., et al., *Multiplexed protein quantitation in Saccharomyces cerevisiae using amine-reactive isobaric tagging reagents*. *Molecular & Cellular Proteomics*, 2004. **3**(12): p. 1154-69.
269. Zhu, W., et al., *Shotgun proteomics of Methanococcus jannaschii and insights into methanogenesis*. *Journal of Proteome Research*, 2004. **3**: p. 538-548.
270. Callister, S.J., et al., *Application of the Accurate Mass and Time Tag Approach to the Proteome Analysis of Sub-cellular Fractions Obtained from Rhodobacter sphaeroides 2.4.1. Aerobic and Photosynthetic Cell Cultures*. *Journal of Proteome Research*, 2006. **5**(8): p. 1940-1947.

271. Coleman, S.E., I. van de Rijn, and A.S. Bleiweis, *Lysis of Grouped and Ungrouped Streptococci by Lysozyme*. Infect Immun, 1970. **2**(5): p. 563-569.
272. Van Huynh, N., et al., *A procedure for the preparation of bacterial DNA that employs dimethyl sulfoxide to induce the lysis of cells*. Analytical Biochemistry, 1989. **176**: p. 464-467.
273. Yu, Y.Q., et al., *Enzyme-friendly, mass spectrometry-compatible surfactant for in-solution enzymatic digestion of proteins*. Analytical Chemistry, 2003. **75**(21): p. 6023-8.
274. Bosserhoff, A., J. Wallach, and R.W. Frank, *Micropreparative separation of peptides derived from sodium dodecyl sulphate-solubilized proteins*. Journal of Chromatography, 1989. **473**(1): p. 71-7.
275. De Leij, L. and B. Witholt, *Structural heterogeneity of the cytoplasmic and outer membranes of Escherichia coli*. Biochimica et Biophysica Acta, 1977. **471**(1): p. 92-104.
276. Guerlava, P., V. Izac, and J.L. Tholozan, *Comparison of different methods of cell lysis and protein measurements in Clostridium perfringens: application to the cell volume determination*. Curr Microbiol, 1998. **36**(3): p. 131-5.
277. Wilkinson, J.M., *Fragmentation of Polypeptides by Enzymic Methods*. Practical Protein Chemistry: A Handbook. , ed. A. Darbre. 1986, New York: John Wiley and Sons.
278. Woese, C.R., *Whither microbiology? Phylogenetic trees*. Curr Biol, 1996. **6**(9): p. 1060-3.

279. Schloss, P.D. and J. Handelsman, *Biotechnological prospects from metagenomics*. Curr Opin Biotechnol, 2003. **14**(3): p. 303-10.
280. Handelsman, J., et al., *Molecular biological access to the chemistry of unknown soil microbes: a new frontier for natural products*. Chemistry & Biology, 1998. **5**(10): p. R245-9.
281. Torsvik, V. and L. Ovreas, *Microbial diversity and function in soil: from genes to ecosystems*. Current Opinion in Microbiology, 2002. **5**(3): p. 240-5.
282. Biron, D.G., et al., *Population proteomics: an emerging discipline to study metapopulation ecology*. Proteomics, 2006. **6**(6): p. 1712-5.
283. Paul, D., et al., *Assessing microbial diversity for bioremediation and environmental restoration*. Trends Biotechnol, 2005. **23**(3): p. 135-42.
284. Wilmes, P. and P.L. Bond, *The application of two-dimensional polyacrylamide gel electrophoresis and downstream analyses to a mixed community of prokaryotic microorganisms*. Environmental Microbiology, 2004. **6**(9): p. 911-20.
285. Wilmes, P. and P.L. Bond, *Towards exposure of elusive metabolic mixed-culture processes: the application of metaproteomic analyses to activated sludge*. Water Science and Technology, 2006. **54**(1): p. 217-26.
286. Powell, M.J., et al., *Marine proteomics: generation of sequence tags for dissolved proteins in seawater using tandem mass spectrometry*. Marine Chemistry, 2005. **95**: p. 183-198.
287. Savidor, A., et al., *Expressed peptide tags: an additional layer of data for genome annotation*. Journal of Proteome Research, 2006. **5**(11): p. 3048-58.

288. Varga, A.R. and L.A. Staehelin, *Spatial differentiation in photosynthetic and non-photosynthetic membranes of Rhodopseudomonas palustris*. Journal of Bacteriology, 1983. **154**(3): p. 1414-30.
289. Deshusses, J.M., et al., *Exploitation of specific properties of trifluoroethanol for extraction and separation of membrane proteins*. Proteomics, 2003. **3**(8): p. 1418-24.
290. Lo, I., et al., *Strain-resolved community proteomics reveals recombining genomes of acidophilic bacteria*. Nature, 2007. **446**(7135): p. 537-41.
291. Gan, C.S., et al., *Technical, experimental, and biological variations in isobaric tags for relative and absolute quantitation (iTRAQ)*. Journal of Proteome Research, 2007. **6**(2): p. 821-7.
292. Larsen, M.R., et al., *Analysis of posttranslational modifications of proteins by tandem mass spectrometry*. Biotechniques, 2006. **40**(6): p. 790-8.
293. Viamajala, S., B.M. Peyton, and J.N. Petersen, *Modeling chromate reduction in Shewanella oneidensis MR-1: Development of a novel dual-enzyme kinetic model*. Biotechnology and Bioengineering, 2003. **83**: p. 790-797.
294. Tang, Y.J., et al., *Evaluation of the effects of various culture conditions on Cr(VI) reduction by Shewanella oneidensis MR-1 in a novel high-throughput mini-bioreactor*. Biotechnology and Bioengineering, 2006. **95**(1): p. 176-84.
295. Hermjakob, H., et al., *The HUPO PSI's molecular interaction format--a community standard for the representation of protein interaction data*. Nature Biotechnology, 2004. **22**(2): p. 177-83.

296. Cuticchia, A.J., *Future vision of the GDB human genome database*. Hum Mutat, 2000. **15**(1): p. 62-7.
297. Karp, P.D., S. Paley, and J. Zhu, *Database verification studies of SWISS-PROT and GenBank*. Bioinformatics, 2001. **17**(6): p. 526-32; discussion 533-4.
298. Ashurst, J.L. and J.E. Collins, *Gene annotation: prediction and testing*. Annu Rev Genomics Hum Genet, 2003. **4**: p. 69-88.
299. Skupski, M.P., et al., *The Genome Sequence DataBase: towards an integrated functional genomics resource*. Nucleic Acids Research, 1999. **27**(1): p. 35-8.
300. Domon, B. and R. Aebersold, *Challenges and Opportunities in Proteomics Data Analysis*. Molecular & Cellular Proteomics, 2006. **5**(10): p. 1921-1926.
301. Norbeck, A.D., et al., *Proteomic approaches to bacterial differentiation*. Journal of Microbiological Methods, 2006. **67**(3): p. 473-86.
302. Lacerda, C.M., L.H. Choe, and K.F. Reardon, *Metaproteomic analysis of a bacterial community response to cadmium exposure*. Journal of Proteome Research, 2007. **6**(3): p. 1145-52.

Appendix

Appendix A1: All Peptides Identified in Cr-Shocked *S. oneidensis* MR-1 using an LTQ Mass Spectrometer

Locus	45 min Control		45 min Cr		90 min Control		90 min Cr		Description
	Run 1	Run 2	Run 1	Run 2	Run 1	Run 2	Run 1	Run 2	
SO0002					2				proton/peptide symporter family protein
SO0003	2	4				3	2	3	tRNA modification GTPase TrmE (trmE)
SO0004	26	18	19	18	24	15	20	16	inner membrane protein, 60 kDa
SO0005		2				3		2	conserved hypothetical protein TIGR00278
SO0006	2	3	3	3	2	3	2	2	ribonuclease P protein component (rnpA)
SO0007		2							ribosomal protein L34 (rpmH)
SO0008	10	12	9	13	13	14	13	14	chromosomal replication initiator protein DnaA (dnaA)
SO0009	6	8	10	12	8	7	9	11	DNA polymerase III, beta subunit (dnaN)
SO0010		2		2		2			DNA replication and repair protein RecF (recF)
SO0011	44	49	48	55	56	44	56	66	DNA gyrase, B subunit (gyrB)
SO0012				2			2		glutathione S-transferase family protein
SO0014	32	42	37	40	34	35	34	44	glycyl-tRNA synthetase, beta subunit (glyS)
SO0015	3				3		2	4	glycyl-tRNA synthetase, alpha subunit (glyQ)
SO0016								2	DNA-3-methyladenine glycosidase I (tag)
SO0017	7	8	2	2	4	8		4	conserved hypothetical protein
SO0018	2	3	2	2			3	2	conserved hypothetical protein
SO0019		5		3			2	3	conserved hypothetical protein
SO0020	23	21	19	20	21	24	13	22	fatty oxidation complex, beta subunit (fadA)
SO0021	43	53	45	48	43	40	47	52	fatty oxidation complex, alpha subunit (fadB)
SO0022		3	2	2			4	4	prolidase (pepQ)
SO0025	2	3			2	2		3	conserved hypothetical protein
SO0026				2			3		transcriptional regulator, ArsR family
SO0027	3				3	5			protoporphyrinogen oxidase, putative
SO0029	9	16	5	9	11	17	6	9	potassium uptake protein TrkA (trkA)
SO0030	10	8	4	7	4	2	4	8	sun protein (sun)
SO0031	7	10	5	7	7		4	7	methionyl-tRNA formyltransferase (fmt)
SO0032	3	6	6	7	8	2	5	6	polypeptide deformylase (def-1)
SO0033	3	4	5	3	2		5	3	LysM domain protein
SO0037		2	2					2	Sua5/YciO/YrdC/YwlC family protein
SO0038	2	3	2	2	2			3	coproporphyrinogen III oxidase, aerobic (hemF)

Locus	45 min Control		45 min Cr		90 min Control		90 min Cr		Description
	Run 1	Run 2	Run 1	Run 2	Run 1	Run 2	Run 1	Run 2	
SO0039	3	3	3	2	4		3	4	conserved hypothetical protein
SO0042	3	3				2			carbonic anhydrase, family 3
SO0045	2			4	2				Rrf2 family protein
SO0048	15	15	8	14	17	7	11	12	peptidase, M23/M37 family phosphoglycerate mutase, 2,3-bisphosphoglycerate-independent
SO0049	16	9	12	12	9	9	14	14	(gpmA)
SO0050	10	11	9	9	10	9	9	10	rhodanese domain protein
SO0052	9	16	20	16	17	14	18	17	protein-export protein SecB (secB)
SO0053	5	7	8	9	4	3	8	7	glycerol-3-phosphate dehydrogenase (NAD(P)+) (gpsA)
SO0054	2								conserved hypothetical protein TIGR00275
SO0055				2			3	3	conserved domain protein
SO0060		2							sensor histidine kinase
SO0061	3			2		2			lipoprotein, NLP/P60 family
SO0062	6	5	3	4	4	3	4	3	hypothetical protein
SO0063			3	2	3		2	2	conserved hypothetical protein
SO0065	9	6	7	3	3	4	2		molybdenum cofactor biosynthesis protein Mog (mog)
SO0066	23	28	22	27	28	27	24	31	conserved hypothetical protein
SO0067								2	penicillin-binding protein 1C, putative
SO0069	3	3	4	4	5	2	5	6	transport protein, putative
SO0070	5	8	6	9	6	8	9	5	ATP-binding transport protein NatA (natA)
SO0071	9	9	10	12	10	6	11	12	hydrolase, alpha/beta hydrolase fold family
SO0072		4				3			transcriptional regulator, GntR family
SO0073	7	9	8	9	5	5	5	8	ABC transporter, ATP-binding protein
SO0075	12	19	11	11	14	18	9	9	AMP-binding family protein
SO0076	38	51	44	50	42	26	27	38	hypothetical protein
SO0080				2					conserved hypothetical protein
SO0084	3	8	10	10	7	7	13	10	HAD-superfamily hydrolase, subfamily IA, variant 1 family protein
SO0095	12	11	7	7	6	8	5	4	imidazolonepropionase (hutI)
SO0096	5	2	3		2				histidine utilization repressor (hutC)
SO0097	23	25	25	25	24	21	20	20	urocanate hydratase (hutU)
SO0098	15	22	13	9	20	10	13	12	histidine ammonia-lyase (hutH)
SO0102	7	12	6	10	6	7	5	5	formate dehydrogenase, nitrate-inducible, iron-sulfur subunit (fdnH)
SO0104	3	4	2	5	4		3	5	fdhE protein (fdhE)

Locus	45 min Control		45 min Cr		90 min Control		90 min Cr		Description
	Run 1	Run 2	Run 1	Run 2	Run 1	Run 2	Run 1	Run 2	
SO0105	7	6	2	4	10	4	3	4	L-seryl-tRNA selenium transferase (selA)
SO0106	6	5	4	5	9	5	6	7	selenocysteine-specific translation elongation factor (selB)
SO0108			2	2					conserved hypothetical protein
SO0109				2	2	2	2	2	conserved hypothetical protein
SO0110	6	6	2	4	8	6	7	4	conserved hypothetical protein
SO0112	4	3	3	4		6	5	5	conserved hypothetical protein
SO0113								2	conserved hypothetical protein
SO0114		2	2	2			2	2	conserved hypothetical protein
SO0118	3		2		3	3	2	2	hypothetical protein
SO0119			2						conserved hypothetical protein
SO0120	2	2	3			2	3	4	hypothetical protein
SO0121	12	10	9	13	10	9	11	12	conserved hypothetical protein
SO0123			3	2	2		2		acyltransferase family protein
SO0130	13	11	3	7	4	5		5	protease, putative
SO0131		2							conserved hypothetical protein
SO0132	2			2		2			flagellar protein FliL, putative
SO0135	7	7	6	6	8	5	7	6	hemolysin protein, putative
SO0137		2		3	2				molybdopterin biosynthesis MoeB protein (moeB)
SO0138	4	3	5	3	5				molybdopterin biosynthesis MoeA protein (moeA)
SO0139	5	9	10	10	5	5	9	10	ferritin (ftn)
SO0141	5	4	3	4	6	6	3	2	sensory box protein
SO0142	2	3	2					3	3,4-dihydroxy-2-butanone 4-phosphate synthase (ribB)
SO0144	12	19	13	17	15	13	9	12	protease II (ptrB)
SO0148		2	2					3	hypothetical protein
SO0152	17	15	13	17	12	10	8	13	conserved hypothetical protein
SO0162	22	29	24	25	28	15	24	30	phosphoenolpyruvate carboxykinase (ATP) (pckA)
SO0163	3				2		2		chaperonin HslO (hslO)
SO0164							2		heat shock protein 15 (hslR)
SO0165	10	17	10	10	10	15	10	15	general secretion pathway protein C (gspC)
SO0166	25	31	33	38	24	31	35	43	general secretion pathway protein D (gspD)
SO0167	17	21	14	17	21	18	14	15	general secretion pathway protein E (gspE)
SO0168	6	11	6	10	9	7	6	9	general secretion pathway protein F (gspF)

Locus	45 min Control		45 min Cr		90 min Control		90 min Cr		Description
	Run 1	Run 2	Run 1	Run 2	Run 1	Run 2	Run 1	Run 2	
SO0169	6	10	8	9	6	9	7	7	general secretion pathway protein G (gspG)
SO0171	2	2							general secretion pathway protein I (gspI)
SO0172		2	3	2	3	6	3	3	general secretion pathway protein J (gspJ)
SO0173	2		2		2		2		general secretion pathway protein K (gspK)
SO0174	12	14	13	8	8	7	9	12	general secretion pathway protein L (gspL)
SO0175	4	5	2	3	6	3	5	5	general secretion pathway protein M (gspM)
SO0176	7	12	10	8	7	6	10	9	general secretion pathway protein N (gspN)
SO0190		2		2			2	2	MutT/nudix family protein
SO0191		2		2			5	6	cysQ protein (cysQ-1)
SO0194		2	2		2	3			acyltransferase family protein
SO0196	6	10	6	9	9	4	4	9	selenide, water dikinase (selD)
SO0197	5	10	4	6	11	13	6	4	fatty acid desaturase, family 1
SO0198	5	6	6	5	5	5	5	2	transcriptional regulator, TetR family
SO0203			2						hypothetical protein
SO0206	4	5	6	4	2		2	6	tRNA (uracil-5-)-methyltransferase (trmA)
SO0208	5	9	8	5	6	6	7	9	RNA-binding protein
SO0215			2		2		2		pantothenate kinase (panK)
SO0217	63	72	65	68	62	65	61	66	translation elongation factor Tu (tufB)
SO0218				2					preprotein translocase, SecE subunit (secE)
SO0219	22	20	14	18	16	18	10	18	transcription antitermination protein NusG (nusG)
SO0220	15	16	18	17	16	22	14	16	ribosomal protein L11 (rplK)
SO0221	47	53	42	47	44	57	43	46	ribosomal protein L1 (rplA)
SO0222	38	41	34	40	39	48	35	34	ribosomal protein L10 (rplJ)
SO0223	17	18	21	18	19	18	21	24	ribosomal protein L7/L12 (rplL)
SO0224	166	194	153	166	170	172	155	175	DNA-directed RNA polymerase, beta subunit (rpoB)
SO0225	121	153	128	134	143	138	142	144	DNA-directed RNA polymerase, beta subunit (rpoC)
SO0226	13	18	15	17	14	12	17	17	ribosomal protein S12 (rpsL)
SO0227	32	37	33	38	38	42	30	33	ribosomal protein S7 (rpsG)
SO0228	44	62	50	46	42	34	29	42	translation elongation factor G (fusA-1)
SO0229	60	70	63	66	60	63	59	64	translation elongation factor Tu (tufA)
SO0230	16	17	17	18	17	18	15	14	ribosomal protein S10 (rpsJ)
SO0231	28	34	29	31	30	34	18	29	ribosomal protein L3 (rplC)

Locus	45 min Control		45 min Cr		90 min Control		90 min Cr		Description
	Run 1	Run 2	Run 1	Run 2	Run 1	Run 2	Run 1	Run 2	
SO0232	25	24	24	28	24	27	22	24	ribosomal protein L4 (rplD)
SO0233	14	12	13	13	12	22	11	10	ribosomal protein L23 (rplW)
SO0234	35	39	41	40	43	38	39	42	ribosomal protein L2 (rplB)
SO0235	11	14	11	13	10	11	12	12	ribosomal protein S19 (rpsS)
SO0236	23	25	22	24	21	23	22	24	ribosomal protein L22 (rplV)
SO0237	42	47	39	42	38	50	40	42	ribosomal protein S3 (rpsC)
SO0238	19	21	21	20	22	23	20	20	ribosomal protein L16 (rplP)
SO0239	11	11	12	15	11	15	11	10	ribosomal protein L29 (rpmC)
SO0240	16	16	15	15	15	16	14	18	ribosomal protein S17 (rpsQ)
SO0241	19	21	20	23	17	18	19	19	ribosomal protein L14 (rplN)
SO0242	21	25	25	25	21	29	26	24	ribosomal protein L24 (rplX)
SO0243	37	40	38	40	33	42	37	40	ribosomal protein L5 (rplE)
SO0244	13	12	10	15	13	10	13	10	ribosomal protein S14 (rpsN)
SO0245	19	16	15	18	17	26	11	15	ribosomal protein S8 (rpsH)
SO0246	28	33	29	30	28	34	26	28	ribosomal protein L6 (rplF)
SO0247	26	27	23	23	20	31	20	22	ribosomal protein L18 (rplR)
SO0248	28	29	29	24	21	30	22	25	ribosomal protein S5 (rpsE)
SO0249	7	11	9	9	7	9	5	7	ribosomal protein L30 (rpmD)
SO0250	24	26	23	26	23	26	21	21	ribosomal protein L15 (rplO)
SO0251	7	11	6	7	5	12	4	5	preprotein translocase, SecY subunit (secY)
SO0253	26	22	24	25	22	26	24	21	ribosomal protein S13 (rpsM)
SO0254	22	25	23	22	22	22	21	20	ribosomal protein S11 (rpsK)
SO0255	31	40	32	35	34	54	28	39	ribosomal protein S4 (rpsD)
SO0256	42	42	42	46	39	36	41	43	DNA-directed RNA polymerase, alpha subunit (rpoA)
SO0257	17	22	19	21	17	24	19	18	ribosomal protein L17 (rplQ)
SO0259	2		2	2		4	3	4	cytochrome c biogenesis protein CcmE (ccmE)
SO0261					3				heme exporter protein CcmC (ccmC)
SO0263	6	7	9	10	9	7	8	8	heme exporter protein CcmA (ccmA)
SO0264	7	6	4	3	4	7	3	3	cytochrome c (scyA)
SO0265	30	27	22	28	36	28	24	31	conserved hypothetical protein
SO0266	8	11	11	7	11	11	9	13	cytochrome c-type biogenesis protein CcmF (ccmF-1)
SO0267	13	21	18	9	17	18	16	15	thiol:disulfide interchange protein DsbE (dsbE)

Locus	45 min Control		45 min Cr		90 min Control		90 min Cr		Description
	Run 1	Run 2	Run 1	Run 2	Run 1	Run 2	Run 1	Run 2	
SO0268	9	9	6	4	6	10	6	9	cytochrome c-type biogenesis protein CcmH (ccmH)
SO0272	2	6	8	9	9	4	10	14	competence/damage-inducible protein CinA (cinA)
SO0273	4	8	9	4	8	4	6	7	conserved hypothetical protein
SO0274	17	14	13	14	19	15	16	19	phosphoenolpyruvate carboxylase (ppc)
SO0278		5	3	5	5		7	6	argininosuccinate synthase (argG)
SO0280	29	31	34	31	28	27	26	25	penicillin-binding protein 1A (mrcA)
SO0281		5	2	4	4	3			type IV pilus biogenesis protein PilM
SO0282	5	7	3	5	5	6	3	2	type IV pilus biogenesis protein PilN
SO0283	2	4			5		3	4	type IV pilus biogenesis protein PilO
SO0284	3	3	2	4		5	3	2	type IV pilus biogenesis protein PilP
SO0285	2	4	4	7	4	9	5	4	type IV pilus biogenesis protein PilQ
SO0286	6	8	7	6	6	8	6	10	shikimate kinase (aroK)
SO0287		2	2						3-dehydroquinate synthase (aroB)
SO0288	2	5	4	6	2	2	3	4	damX domain protein
SO0289	2	3		2			3	3	DNA adenine methylase (dam)
SO0292	7	7	5	6	7	5	6	7	ribulose-phosphate 3-epimerase (rpe)
SO0293	2								phosphoglycolate phosphatase (gph)
SO0294	8	9	13	13	9	8	4	10	tryptophanyl-tRNA synthetase (trpS)
SO0295						2			transcriptional regulator, LysR family
SO0297	6	6	7	8	6	7	10	8	lipoprotein, putative
SO0298	6	5	4	10	7	4	4	6	phosphoheptose isomerase (gmhA)
SO0300	19	25	15	19	21	16	24	26	lipoprotein, putative
SO0301	5	8	3	6	6	2	3	6	conserved hypothetical protein TIGR00096
SO0302			2				2	2	hypothetical protein
SO0311	4	16	3	8	7	6	4	7	conserved hypothetical protein
SO0314	11	17	5	6	37	16	3	11	ornithine decarboxylase, inducible (speF)
SO0316			2						conserved hypothetical protein TIGR00481
SO0322		2							hypothetical protein
SO0323								2	hypothetical protein
SO0325		2		2	3	2			dsrE-related protein
SO0326	5	4	5	8	7	7	5	4	hypothetical protein
SO0330								2	conserved hypothetical protein

Locus	45 min Control		45 min Cr		90 min Control		90 min Cr		Description
	Run 1	Run 2	Run 1	Run 2	Run 1	Run 2	Run 1	Run 2	
SO0333	8	11	16	17	11	8	13	16	thiol:disulfide interchange protein DsbA (dsbA)
SO0335	8	8	8	7	6	8	6	7	conserved hypothetical protein
SO0340	6	9	8	12	11	3	10	13	branched-chain amino acid aminotransferase (ilvE)
SO0341	4	6			3	5		4	sensory box protein
SO0342			3	4	2	5	2	6	conserved hypothetical protein
SO0343	13	9	21	32	11	10	28	27	aconitate hydratase 1 (acnA)
SO0344	3	10	18	24	19	3	21	29	methylcitrate synthase (prpC)
SO0345	8	9	13	16	11	9	15	17	methylisocitrate lyase (prpB)
SO0346	2		3	5		3	4	5	transcriptional regulator. GntR family
SO0347	6	5	6	6	5	3	5	9	acyltransferase family protein
SO0348	12	17	15	15	16	11	16	18	acyltransferase family protein
SO0350		2	2	4			3		hypothetical protein
SO0352						2		2	sensor histidine kinase, putative
SO0355	16	16	17	15	18	13	18	19	AMP-binding protein
SO0356	15	22	15	15	16	18	15	15	ISSo4, transposase
SO0358	3	3	5	3	2	4	2		endoribonuclease L-PSP, putative
SO0359	7	11	4	14	13	9	16	14	guanosine-3,5-bis(diphosphate) 3-pyrophosphohydrolase (spoT)
SO0360	7	8	11	8	7	4	10	10	DNA-directed RNA polymerase, omega subunit (rpoZ)
SO0361	2	2	2	2	2	2	2		guanylate kinase (gmK)
SO0362	15	18	18	27	20	18	23	23	hypothetical protein
SO0364		2		3			2	3	conserved hypothetical protein
SO0367								2	conserved hypothetical protein
SO0368			2						helicase
SO0369			3	4		2	2	2	transcriptional regulator, LysR family
SO0374				2					ISSo1, transposase OrfB
SO0375	5	3	7	7	10	2	8	12	ISSo1, transposase OrfA
SO0378	15	22	15	15	16	18	15	15	
SO0379						2			conserved hypothetical protein
SO0380				2				2	type I restriction-modification system, R subunit (hsdR-1)
SO0382	2	3	2	3	3	3	3	2	type I restriction-modification system, S subunit (hsdS-1)
SO0383	4	7	2	3	4	3	4	6	type I restriction-modification system, M subunit (hsdM-1)
SO0388	5	3	3	4	5	2	3	3	site-specific recombinase, phage integrase family

Locus	45 min Control		45 min Cr		90 min Control		90 min Cr		Description
	Run 1	Run 2	Run 1	Run 2	Run 1	Run 2	Run 1	Run 2	
SO0391					2				hypothetical protein
SO0393	8	9	10	10	7	11	5	8	DNA-binding protein Fis (fis)
SO0394		4						2	conserved hypothetical protein
SO0395	6	4	2	6	3		8	6	ribosomal protein L11 methyltransferase (prmA)
SO0398	11	5	2		23	11		2	fumarate reductase flavoprotein subunit (frdA)
SO0401				3			5	2	alcohol dehydrogenase, zinc-containing
SO0402	2	4	2	6	3	2		2	transcriptional regulator, LysR family
SO0403	2			3	2	3	2	2	hypothetical protein
SO0404	101	128	98	99	128	125	68	71	hypothetical protein
SO0405	46	48	44	47	41	43	43	42	transcription termination factor Rho (rho)
SO0406	15	15	14	14	12	21	10	11	thioredoxin 1 (trxA)
SO0407	26	28	21	23	27	18	25	16	ATP-dependent RNA helicase, DEAD box family
SO0409			2	2	2		3	3	hypothetical protein
SO0414					3	4			type 4 prepilin-like proteins leader peptide processing enzyme (pilD)
SO0415	2	3		3	4	3	6	5	type IV pilus biogenesis protein PilC
SO0416	2	6	5	3	5		6	6	type IV pilus biogenesis protein PilB
SO0417	3	4	4	5	3	2	3	5	pilin, putative
SO0421							2	2	AmpD protein (ampD)
SO0423		5	3	3	2		6	6	pyruvate dehydrogenase complex repressor (pdhR)
SO0424	82	96	103	110	93	78	115	114	pyruvate dehydrogenase complex, E1 component, pyruvate dehydrogenase (aceE)
SO0425	31	38	33	36	30	35	31	31	pyruvate dehydrogenase complex, E2 component, dihydrolipoamide acetyltransferase (aceF)
SO0426	56	64	50	56	51	56	60	52	pyruvate dehydrogenase complex, E3 component, lipoamide dehydrogenase (lpdA)
SO0427			2	2		2	2	2	sensory box protein
SO0428	9	7	10	5	11	13	7	13	conserved hypothetical protein
SO0429	80	93	79	80	79	80	89	92	peptidase, M13 family
SO0430		2		3					conserved hypothetical protein
SO0431		2	2	2				3	HAD-superfamily hydrolase, subfamily IA, variant 3 protein family
SO0432	78	87	67	74	75	62	63	74	aconitate hydratase 2 (acnB)
SO0433	3	2	3	6	2		4	3	regulator of sigma D (rsd)
SO0435	8	13	8	10	8	8	7	10	uroporphyrinogen decarboxylase (hemE)

Locus	45 min Control		45 min Cr		90 min Control		90 min Cr		Description
	Run 1	Run 2	Run 1	Run 2	Run 1	Run 2	Run 1	Run 2	
SO0437	3	4	4	6		4	4	6	sensory box protein
SO0438	2	4		3	4	3	6	6	oxidoreductase, short chain dehydrogenase/reductase family
SO0439					2				hypothetical protein
SO0440	3	6	4	4	3	5	2	6	conserved hypothetical protein
SO0441	14	22	16	16	16	16	8	12	phosphoribosylamine--glycine ligase (purD) phosphoribosylaminoimidazolecarboxamide formyltransferase/IMP
SO0442	23	31	23	26	21	16	13	20	cyclohydrolase (purH)
SO0443			2	2					transcriptional regulator, MerR family
SO0444	7	6	11	13	6		10	7	hypothetical protein
SO0445					4	4			hflC protein, putative
SO0449	8	10	8	7	4	4	9	7	conserved hypothetical protein
SO0452	6	3	5	9	3	3	7	7	thioredoxin 2 (trxC)
SO0453	9	8	8	8	6	2	5	8	peptidyl-prolyl cis-trans isomerase FkbP (fkbP-1)
SO0456	8	8	9	9	7	5	7	10	immunogenic-related protein
SO0459		3	2		3	2	2	2	conserved hypothetical protein
SO0463			2						conserved hypothetical protein
SO0466								2	hypothetical protein
SO0467	8	11	3	4	6	2	3	7	DNA helicase II (uvrD)
SO0470				2					hypothetical protein
SO0471		2			2				conserved hypothetical protein
SO0474		2	2	3	5	2	2		conserved hypothetical protein
SO0481				2					peptidyl-prolyl cis-trans isomerase, FKBP-type
SO0490	2	4			9	6	4		transcriptional regulator
SO0491	32	46	36	32	36	33	31	34	peptidase, M13 family
SO0492		2		2		2		2	conserved hypothetical protein
SO0494	5	3	7	7	10	2	8	12	ISSo1, transposase OrfA
SO0495				2					ISSo1, transposase OrfB
SO0496			3		2	2			conserved hypothetical protein
SO0500	4	3	2	4	2	3	2	2	methyl-accepting chemotaxis protein
SO0501	17	19	22	23	18	17	20	24	conserved hypothetical protein
SO0502							2		transcriptional regulator, ArsR family
SO0506	8	8	11	10	13	8	9	12	conserved hypothetical protein TIGR00148
SO0508	2	3	4	3	3	3		3	hypothetical protein

Locus	45 min Control		45 min Cr		90 min Control		90 min Cr		Description
	Run 1	Run 2	Run 1	Run 2	Run 1	Run 2	Run 1	Run 2	
SO0510				2					oxidoreductase, short-chain dehydrogenase/reductase family
SO0511		2							acetyl-CoA carboxylase, biotin carboxyl carrier protein (accB)
SO0513	2					2			prokaryotic and mitochondrial release factors family protein
SO0514					2				hypothetical protein
SO0515	2	2	3				2	2	hypothetical protein
SO0518	9	13	15	14	9	16	15	19	outer membrane efflux family protein, putative
SO0519	3	5	9	6	4	2	9	9	cation efflux protein, putative
SO0520	10	18	11	11	14	12	17	18	heavy metal efflux pump, CzcA family
SO0521	2	2	4		4		2	4	conserved hypothetical protein
SO0526								2	acetyltransferase, GNAT family
SO0527		4	3	4	4		4	3	conserved hypothetical protein
SO0528	2		2		2		2	3	conserved hypothetical protein
SO0532	3								arsenical resistance operon repressor (arsR)
SO0538	4	2	5	6	5	3	8	6	glyceraldehyde 3-phosphate dehydrogenase (gapA-1)
SO0541							2		metallo-beta-lactamase family protein
SO0542	4	3	4		5		4	5	conserved hypothetical protein
SO0543								2	hypothetical protein
SO0544							2		sensory box histidine kinase
SO0546					3	2	2		ribosomal protein S6 modification protein (rimK-1)
SO0548	7	14	5	10	14	13	4	5	DNA-binding protein, HU family
SO0549						2			chemotaxis protein CheY/response regulator receiver domain protein
SO0551				2			2		conserved hypothetical protein
SO0554	2	5	5	5	3	2		4	hypothetical protein
SO0555	2								conserved hypothetical protein
SO0556					3			2	hypothetical protein
SO0558	2	4	2	2	2			2	smtA protein (smtA)
SO0559		3	2	3	3		3	3	MaoC domain protein
SO0560	3				5				formate--tetrahydrofolate ligase (fhs)
SO0564		3	2			2	5	3	conserved hypothetical protein
SO0565	2	3	2	2	2	3		3	adhesion protein, putative
SO0567	4	7	2	8	4	3	2	5	1-acyl-sn-glycerol-3-phosphate acyltransferase (plsC)
SO0568		3	2	2			3	4	conserved hypothetical protein

Locus	45 min Control		45 min Cr		90 min Control		90 min Cr		Description
	Run 1	Run 2	Run 1	Run 2	Run 1	Run 2	Run 1	Run 2	
SO0570								2	response regulator
SO0572				2					enoyl-CoA hydratase/isomerase family protein
SO0575	27	27	18	22	21	12	19	17	RNA polymerase-associated protein HepA (hepA)
SO0576							5	2	PhoH family protein
SO0577	14	17	8	11	12	10	16	20	sensory box histidine kinase/response regulator
SO0578	24	27	32	30	26	26	29	35	hypothetical protein
SO0583				2					bacterioferritin-associated ferredoxin (bfd)
SO0584	3	2	2	2	4	2	2	2	methyl-accepting chemotaxis protein
SO0585							2		D-isomer specific 2-hydroxyacid dehydrogenase family protein
SO0588	15	22	20	21	15	26	18	20	transporter, putative
SO0591	10	12	9	11	9	5	11	18	conserved hypothetical protein TIGR00157
SO0592		5	4	4	3			3	oligoribonuclease (orn)
SO0595	3	2	2	3	3				hypothetical protein
SO0596	15	22	15	15	16	18	15	15	ISSo4, transposase
SO0598					3				yjeF protein (yjeF)
SO0600	10	9	9	6	8	10	7	5	N-acetylmuramoyl-L-alanine amidase (amiB)
SO0601	3	4	3	4	4	3	4	4	DNA mismatch repair protein MutL (mutL)
SO0602	6	10	9	7	8	3	6	12	tRNA delta(2)-isopentenylpyrophosphate transferase (miaA)
SO0603	7	8	8	9	7	6	8	6	host factor-I protein (hfq)
SO0604	3	4	3	3	2		5	5	GTP-binding protein HflX (hflX)
SO0605	29	43	40	37	29	31	35	43	hflK protein (hflK)
SO0606	42	57	46	46	41	43	51	52	hflC protein (hflC)
SO0608	14	19	16	14	11	18	14	15	ubiquinol-cytochrome c reductase, iron-sulfur subunit (petA)
SO0609	4	6	5	4	6	4	5	5	ubiquinol-cytochrome c reductase, cytochrome b (petB)
SO0610	13	15	12	11	13	9	14	15	ubiquinol-cytochrome c reductase, cytochrome c1 (petC)
SO0611	5	4	4	5	3	5	6	6	stringent starvation protein a (sspA)
SO0612	6	4	5	3	4	2	3	3	stringent starvation protein b (sspB)
SO0614	23	24	20	14	18	21	16	17	dipeptidyl peptidase IV, putative
SO0617	19	22	15	13	14	18	16	19	acetylornithine aminotransferase (argD)
SO0618	4	3	4	4	8	2	3	4	arginine N-succinyltransferase (astA)
SO0619	13	13	9	11	10	12	9	11	succinylglutamic semialdehyde dehydrogenase (astD)
SO0620								2	conserved hypothetical protein

Locus	45 min Control		45 min Cr		90 min Control		90 min Cr		Description
	Run 1	Run 2	Run 1	Run 2	Run 1	Run 2	Run 1	Run 2	
SO0621			2		2		2	5	sensor histidine kinase
SO0622					4			3	DNA-binding response regulator
SO0624	13	17	16	17	18	13	12	21	catabolite gene activator (crp)
SO0625			3	2		2			conserved domain protein
SO0630	3		4	5		2	4	7	TonB-dependent receptor (nosA)
SO0632					4		2		ATP-dependent helicase HrpB (hrpB)
SO0633	25	27	20	17	28	12	23	20	penicillin-binding protein 1B (mrcB)
SO0635	2	2	2	2	3	7	6	7	peptidyl-prolyl cis-trans isomerase C (ppiC-1)
SO0636			2	2	2		2	2	acetyltransferase, GNAT family
SO0640	4	3	2	3	4	3	3	3	alcohol dehydrogenase, zinc-containing
SO0641	2		3		3				prophage MuSo1, transcriptional regulator, Cro/CI family
SO0643								2	transposase, putative
SO0644				2				2	prophage MuSo1, DNA transposition protein, putative
SO0646				2			2		hypothetical protein
SO0653				2					hypothetical protein
SO0655			2	2					hypothetical protein
SO0656	5	3	7	7	10	2	8	12	ISSo1, transposase OrfA
SO0657				2					ISSo1, transposase OrfB
SO0667	2								conserved hypothetical protein
SO0670	3		3	2	4		2	6	hypothetical protein
SO0672			2						hypothetical protein
SO0673	4	2		3	3		3	4	hypothetical protein
SO0680		3		2		4	2	3	hypothetical protein
SO0684				2					ISSo1, transposase OrfB
SO0685	5	3	7	7	10	2	8	12	ISSo1, transposase OrfA
SO0688							2		hypothetical protein
SO0691	9	15	12	12	10	15	8	10	hypothetical protein
SO0693				4				2	aldose 1-epimerase (galM)
SO0694								2	galactokinase (galK)
SO0695	8	9	11	10	8	4	8	8	glutathione-regulated potassium-efflux system protein KefC, putative
SO0696	7	9	6	6	10	6	8	9	thiol:disulfide interchange protein DsbD (dsbD)
SO0698		2				2		4	fxsA protein (fxsA)

Locus	45 min Control		45 min Cr		90 min Control		90 min Cr		Description
	Run 1	Run 2	Run 1	Run 2	Run 1	Run 2	Run 1	Run 2	
SO0701			3		2	2		2	transcriptional regulator, LysR family
SO0703	13	15	18	18	14	19	16	15	chaperonin GroES (groES)
SO0704	122	125	129	133	114	140	132	135	chaperonin GroEL (groEL)
SO0708				2					transposase, mutator family
SO0709			2						hypothetical protein
SO0719	22	27	26	28	21	19	27	29	TonB-dependent receptor, putative
SO0728	2								conserved hypothetical protein
SO0730	2	2		3	6	2		3	hypothetical protein
SO0733		3		3	3	3		2	cold shock domain family protein
SO0740	3	4	5	5	3	4	6	6	melanin biosynthesis protein TyrA, putative
SO0741		7			2				gamma-glutamyltranspeptidase (ggt-1)
SO0742		2	4	4			4		iron(III) ABC transporter, ATP-binding protein
SO0744	6	5	5			2	2	2	iron(III) ABC transporter, periplasmic iron(III)-binding protein
SO0746							2		glutathione S-transferase family protein
SO0747		2							ferredoxin--NADP reductase (fpr)
SO0749							2	2	conserved hypothetical protein
SO0750	4	8	5	6	8	7	6	4	glutamate synthase, putative
SO0752	2			3				2	hypothetical protein
SO0754	2	3	2	3		3	4	4	ABC transporter, ATP-binding protein
SO0756	12	13	14	12	16	10	14	14	phospho-2-dehydro-3-deoxyheptonate aldolase, phe-sensitive (aroG)
SO0764	2	5	7	5	2		6	2	hypothetical protein
SO0768	2	3		2		3	4		conserved hypothetical protein
SO0769	7	10	7	7	6	9	6	5	arginine repressor (argR)
SO0770	34	30	31	38	26	29	30	33	malate dehydrogenase (mdh)
SO0775	5	4		4	3		2	2	conserved hypothetical protein
SO0777	2	4	2	2	4	2	2	2	2-octaprenyl-6-methoxyphenol hydroxylase (ubiH)
SO0778	8	10	7	8	10	8	2	7	oxidoreductase, FAD-binding, UbiH/Coq6 family
SO0779	12	19	18	22	15	13	14	18	glycine cleavage system T protein (gcvT)
SO0781	24	39	27	42	40	21	39	41	glycine cleavage system P protein (gcvP)
SO0783	4	7	9	14	10	4	8	12	hypothetical protein
SO0788	5			2	2		3		conserved hypothetical protein
SO0789		2	2				2		conserved hypothetical protein

Locus	45 min Control		45 min Cr		90 min Control		90 min Cr		Description
	Run 1	Run 2	Run 1	Run 2	Run 1	Run 2	Run 1	Run 2	
SO0795	3	12	3	8	10		11	12	conserved hypothetical protein
SO0798	3	2	6	12			11	13	conserved hypothetical protein
SO0801		2					2		conserved hypothetical protein
SO0804		2							hypothetical protein
SO0805	7	5	7	5	4	3	5	9	CBS domain protein
SO0807	5	8	6	5	5	3	3	5	hypoxanthine-guanine phosphoribosyltransferase (hpt-1)
SO0808	2	4	2	3	3		2	2	conserved hypothetical protein
SO0809	2	2	3	3		2	2	3	azurin (azu)
SO0810	2	3	3	2	3	3	4		ribokinase (rbsK)
SO0811	4	2	2	7	4	2	2	5	inosine-uridine preferring nucleoside hydrolase family protein
SO0812					2				hypothetical protein
SO0813	16	17	12	11	14	12	15	18	hypothetical protein
SO0815	28	36	28	33	29	25	43	41	TonB-dependent receptor C-terminal domain protein
SO0816	2	2	3	3	2	2	2	3	hypothetical protein
SO0818						2			5-methyltetrahydropteroyltriglutamate--homocysteine methyltransferase (metE)
SO0820				2			4		HlyD family secretion protein
SO0821			3	2		2	3	3	ABC transporter, ATP-binding/permease protein
SO0822				2					outer membrane efflux family protein
SO0823				3	2	3	3		conserved hypothetical protein
SO0828	4	5	2	3	3	2	2	5	conserved hypothetical protein
SO0830	2	6	4	8	3	4	5	4	alkaline phosphatase
SO0831	9	12	8	13	11	3	9	12	glutathione synthetase (gshB)
SO0832	8	9	7	9	6	4	5	7	conserved hypothetical protein TIGR00046
SO0833		3			2				endonuclease I (endA)
SO0834	2	2	2	2	2	2			sprT protein, putative
SO0835		3	2	2					conserved hypothetical protein
SO0837				2			2	2	beta-lactamase, putative
SO0839				2	2				transcriptional regulator, LysR family
SO0840	148	154	133	136	166	139	156	159	acetyl-CoA carboxylase multifunctional enzyme accADC, carboxyl transferase subunit alpha/carboxyl transferase subunit beta/biotin carboxylase
SO0842	71	82	71	79	70	57	85	81	translation elongation factor G (fusA-2)

Locus	45 min Control		45 min Cr		90 min Control		90 min Cr		Description
	Run 1	Run 2	Run 1	Run 2	Run 1	Run 2	Run 1	Run 2	
SO0845	6	6	3	3	6	6	4	3	cytochrome c-type protein NapB (napB)
SO0846		2				3			iron-sulfur cluster-binding protein napH (napH)
SO0847	4	2			8	6			iron-sulfur cluster-binding protein NapG (napG)
SO0848	49	59	33	45	74	66	23	34	periplasmic nitrate reductase (napA)
SO0853							2		pilin, putative
SO0855		2			3	2		2	conserved hypothetical protein
SO0856					2				conserved hypothetical protein
SO0859	2	4	9		4	5	3	9	sensory box histidine kinase/response regulator
SO0860		2					4	2	response regulator
SO0861		2	2	2				2	conserved hypothetical protein
SO0862	11	15	17	16	17	11	15	15	D-3-phosphoglycerate dehydrogenase (serA)
SO0864								3	transcriptional regulator, LuxR family
SO0869	6	6		3	3		5	2	pantoate--beta-alanine ligase (panC)
SO0870	5	6	3	3	4	4	4	5	3-methyl-2-oxobutanoate hydroxymethyltransferase (panB)
									2-amino-4-hydroxy-6-hydroxymethyldihydropteridine
SO0871		3	3	4	2		2	2	pyrophosphokinase (folK-1)
SO0872	12	13	11	17	18	11	11	16	polyA polymerase (pcnB)
SO0874	8	12	8	11	10	9	5	9	DnaK suppressor protein (dksA)
SO0876	10	9	7	10	12	4	10	10	peptidase B (pepB)
SO0880	2								conserved hypothetical protein
SO0881	2								conserved hypothetical protein
SO0882	4	5	2	2	5	6	4	3	oxidoreductase, GMC family
SO0885	2	4	2	4	2	2	3	2	ABC transporter, ATP-binding protein
SO0887	16	15	14	13	7	11	7	18	conserved hypothetical protein
SO0888	11	19	10	20	8	6	12	17	amidase family protein
SO0891	5	3	7	7	10	2	8	12	ISSo1, transposase OrfA
SO0892				2					ISSo1, transposase OrfB
SO0897	11	11	3	2	7	8	7	6	ATP-dependent RNA helicase DbpA (dbpA)
SO0899				3					glyoxalase family protein
SO0900	5	5	3	6	8	3	8	10	oxidoreductase, aldo/keto reductase family
									NADH:ubiquinone oxidoreductase, Na translocating, alpha subunit
SO0902	19	24	10	8	23	18	7	4	(nqrA-1)
SO0904	2	4	2	5	7	6	3	4	NADH:ubiquinone oxidoreductase, gamma subunit (nqrC-1)

Locus	45 min Control		45 min Cr		90 min Control		90 min Cr		Description
	Run 1	Run 2	Run 1	Run 2	Run 1	Run 2	Run 1	Run 2	
SO0907	12	13	7	9	16	11	9	9	NADH:ubiquinone oxidoreductase, Na translocating, beta subunit (nqrF-1)
SO0912							3	3	hypothetical protein
SO0915			2					2	ankyrin domain protein
SO0916	2			2			3		transcriptional regulator, MarR family
SO0918	11	11	7	7	7	15	5	4	aculeacin A acylase (aac)
SO0919	2	3	2		2		2	2	serine transporter, putative
SO0923	13	10	13	12	12	9	12	11	conserved hypothetical protein
SO0929	21	21	21	21	13	17	15	27	S-adenosylmethionine synthetase (metK)
SO0930	28	36	29	33	32	21	32	36	transketolase (tkt)
SO0931	3	5	2	3		2	5	6	D-erythrose-4-phosphate dehydrogenase (epd)
SO0932	25	21	21	23	17	19	11	16	phosphoglycerate kinase (pgk)
SO0933	21	34	29	27	23	33	31	32	fructose-bisphosphate aldolase, class II, Calvin cycle subtype (fba)
SO0934	9	10	12	14	2	12	22	24	conserved hypothetical protein
SO0940					2				transcriptional regulator-related protein
SO0942		2		2	2	2		3	conserved hypothetical protein
SO0943	6	9	6	5	5	5	6	6	sensory box protein, putative
SO0945		2					2		AcrB/AcrD/AcrF family protein
SO0946	2	3			2				conserved hypothetical protein
SO0947	17	19	12	14	15	11	11	10	ATP-dependent RNA helicase SrmB (srmB)
SO0951	10	8	13	11	4	4	9	8	thiol:disulfide interchange protein DsbC (dsbC)
SO0952							3		single-stranded-DNA-specific exonuclease RecJ (recJ)
SO0956	4		2	4		2	2	7	alkyl hydroperoxide reductase, F subunit (ahpF)
SO0958	14	19	18	19	15	11	12	14	alkyl hydroperoxide reductase, C subunit (ahpC)
SO0959	22	20	23	18	13	18	17	15	cytosol aminopeptidase (pepA-1)
SO0961		2	3	3					conserved hypothetical protein
SO0968	2	3	2	4	3			3	D-lactate dehydrogenase (ldhA)
SO0970	24	22	31	27	39	37	14	18	fumarate reductase flavoprotein subunit precursor
SO0976						2			organic hydroperoxide resistance protein (ohr)
SO0977			2	3	2			5	transcriptional regulator, MarR family
SO0978						2			FAD-dependent glycerol-3-phosphate dehydrogenase, family protein
SO0980		2							RNA methyltransferase, TrmA family
SO0982	5	3	7	7	10	2	8	12	ISSo1, transposase OrfA

Locus	45 min Control		45 min Cr		90 min Control		90 min Cr		Description
	Run 1	Run 2	Run 1	Run 2	Run 1	Run 2	Run 1	Run 2	
SO0983				2					ISSo1, transposase OrfB
SO0987	21	23	10	16	24	24	17	21	methyl-accepting chemotaxis protein
SO0988	3	2			6	3	2		formate dehydrogenase, alpha subunit
SO0992	11	18	9	20	9	11	14	16	lysyl-tRNA synthetase (lysS)
SO0994	11	10	9	11	14	6	7	11	conserved hypothetical protein
SO0996	2	3	5	4	2		2	3	glyoxalase family protein
SO1002	2	3				3		2	hypothetical protein
SO1003	7	13	8	9	13	21	12	8	hypothetical protein
SO1004	17	26	25	17	21	26	25	22	hypothetical protein
SO1006							2		dienelactone hydrolase family protein
SO1014	9	14	16	10	12	9	16	11	NADH dehydrogenase I, I subunit (nuoI)
SO1016	16	29	20	24	23	18	29	29	NADH dehydrogenase I, G subunit (nuoG)
SO1017	21	25	23	22	22	19	20	14	NADH dehydrogenase I, F subunit (nuoF)
SO1018	4	2	3		2		2	3	NADH dehydrogenase I, E subunit (nuoE)
SO1019	23	34	19	20	27	22	19	22	NADH dehydrogenase I, C/D subunits (nuoCD)
SO1020	7	9	5	7	7	7	4	6	NADH dehydrogenase I, B subunit (nuoB)
SO1021		3						2	NADH dehydrogenase I, A subunit (nuoA)
SO1024				2					ISSo1, transposase OrfB
SO1025	5	3	7	7	10	2	8	12	ISSo1, transposase OrfA
SO1026	15	22	15	15	16	18	15	15	ISSo4, transposase
SO1030		5		4	4		7	3	5-methyltetrahydrofolate--homocysteine methyltransferase (metH)
SO1033					2				iron-compound ABC transporter, ATP-binding protein, putative nicotinate-nucleotide--dimethylbenzimidazole
SO1035			3	3			4	4	phosphoribosyltransferase (cobT)
SO1037	2								cobinamide kinase/cobinamide phosphate guanylyltransferase (cobU)
SO1038		4	2						cobyric acid synthase CobQ (cobQ)
SO1039			2	2					cob(I)alamin adenosyltransferase (cobO)
SO1042								2	amino acid ABC transporter, ATP-binding protein
SO1043							2		amino acid ABC transporter, permease protein
SO1044			2						amino acid ABC transporter, periplasmic amino acid-binding protein
SO1045				3			5	5	hypothetical protein
SO1051	35	41	34	37	37	27	35	36	periplasmic glucan biosynthesis protein, putative

Locus	45 min Control		45 min Cr		90 min Control		90 min Cr		Description
	Run 1	Run 2	Run 1	Run 2	Run 1	Run 2	Run 1	Run 2	
SO1052	3	3	2	2	2				low-affinity inorganic phosphate transporter (pit)
SO1056	27	31	21	20	31	16	25	25	methyl-accepting chemotaxis protein
SO1059	14	31	16	22	13	21	14	12	aminopeptidase N
SO1060	15	20	19	20	22	13	24	24	conserved hypothetical protein
SO1061	10	17	12	12	10	13	14	11	TPR domain protein
SO1062	3		3	3	2		3	2	polypeptide deformylase (def-2)
SO1063	2								slyX protein (slyX)
SO1065	33	40	29	32	37	43	39	38	FKBP-type peptidyl-prolyl cis-trans isomerase FkpA (fkpA)
SO1066	11	8	8	5	19	24	7	17	extracellular nuclease
SO1068			2	3			2	2	conserved hypothetical protein
SO1070					3			2	catalase (katB)
SO1072	5	6	12	12		2	4	4	chitin-binding protein, putative
SO1075	24	23	17	23	20	24	14	20	conserved hypothetical protein
SO1079				2					ISSo1, transposase OrfB
SO1080	5	3	7	7	10	2	8	12	ISSo1, transposase OrfA
SO1082	5	3	7	7	10	2	8	12	ISSo1, transposase OrfA
SO1083				2					ISSo1, transposase OrfB
SO1093			2	3				3	ISSo7, transposase
SO1094			2						conserved hypothetical protein
SO1095	3	6	8	11	10	3	9	14	O-acetylhomoserine (thiol)-lyase, putative
SO1096		3	3		2	2	2	2	hypothetical protein
SO1097	2			2	2				conserved hypothetical protein
SO1099		2	2		2			2	bolA protein (bolA)
SO1101	9	8	6	8	5	4	5	8	autoinducer-2 production protein LuxS (luxS)
SO1103	44	55	47	42	45	48	49	55	NADH:ubiquinone oxidoreductase, Na translocating, alpha subunit (nqrA-2)
SO1104	3	2	2		2	2	2		NADH:ubiquinone oxidoreductase, Na translocating, hydrophobic membrane protein NqrB (nqrB-2)
SO1105	16	27	18	21	18	16	15	14	NADH:ubiquinone oxidoreductase, Na translocating, gamma subunit (nqrC-2)
SO1108	43	42	36	37	42	31	44	43	NADH:ubiquinone oxidoreductase, Na translocating, beta subunit (nqrF-2)
SO1109	15	15	12	12	13	11	15	12	thiamin biosynthesis lipoprotein ApbE (apbE)

Locus	45 min Control		45 min Cr		90 min Control		90 min Cr		Description
	Run 1	Run 2	Run 1	Run 2	Run 1	Run 2	Run 1	Run 2	
SO1111	5	5	2	5	8	12	3	4	bacterioferritin subunit 2 (bfr2)
SO1112	4	7	3	2	8	10	3	3	bacterioferritin subunit 1 (bfr1)
SO1114		2	6	11			5	13	DNA-damage-inducible protein P (dinP)
SO1115	7	10	9	10	10	5	16	12	aminoacyl-histidine dipeptidase (pepD)
SO1117	16	16	15	17	22	16	15	20	cytosol aminopeptidase, putative
SO1121	7	3	4	3	6	5	4	4	glutamate 5-kinase (proB)
SO1122	5	3	4	4	2	4	4	5	gamma-glutamyl phosphate reductase (proA)
SO1124	3	3				3		3	conserved hypothetical protein TIGR00011
SO1126	108	121	138	147	114	125	137	131	chaperone protein DnaK (dnaK)
SO1127	39	44	42	50	51	39	47	56	chaperone protein DnaJ (dnaJ)
SO1129				2					ISSo1, transposase OrfB
SO1130	5	3	7	7	10	2	8	12	ISSo1, transposase OrfA
SO1133	5	3	7	7	10	2	8	12	ISSo1, transposase OrfA
SO1134				2					ISSo1, transposase OrfB
SO1136	2	3	3	2	2		2	2	ATP-dependent RNA helicase, DEAD box family
SO1137	8	7	13	6	7	6	13	11	conserved hypothetical protein
SO1139	7	10	8	8	7	7	6	9	peptidyl-prolyl cis-trans isomerase FklB (fklB)
SO1140	5	4	7	6	5	5	9	8	dihydrodipicolinate reductase (dapB)
SO1141	25	25	21	23	21	28	14	16	carbamoyl-phosphate synthase, small subunit (carA)
SO1142	71	66	52	44	67	47	43	44	carbamoyl-phosphate synthase, large subunit (carB)
SO1144	15	13	16	15	15	12	13	16	methyl-accepting chemotaxis protein
SO1149	5	7	4	5	5	6	6	6	conserved hypothetical protein
SO1150	9	8	7	8	8	10	8	7	ribose 5-phosphate isomerase (rpiA)
SO1154	2								hypothetical protein
SO1156						2			TonB-dependent receptor
SO1158	2			2					Dps family protein
SO1161	14	19	12	20	14	15	17	17	lipoic acid synthetase (lipA)
SO1162				5	5		6	6	lipoate-protein ligase B (lipB)
SO1163	7	8	9	12	8	2	9	10	conserved hypothetical protein
SO1164	51	61	56	46	51	41	50	50	D-alanyl-D-alanine carboxypeptidase (dacA-1)
SO1165	10	6	7	6	7	2	8	7	rare lipoprotein A
SO1166	3	4	4	7	4	2	4	7	membrane-bound lytic transglycosylase, putative

Locus	45 min Control		45 min Cr		90 min Control		90 min Cr		Description
	Run 1	Run 2	Run 1	Run 2	Run 1	Run 2	Run 1	Run 2	
SO1168	9	15	18	11	15	23	15	11	penicillin-binding protein 2 (mrdA)
SO1169	3	3	5	2	4		2		conserved hypothetical protein TIGR00246
SO1170		3	4	8	3	4	6	6	iojap domain protein
SO1173		2	4	5			2	2	rare lipoprotein B
SO1174	32	29	26	24	24	14	21	24	leucyl-tRNA synthetase (leuS)
SO1175	2		2	3	2	2	3	2	conserved hypothetical protein
SO1177		4		2	3	5		4	apolipoprotein N-acyltransferase (cutE)
SO1178	4	7	11	10	4	2	8	7	magnesium and cobalt efflux protein CorC (corC)
SO1180	23	25	34	32	27	22	33	39	PhoH family protein
SO1181	9	17	13	13	16	6	11	17	tRNA-i(6)A37 modification enzyme MiaB (miaB)
SO1183	5	5	2	4	5	4		5	oxidoreductase, FAD-binding
SO1184	7	5	6	8	3	8	3	5	peptidyl-tRNA hydrolase (pth)
SO1185	8	15	11	10	11	8	6	10	conserved hypothetical protein TIGR00092
SO1188			3	2					conserved hypothetical protein
SO1189			4	3			3	4	conserved hypothetical protein
SO1190	17	14	28	28	9	6	24	22	conserved hypothetical protein
SO1191	8	13	10	12	12	12	6	11	transcription elongation factor GreA (greA)
SO1193	5	7	3	4	3	2	7	4	protein-export membrane protein SecD (secD-1)
SO1194		2							protein-export membrane protein SecF (secF-1)
SO1195					3			2	conserved hypothetical protein TIGR00253
SO1196	12	13	15	15	10	12	16	21	ribosomal RNA large subunit methyltransferase J (rrmJ)
SO1197	54	67	63	71	66	42	72	84	cell division protein FtsH (ftsH)
SO1198		7	2	5	4	2	3	2	dihydropteroate synthase (folP)
SO1199	8	10	9	10	14	6	14	17	phosphoglucosamine mutase (glmM)
SO1200	22	20	17	16	17	22	18	15	triosephosphate isomerase (tpiA)
SO1201		3	4				3	5	preprotein translocase, SecG subunit (secG)
SO1202	7	3	4	7	8	6	2	4	conserved hypothetical protein
SO1203	35	45	35	43	38	43	33	32	N utilization substance protein A (nusA)
SO1204	82	109	82	90	87	91	74	83	translation initiation factor IF-2 (infB)
SO1205	12	8	5	4	7	7	4	3	ribosome-binding factor A (rbfA)
SO1206	11	12	6	5	9	7	4	9	tRNA pseudouridine synthase B (truB)
SO1207	12	12	13	15	14	10	14	17	ribosomal protein S15 (rpsO)

Locus	45 min Control		45 min Cr		90 min Control		90 min Cr		Description
	Run 1	Run 2	Run 1	Run 2	Run 1	Run 2	Run 1	Run 2	
SO1208	4	4	2	2	8	2	6	7	GGDEF domain protein
SO1209	73	76	66	76	81	67	66	81	polyribonucleotide nucleotidyltransferase (pnp)
SO1210	4	6	5	5	7	4	4	2	TPR domain protein
SO1214	2	2			2		2	2	NupC family protein
SO1215	8	7	11	10	7	10	16	13	outer membrane protein OmpK, putative
SO1217	9	14	11	10	8	9	13	12	deoxyribose-phosphate aldolase (deoC)
SO1218	13	11	13	12	15	8	12	12	thymidine phosphorylase (deoA)
SO1219	7	12	6	6	12	13	7	12	phosphopentomutase (deoB)
SO1221	17	21	19	22	21	16	19	24	purine nucleoside phosphorylase (deoD-2)
SO1222	4	5	3	5	5	2	11	11	hypothetical protein
SO1223				2			2		phosphoserine phosphatase (serB)
SO1224			2					2	conserved hypothetical protein
SO1225		2							conserved hypothetical protein
SO1226	4	4		2		5	2	2	DNA repair protein RadA (radA)
SO1230	2		3		3		2	2	sensor histidine kinase/response regulator TorS (torS)
SO1236					2				xanthine/uracil permease family protein
SO1242	2	2			2			3	hypothetical protein
SO1250						2			conserved hypothetical protein
SO1252	9	19	18	8	19	7	5	17	peptidase, U32 family
SO1254					2				conserved hypothetical protein
SO1255								2	cyclic nucleotide phosphodiesterase, putative
SO1258	7	8	5	3	6	4	2	3	adenylosuccinate synthetase, putative
SO1259							2	2	transcriptional regulator, LysR family
SO1262						2			hypothetical protein
SO1264	5	3		3	8	2	2	2	conserved hypothetical protein
SO1265	4	4	2	3	2	4			transcriptional regulator, putative
SO1267	2	2							conserved hypothetical protein
SO1268		4	2		4		4	2	glutamine synthetase
SO1269	15	22	15	15	16	18	15	15	ISSo4, transposase
SO1270	3	3	10	5	5	5		5	polyamine ABC transporter, periplasmic polyamine-binding protein
SO1271	9	9	9	8	8	5	6	6	polyamine ABC transporter, ATP-binding protein
SO1274	3		5	6	6	3	4	6	conserved hypothetical protein

Locus	45 min Control		45 min Cr		90 min Control		90 min Cr		Description
	Run 1	Run 2	Run 1	Run 2	Run 1	Run 2	Run 1	Run 2	
SO1275	5	7	3	2	4	3	6	8	succinate-semialdehyde dehydrogenase (gabD)
SO1276	8	13	10	6	9	7	8	6	4-aminobutyrate aminotransferase (gabT)
SO1278	4	5	5	7	7	5	8	9	methyl-accepting chemotaxis protein
SO1284	22	25	25	31	23	17	18	36	RNA polymerase sigma-70 factor (rpoD)
SO1286		5		4	2	4	3	7	DNA primase (dnaG)
SO1287	4	4	6	4	3	6	2	4	conserved hypothetical protein
SO1288	13	17	13	15	11	16	11	14	ribosomal protein S21 (rpsU)
SO1289	4	6	5	5	4	3	2	8	O-sialoglycoprotein endopeptidase (gcp)
SO1295	9	15	11	10	12	15	18	17	major outer membrane lipoprotein, putative
SO1297	10	12	12	4	11	7	10	11	general secretion pathway protein a (gspA)
SO1298	3	3	4	3	2	6	4	4	general secretion pathway protein B (gspB)
SO1300	16	22	12	15	18	15	8	11	glutamate-1-semialdehyde-2,1-aminomutase (hemL)
SO1301	5	14	12	11	13	4	10	15	aspartate carbamoyltransferase (pyrB)
SO1303	9	10	10	7	12	5	11	12	hypothetical protein
SO1304	6	6	7	6	5	5		2	HesB/YadR/YfhF family protein
SO1306				2				2	conserved hypothetical protein
SO1309				2					conserved hypothetical protein
SO1313		4	3				2	3	conserved hypothetical protein
SO1314		5	2	2	2	2			peptidase, M23/M37 family
SO1315	23	28	28	31	27	15	24	22	tyrosyl-tRNA synthetase (tyrS)
SO1322	2	2	2						5-methylthioadenosine nucleosidase/S-adenosylhomocysteine nucleosidase (pfs)
SO1324	4	3	2		5	4			glutamate synthase, small subunit (gltD)
SO1325		4		2	2	2	2		glutamate synthase, large subunit (gltB)
SO1327	4	5	4	6	7		6	12	sensor histidine kinase-related protein
SO1328	6	7	7	6	9	4	2	7	transcriptional regulator, LysR family
SO1329	5	2	3	3	4		2		adenylate cyclase-related protein
SO1330					2		2		DNA mismatch repair protein MutH (mutH)
SO1332	4	6	4	5	7	3	4	2	phosphoenolpyruvate-protein phosphotransferase PtsP (ptsP)
SO1334					2	2		2	prolipoprotein diacylglycerol transferase (lgt)
SO1335	4			4	2	2			thymidylate synthase (thyA)
SO1339	4	2	2	2	2	2			conserved hypothetical protein
SO1341	8	8	7	7	8	4	9	9	L-aspartate oxidase (nadB)

Locus	45 min Control		45 min Cr		90 min Control		90 min Cr		Description
	Run 1	Run 2	Run 1	Run 2	Run 1	Run 2	Run 1	Run 2	
SO1342	3	4	4	5	4	7	8	6	RNA polymerase sigma-24 factor (rpoE)
SO1343	2	4	3	3	3			4	sigma-E factor negative regulatory protein (rseA)
SO1344	4	5	3	7	5	5	2	2	sigma-E factor regulatory protein RseB (rseB)
SO1345			2	4					sigma-E factor regulatory protein RseC (rseC)
SO1346	9	11	6	12	17	8	17	14	GTP-binding protein LepA (lepA)
SO1347	21	29	25	19	22	23	23	19	signal peptidase I (lepB)
SO1348	3	6		2	5	4	4	4	ribonuclease III (rnc)
SO1349	8	12	10	10	6	6	11	9	GTP-binding protein Era (era)
SO1351	7	7	6	4	5	7	7	7	pyridoxal phosphate biosynthetic protein PdxJ (pdxJ)
SO1353		2		3	2	3			conserved hypothetical protein
SO1354	2	4	3	4	3	9	4	3	hemolysin protein, putative
SO1356	36	52	39	46	38	39	38	42	signal recognition particle protein Ffh (ffh)
SO1357	8	11	11	10	10	12	9	10	ribosomal protein S16 (rpsP)
SO1358	5	5	2	3	3			3	16S rRNA processing protein RimM (rimM)
SO1359		3	2						tRNA (guanine-N1)-methyltransferase (trmD)
SO1360	23	22	20	17	19	23	18	19	ribosomal protein L19 (rplS)
SO1361		3		2					phospho-2-dehydro-3-deoxyheptonate aldolase, tyr-sensitive (aroF)
SO1362				2				2	chorismate mutase/prephenate dehydrogenase (tyrA)
SO1366						2			sodium/hydrogen exchanger family protein
SO1367	4	4	2	4	4	2		3	chorismate mutase/prephenate dehydratase (pheA)
SO1368	26	28	23	21	27	19	22	21	cytosol aminopeptidase (pepA-2)
SO1369	6	7	4	5	3	4	6	6	conserved hypothetical protein
SO1370	3	4		5	4	2	2	2	conserved hypothetical protein
SO1371	2			2					conserved hypothetical protein
SO1372	2		2		3		3	2	conserved hypothetical protein
SO1375		4	5	3	4	2	9	3	carboxypeptidase
SO1377	35	46	40	41	46	50	41	54	conserved hypothetical protein
SO1378							2	3	ThiJ/PfpI family protein
SO1380						2			conserved hypothetical protein
SO1383	20	22	10	11	17	23	11	13	ATP-dependent RNA helicase, DEAD box family
SO1385	5	8	3	9	4	6	6	8	methyl-accepting chemotaxis protein
SO1388	15	24	13	12	15	14	11	10	aminopeptidase P, putative

Locus	45 min Control		45 min Cr		90 min Control		90 min Cr		Description
	Run 1	Run 2	Run 1	Run 2	Run 1	Run 2	Run 1	Run 2	
SO1389	2				2				ROK family protein
SO1390	12	11	10	6	11	12	8	7	peptidyl-prolyl cis-trans isomerase, FKBP-type
SO1401	13	12	9	8	14	13	11	15	hypothetical protein
SO1402	6	3	2		3	4		2	conserved hypothetical protein
SO1403		2	2						conserved hypothetical protein
SO1404	4	7	4	4	4	3	2	3	endoribonuclease L-PSP, putative
SO1405	3	4	4	2	10	7	2		transglutaminase family protein
SO1407					2				mercuric transport periplasmic protein MerP, putative
SO1408	2	5	2	2	2				helicase, putative
SO1410	2	2		4	3	3			hypothetical protein
SO1412			3					2	conserved hypothetical protein
SO1417	2		2		3				sensor histidine kinase
SO1424	18	27	7	20	21	26	16	23	hypothetical protein
SO1425	13	18	13	20	19	14	17	12	hypothetical protein
SO1429	2	3		4	24	23			anaerobic dimethyl sulfoxide reductase, A subunit (dmaA-1)
SO1430	2				8	7			anaerobic dimethyl sulfoxide reductase, B subunit (dmsB-1)
SO1434	3	4	3	3	4	3	3	4	methyl-accepting chemotaxis protein
SO1438	15	22	15	15	16	18	15	15	ISSo4, transposase
SO1441		2	4	3	3		4	4	hypothetical protein
SO1457	13	15	15	14	15	8	17	18	type I restriction-modification system, M subunit, putative
SO1458		2							hypothetical protein
SO1460	17	16	14	10	16	12	14	12	type I restriction-modification system, S subunit, putative
SO1461	10	8	11	11	14	11	12	13	protein kinase, putative
SO1462	6	2	4		5	4	2	2	hypothetical protein
SO1463	2	3	4			2			hypothetical protein
SO1464	5	3	7	7	10	2	8	12	ISSo1, transposase OrfA
SO1465				2					ISSo1, transposase OrfB
SO1468			2			2			conserved hypothetical protein
SO1471	2	3	4	4	7	2	5	6	site-specific recombinase, phage integrase family
SO1473	8	8	9	11	10	7	4	6	SsrA-binding protein (smpB)
SO1474	2			2					conserved hypothetical protein
SO1475	7	10	5	4	8	8	4	4	conserved hypothetical protein

Locus	45 min Control		45 min Cr		90 min Control		90 min Cr		Description
	Run 1	Run 2	Run 1	Run 2	Run 1	Run 2	Run 1	Run 2	
SO1476	6	11	7	8	8	9	8	8	small protein A (smpA)
SO1481	2	3	2	2	5	4	5	6	glutathione-regulated potassium-efflux system protein
SO1482	34	36	66	61	14	16	87	88	TonB-dependent receptor, putative
SO1483				5			2	5	malate synthase A (aceB)
SO1484	5	6	12	12	12	3	9	16	isocitrate lyase (aceA)
SO1487	3				3	4	2	3	hypothetical protein
SO1489	3	5	4	7	10	5	4	4	hypothetical protein
SO1490	16	16	9	10	23	27	5	11	alcohol dehydrogenase II (adhB)
SO1496			2						glycogen phosphorylase family protein
SO1500	3			3	3		4		sensory box protein
SO1501	2	2					2	3	ATP-dependent RNA helicase, DEAD box family
SO1502	4	3	2	3	2	3	3	3	cobalamin synthesis protein/P47K family protein
SO1507	8	6	11	11	5	2	4	7	hypothetical protein
SO1511						2			transposase, IS91 family, putative
SO1512	2			2		2			hypothetical protein
SO1514	5	3	7	7	10	2	8	12	ISSo1, transposase OrfA
SO1515				2					ISSo1, transposase OrfB
SO1518	12	14	13	13	16	15	7	8	conserved hypothetical protein
SO1519	35	39	23	27	36	36	21	27	iron-sulfur cluster-binding protein
SO1520	8	7	6	9	13	5	4	9	conserved hypothetical protein
SO1521	89	95	80	78	99	92	71	70	iron-sulfur cluster-binding protein
SO1522					2				L-lactate permease, putative
SO1523	2								conserved hypothetical protein
SO1524	22	21	25	26	18	25	21	26	heat shock protein GrpE (grpE)
SO1525	8	10	10	11	13	2	10	6	deoxyxylulose-5-phosphate synthase (dxs)
SO1526		2							geranyltranstransferase (ispA)
SO1529	6	6	6	2	3	2		4	chemotaxis motA protein (pomA)
SO1530	5	3	2	6	3	5	3	7	sodium-driven polar flagellar protein PomB (pomB)
SO1531	14	10	9	9	16	11	10	10	thiamine biosynthesis protein ThiI (thiI)
SO1533	2		2		2				glycine cleavage system transcriptional activator, putative
SO1536	9	13	11	6	10	7	7	12	conserved hypothetical protein
SO1538	13	13	15	17	13	7	17	19	isocitrate dehydrogenase, NAD-dependent

Locus	45 min Control		45 min Cr		90 min Control		90 min Cr		Description
	Run 1	Run 2	Run 1	Run 2	Run 1	Run 2	Run 1	Run 2	
SO1539	11	21	15	22	19	15	21	22	conserved hypothetical protein
SO1548	4	3		4	5	5	3	7	hypothetical protein
SO1549	4	3	5	6			4	5	exodeoxyribonuclease IX (xni)
SO1550	5	10	11	5	7	5	8	5	conserved hypothetical protein
SO1551	12	10	9	12	17	12	15	7	GGDEF domain protein
SO1552	7	9	5	6	8	9	6	7	TPR domain protein
SO1556	19	29	18	18	21	9	13	23	conserved hypothetical protein
SO1559	4	7	5	5	7	6	4	5	phosphate regulon sensor protein PhoR (phoR)
SO1560	2			2					phosphate-binding protein
SO1563				2			2		glutathione peroxidase, putative
SO1565		2	3		4		2	2	magnesium transporter, putative
SO1568	7	11	10	9	5	6	11	10	hypothetical protein
SO1571	3	10	4	5	10	4	11	12	hypothetical protein
SO1575	5			3	2			2	NOL1/NOP2/sun family putative RNA methylase
SO1576	2	5	7	6	3		6	11	glutathione S-transferase family protein
SO1579					2			3	conserved hypothetical protein
SO1580	11	13	22	21	3	7	19	26	TonB-dependent heme receptor
SO1581	7	6	6	5	4		3	4	phnA protein (phnA)
SO1582	2	3		2	2				transcriptional regulator, MarR family
SO1589	4	3	3	3	5	2	2	4	hypothetical protein
SO1595								2	hypothetical protein
SO1597	3	3	4	6	3		3	3	conserved hypothetical protein
SO1599	18	14	24	19	18	5	12	17	beta-ketoacyl synthase
SO1602	37	35	44	49	35	33	29	36	multi-domain beta-ketoacyl synthase
SO1603			2						transcriptional regulator, putative
SO1605	2			2			3	2	lipoprotein, putative
SO1606	2		3	3	2			6	metallo-beta-lactamase superfamily protein
SO1608	3	7	4	4	5	2	3	4	conserved hypothetical protein
SO1610	4	6	4	3	2	2	5	4	conserved hypothetical protein
SO1611	3	6	2	4	2	3	4	4	hypothetical protein
SO1616	15	22	15	15	16	18	15	15	ISSo4, transposase
SO1617	3								conserved hypothetical protein

Locus	45 min Control		45 min Cr		90 min Control		90 min Cr		Description
	Run 1	Run 2	Run 1	Run 2	Run 1	Run 2	Run 1	Run 2	
SO1620					2		2		RNA pseudouridylate synthase family protein
SO1624					2				formyltetrahydrofolate deformylase (purU)
SO1625	10	9	15	18	10	9	18	15	2,3,4,5-tetrahydropyridine-2,6-dicarboxylate N-succinyltransferase (dapD)
SO1626	7	4	4	5	7	5	6	4	protein-P-II uridylyltransferase (glnD)
SO1627	15	17	13	17	11	12	10	12	methionine aminopeptidase, type I (map)
SO1629	36	43	39	42	39	41	44	41	ribosomal protein S2 (rpsB)
SO1630	44	43	40	49	37	47	29	34	translation elongation factor Ts (tsf)
SO1631	12	17	15	17	15	9	8	10	uridylate kinase (pyrH)
SO1632	22	18	17	24	14	19	11	19	ribosome recycling factor (frr)
SO1633	2					2	2	2	undecaprenyl diphosphate synthase (uppS)
SO1635	2	2	2	2	3			3	1-deoxy-D-xylulose 5-phosphate reductoisomerase (dxr)
SO1636	2	6	6	3	5	2	4	5	membrane-associated zinc metalloprotease, putative
SO1637	46	55	47	55	38	42	46	46	bacterial surface antigen
SO1638	22	21	25	21	17	25	19	22	outer membrane protein OmpH (ompH)
SO1639	5	6	6	7	6	10	7	7	UDP-3-O-(3-hydroxymyristoyl) glucosamine n-acyltransferase (lpxD)
SO1641	8	10	5	7	8	5	4	5	acyl-(acyl-carrier-protein)--UDP-N-acetylglucosamine O-acyltransferase (lpxA)
SO1642	6	7	4	8	8	3	13	10	lipid A disaccharide synthase (lpxB)
SO1643	2	2	3	4	2	2	2	2	ribonuclease HII (rnhB)
SO1644	2	3	4	6	6	4	4	9	DNA polymerase III, alpha subunit (dnaE)
SO1648	5	7	4	5	5	5	4	3	cold shock domain family protein
SO1651	2	5	5	2	3		4	3	Snf2 family protein
SO1652	2		2	2	4		3	2	conserved hypothetical protein
SO1655	2	2	3	4			4	4	cysQ protein (cysQ-2)
SO1656		3	3	5	2	2	3	8	ROK family protein
SO1657	4	3	3	2	3	4	3	2	conserved hypothetical protein
SO1659		3	2						decaheme cytochrome c
SO1662	2	3	3	2	2	3	3	4	conserved hypothetical protein
SO1664	5	8	7	6	4	2	8	7	UDP-glucose 4-epimerase (galE)
SO1665	24	22	21	22	18	22	18	25	UTP-glucose-1-phosphate uridylyltransferase (galU)
SO1669	12	12	9	10	15	9	9	11	transcriptional regulatory protein TyrR (tyrR)

Locus	45 min Control		45 min Cr		90 min Control		90 min Cr		Description
	Run 1	Run 2	Run 1	Run 2	Run 1	Run 2	Run 1	Run 2	
SO1670	9	9	6	7	8	7	10	10	fumarylacetoacetate hydrolase family protein
SO1674	6	13	4	5	8	5	4	8	oxidoreductase, short chain dehydrogenase/reductase family
SO1675	14	15	12	12	13	9	9	11	conserved hypothetical protein
SO1676	2	3	2	2			3	4	homoserine O-succinyltransferase (metA)
SO1677	29	38	36	38	32	31	28	33	acetyl-CoA acetyltransferase (atoB)
SO1678	8	10	11	11	17	10	11	16	methylmalonate-semialdehyde dehydrogenase (mmsA)
SO1679	19	18	24	22	31	23	19	21	acyl-CoA dehydrogenase family protein
SO1680	10	17	14	15	17	19	15	16	enoyl-CoA hydratase/isomerase family protein
SO1681		3	3	5	4		2	2	enoyl-CoA hydratase/isomerase family protein
SO1682	4	6	3	6	4	2	2	3	3-hydroxyisobutyrate dehydrogenase (mmsB)
SO1683	11	11	9	7	13	21	10	13	3-oxoacyl-(acyl-carrier-protein) reductase, putative
SO1686	3	4	3		2	6	3	4	prolyl oligopeptidase family protein
SO1689	4	2	2	8	3	2	4	3	cation transport ATPase, E1-E2 family
SO1690	17	18	21	15	16	12	23	16	ABC transporter, ATP-binding protein
SO1691	3	3	3	4	2	2	3	5	lipoprotein Blc (blc)
SO1700	5	9	12	15	4	5	9	8	hypothetical protein
SO1701			5		3	2	3	2	hypothetical protein
SO1717	3	5	6	7	6		7	9	hypothetical protein
SO1718	2			2	2	2		5	conserved hypothetical protein
SO1723	4	5	3	3	2	4	2	2	phosphate ABC transporter, permease protein, putative
SO1724	6	6	8	3	4	4	6	3	phosphate ABC transporter, permease protein, putative
SO1725	10	12	16	19	12	7	11	18	phosphate ABC transporter, ATP-binding protein (pstB-1)
SO1726	3	4		4	3	2	2	3	phosphate transport system regulatory protein PhoU (phoU)
SO1732		3		3	3			2	cold shock domain family protein
SO1734			2					3	glyoxalase family protein
SO1738							4		conserved hypothetical protein
SO1742				4	2			3	conserved hypothetical protein
SO1743	6	9	3	4	5	6	4	5	hydrolase, alpha/beta hydrolase fold family
SO1744	4	2		2	4	4	2	3	AMP-binding protein
SO1745	7	6	5	4	6	5	3	5	3-beta hydroxysteroid dehydrogenase/isomerase family protein
SO1750	22	25	20	20	25	20	20	23	ABC transporter, ATP-binding protein
SO1751	12	12	9	9	19	15	11	13	membrane protein, putative

Locus	45 min Control		45 min Cr		90 min Control		90 min Cr		Description
	Run 1	Run 2	Run 1	Run 2	Run 1	Run 2	Run 1	Run 2	
SO1755	7	16	12	14	6	4	16	21	phosphoglucomutase/phosphomannomutase family protein
SO1756				2				3	glyoxalase family protein
SO1767	15	22	15	15	16	18	15	15	ISSo4, transposase
SO1769		2					3	2	glutamate decarboxylase, putative
SO1770		2							glycerate kinase, putative
SO1776	13	20	14	9	32	26	12	18	outer membrane protein precursor MtrB (mtrB)
SO1777		2		2	4	3			decaheme cytochrome c MtrA (mtrA)
SO1778	30	34	29	29	42	44	14	12	decaheme cytochrome c (omcB)
SO1779	35	39	21	29	56	55	18	18	decaheme cytochrome c (omcA)
SO1783	7	7	8	8	2	3	2	8	ferrous iron transport protein A (feoA)
SO1784	20	19	21	20	14	13	23	26	ferrous iron transport protein B (feoB)
SO1786	11	18	11	17	21	6	21	13	glutaminyl-tRNA synthetase (glnS)
SO1788							4		tRNA-(MS[2]IO[6]A)-hydroxylase (miaE)
SO1790	12	12	11	7	9	11	8	11	peptidyl-prolyl cis-trans isomerase B (ppiB-1)
SO1791	7	13	6	12	9	4	13	9	cysteinyl-tRNA synthetase (cysS)
									methylenetetrahydrofolate dehydrogenase/methylenetetrahydrofolate
SO1792	4	2	4	4	4	4	5	5	cyclohydrolase (folD)
SO1793	69	76	78	77	69	81	70	70	trigger factor (tig)
SO1794	5	9	7	6	6	2	6	9	ATP-dependent Clp protease, proteolytic subunit (clpP)
SO1795	19	20	24	25	13	14	18	22	ATP-dependent Clp protease, ATP-binding subunit ClpX (clpX)
SO1796	51	65	60	71	56	48	69	74	ATP-dependent protease La (lon)
SO1797	22	23	22	23	23	31	23	21	DNA-binding protein, HU family
SO1798	88	112	100	95	77	99	85	100	peptidyl-prolyl cis-trans isomerase D (ppiD)
SO1800	18	29	26	23	19	12	19	22	conserved hypothetical protein
SO1801	9	10	8	8	10	8	8	5	peptide ABC transporter, ATP-binding protein (sapF)
SO1802	7	9	7		10	7	6	6	peptide ABC transporter, ATP-binding protein (sapD)
SO1805	8	10	7	5	4	3	6	8	peptide ABC transporter, periplasmic peptide-binding protein (sapA)
SO1806	2						2	2	psp operon transcriptional activator (pspF)
SO1807	36	39	33	40	39	33	41	40	phage shock protein A (pspA)
SO1808	2	2	2	3	3	2	2	2	phage shock protein B (pspB)
SO1809		4	3	5	4	5	4	2	phage shock protein C (pspC)
SO1810			2		2	3	2		conserved hypothetical protein
SO1811	3	4	4	4	6	3	8	11	conserved hypothetical protein

Locus	45 min Control		45 min Cr		90 min Control		90 min Cr		Description
	Run 1	Run 2	Run 1	Run 2	Run 1	Run 2	Run 1	Run 2	
SO1812			2	2				2	methionine gamma-lyase (mdeA)
SO1816	8	10	8	10	7	5	5	9	conserved hypothetical protein
SO1817		4	3	3	3			3	primosomal replication protein n, putative
SO1819	4	3		4	3		3	2	ATP-dependent helicase DinG (dinG)
SO1821	10	14	16	19	14	18	22	22	outer membrane porin, putative
SO1824	49	61	52	51	51	51	52	52	conserved hypothetical protein
SO1825	92	119	87	93	97	120	97	112	MotA/TolQ/ExbB proton channel family protein
SO1826	5	6	4	4	6	6	2	4	TonB system transport protein ExbB2 (exbB2)
SO1827	12	10	13	11	10	8	11	11	TonB system transport protein ExbD2 (exbD2)
SO1828	14	18	13	17	17	12	15	15	TonB2 protein (tonB2)
SO1829	74	85	73	66	77	64	70	72	TPR domain protein
SO1831	34	44	30	28	38	21	33	31	conserved hypothetical protein
SO1832	2	5	7	4	4	3	5	8	peptidyl-prolyl cis-trans isomerase C (ppiC-2)
SO1833			2	3				3	ISSo7, transposase
SO1839		2			2				hypothetical protein
SO1844		4		4	4	4	2	3	extracellular nuclease, putative
SO1846								3	hypothetical protein
SO1848	6	5	6	5	4	3	4	5	hypothetical protein
SO1849	7	8	4	3	6	2	2	5	hypothetical protein
SO1850	2	3	2	3	2	2	3	4	DnaJ domain protein
SO1851	7	5	6	6	8	2	3	6	conserved hypothetical protein
SO1853	10	15	6	9	6	10	7	13	ABC transporter, ATP-binding protein
SO1854	27	37	29	29	29	29	32	36	hypothetical protein
SO1855			2				3	2	ribosome modulation factor (rmf)
SO1856	9	5	3	5	4	2	4	3	3-hydroxydecanoyl-(acyl-carrier-protein) dehydratase (fabA)
SO1857	7	9	3	7	6	6	4	9	conserved hypothetical protein
SO1860	5	3	3	6	4	2	7	7	DNA-binding response regulator, LuxR family
SO1861	2	2	3	2	4	2		4	excinuclease ABC, C subunit (uvrC)
SO1863	4	6	3	2	3	2		2	DNA-binding protein, HU family
SO1865	8	3	5	8	5	4	6	4	ABC transporter, ATP-binding protein
SO1867	7	6	5	5	6	3	2	7	conserved hypothetical protein
SO1868	3	7		4	4		4	3	conserved hypothetical protein

Locus	45 min Control		45 min Cr		90 min Control		90 min Cr		Description
	Run 1	Run 2	Run 1	Run 2	Run 1	Run 2	Run 1	Run 2	
SO1870	19	18	15	15	19	9	17	21	biosynthetic arginine decarboxylase (speA)
SO1875	15	22	15	15	16	18	15	15	ISSo4, transposase
SO1877	6	8	3	7	9	3		3	bacterioferritin comigratory protein (bcp)
SO1878	3		2	3	3		2	2	glycine cleavage system transcriptional repressor, putative
SO1879	13	17	11	13	11	10	11	11	dihydrodipicolinate synthase (dapA)
SO1880	18	36	26	28	24	29	25	30	lipoprotein-34 NlpB (nlpB)
SO1881	7	11	6	6	3	4	2	6	HlyD family-related protein
SO1882	5	2	4	3	4	2	2	2	AcrB/AcrD/AcrF family protein
SO1891	5	11	10	9	8	6	8	14	3-oxoadipate CoA-succinyl transferase, beta subunit
SO1892	9	6	6	6	9	10	6	8	acetate CoA-transferase, subunit A (atoD)
SO1893	11	6	5	5	11	10	3	8	hydroxymethylglutaryl-CoA lyase (mvaB)
SO1894	34	39	34	33	49	32	32	33	acetyl-CoA carboxylase, biotin carboxylase, putative
SO1895	7	3	3	5	8	5	6	7	enoyl-CoA hydratase/isomerase family protein
SO1896	23	24	14	21	28	35	19	25	3-methylcrotonyl CoA carboxylase, beta subunit (pccB-1)
SO1897	20	19	19	27	28	26	20	24	isovaleryl-CoA dehydrogenase (ivd)
SO1898	7	9	11	8	7	7	9	11	transcriptional regulator, putative
SO1899				2	3			2	conserved hypothetical protein
SO1902	6	7	4	3	8	6	3	2	6-phosphogluconate dehydrogenase, decarboxylating (gnd)
SO1904				2					ISSo1, transposase OrfB
SO1905	5	3	7	7	10	2	8	12	ISSo1, transposase OrfA
SO1912	2	3	2	4	3	2	3	3	acyl-CoA thioesterase II (tesB)
SO1913	3	4	3	4		5	4	3	conserved hypothetical protein
SO1915	3	2				2			serine protease, subtilase family
SO1916	2	2	2		2				transcriptional regulator, LysR family
SO1921	3	5	2	2	3	3	4	2	hypothetical protein
SO1923		3			2				AcrB/AcrD/AcrF family protein
SO1924		2					3		AcrB/AcrD/AcrF family protein
SO1925			2						HlyD family secretion protein
SO1926	34	33	29	34	42	19	40	41	citrate synthase (gltA)
SO1928	67	69	66	73	63	56	55	59	succinate dehydrogenase, flavoprotein subunit (sdhA)
SO1929	32	32	29	27	31	27	28	35	succinate dehydrogenase, iron-sulfur protein (sdhB)
SO1930	63	76	68	67	75	61	92	91	2-oxoglutarate dehydrogenase, E1 component (sucA)

Locus	45 min Control		45 min Cr		90 min Control		90 min Cr		Description
	Run 1	Run 2	Run 1	Run 2	Run 1	Run 2	Run 1	Run 2	
SO1931	45	48	45	38	42	44	43	39	2-oxoglutarate dehydrogenase, E2 component, dihydrolipoamide succinyltransferase (sucB)
SO1932	41	49	38	46	34	43	27	40	succinyl-CoA synthase, beta subunit (sucC)
SO1933	17	25	17	16	19	18	14	18	succinyl-CoA synthase, alpha subunit (sucD)
SO1935	3	2	3	2	3		3	2	regulator of nucleoside diphosphate kinase (rnk)
SO1936				2				2	acetyltransferase, GNAT family
SO1937	6	13	12	12	9	8	9	12	ferric uptake regulation protein (fur)
SO1940					2				hypothetical protein
SO1941		2	2	2	2	2	3		magnesium and cobalt transport protein CorA (corA)
SO1942				2					HDIG domain protein
SO1945	5	10	5	6	7	7	7	8	sensor protein PhoQ (phoQ)
SO1946		2		3	2		4	3	transcriptional regulatory protein PhoP (phoP)
SO1948	3	4	3	2	2	4			sodium:dicarboxylate symporter family protein
SO1949	18	29	13	16	26	32	10	18	invasin domain protein
SO1952	3	6	5	10	2		5	2	gamma-glutamyltranspeptidase (ggt-2)
SO1959			2						ABC transporter, periplasmic substrate-binding protein, putative
SO1961								3	maltose O-acetyltransferase (maa)
SO1962			2	2	4			2	4-hydroxyphenylpyruvate dioxygenase
SO1966		2	6	2	3	4	4	2	conserved hypothetical protein TIGR00266
SO1968					2				hypothetical protein
SO1970				2					hypothetical protein
SO1975								2	Zinc carboxypeptidase-related protein
SO1980								2	phosphoribosyl transferase domain protein
SO1981	2			5	2	2	2		conserved hypothetical protein
SO1986		2					2		RNA polymerase sigma-70 factor, ECF subfamily
SO1988								2	conserved hypothetical protein
SO1989				2	2		2	2	chemotaxis protein CheV (cheV-1)
SO1994	16	17	15	16	17	17	18	18	membrane-bound lytic transglycolase-related protein
SO1995	7	8	4	4	9	6	6	7	peptidyl-prolyl cis-trans isomerase, FkbP family
SO2001	45	47	48	44	55	60	39	44	5-nucleotidase (ushA)
SO2006	2	2		2				2	NifR3/Smm1 family protein
SO2007								2	conserved hypothetical protein
SO2008		4							conserved hypothetical protein

Locus	45 min Control		45 min Cr		90 min Control		90 min Cr		Description
	Run 1	Run 2	Run 1	Run 2	Run 1	Run 2	Run 1	Run 2	
SO2012	2	2	2	2		2		2	adenine phosphoribosyltransferase (apt)
SO2013	9	8	2	6	5	5	4	7	DNA polymerase III, gamma and tau subunits (dnaX)
SO2014	8	9	12	11	9	11	6	8	conserved hypothetical protein TIGR00103
SO2015		2		3					recombination protein RecR (recR)
SO2016	63	75	92	100	82	72	113	124	heat shock protein HtpG (htpG)
SO2017			4	5	3		6	8	conserved hypothetical protein
SO2018	24	32	27	26	25	19	18	22	adenylate kinase (adk)
SO2019	4	5	2	2	6	7	3	3	ferrochelatase (hemH-1)
SO2020	4	6	2	2	7	2	4	2	inosine-guanosine kinase (gsk)
SO2021	6	7	5	9	3	4	3	7	NH(3)-dependent NAD(+) synthetase (nadE)
SO2025	5	3	7	7	10	2	8	12	ISSo1, transposase OrfA
SO2026				2					ISSo1, transposase OrfB
SO2027	3	4	3	2	2	2	5	2	hypothetical protein
SO2031				2					ISSo1, transposase OrfB
SO2032	5	3	7	7	10	2	8	12	ISSo1, transposase OrfA
SO2034			2				4		hypothetical protein
SO2035						2			transposase, putative
SO2037		2							site-specific recombinase, phage integrase family
SO2040	6	6	5	13	8	5	10	9	soluble lytic murein transglycosylase, putative
SO2041	14	24	19	25	21	26	20	26	conserved hypothetical protein
SO2042				3	2			2	conserved hypothetical protein
SO2044	2	4	2	4	2			4	lactoylglutathione lyase (gloA)
SO2045	2	5			3	3	3		cation efflux family protein
SO2046				2			2		transcriptional regulator, MarR family
SO2047	3		4	4			2	3	prolyl oligopeptidase family protein
SO2048	9	9	8	2	10	11	6	7	membrane protein, putative
SO2052		2			2		2		conserved hypothetical protein
SO2056				2					ISSo1, transposase OrfB
SO2057	5	3	7	7	10	2	8	12	ISSo1, transposase OrfA
SO2062	4	8	6	6	3	13	7	8	conserved hypothetical protein
SO2064			2		2		4		conserved domain protein
SO2067							2	2	phosphoribosyl-ATP pyrophosphatase/phosphoribosyl-AMP cyclohydrolase (hisI)

Locus	45 min Control		45 min Cr		90 min Control		90 min Cr		Description
	Run 1	Run 2	Run 1	Run 2	Run 1	Run 2	Run 1	Run 2	
SO2069				2					phosphoribosylformimino-5-aminoimidazole carboxamide ribotide isomerase (hisA)
SO2071							2	2	imidazoleglycerol-phosphate dehydratase/histidinol-phosphatase (hisB)
SO2072								2	histidinol-phosphate aminotransferase (hisC)
SO2074		3							ATP phosphoribosyltransferase (hisG)
SO2078	15	22	15	15	16	18	15	15	ISSo4, transposase
SO2082		5	3	4	3	2	2	2	rod shape-determining-related protein
SO2083	5	6	5	5	5	7	5	6	methyl-accepting chemotaxis protein
SO2085	24	26	21	24	27	23	16	18	phenylalanyl-tRNA synthetase, alpha subunit (pheS)
SO2086	35	37	28	30	37	31	33	38	phenylalanyl-tRNA synthetase, beta subunit (pheT)
SO2087	12	16	13	16	13	12	16	13	integration host factor, alpha subunit (ihfA)
SO2088	13	8	8	5	11	10	5	9	lipid A biosynthesis acyltransferase, putative
SO2098					4	2			quinone-reactive Ni/Fe hydrogenase, large subunit (hyaB)
SO2099					2				quinone-reactive Ni/Fe hydrogenase, small subunit precursor (hoxK)
SO2107	5	12	11	11	8	6	10	10	periplasmic glucans biosynthesis protein MdoG (mdoG-1)
SO2108	14	17	8	13	19	17	14	16	periplasmic glucans biosynthesis protein MdoH (mdoH)
SO2110			2						conserved hypothetical protein
SO2112	4	5	3	3	3	4	7	4	ribosomal protein L25 (rplY)
SO2113	11	11	10	4	15	18	6	10	conserved hypothetical protein
SO2114	5	4	3	4	5	5	7	4	conserved hypothetical protein
SO2116	3	3		5	4		5	2	acetyltransferase, GNAT family
SO2117	3	4	3	4	4	3	3	4	methyl-accepting chemotaxis protein
SO2123				2	3				methyl-accepting chemotaxis protein
SO2130				2					ISSo1, transposase OrfB
SO2131	5	3	7	7	10	2	8	12	ISSo1, transposase OrfA
SO2133	2								hypothetical protein
SO2134	5	3	7	7	10	2	8	12	ISSo1, transposase OrfA
SO2135				2					ISSo1, transposase OrfB
SO2136		4						2	aldehyde-alcohol dehydrogenase (adhE)
SO2147	2								exodeoxyribonuclease V, alpha subunit (recD)
SO2148	2		2		2		2		exodeoxyribonuclease V, beta subunit (recB)
SO2149	3	2			2			2	exodeoxyribonuclease V, gamma subunit (recC)

Locus	45 min Control		45 min Cr		90 min Control		90 min Cr		Description
	Run 1	Run 2	Run 1	Run 2	Run 1	Run 2	Run 1	Run 2	
SO2150	2					2		2	transglutaminase family protein
SO2151	2	3	3		2	2	2	3	conserved hypothetical protein
SO2165						2			transposase, IS91 family, putative
SO2168	5	3	7	7	10	2	8	12	ISSo1, transposase OrfA
SO2169				2					ISSo1, transposase OrfB
SO2171				2					ISSo1, transposase OrfB
SO2172	5	3	7	7	10	2	8	12	ISSo1, transposase OrfA
SO2175	7	8	9	8	8	3	11	8	conserved hypothetical protein
SO2176				2			2		conserved hypothetical protein
SO2177	10	14	5	13	8	13	10	12	conserved hypothetical protein
SO2178	2	2	4	3	3	3			cytochrome c551 peroxidase (ccpA)
SO2180	4	5	9	7		3		4	peptidase, M23/M37 family
SO2183	2	3	3	3	3		3	2	conserved hypothetical protein
SO2189	2	5		3	3				conserved hypothetical protein
SO2190	3	3	4		3	5	3	2	creA protein (creA)
SO2191		2	2	4	2		2	2	cystathionine beta-lyase (metC)
SO2192	5	4	3		2	3	2	4	sensor histidine kinase
SO2193					2				DNA-binding response regulator
SO2195						2			inter-alpha-trypsin inhibitor domain protein
SO2197								2	GGDEF family protein
SO2198	4	6	7	6	6		2	6	conserved hypothetical protein
SO2200	4	5	2	5	4	5	2		ribosomal protein S6 modification protein, putative
SO2201				4			4	3	conserved hypothetical protein
SO2202							2		transcriptional regulator, LysR family
SO2212						2			transposase, IS91 family, putative
SO2215	8	13	5	5	7	7		6	sun protein, putative
SO2217	2	2	2	2	2		2	2	D-alanine--D-alanine ligase (ddlA)
SO2218	17	21	24	24	22	9	21	33	asparaginyl-tRNA synthetase (asnS)
SO2220								2	MutT/nudix family protein
SO2221			2				2	2	para-aminobenzoate synthase, component I (pabB)
SO2222	26	38	26	30	25	17	23	22	fumarate hydratase, class I, anaerobic, putative
SO2223	11	14	14	14	15	9	19	10	peptidase, putative

Locus	45 min Control		45 min Cr		90 min Control		90 min Cr		Description
	Run 1	Run 2	Run 1	Run 2	Run 1	Run 2	Run 1	Run 2	
SO2228							2		CBS domain protein
SO2229	11	14	9	5	9	8	5	12	ATP-dependent helicase HrpA (hrpA)
SO2236	3			3				3	PTS system, glucose-specific IIA component (crr)
SO2237			3		3			2	phosphoenolpyruvate-protein phosphotransferase (ptsI)
SO2240	12	12	13	12	19	12	10	12	methyl-accepting chemotaxis protein
SO2244	2								transcriptional regulator, LacI family
SO2247		4	5	9	5	5	6	7	hypothetical protein
SO2248	5	16	13	14	11	3	12	15	L-serine dehydratase 1 (sdaA)
SO2250	2		2		2	2	2	2	beta-hexosaminidase (nagZ)
SO2251					4	2			conserved hypothetical protein
SO2254	11	11	14	11	13	7	9	12	conserved hypothetical protein
SO2255	3	8	5		5	4	6	8	transcription-repair coupling factor (mfd)
SO2257	2	5		2	3	4	5	4	lipoprotein releasing system transmembrane protein LolE (lolE)
SO2258	6	8	5	11	7	3	8	5	lipoprotein releasing system ATP-binding protein LolD (lolD)
SO2259	4	4	3	3	4	2	3	5	lipoprotein releasing system transmembrane protein LolC, putative
SO2260	16	17	14	15	15	10	15	10	extragenic suppressor protein SuhB (suhB)
SO2261	7	4	7	5	5	3	2	5	RNA methyltransferase, TrmH family, group 1
SO2262	15	19	20	16	17	20	18	22	serine acetyltransferase (cysE)
SO2263	6	4	10	6	3		8	9	Rrf2 family protein
SO2264	27	35	38	40	29	29	36	39	cysteine desulfurase (iscS)
SO2265	8	10	11	13	5	6	10	13	NifU family protein
SO2267	2	5	4	3	3		4	6	co-chaperone Hsc20 (hscB)
SO2268	12	16	16	14	15	9	19	20	chaperone protein HscA (hscA)
SO2269	4	3	3	2	2	3			ferredoxin, 2Fe-2S
SO2270	9	9	4	5	6	5		7	ribosomal protein S6 modification protein (rimK-2)
SO2272	15	22	15	15	16	18	15	15	ISSo4, transposase
SO2274	13	16	16	16	17	16	16	16	nucleoside diphosphate kinase (ndk)
SO2277	11	12	20	19	10	14	18	19	16 kDa heat shock protein A (ibpA)
SO2278	4	2				3			acetolactate synthase III, small subunit (ilvH)
SO2279	5	4	4	4	6	3	8	8	acetolactate synthase III, large subunit (ilvI)
SO2286	4	5	4	2	5	2	3	7	sulfate permease family protein
SO2290	6	10	12	13	5	3	17	14	rhodanese domain protein

Locus	45 min Control		45 min Cr		90 min Control		90 min Cr		Description
	Run 1	Run 2	Run 1	Run 2	Run 1	Run 2	Run 1	Run 2	
SO2292	15	19	13	13	15	16	14	14	ISSo4, transposase
SO2299	18	23	19	22	29	9	30	28	threonyl-tRNA synthetase (thrS)
SO2300	15	19	18	14	16	23	13	13	translation initiation factor IF-3 (infC)
SO2301	4	5	3	4	4	2			ribosomal protein L35 (rpmI)
SO2302	19	20	16	20	19	25	16	18	ribosomal protein L20 (rplT)
SO2303	11	17	14	17	15	14	14	14	thioredoxin reductase (trxB)
SO2304	20	21	11	9	13	18	10	10	alanine dehydrogenase, authentic point mutation (ald)
SO2305	11	13	10	6	10	12	8	9	leucine-responsive regulatory protein (lrp)
SO2306	20	25	24	21	28	21	27	31	cell division protein FtsK, putative
SO2307		3		2			2		outer membrane lipoprotein carrier protein LolA (lolA)
SO2308	3			2	3	5	6	4	ATPase, AAA family
SO2310	22	28	22	20	26	26	20	21	seryl-tRNA synthetase (serS)
SO2317	2	2	3	3	2	3	3	3	methyl-accepting chemotaxis protein, truncation
SO2320								2	chemotaxis protein CheA, interruption-N
SO2321	15	22	15	15	16	18	15	15	ISSo4, transposase
SO2323	6	6	7	7	7	3	3	7	methyl-accepting chemotaxis protein
SO2328	14	15	13	14	14	13	16	14	translation elongation factor P (efp)
SO2330	3	5	3	7	5	3	5	6	flavodoxin
SO2331	5		2						conserved hypothetical protein
SO2333		2		2	3	2	4	2	hydrolase, alpha/beta fold family
SO2335	4	7	6	3	7	5	2	3	seqA protein (seqA)
SO2336	4	4	4	5	6	2	4	5	phosphoglucosyltransferase, alpha-D-glucose phosphate-specific (pgm)
SO2338	8	6	8	8	9	5	5	5	succinylglutamate desuccinylase (astE)
SO2339	45	54	43	47	50	53	45	50	alpha keto acid dehydrogenase complex, E1 component, alpha subunit
SO2340	30	31	25	28	33	36	24	27	alpha keto acid dehydrogenase complex, E1 component, beta subunit
SO2341	35	33	35	36	34	33	36	33	alpha keto acid dehydrogenase complex, E2 component
SO2342	4	6	5	6	9	3	2	4	quinolinate synthetase complex, subunit A (nadA)
SO2344	15	22	15	15	16	18	15	15	ISSo4, transposase
SO2345	22	26	29	29	24	21	25	25	glyceraldehyde 3-phosphate dehydrogenase (gapA-2)
SO2346						3		3	conserved hypothetical protein
SO2347	37	43	34	42	34	31	33	37	glyceraldehyde 3-phosphate dehydrogenase (gapA-3)
SO2350	15	14	8	16	18	4	6	13	aspartate aminotransferase (aspC-1)

Locus	45 min Control		45 min Cr		90 min Control		90 min Cr		Description
	Run 1	Run 2	Run 1	Run 2	Run 1	Run 2	Run 1	Run 2	
SO2352		3	2	2	2	4			bax protein, putative
SO2353	2	4		4	2	2		2	hypothetical protein
SO2354		2		3	2	2			conserved hypothetical protein
SO2355	4	9	7	7	9	4	3	7	universal stress protein family
SO2356	2							2	electron transport regulator A (etrA)
SO2359	6	4	6	5	6	9	6	3	cation transport ATPase, E1-E2 family
SO2360	6	10	6	6	6	10	6	6	conserved hypothetical protein
SO2361	32	38	28	31	31	27	24	29	cytochrome c oxidase, cbb3-type, subunit III (ccoP)
SO2363	17	24	18	20	24	11	16	20	cytochrome c oxidase, cbb3-type, subunit II (ccoO)
SO2365			3	3			2	2	conserved hypothetical protein
SO2366								2	response regulator
SO2374	5	4	2		4	3	4	4	transcriptional regulator, LysR family
SO2379					2				conserved hypothetical protein
SO2380					3	2		3	RecQ domain protein
SO2387		2							conserved hypothetical protein
SO2388		2	3	3			3	2	beta-lactamase
SO2390	8	8	8	6	12	6	13	14	CDP-diacylglycerol--serine O-phosphatidyltransferase (pssA)
SO2392	15	22	15	15	16	18	15	15	ISSo4, transposase
SO2394							2		penicillin-binding protein 4 (dacB)
SO2395	6	12	7	8	10	3	6	7	acyl-CoA dehydrogenase family protein
SO2396	3	3	5	3	4	4	5	4	conserved hypothetical protein
SO2398	11	12	9	12	7	7	7	9	orotidine 5'-phosphate decarboxylase (pyrF)
SO2399	4	4	9		4	3	4	8	conserved hypothetical protein
SO2400						2			conserved hypothetical protein
SO2401	9	6	8	8	6	9	9	6	integration host factor, beta subunit (ihfB)
SO2402	83	119	96	110	97	99	100	108	ribosomal protein S1 (rpsA)
SO2403	8	9	8	9	7	7	10	8	cytidylate kinase (cmk)
SO2404	6	7	5	5	5		5	4	3-phosphoshikimate 1-carboxyvinyltransferase (aroA)
SO2406	12	11	15	16	16	4	6	13	aspartate aminotransferase (aspC-2)
SO2407	2	2	3	2	3	2			conserved hypothetical protein
SO2410	3						3	3	phosphoserine aminotransferase (serC)
SO2411	42	49	37	48	39	38	33	42	DNA gyrase, A subunit (gyrA)

Locus	45 min Control		45 min Cr		90 min Control		90 min Cr		Description
	Run 1	Run 2	Run 1	Run 2	Run 1	Run 2	Run 1	Run 2	
SO2413	7	11	9	8	4	9	8	13	3-demethylubiquinone-9 3-methyltransferase (ubiG)
SO2415	24	37	24	21	32	31	37	35	ribonucleoside-diphosphate reductase, alpha subunit (nrdA)
SO2416		4	3	3	2		4	7	ribonucleoside-diphosphate reductase, beta subunit (nrdB)
SO2418	3		3		2	3	2	2	ISSo5, transposase
SO2419	25	33	30	17	25	22	19	27	2,4-dienoyl-CoA reductase, putative
SO2420	10	17	10	13	13	10	9	15	signal peptide peptidase SppA, 67K type (sppA)
SO2421	3								L-asparaginase I (ansA)
SO2422			2	5			3		conserved hypothetical protein
SO2423								5	hypothetical protein
SO2424	6	6	5	8	8	4	5	7	zinc carboxypeptidase domain protein
SO2426		4	9	9			9	12	DNA-binding response regulator
SO2427	55	62	56	59	51	50	51	51	TonB-dependent receptor, putative
SO2429	3	7	3	5	2	5	5	7	Holliday junction DNA helicase RuvB (ruvB)
SO2430				2					Holliday junction DNA helicase RuvA (ruvA)
SO2431	2								crossover junction endodeoxyribonuclease RuvC (ruvC)
SO2432		4	2	2		5		2	conserved hypothetical protein TIGR01033
SO2433	34	50	32	30	39	23	42	39	aspartyl-tRNA synthetase (aspS)
SO2434					2				extracellular solute-binding proteins, family 3/GGDEF domain protein
SO2435		3	3				2	3	methyltransferase, putative
SO2436	3	3	5		6	4	9	9	methyltransferase, putative
SO2437	5	9	10	12	10	11	3	4	hypothetical protein
SO2438	2			3				2	transcriptional regulator, LysR family
SO2441		2						2	thiG protein (thiG)
SO2446			2				2		hypothetical protein
SO2453		2			3		2	2	N-ethylmaleimide reductase, putative
SO2460	2				3				hypothetical protein
SO2469	5	8	7	5	17	16	4	7	conserved hypothetical protein
SO2470			2		4	2	2	4	conserved hypothetical protein
SO2471	2	5			2			3	succinyl-diaminopimelate desuccinylase (dapE)
SO2474	2	3	7	4	2		5	7	carbonic anhydrase family protein
SO2476	17	20	18	22	15	15	20	22	polysaccharide biosynthesis protein
SO2477	11	9	12	9	8	4	12	9	alcohol dehydrogenase, iron-containing

Locus	45 min Control		45 min Cr		90 min Control		90 min Cr		Description
	Run 1	Run 2	Run 1	Run 2	Run 1	Run 2	Run 1	Run 2	
SO2478	5	2	2	2	3	2		2	3-deoxy-D-manno-octulosonate cytidyltransferase (kdsB)
SO2479						2		2	hypothetical protein
SO2481						2			conserved hypothetical protein
SO2483	19	13	8	14	18	9	12	15	aspartate aminotransferase, putative
SO2484	3		3	4			3		conserved hypothetical protein
SO2485	2		3	4	5		3	3	deoxyguanosinetriphosphate triphosphohydrolase, putative
SO2486	12	13	5	7	6	5	8	8	2-dehydro-3-deoxyphosphogluconate aldolase/4-hydroxy-2-oxoglutarate aldolase (eda)
SO2487	14	19	14	17	10	4	12	15	6-phosphogluconate dehydratase (edd)
SO2488	7	4	3	4	2	3	2	5	6-phosphogluconolactonase (pgl)
SO2489	6	18	12	9	11	3	10	18	glucose-6-phosphate 1-dehydrogenase (zwf)
SO2490	14	13	11	17	12	20	6	7	transcriptional regulator, RpiR family
SO2491	21	24	24	26	25	15	16	24	pyruvate kinase II (pykA)
SO2492	43	36	43	40	45	24	28	40	oxidoreductase, acyl-CoA dehydrogenase family
SO2493	4	2	2	3		3	2	3	transcriptional regulator, TetR family
SO2494	23	35	28	24	24	26	19	31	zinc-dependent metalloproteinase
SO2495		2	2	5			3	3	Smr domain protein
SO2497			2		2				conserved hypothetical protein
SO2501		3		3	3			2	radical activating enzyme
SO2503			2		2				exsB protein (exsB)
SO2506		3	2	4	6	2	6	5	excinuclease ABC, B subunit (uvrB)
SO2507	4	4	4	7	5	4	5	7	GGDEF domain protein
SO2509	5	4	4	3	3	2	3	2	iron-sulfur cluster-binding protein
SO2510	24	27	15	24	21	21	18	22	iron-sulfur cluster-binding protein
SO2512	8	7	4	4	5	10	12	8	conserved hypothetical protein
SO2514				2			3	4	Endonuclease III (nth)
SO2525	4	3	3	3	5	3	3	3	ABC transporter, ATP-binding protein
SO2527						2			transposase, IS91 family, putative
SO2529	4	7	3	3	6	7	5	8	hypothetical protein
SO2530								2	polypeptide deformylase (def-3)
SO2533	3	4	9	7	4	2	4	9	conserved hypothetical protein
SO2535			2						conserved hypothetical protein
SO2536	28	30	30	29	36	27	34	35	oxidoreductase, acyl-CoA dehydrogenase family

Locus	45 min Control		45 min Cr		90 min Control		90 min Cr		Description
	Run 1	Run 2	Run 1	Run 2	Run 1	Run 2	Run 1	Run 2	
SO2537	4	6	5	6	7	10	7	11	sodium/hydrogen exchanger family protein
SO2540		2							response regulator
SO2543				2					sensor histidine kinase
SO2553								2	conserved hypothetical protein
SO2557		4		2	2	4	3	6	conserved hypothetical protein
SO2559		2	4	4	3	2	3	3	DNA polymerase III, epsilon subunit (dnaQ-2)
SO2560		3	2						ribonuclease HI (rnhA)
SO2564	6	10	6	3	8	4	3	2	transglycosylase, Slt family
SO2566	12	19	22	23	25	27	38	33	asmA protein (asmA)
SO2567	3	2	2	3	2				S-adenosylmethionine:2-demethylmenaquinone methyltransferase (menG-1)
SO2569	3	5	6	9	5	7	7	7	hypothetical protein
SO2570	17	22	15	18	17	21	18	19	lipoprotein, putative
SO2571	14	10	10	9	12	12	6	5	ATP-dependent RNA helicase, DEAD box family
SO2572				2	2			2	peptidyl-prolyl cis-trans isomerase B (ppiB-2)
SO2573					2				conserved hypothetical protein
SO2575			2						conserved hypothetical protein
SO2576								2	septum site-determining protein MinC (minC)
SO2577	3	6	8	10	4	4	12	12	septum site-determining protein MinD (minD)
SO2578	5	2	6	3	4			4	cell division topological specificity factor MinE (minE)
SO2580	2	2	3	7	4			2	ribonuclease D (rnd)
SO2581	24	20	22	27	31	28	27	20	long-chain-fatty-acid--CoA ligase (fadD-1)
SO2583	9	9	10	15	8	3	6	9	hypothetical protein
SO2587	8	10	8	10	19	13	10	11	delta-aminolevulinic acid dehydratase (hemB-1)
SO2588		4	2		2	2	2	2	protein-methionine-S-oxide reductase, PilB family
SO2589					2				oxidoreductase, iron/ascorbate family
SO2590	10	9	6	11	4	7	3	6	GTP-binding protein
SO2592	24	21	24	25	22	23	17	24	dihydroorotate dehydrogenase (pyrD)
SO2593	80	99	80	99	101	71	79	100	conserved hypothetical protein
SO2594		2			2	2			conserved hypothetical protein
SO2596	2	2		3	2		2		conserved hypothetical protein
SO2600	3	3	3	6	4		3	6	aminopeptidase N (pepN)
SO2601	20	26	26	30	22	15	18	25	carboxyl-terminal protease

Locus	45 min Control		45 min Cr		90 min Control		90 min Cr		Description
	Run 1	Run 2	Run 1	Run 2	Run 1	Run 2	Run 1	Run 2	
SO2602	13	19	10	15	9	17	12	13	conserved hypothetical protein
SO2603								3	conserved hypothetical protein
SO2604	2		2	2	2			2	conserved hypothetical protein
SO2606	29	39	32	31	29	31	26	24	PqiB family protein
SO2610		8	7	9	4		3	7	hydrolase, TatD family
SO2612				2					DNA polymerase III, delta prime subunit (holB)
SO2613	2		2		3			2	thymidylate kinase (tmk)
SO2614	7	11	5	9	6	9	7	5	conserved hypothetical protein TIGR00247
SO2616	3	5	3	6	2	2	4	4	deoxycytidine triphosphate deaminase (dcd)
SO2617	9	4	6	4	6	4	6	7	uridine kinase (udk)
SO2618	9	9	7	8	7	4	8	6	ATP-binding protein, Mrp/Nbp35 family
SO2619	14	27	23	27	22	9	22	28	methionyl-tRNA synthetase (metG)
SO2621	2	2	2	3				3	conserved hypothetical protein TIGR00486
SO2622		4		6			2		conserved hypothetical protein
SO2625	6	4	5	3	3	4	2	4	translation initiation factor IF-1 (infA)
SO2626	8	11	10	19	10	10	12	19	ATP-dependent Clp protease, ATP-binding subunit ClpA (clpA)
SO2628	2								stress response protein CspD (cspD)
SO2629	54	60	57	68	51	44	51	55	isocitrate dehydrogenase, NADP-dependent (icd)
SO2630	2	2	3			2		2	RNA pseudouridylate synthase family protein
SO2633	5	9	9	10	6	2	8	7	tRNA (5-methylaminomethyl-2-thiouridylate)-methyltransferase (trmU)
SO2634	9	10	10	9	12	7	8	12	conserved hypothetical protein
SO2635	16	27	16	19	23	12	21	18	adenylosuccinate lyase (purB)
SO2636	9	7	6	4	4	4	7	4	conserved hypothetical protein
SO2637	7	7	5	9	3	12	4	5	hypothetical protein
SO2638	17	14	16	14	16	20	19	20	leucine dehydrogenase (ldh)
SO2643	30	35	22	19	36	34	21	16	oxidoreductase, FAD-binding, putative
SO2644	56	68	58	62	69	50	51	63	phosphoenolpyruvate synthase (ppsA)
SO2645	4	3	4	4	3	3	3	4	conserved hypothetical protein
SO2646	10	11	7	8	8	3	8	9	phospho-2-dehydro-3-deoxyheptonate aldolase, trp-sensitive (aroH)
SO2649	9	12	10	8	13	6	13	7	cys regulon transcriptional activator (cysB)
SO2650	5	10	7	7	10	9	9	9	conserved hypothetical protein
SO2652	10	6	8	4	12	6	5	8	prophage MuSo2, transcriptional regulator, Cro/CI family

Locus	45 min Control		45 min Cr		90 min Control		90 min Cr		Description
	Run 1	Run 2	Run 1	Run 2	Run 1	Run 2	Run 1	Run 2	
SO2654		2							transposase, putative
SO2655	2	2	2		4				prophage MuSo2, DNA transposition protein, putative
SO2660							2		conserved hypothetical protein
SO2663						2	2		conserved hypothetical protein
SO2681		2							prophage MuSo2, F protein, putative
SO2682	4	3	3	3	3	3		3	hypothetical protein
SO2683				2		2			hypothetical protein
SO2697		2							conserved hypothetical protein
SO2698	2								prophage MuSo2, DNA circulation protein, putative
SO2705	34	40	35	31	33	35	21	31	DNA topoisomerase I (topA)
SO2706	12	8	6	9	4	4	3	7	succinylarginine dihydrolase (astB)
SO2707	2								acetyltransferase, GNAT family
SO2708	3	4	2	3	2	2	3	3	nitroreductase family protein
SO2714	2	2		2		2			hypothetical protein
SO2715		3						3	TonB-dependent receptor
SO2720	3	3	2	3	2	4		2	conserved hypothetical protein
SO2721							3	2	conserved hypothetical protein
SO2722	2	3					3	3	conserved hypothetical protein
SO2723	2	5		3	3	4	2	4	HIT family protein
SO2725	2						2	3	transcriptional regulator, LuxR family
SO2726						3			cytochrome b, putative
SO2728	6	5	8	9	6		15	10	peptidase HtpX (htpX)
SO2730	4	6	5	6	3	3	4	8	peptidase E (pepE)
SO2731	19	22	24	28	21	10	15	17	periplasmic glucans biosynthesis protein MdoG (mdoG-2)
SO2737	3	2	2	3	2		3		dethiobiotin synthase (bioD)
SO2739	2		4		2	2	3	5	8-amino-7-oxononanoate synthase (bioF)
SO2740	7	10	10	9	7	7	6	12	biotin synthase (bioB)
SO2741	2			2	2			2	adenosylmethionine--8-amino-7-oxononanoate aminotransferase (bioA)
SO2742	4	7	3	7	9	9	4	6	sensor histidine kinase/response regulator
SO2743	13	15	13	15	10	10	15	18	acetyl-coenzyme A synthetase (acs)
SO2744								2	helicase
SO2745	7	7	7	9	6	3	8	13	glutaredoxin

Locus	45 min Control		45 min Cr		90 min Control		90 min Cr		Description
	Run 1	Run 2	Run 1	Run 2	Run 1	Run 2	Run 1	Run 2	
SO2746	13	15	12	15	11	8	7	9	conserved hypothetical protein
SO2747	13	21	15	18	12	16	17	17	peptidoglycan-associated lipoprotein (pal)
SO2748	25	15	21	17	16	16	9	14	tolB protein (tolB)
SO2749	12	23	14	19	10	19	15	21	tolA protein (tolA)
SO2750		2			2			2	tolR protein (tolR)
SO2751	9	20	12	11	15	14	10	16	MotA/TolQ/ExbB proton channel family protein
SO2752				2					conserved hypothetical protein TIGR00051
SO2753	28	32	24	28	38	27	22	23	prolyl endopeptidase
SO2755		2	3	3	3		2	3	ribonuclease T (rnt)
SO2756	21	21	25	29	23	26	26	25	antioxidant, AhpC/Tsa family, authentic frameshift
SO2759	10	14	11	12	14	12	8	9	uracil phosphoribosyltransferase (upp)
SO2760	13	18	11	17	13	9	13	16	phosphoribosylformylglycinamide cyclo-ligase (purM)
SO2761	9	11	12	12	11	5	8	10	phosphoribosylglycinamide formyltransferase (purN)
SO2762	4	7	5	8	8	3	5	8	nagD protein
SO2763	11	6	5	8	4	12	4	5	conserved hypothetical protein
SO2766	30	35	34	26	31	31	35	26	conserved hypothetical protein
SO2768					2		2		acyl-CoA dehydrogenase family protein
SO2769							2		conserved hypothetical protein
SO2771	2	5	4	3	7			7	2-hydroxy-3-oxopropionate reductase (garR)
SO2774	12	14	11	13	9	7	7	10	3-oxoacyl-(acyl-carrier-protein) synthase II (fabF-1)
SO2775	6	5		4	4	4	3	4	acyl carrier protein (acpP)
SO2776	16	16	14	16	11	16	14	8	3-oxoacyl-(acyl-carrier-protein) reductase (fabG-1)
SO2777	9	10	7	6	5	9	2	4	malonyl CoA-acyl carrier protein transacylase (fabD)
SO2778	5	9	9	7	7	3	6	9	3-oxoacyl-(acyl-carrier-protein) synthase III (fabH-1)
SO2779	4	3	3	2	5	3	2	2	fatty acid/phospholipid synthesis protein PlsX (plsX)
SO2780	6	8	10	9	9	7	10	9	ribosomal protein L32 (rpmF)
SO2781	3	3	5	3	2	2	2	4	conserved hypothetical protein
SO2782	2	2	2	2	3		4	3	maf protein, putative
SO2784	10	12	3	8	6	9	6	6	ribosomal large subunit pseudouridine synthase C (rluC)
SO2785	82	94	87	95	91	93	87	100	ribonuclease E (rne)
SO2787	20	18	19	17	18	14	19	18	cold shock domain family protein
SO2788		4	2	3	5	2			ribosomal RNA large subunit methyltransferase A (rrmA)

Locus	45 min Control		45 min Cr		90 min Control		90 min Cr		Description
	Run 1	Run 2	Run 1	Run 2	Run 1	Run 2	Run 1	Run 2	
SO2790	4	5	4	8	3	3	6	6	exodeoxyribonuclease I (sbcB)
SO2794		3		3	2	3		2	conserved hypothetical protein
SO2796	56	65	49	56	61	57	51	56	conserved hypothetical protein
SO2797		2	4	2			2	2	conserved hypothetical protein
SO2799	3	5		5	3	2	2	6	lipoprotein, putative
SO2800	3	2			4	3	8	7	conserved hypothetical protein
SO2801	3	3	2	6		4	4	6	tetraacyldisaccharide 4-kinase (lpxK)
SO2802	15	13	16	16	12	8	15	15	ABC transporter, ATP-binding protein MsbA (msbA)
SO2807				2			3		hypothetical protein
SO2811	15	22	15	15	16	18	15	15	ISSo4, transposase
SO2813	2	2	2	2	2				oxidoreductase, short chain dehydrogenase/reductase family
SO2815	3		3	2	3	2	3	5	CBS domain protein
SO2817	15	22	15	15	16	18	15	15	ISSo4, transposase
SO2822							2	2	sensor histidine kinase
SO2827	4	2	3	2	3				conserved hypothetical protein
SO2831	3	4	2	2	2	2		2	GTP cyclohydrolase II (ribA)
SO2832	7	12	7	9	5	8	3	7	conserved hypothetical protein
SO2834					5	5		2	anaerobic ribonucleoside-triphosphate reductase (nrdD)
SO2836								2	conserved hypothetical protein
SO2838	15	8	3	6	9	6	5	12	ATP-dependent RNA helicase, DEAD box family
SO2839	3	6	5	7	7	5	7	6	hypothetical protein
SO2840							2		conserved hypothetical protein
SO2841			3	2			2	5	hypothetical protein
SO2842	3	4	2	4	4	6	3	3	peptidase, M23/M37 family
SO2843	8	10	7	7	9	8	7	7	exonuclease SbcC, putative
SO2844				2	3			4	exonuclease SbcD, putative
SO2847				2					transcriptional regulator, LysR family
SO2848			4	2	2				hypothetical protein
SO2849					2				acetyltransferase, GNAT family
SO2851	3	3	4	7	4	4	4	7	histidinol phosphatase domain protein
SO2852	2	4	2	5	2	3	5	4	transcriptional regulator, GntR family
SO2853	8	7	5	5	4	5	3	4	3-oxoacyl-(acyl-carrier-protein) synthase III, putative

Locus	45 min Control		45 min Cr		90 min Control		90 min Cr		Description
	Run 1	Run 2	Run 1	Run 2	Run 1	Run 2	Run 1	Run 2	
SO2856	2								CBS domain protein
SO2857		2	2	2			2		sodium/solute symporter family protein
SO2860								3	thiol:disulfide interchange protein, DsbA family
SO2861			3	2					conserved hypothetical protein
SO2862							2		HDIG domain protein
SO2866	3	2	2		3	2			chromosome initiation inhibitor (iciA)
SO2869		4	3	7	2			5	conserved hypothetical protein
SO2871			3	4				2	arsenate reductase, putative
SO2877			2	2					conserved hypothetical protein
SO2878	9	10	11	8	11	11	6	8	conserved hypothetical protein
SO2880							2		glutaredoxin domain protein
SO2881	5	3	4	7	3		3	7	superoxide dismutase, Fe (sodB)
SO2882							2	2	conserved hypothetical protein
SO2885	3						2	4	fatty acid metabolism regulator protein (fadR)
SO2886					2				Na ⁺ /H ⁺ antiporter (nhaB)
SO2889	3	5	3	3			2	2	sensory box histidine kinase
SO2893							2		conserved hypothetical protein
SO2894	3		2	3				2	YaiI/YqxJ family protein
SO2895	3	3	6		2	4			pyridoxamine 5-phosphate oxidase (pdxH)
SO2896	23	16	18	20	19	16	8	15	DNA ligase, NAD-dependent (ligA)
SO2897	16	23	18	17	16	15	13	19	cell division protein ZipA (zipA)
SO2898	2			3	3	4	2	4	SMC family protein
SO2901							2	3	3-oxoacyl-(acyl-carrier-protein) synthase III (fabH-2)
SO2902							2		hypothetical protein
SO2903	37	50	52	58	37	41	52	53	cysteine synthase A (cysK)
SO2907	40	63	34	37	41	48	32	32	TonB-dependent receptor domain protein
SO2912	13	13	33	45	23	13	48	45	formate acetyltransferase (pflB)
SO2915	6	7	9	10	5	3	16	17	acetate kinase (ackA)
SO2916	24	31	32	35	32	25	30	42	phosphate acetyltransferase (pta)
SO2917	2			2	2			2	hypothetical protein
SO2919		2							conserved hypothetical protein
SO2921					2		2		D-erythro-7,8-dihydroneopterin triphosphate epimerase (folX)

Locus	45 min Control		45 min Cr		90 min Control		90 min Cr		Description
	Run 1	Run 2	Run 1	Run 2	Run 1	Run 2	Run 1	Run 2	
SO2923			2		2	2		2	sodium/glutamate symporter (gltS)
SO2926	9	10	6	9	12	8	7	11	ABC transporter, permease, putative
SO2927	3	6	5	4	4	7	3	4	ABC transporter, ATP-binding protein
SO2929	30	31	8	13	36	34	14	12	hypothetical protein
SO2933	14	20	14	13	12	11	7	12	sohB protein, peptidase U7 family
SO2934	3	5	2	4	4	7		4	conserved hypothetical protein
SO2935	5	6	5	8	6	5	5	9	oxidoreductase, short-chain dehydrogenase/reductase family
SO2937	13	15	12	15	16	12	10	12	RNA pseudouridylate synthase family protein
SO2938	6	7	8	9	5	6	8	7	hypothetical protein
SO2939						2			hypothetical protein
SO2942				2					hypothetical protein
SO2945		2			2	3		2	hypothetical protein
SO2951					4	6			hypothetical protein
SO2953					4	2			prophage LambdaSo, tail length tape measure protein (H)
SO2963	4	5		3	8	6	4	7	prophage LambdaSo, major capsid protein, HK97 family
SO2967	2		2				2		conserved hypothetical protein
SO2968		2	2	2		2		2	conserved hypothetical protein
SO2969								2	prophage LambdaSo, holin, putative
SO2988			2		3		3	2	conserved hypothetical protein
SO2990	2	3	2			4			prophage LambdaSo, transcriptional regulator, Cro/CI family
SO2991	4	8	6	4	3	4	6	5	conserved hypothetical protein
SO2992		2	2	3			2	3	hypothetical protein
SO2993			2		3		9	8	prophage LambdaSo, type II DNA modification methyltransferase, putative, truncation
SO3000							3	2	conserved hypothetical protein
SO3002								2	conserved hypothetical protein
SO3004							2	2	prophage LambdaSo, DNA modification methyltransferase, putative
SO3006	2	2					3		prophage LambdaSo, type II DNA modification methyltransferase, putative
SO3008	2								hypothetical protein
SO3013		2	2	2		2	2		site-specific recombinase, phage integrase family
SO3016	4			2		3	2		Sua5/YciO/YrdC/YwIC family protein
SO3017	2	2					3		TrpH family protein

Locus	45 min Control		45 min Cr		90 min Control		90 min Cr		Description
	Run 1	Run 2	Run 1	Run 2	Run 1	Run 2	Run 1	Run 2	
SO3019		2			3				anthranilate synthase component I (trpE)
SO3022			2		2				indole-3-glycerol phosphate synthase/phosphoribosylanthranilate isomerase (trpC/F)
SO3023	4	7	6	6	5	2	6	7	tryptophan synthase, beta subunit (trpB)
SO3024	7	8	6	5	2	8	2	2	tryptophan synthase, alpha subunit (trpA)
SO3025				2			2	2	conserved hypothetical protein
SO3030	10	8	28	28	3		33	36	siderophore biosynthesis protein (alcA)
SO3031			3	3				2	siderophore biosynthesis protein, putative
SO3032	5	5	12	16	3		19	17	siderophore biosynthesis protein, putative
SO3033	23	19	44	43	4	2	54	52	ferric alcaligin siderophore receptor
SO3034							2	3	ferric iron reductase protein, putative
SO3036	2	2	2		2	2	2		conserved hypothetical protein
SO3037	8	13	6	5	7	9	8	5	exodeoxyribonuclease III (xth)
SO3043							2		hypothetical protein
SO3044	15	22	15	15	16	18	15	15	ISSo4, transposase
SO3048		2					2		isoquinoline 1-oxidoreductase, beta subunit, putative
SO3049						2			isoquinoline 1-oxidoreductase, alpha subunit, putative
SO3052	8	7	10	10	9	6	17	13	methyl-accepting chemotaxis protein
SO3054					3	2			metallo-beta-lactamase family protein
SO3055							2	2	proline iminopeptidase (pip)
SO3057					2		3	2	Pal/histidase family protein
SO3061	6	2	5	8	3	2	11	13	DNA topoisomerase III (topB)
SO3063				2				3	sodium:alanine symporter family protein
SO3064	23	28	22	29	28	18	23	26	amidophosphoribosyltransferase (purF)
SO3066	10	25	15	18	13	23	14	22	conserved hypothetical protein
SO3067		2	2	4	3			4	FolC bifunctional protein (folC)
SO3068	2	2				2			tRNA pseudouridine synthase A (truA)
SO3069	14	18	18	21	14	17	16	24	conserved hypothetical protein
SO3070	18	18	15	19	18	14	17	17	aspartate semialdehyde dehydrogenase (asd)
SO3071	2	2							erythronate-4-phosphate dehydrogenase (pdxB)
SO3072	21	31	30	27	25	19	25	21	3-oxoacyl-(acyl-carrier-protein) synthase I (fabB)
SO3073	2	2							conserved hypothetical protein
SO3077	3	5	3	5	2				conserved hypothetical protein

Locus	45 min Control		45 min Cr		90 min Control		90 min Cr		Description
	Run 1	Run 2	Run 1	Run 2	Run 1	Run 2	Run 1	Run 2	
SO3080	2							2	hemK family protein
SO3081								2	Smr domain protein
SO3083							2		peptidase, M16 family
SO3084	2	3	5	4	4	4	4	6	sensory box protein
SO3088	14	17	23	11	15	6	21	23	fatty oxidation complex, alpha subunit
SO3089	9	12	10	11	11	5	11	13	fatty oxidation complex, beta subunit
SO3090	14	14	8	17	13	13	12	17	MoxR domain protein
SO3091	5		2		3				conserved hypothetical protein
SO3092	6	9	5	9	10	12	8	8	hypothetical protein
SO3093	3	3	3	4		2	3	8	von Willebrand factor type A domain protein
SO3094	6	11	5	4	8	10	7	12	TPR domain protein
SO3095	6	15	16	14	17	6	16	11	conserved hypothetical protein
SO3096	5	5	7	4	7	3	2	6	RNA polymerase sigma-70 factor, ECF subfamily
SO3097	4	4	4	2	4		5	2	conserved hypothetical protein
SO3099	17	21	16	22	14	19	23	26	long-chain fatty acid transport protein, putative
SO3101	14	21	17	14	19	18	17	19	conserved hypothetical protein
SO3102	3							2	AcrA/AcrE family protein
SO3103	6	11	7	9	16	12	15	11	AcrB/AcrD/AcrF family protein
SO3105	2	3	4	2		3		2	phage shock protein E (pspE-1)
SO3108		4	6	7	5		4	9	siroheme synthase, N-terminal component, putative
SO3110	11	10	11	12	12	11	9	7	protein-export membrane protein SecF (secF-2)
SO3111	38	52	45	52	39	37	44	45	protein-export membrane protein SecD (secD-2)
SO3112	4	6	6	9	2	4	5	7	preprotein translocase, YajC subunit (yajC)
SO3113	17	23	19	21	13	17	16	21	queuine tRNA-ribosyltransferase (tgt)
SO3114	5	9	4	6	6	2	4	5	S-adenosylmethionine:tRNA ribosyltransferase-isomerase (queA)
SO3116			2		2				conserved hypothetical protein
SO3118	5	4	4	2	3	2	2	6	ribosomal large subunit pseudouridine synthase A (rluA-1)
SO3120		4	6	7	6	2	8	7	oxidoreductase, Gfo/Idh/MocA family
SO3122	3	3	4	3	4		2		sodium/dicarboxylate symporter
SO3124			3	4	2			4	tyrosine-specific protein phosphatase, putative
SO3125	9	12	3	7	4	3	7	6	ATP-dependent RNA helicase, DEAD box family
SO3126					2				methylated-DNA--protein-cysteine methyltransferase (ogt)

Locus	45 min Control		45 min Cr		90 min Control		90 min Cr		Description
	Run 1	Run 2	Run 1	Run 2	Run 1	Run 2	Run 1	Run 2	
SO3127							2		Ada regulatory protein, putative
SO3128	8	9	10	6	7	7	9	6	ABC transporter, ATP-binding/permease protein, putative
SO3133			2						hypothetical protein
SO3134	2								C4-dicarboxylate-binding periplasmic protein (dctP)
SO3138			2	3	3			3	C4-dicarboxylate transport transcriptional regulatory protein (dctD)
SO3140	3		2						thymidine kinase
SO3142	43	45	43	54	46	41	51	52	peptidyl-dipeptidase Dcp (dcp-1)
SO3144	8	9	8	5	9	6	6	7	electron transfer flavoprotein, alpha subunit (etfA)
SO3145	12	9	10	9	7	12	11	9	electron transfer flavoprotein, beta subunit (etfB)
SO3146	28	37	33	33	32	36	34	36	DNA-binding protein, H-NS family
SO3148		2							conserved hypothetical protein
SO3149		3		3					conserved hypothetical protein
SO3150	3	7	8	8	4	7	4	7	lipoprotein, putative
SO3154	22	32	21	29	29	11	27	38	prolyl-tRNA synthetase (proS)
SO3155	2	2	4			4		3	conserved hypothetical protein
SO3157	5	5	4	6	5	5	3	5	lipoprotein, putative
SO3158	8	9	7	6	5	9	6	4	polysaccharide synthesis-related protein
SO3159	14	20	19	13	15	10	10	17	conserved hypothetical protein
SO3163	2	2	3		5	5	4	4	lipoprotein
SO3166				2					conserved hypothetical protein
SO3168	2	2	4	4	5	2	7	5	DnaJ domain protein
SO3171	14	19	13	11	13	10	7	11	polysaccharide biosynthesis protein
SO3172	8	14	12	12	13	12	13	13	galactosyl transferase
SO3173	6	3	6	6	6	5	6	7	UDP-galactose 4-epimerase, putative
SO3174	13	6	12	11	11	10	12	16	glycosyl transferase, group 1 family protein
SO3175	18	23	17	23	20	15	19	18	asparagine synthetase, glutamine-hydrolyzing (asnB-2)
SO3176	3	7			2	6			glycosyl transferase, group 1 family protein
SO3177	12	11	10	7	9	12	5	4	formyl transferase domain protein
SO3178	18	23	21	18	18	17	22	19	hypothetical protein
SO3180	4	5	3	2	5	2	3	3	glycosyl transferase, group 2 family protein
SO3182	2					2		2	acetyltransferase, GNAT family
SO3183	3	3	5	4	4	3		5	perosamine synthetase-related protein

Locus	45 min Control		45 min Cr		90 min Control		90 min Cr		Description
	Run 1	Run 2	Run 1	Run 2	Run 1	Run 2	Run 1	Run 2	
SO3184	5	2		4	6		7	7	conserved hypothetical protein
SO3185	5	7	6	8	10	3	5	6	polysaccharide biosynthesis protein
SO3186	6	9	6	8	11	4	9	9	glucose-1-phosphate-thymidyltransferase (rfbA)
SO3188	5	7	7	9	9	3	8	11	dTDP-glucose 4,6-dehydratase (rfbB)
SO3189	9	11	8	9	6	5	7	10	polysaccharide biosynthesis protein
SO3190	22	34	33	28	28	20	26	33	polysaccharide biosynthesis protein
SO3191	9	15	7	14	15	13	11	13	chain length determinant protein
SO3193	53	73	62	54	49	59	63	56	polysaccharide biosynthesis protein
SO3194	3	5	5	5	4	5	5	2	transcriptional activator rfaH, putative
SO3197	10	11	9	9	9	8	9	9	vacJ lipoprotein, putative
SO3198	3	4	3		5	2	2		hypothetical protein
SO3200		2	3	5			2	3	conserved hypothetical protein
SO3202	2			2	4	2	5	4	purine-binding chemotaxis protein CheW (cheW-3)
SO3203	2				3				CheW domain protein
SO3204	9	7	6	3	3	4	7	6	ParA family protein
SO3205	2	2	5	5	2	3	4	3	hypothetical protein
SO3206	4	10	4	8		7	2	3	protein-glutamate methylesterase CheB (cheB-3)
SO3207	20	27	22	20	22	20	21	30	chemotaxis protein
SO3208	3	3	5	5	4	2	7	4	chemotaxis protein CheZ (cheZ)
SO3209	2	5		5	3	4	10	8	chemotaxis protein CheY (cheY-3)
SO3210	4	4	3	4	3		3	6	RNA polymerase sigma-27 factor (fliA)
SO3211	8	10	6	9	10	9	8	6	flagellar biosynthetic protein FlhG (flhG)
SO3212	8	13	17	19	8	13	9	17	flagellar biosynthetic protein FlhF (flhF)
SO3213	3		2	2	6	2	4	3	flagellar biosynthesis protein FlhA (flhA)
SO3215		2						3	flagellar biosynthetic protein FlhB (flhB)
SO3219				3			2		flagellar protein FliO (fliO)
SO3220				2				2	flagellar motor switch protein FliN (fliN)
SO3221	2			2	2		2	2	flagellar motor switch protein FliM (fliM)
SO3222	3	4	4	2	3	12	4	6	flagellar protein FliL (fliL)
SO3223			5				4		flagellar hook-length control protein FliK (fliK)
SO3224								2	flagellar protein FliJ (fliJ)
SO3225				3				2	flagellum-specific ATP synthase FliI (fliI)

Locus	45 min Control		45 min Cr		90 min Control		90 min Cr		Description
	Run 1	Run 2	Run 1	Run 2	Run 1	Run 2	Run 1	Run 2	
SO3226		5	2	4	4	4		6	flagellar assembly protein FliH (fliH)
SO3227	9	13	12	10	9	4	14	12	flagellar motor switch protein FliG (fliG)
SO3228	9	11	12	13	8	14	9	5	flagellar M-ring protein FliF (fliF)
SO3230		4			4	3		2	flagellar regulatory protein C (flrC)
SO3231	2	3	2	6	5	7	5	8	flagellar regulatory protein B (flrB)
SO3232	5	8	5	10	8	7	8	11	flagellar regulatory protein A (flrA)
SO3233	6	9	9	8	5	6	8	8	flagellar protein FliS (fliS)
SO3235	4	2	5	5	2	2		7	flagellar hook-associated protein FliD (fliD)
SO3237	24	21	23	23	21	16	18	18	flagellin
SO3238	22	20	20	22	22	15	18	18	flagellin
SO3239	4	2		3	3	2			flagellar hook-associated protein FlgL (flgL)
SO3241				2					flagellar protein FlgJ (flgJ)
SO3242	3	6	3	4	3		2	4	flagellar P-ring protein FlgI (flgI)
SO3243	3	5	10	5			5	5	flagellar L-ring protein FlgH (flgH)
SO3244	2	2						4	flagellar basal-body rod protein FlgG (flgG)
SO3245				3					flagellar basal-body rod protein FlgF (flgF)
SO3247	8	12	8	8	6	7	5	3	flagellar hook protein FlgE (flgE)
SO3248		3		2	2				basal-body rod modification protein FlgD (flgD)
SO3251	6	5	5	3	3	3	2	7	chemotaxis protein methyltransferase CheR (cheR-2)
SO3252						2			chemotaxis protein CheV (cheV-3)
SO3254			4	4		4	2		negative regulator of flagellin synthesis FlgM (flgM)
SO3255			2	4			2	2	flagellar biosynthetic protein FlgN (flgN)
SO3256	3	3	2			2	2	2	conserved hypothetical protein
SO3257	2		2	3	4		2		conserved hypothetical protein
SO3259			2		3	3		2	conserved domain protein
SO3261	2								polysaccharide biosynthesis related-protein
SO3262	4	6	9	4	9	2	4	6	acetolactate synthase isozyme I, large subunit (ilvB)
SO3263					3			2	3-oxoacyl-(acyl-carrier-protein) reductase, putative
SO3264								2	hypothetical protein
SO3265	5	6	7	6	3			4	conserved hypothetical protein
SO3266			3	2			2	3	conserved domain protein

Locus	45 min Control		45 min Cr		90 min Control		90 min Cr		Description
	Run 1	Run 2	Run 1	Run 2	Run 1	Run 2	Run 1	Run 2	
SO3267	5	2	4		5		3	2	conserved domain protein
SO3268				2					alpha amylase domain protein
SO3271	10	11	9	6	13	9	7	8	polysaccharide biosynthesis protein
SO3273							2		conserved hypothetical protein
SO3275		3	2	2	2		2	2	hypothetical protein
SO3279					2			2	AcrB/AcrD/AcrF family protein
SO3282	8	12	3	6	18	20	6	11	methyl-accepting chemotaxis protein
SO3285		2			3				cytochrome d ubiquinol oxidase, subunit II (cydB)
SO3286	19	19	16	19	26	21	14	17	cytochrome d ubiquinol oxidase, subunit I (cydA)
SO3287	42	57	38	47	52	26	33	49	phosphoribosylformylglycinamide synthase (purL)
SO3288	2	3	2		4	3	6	2	transglycosylase, Slt family
SO3291	2								cytidine/deoxycytidylate deaminase family protein
SO3292	11	17	16	13	19	4	16	16	GMP synthase (guaA)
SO3293	51	62	50	49	48	55	47	47	inosine-5-monophosphate dehydrogenase (guaB)
SO3294	3		3		2				exodeoxyribonuclease VII, large subunit (xseA)
SO3297		2			2	2			transcriptional regulator, LysR family
SO3298								2	conserved hypothetical protein
SO3299	2	5	5	8	6	3	3	8	Pal/histidase family protein
SO3306							2		sensor histidine kinase
SO3308	19	23	17	14	20	14	14	18	GTP-binding protein EngA (engA)
SO3309	14	13	11	14	13	12	12	13	PQQ enzyme repeat domain protein
SO3310	33	42	32	37	35	35	33	36	conserved hypothetical protein
SO3311	11	12	12	11	16	11	4	16	histidyl-tRNA synthetase (hisS)
SO3312	9	7	4	7	5	6	7	9	1-hydroxy-2-methyl-2-(E)-butenyl 4-diphosphate synthase (ispG)
SO3313	13	12	11	11	12	11	13	14	conserved hypothetical protein
SO3314	13	7	11	11	8	5	8	10	fimbrial biogenesis and twitching motility protein, putative
SO3315	4	4	3	3	5		3	5	conserved hypothetical protein TIGR00048
SO3316	13	20	16	21	14	11	11	13	conserved hypothetical protein
SO3317	2	2	2	5	3		4	5	5-nucleotidase, putative
SO3325	3	2	2	4	5	5	2	4	nrfJ-related protein
SO3335				2		2		2	conserved hypothetical protein
SO3338	7	2	6	6	4	7	2	7	L-allo-threonine aldolase (ybjU)

Locus	45 min Control		45 min Cr		90 min Control		90 min Cr		Description
	Run 1	Run 2	Run 1	Run 2	Run 1	Run 2	Run 1	Run 2	
SO3339		2	3	5					OmpA family protein
SO3340	5	6	7	5	10		8	11	conserved hypothetical protein
SO3341	9	12	13	17	9	5	8	10	antioxidant, AhpC/TSA family
SO3343	17	19	19	21	17	10	15	15	conserved hypothetical protein
SO3345	3	4	6	4	2	4	3	4	translation initiation factor, putative
SO3346		2	3	2	3		4	6	conserved hypothetical protein
SO3347	2	3	3	2					conserved hypothetical protein TIGR00250
SO3348	8	9	7	6	4	4	9	7	ferrochelatase (hemH-2)
SO3349			2					2	glutathione peroxidase, putative
SO3350		3			6		4	3	twitching motility protein PilU (pilU)
SO3351	15	7	9	6	11	3	18	14	twitching motility protein PilT (pilT)
SO3352	3	2		2		2	2		conserved hypothetical protein TIGR00044
SO3354	8	5	5	7	3	5	3	3	pyrroline-5-carboxylate reductase (proC)
SO3355							2		conserved hypothetical protein
SO3358	5	3	2	3		2		4	HAM1 protein
SO3360	4	3	3		2	4	3	2	ISSo5, transposase
SO3361	9	9	11	11	6	7		4	conserved hypothetical protein
SO3363	4	2	3	5	5	2	4	4	transcriptional regulator, LysR family
SO3364					2				conserved hypothetical protein
SO3365					2		3		glutaminase A (glsA)
SO3367	7	9	7	9	4	4	9	12	conserved hypothetical protein TIGR00091
SO3368	2	5	2	3	3		4	3	A/G-specific adenine glycosylase (mutY)
SO3369	5	7	7	8	6	4	5	9	conserved hypothetical protein
SO3370	2	4	4	6			4	5	conserved hypothetical protein
SO3374	2	2		2	3	3	3	3	conserved hypothetical protein
SO3379			3	5				2	cyclopropane-fatty-acyl-phospholipid synthase (cfa)
SO3380			2					2	conserved hypothetical protein
SO3381					2	2	2	2	conserved hypothetical protein
SO3384			3	2	2		2		deoxyribodipyrimidine photolyase (phrB)
SO3388	5	7	4	5	7	2	5	6	ATP-dependent RNA helicase, DEAD box family
SO3389				2					sensory box protein
SO3391	7	10	5	7	7	5	7	7	ATP-dependent protease, putative

Locus	45 min Control		45 min Cr		90 min Control		90 min Cr		Description
	Run 1	Run 2	Run 1	Run 2	Run 1	Run 2	Run 1	Run 2	
SO3392	2	4	3	3	3		4	6	oxidoreductase, FMN-binding
SO3396	4	4	3	6	5	4	4	5	methyl-accepting chemotaxis protein, truncation
SO3399	15	22	15	15	16	18	15	15	ISSo4, transposase
SO3401	10	6	7	11	7	8	4	4	conserved hypothetical protein TIGR01033
SO3403	4	8	11	10	10	10	12	14	ribosomal subunit interface protein (yfiA-1)
SO3404	3	3	3	2	3	5	2	3	methyl-accepting chemotaxis protein
SO3407	5	8	8	10	4	3	13	14	conserved hypothetical protein
SO3409	2	4	2		3	3	4	3	OsmC/Ohr family protein
SO3411	26	21	18	23	19	22	20	25	protease, putative
SO3413	3		2						threonine synthase (thrC)
									aspartokinase I/homoserine dehydrogenase, threonine-sensitive (thrA)
SO3415			2	3	2			5	
SO3417	6	6	7	5	5	6	8	5	peptidyl-prolyl cis-trans isomerase SlyD (slyD)
SO3420	11	16	19	21	13	10	15	17	cytochrome c
SO3422	4	4	8	5	5	4	5	5	ribosomal subunit interface protein (yfiA-2)
SO3424	23	32	24	34	27	17	27	40	valyl-tRNA synthetase (valS)
SO3426	4	3	3	5	4	4	6	3	carbon storage regulator (csrA)
SO3427	3	2			3	3	2		aspartokinase
SO3428	48	41	34	43	42	36	33	41	alanyl-tRNA synthetase (alaS)
SO3430	40	41	47	47	38	42	51	52	recA protein (recA)
SO3431	13	11	12	14	20	7	12	13	DNA mismatch repair protein MutS (mutS)
SO3432					3				RNA polymerase sigma-38 factor (rpoS)
SO3433	2	2	4		5	7	6	5	lipoprotein NlpD (nlpD)
SO3434	3	3		2	2			2	protein-L-isoaspartate O-methyltransferase (pcm)
SO3435	2								stationary-phase survival protein SurE (surE)
SO3436	7	5	5	7	6	4	11	9	conserved hypothetical protein
SO3437		2					3		2C-methyl-D-erythritol 2,4-cyclodiphosphate synthase (ispF)
SO3438	2	7	5	5	5	2	8	7	4-diphosphocytidyl-2C-methyl-D-erythritol synthase (ispD)
SO3439	2	3	2	2	3		2	4	conserved hypothetical protein
SO3440	24	29	36	37	22	29	34	32	enolase (eno)
SO3441	37	43	29	35	33	23	26	34	CTP synthase (pyrG)
SO3442	3		2	6		3	4	2	MazG family protein
SO3443	15	22	15	15	16	18	15	15	ISSo4, transposase

Locus	45 min Control		45 min Cr		90 min Control		90 min Cr		Description
	Run 1	Run 2	Run 1	Run 2	Run 1	Run 2	Run 1	Run 2	
SO3444							2		hypothetical protein
SO3449	2	6	2	4	4		2	4	conserved domain protein
SO3451	15	22	15	15	16	18	15	15	ISSo4, transposase
SO3455	16	15	21	19	28	20	21	26	GTP pyrophosphokinase (relA)
SO3456	9	11	3	5	7	4	2	6	RNA methyltransferase, TrmA family
SO3457	6	6	5	5	7	7	5	8	sensor histidine kinase/response regulator
SO3458					3		2	2	conserved hypothetical protein
SO3462	4		6	12			2	12	DNA repair protein RecN (recN)
SO3463	2								phosphatidylglycerophosphatase A (pgpA)
SO3464	2	3	2	4			2	7	thiamin-monophosphate kinase (thiL)
SO3465	3	8	8	8	7	7	9	9	N utilization substance protein B (nusB)
SO3466	19	23	18	18	21	22	19	20	riboflavin synthase, beta subunit (ribH)
SO3467	19	20	14	19	19	15	15	12	3,4-dihydroxy-2-butanone 4-phosphate synthase/GTP cyclohydrolase II, putative (ribBA)
SO3468		2	3	2	5	3	3	3	riboflavin synthase, alpha subunit (ribE-2)
SO3469	2	4	2	2	2			4	riboflavin biosynthesis protein RibD (ribD)
SO3470	4	4	6	7	2			4	conserved hypothetical protein TIGR00244
SO3471	26	32	31	28	29	20	22	28	serine hydroxymethyltransferase (glyA)
SO3472	41	32	39	46	30	32	31	33	ABC transporter, ATP-binding protein
SO3480				2					conserved hypothetical protein
SO3483	13	9	13	17	8	9	7	13	HlyD family secretion protein
SO3484	10	11	12	6	9	8	8	9	AcrB/AcrD/AcrF family protein
SO3494	2	5	4	2				2	transcriptional regulator, TetR family
SO3496		3		4	4	2	3	2	aldehyde dehydrogenase
SO3506			2	4			2	2	SIS domain protein
SO3509	11	14	14	13	18	12	16	18	beta-hexosaminidase b precursor (hex)
SO3516	6	2	4	4	4	4		4	transcriptional regulator, LacI family
SO3517	13	12	12	9	12	14	9	8	NADH dehydrogenase (ndh)
SO3518		3	2	2			2		ISSo4, transposase
SO3519	6			4			3	4	nitrogen regulatory protein P-II 1 (glnB-2)
SO3521			2	2	2		2		type IV pilus biogenesis protein, putative
SO3524	2			4			2	2	type IV pilus biogenesis protein PilE (pilE)
SO3529	9	10	7	9	5	3	7	10	penicillin tolerance protein LytB (lytB)

Locus	45 min Control		45 min Cr		90 min Control		90 min Cr		Description
	Run 1	Run 2	Run 1	Run 2	Run 1	Run 2	Run 1	Run 2	
SO3532	17	27	23	29	27	13	24	35	isoleucyl-tRNA synthetase (ileS)
SO3533				2	3		4		riboflavin biosynthesis protein RibF (ribF)
SO3537	7	6	7	8	6	7	6	6	ribosomal protein S20 (rpsT)
SO3538	5	3			6	3			transcriptional regulator HlyU (hlyU)
SO3539	23	30	25	24	28	23	25	26	peptidase, M28D family
SO3540	2		2						conserved hypothetical protein
SO3541	4	2	3	3	3	2	3	3	sodium:alanine symporter family protein
SO3542	2	5		2	6				conserved hypothetical protein
SO3543								2	ISSo13, transposase
SO3544			2	3				3	ISSo7, transposase
SO3545	48	56	50	52	51	48	59	59	OmpA family protein
SO3546	11	11	10	9	10	9	7	7	transaldolase (tal)
SO3547	10	7	6	6	6	6	2	5	glucose-6-phosphate isomerase (pgi)
SO3550	2	4	3	3	3		7	8	hypothetical protein
SO3551			2		2			3	RNA polymerase sigma-70 factor, ECF subfamily
SO3552								2	von Willebrand factor type A domain protein
SO3553	2	4	3		5	2			sulfate permease family protein
SO3554	9	13	6	6	6	4	6	6	phosphoribosylaminoimidazole carboxylase, catalytic subunit (purE)
SO3555	3	5	3	6	3	2	2		phosphoribosylaminoimidazole carboxylase, ATPase subunit (purK)
SO3556	4	5	2	3	8	6	6	3	GAF/GGDEF domain protein
SO3557			2	7	4	2	4	3	conserved hypothetical protein
SO3558			2					2	hypothetical protein
SO3559	5	6	3	6	4			3	glutamate--cysteine ligase (gshA)
SO3560	62	66	63	58	74	56	61	59	peptidase, M16 family
SO3562	2	5	5	4	2	3	2	3	proton/glutamate symporter, putative
SO3564	54	64	46	54	58	57	46	57	peptidyl-dipeptidase Dcp (dcp-2)
SO3565	34	47	29	31	44	44	22	21	2,3-cyclic-nucleotide 2-phosphodiesterase (cpdB)
SO3571	4	5	4	3		3	3	3	conserved hypothetical protein
SO3575		3			2	2	2	2	CDP-diacylglycerol--serine O-phosphatidyltransferase, putative
SO3577	30	37	55	71	39	41	66	67	clpB protein (clpB)
SO3578							3	2	conserved hypothetical protein TIGR00726
SO3579	4	7	5	4	3	4	3	6	ribosomal large subunit pseudouridine synthase D (rluD)

Locus	45 min Control		45 min Cr		90 min Control		90 min Cr		Description
	Run 1	Run 2	Run 1	Run 2	Run 1	Run 2	Run 1	Run 2	
SO3580	14	21	13	16	12	15	12	12	conserved hypothetical protein
SO3582	8	12	8	7	8	11	9	12	methyl-accepting chemotaxis protein
SO3584		2		2				5	conserved hypothetical protein
SO3585			10	9			5	4	Azoreductase, putative
SO3586			5	6			8	3	glyoxalase family protein
SO3587		2	5	7	3	2	4	3	hypothetical protein
SO3594	2	5	7	6	6	2	6	7	transcriptional regulatory protein RstA, putative
SO3595	2	3	5	3	4	5	3	4	sensor protein RstB, putative
SO3597	4	10	8	7	5	6	7	8	conserved hypothetical protein
SO3598	6	6	4	5	3		6	6	cysteine synthase B (cysM)
SO3599	11	20	28	32	2	5	23	23	sulfate ABC transporter, periplasmic sulfate-binding protein (cysP)
SO3602	11	25	21	14	11	13	17	23	sulfate ABC transporter, ATP-binding protein (cysA-1)
SO3611		2						2	ATPase, AAA family
SO3613	2	3	3		3	4			phosphoribosylglycinamide formyltransferase 2 (purT)
SO3614								2	hypothetical protein
SO3615	16	22	12	14	19	15	12	15	hypothetical protein
SO3622	3	2	5	8		3	2	5	conserved domain protein
SO3631	3	4	3	4	2	3	6		glycerate dehydrogenase (hprA)
SO3633	7	6	4	4	7	3	6	8	DnaJ domain protein
SO3636	10	16	8	12	9	8	13	15	organic solvent tolerance protein (imp)
SO3637	19	17	17	22	17	13	20	19	survival protein surA (surA)
SO3638			2	2	3	2		3	pyridoxal phosphate biosynthetic protein PdxA (pdxA)
SO3639	3	4	2	4	6	2	2	6	dimethyladenosine transferase (ksgA)
SO3642	20	36	21	25	27	31	23	25	methyl-accepting chemotaxis protein
SO3646	3	4		2	2		2	2	dihydrofolate reductase (folA)
SO3649	14	13	16	11	16	10	12	17	GTP-binding protein, GTP1/Obg family
SO3651	8	10	11	11	7	9	11	11	ribosomal protein L27 (rpmA)
SO3652	16	18	13	14	16	17	14	17	ribosomal protein L21 (rplU)
SO3653	3	8	4	8	4	2		5	octaprenyl-diphosphate synthase (ispB)
SO3654		2						2	uracil-DNA glycosylase (ung)
SO3655		2		2		2			pilin, putative
SO3656	3	2	2	3	4	3			hypothetical protein

Locus	45 min Control		45 min Cr		90 min Control		90 min Cr		Description
	Run 1	Run 2	Run 1	Run 2	Run 1	Run 2	Run 1	Run 2	
SO3664	13	13	6	10	7	4	4	6	long-chain-fatty-acid--CoA ligase (fadD-2)
SO3665	4	3	5	4	2	4	5	6	ABC transporter, ATP-binding/permease protein, putative
SO3667	4	10	30	27			29	31	conserved hypothetical protein
SO3668			5	6				3	conserved hypothetical protein
SO3669	14	14	53	64	3	5	67	71	heme transport protein (hugA)
SO3670			3	4			3	4	TonB1 protein (tonB1)
SO3671	3	4	5	4			6	7	TonB system transport protein ExbB1 (exbB1)
SO3673	2	6	22	22			16	17	hemin ABC transporter, periplasmic hemin-binding protein (hmuT)
SO3675	4	3	13	9			12	9	hemin ABC transporter, ATP-binding protein (hmuV)
SO3676		3	2	4	3		2	4	hypothetical protein
SO3678	2	3			2	3			conserved hypothetical protein
SO3680	2	2	2			2	3		universal stress protein family
SO3681	3	5	5	6	6	5	8	7	universal stress protein family
SO3683	13	15	17	14	13	13	19	10	coniferyl aldehyde dehydrogenase
SO3689			2					2	sigma-54 dependent nitrogen response regulator
SO3692			2	2				3	ABC transporter, ATP-binding protein
SO3695	7	12	7	6	8	8	9	6	dihydroorotase, homodimeric type (pyrC)
SO3696		2	2						hypothetical protein
SO3698								3	hypothetical protein
SO3705	3	2	4	4	3		7	4	5-methylthioadenosine nucleosidase/S-adenosylhomocysteine nucleosidase, putative
SO3711					3				conserved hypothetical protein
SO3714				2					sugar-binding protein, putative
SO3715	8	8	14	12	9	5	11	13	oxygen-insensitive NAD(P)H nitroreductase
SO3718	7	9	8	7	9	8	5	10	thiol:disulfide interchange protein, DsbA family
SO3720	6	5	6	4	12	7	6	4	conserved hypothetical protein
SO3722	3	5			5	4		2	conserved hypothetical protein
SO3723				3			5	4	adenylylsulfate kinase (cysC)
SO3726	5	11	17	19	7	2	17	23	sulfate adenylyltransferase, subunit 1 (cysN)
SO3727	14	15	24	23	10	5	28	32	sulfate adenylyltransferase, subunit 2 (cysD)
SO3728				2			4	4	uroporphyrin-III C-methyltransferase (cobA)
SO3731						2			hypothetical protein
SO3733	28	34	30	30	38	24	37	30	hypothetical protein

Locus	45 min Control		45 min Cr		90 min Control		90 min Cr		Description
	Run 1	Run 2	Run 1	Run 2	Run 1	Run 2	Run 1	Run 2	
SO3735	2			2				2	monofunctional biosynthetic peptidoglycan transglycosylase (mtgA)
SO3736	4	3	4	4	2		5	5	phosphoadenosine phosphosulfate reductase (cysH) sulfite reductase (NADPH) hemoprotein beta-component (cysI)
SO3737	19	17	35	39	13	8	41	57	(cysI)
SO3738	2	5	11	9	2		13	15	sulfite reductase (NADPH) flavoprotein alpha-component (cysJ)
SO3740	35	35	33	36	39	34	43	43	NAD(P) transhydrogenase, alpha subunit (pntA)
SO3741	13	15	14	14	16	8	16	15	NAD(P) transhydrogenase, beta subunit (pntB)
SO3743	4	8	7	6	5	3	4	7	transcriptional regulator, TetR family
SO3745	7	9	4	6	7	4	4	8	ADP-heptose synthase (rfaE)
SO3746	9	15	12	11	12	9	13	17	lipid A biosynthesis lauroyl acyltransferase (htrB)
SO3747	2	3		3			2	3	sodium/hydrogen exchanger family/TrkA domain protein
SO3748	22	27	21	19	19	23	21	21	LysM domain protein
SO3749		2	3	3	2		2	2	hypothetical protein
SO3757								2	rubisco operon transcriptional regulator (rbcR)
SO3760	3	3	2						glutamate-ammonia-ligase adenyltransferase (glnE)
SO3761	2	14	9	8	9	11	8	12	hypothetical protein
SO3763	6	4	3	2	4	3	3	5	spermine/spermidine synthase family protein
SO3765	32	40	37	45	37	41	43	49	conserved hypothetical protein
SO3767			2		2				hypothetical protein
SO3768			2	2			2		ion transporter
SO3769								2	conserved hypothetical protein
SO3770	17	15	14	15	11	8	10	16	conserved hypothetical protein TIGR00153
SO3772	16	26	19	23	18	20	21	21	conserved hypothetical protein proline dehydrogenase/delta-1-pyrroline-5-carboxylate
SO3774	71	75	40	57	65	62	47	46	dehydrogenase, putative
SO3775	5		3	3	5	5	5	9	hypothetical protein
SO3776		2				2		2	conserved hypothetical protein
SO3777								2	hypothetical protein
SO3778							2		adenylate cyclase CyaB, putative
SO3779	3	2	2	4	8	3	6	6	ABC transporter, ATP-binding protein CydC (cydC)
SO3780	4	8	4		7	7		3	ABC transporter, ATP-binding protein CydD (cydD)
SO3781	4	5	7	5	5	5	5	4	hypothetical protein
SO3783	9	11	2	5	5	6		2	ATP-dependent RNA helicase, DEAD box family

Locus	45 min Control		45 min Cr		90 min Control		90 min Cr		Description
	Run 1	Run 2	Run 1	Run 2	Run 1	Run 2	Run 1	Run 2	
SO3786	2	3	4	5	3	2	4	7	hypothetical protein
SO3787	3	3	4	5		3	4	4	hypothetical protein
SO3789		2	2				2		aminotransferase, class V
SO3790				2	3		4		conserved hypothetical protein
SO3791			2				2	3	renal dipeptidase family protein
SO3796					3				conserved hypothetical protein
SO3797	9	8	3	8	4	6	5	4	peptidase, U32 family
SO3798		3	2	2	2		2		ribosomal large subunit pseudouridine synthase A (rluA-2)
SO3799	4	4	4	3	5		2	5	regulatory protein AsnC (asnC)
SO3800	7	5	3		6	5			serine protease, subtilase family
SO3802	8	9	13	18	10	7	13	12	ABC transporter, ATP-binding protein
SO3803	5	9	5	10	9	3	8	10	hypoxanthine phosphoribosyltransferase (hpt-2)
SO3804			3	3	2		4	2	phenylacrylic acid decarboxylase, 3-octaprenyl-4-hydroxybenzoate carboxy-lyase, putative
SO3805	9	12	7	10	6	5	6	10	UDP-N-acetylmuramate:L-alanyl-gamma-D-glutamyl-meso- diaminopimelate ligase (mpl)
SO3810	2						2	3	OmpA-like transmembrane domain protein
SO3811	16	16	14	12	17	10	17	19	lipoprotein, putative
SO3812	4	7	5	5	4	3	3	4	peptidyl-prolyl cis-trans isomerase A (ppiA)
SO3815	9	8	11	11	10	8	5	11	conserved hypothetical protein
SO3817			2						2-dehydropantoate 2-reductase (panE)
SO3821	2	2							rtn protein
SO3827	9	12	10	11	7	9	10	9	2-dehydro-3-deoxyphosphooctonate aldolase (kdsA)
SO3828					2				conserved hypothetical protein
SO3832	3		2	3	3		2	3	hemK family protein
SO3833	8	15	10	12	7	7	11	11	peptide chain release factor 1 (prfA)
SO3834	12	15	8	6	16	14	10	5	glutamyl-tRNA reductase (hemA)
SO3835	6	4	6	5	3	4	5	4	outer membrane lipoprotein LolB (lolB)
SO3836	3	7	7	8	5			4	4-diphosphocytidyl-2C-methyl-D-erythritol kinase (ispE)
SO3837	29	31	26	26	27	29	17	25	ribose-phosphate pyrophosphokinase (prsA)
SO3838	16	15	14	21	17	13	14	18	methyl-accepting chemotaxis protein
SO3841				2					hypothetical protein
SO3842	12	12	11	17	8	8	11	9	conserved hypothetical protein

Locus	45 min Control		45 min Cr		90 min Control		90 min Cr		Description
	Run 1	Run 2	Run 1	Run 2	Run 1	Run 2	Run 1	Run 2	
SO3843		4	3	4				2	ribosomal small subunit pseudouridine synthase A (rsuA-2)
SO3844	89	112	90	81	91	97	80	93	peptidase, M13 family
SO3848	2	4	2			2		2	hypothetical protein
SO3854					2		2	2	ISSo12, transposase
SO3855	21	30	21	23	25	16	24	25	malate oxidoreductase (sfcA)
SO3856	8	12	6	5	6	9	4	6	hypothetical protein
SO3862								2	molybdenum transport regulatory protein ModE (modE)
									molybdenum ABC transporter, periplasmic molybdenum-binding
SO3863	12	14	12	15	10	19	6	9	protein (modA)
SO3865	17	16	9	13	25	17	13	10	molybdenum ABC transporter, ATP-binding protein (modC)
SO3866	2			3		2	2		site-specific recombinase, phage integrase family
SO3867	2							2	transcriptional regulator, Cro/CI family
SO3872							2		arylsulfate sulfotransferase
SO3878	4	3	3		2	4	3	2	ISSo5, transposase
SO3880								2	ISSo13, transposase
SO3888	2								conserved hypothetical protein
SO3890	4	3	5	5	6	3	5	8	methyl-accepting chemotaxis protein
SO3892		2	3		2	2	4		hypothetical protein
SO3895	4	4		4	3	2		3	HesA/MoeB/ThiF family protein
SO3896	50	57	49	49	56	64	55	51	outer membrane porin, putative
SO3897	13	14	7	8	11	10	7	14	DNA topoisomerase IV, A subunit (parC)
SO3899	4	6	4	8	5	2	8	6	DNA topoisomerase IV, B subunit (parE)
SO3901					3				lacZ expression regulator (icc)
SO3904	56	72	63	68	63	63	66	65	outer membrane protein TolC (tolC)
SO3905	2	3			2			3	conserved hypothetical protein
SO3906	9	13	18	17	13	14	18	17	conserved hypothetical protein
SO3907	2	2	5	5			3	6	conserved hypothetical protein
SO3908	2		4		3		2	3	enoyl-CoA hydratase/isomerase family protein
SO3912	2	2	5	7	2			6	TIM-barrel protein, yjbN family
SO3913			5	4			4	4	conserved hypothetical protein
SO3914	33	41	59	60	9	9	67	67	TonB-dependent receptor, putative
SO3917	8	7	4	4	5	5	2	5	replicative DNA helicase (dnaB)
SO3918	26	28	28	25	26	19	23	27	conserved hypothetical protein

Locus	45 min Control		45 min Cr		90 min Control		90 min Cr		Description
	Run 1	Run 2	Run 1	Run 2	Run 1	Run 2	Run 1	Run 2	
SO3920					8	7			periplasmic Fe hydrogenase, large subunit (hydA)
SO3921					3	4			periplasmic Fe hydrogenase, small subunit (hydB)
SO3927	30	33	32	29	28	44	25	26	ribosomal protein L9 (rplI)
SO3928	16	19	16	17	18	17	13	17	ribosomal protein S18 (rpsR)
SO3930	22	24	20	23	19	26	23	22	ribosomal protein S6 (rpsF)
SO3931		2	2		3		6	6	conserved hypothetical protein
SO3934	14	15	8	11	10	11	12	11	RNA methyltransferase, TrmH family, group 3
SO3935	8	15	10	11	13	9	14	21	ribonuclease R (vacB)
SO3936	3		3	4	2				sodium-type flagellar protein MotX (motX)
SO3937	19	17	17	20	21	6	16	14	adenylosuccinate synthetase (purA)
SO3939	10	10	12	13	10	6	9	11	ribosomal protein S9 (rpsI)
SO3940	21	30	25	27	23	26	26	25	ribosomal protein L13 (rplM)
SO3941						2	2		conserved hypothetical protein
SO3942	34	37	43	51	43	40	44	47	serine protease, HtrA/DegQ/DegS family
SO3943	5	13	6	6	9	13	8	10	protease DegS (degS)
SO3948	7	5	8	11	5	7	8	10	UDP-N-acetylglucosamine 1-carboxyvinyltransferase (murA)
SO3949	2	8	4	4	7		3	4	BolA/YrbA family protein
SO3950	7	3	4	4	4	5	6	3	SpoIIAA family protein
SO3951				2	3		2	3	conserved hypothetical protein
SO3952	4	6	4	4	2	2	4	5	mce-related protein
SO3954	17	18	14	14	15	15	15	16	ABC transporter, ATP-binding protein, putative
SO3956	10	9	8	14	6	9	15	7	carbohydrate isomerase, KpsF/GutQ family
SO3957	2	4	2	5	2		2	5	conserved hypothetical protein
SO3958			3	2			2	2	conserved hypothetical protein
SO3959	7	12	9	10	6	11	5	7	conserved hypothetical protein
SO3960	14	23	13	16	19	20	15	19	ABC transporter, ATP-binding protein
SO3961	11	8	7	11	8	8	7	14	RNA polymerase sigma-54 factor (rpoN)
SO3962							2		ribosomal subunit interface protein (yfiA-3)
SO3963	2	5	3	3	2	4	2	3	nitrogen regulatory IIA protein (ptsN)
SO3964		3			2			2	conserved hypothetical protein
SO3965							2		phosphocarrier protein NPR (ptsO)
SO3966	7	8	8	9	5	4	7	11	magnesium transporter (mgtE-2)

Locus	45 min Control		45 min Cr		90 min Control		90 min Cr		Description
	Run 1	Run 2	Run 1	Run 2	Run 1	Run 2	Run 1	Run 2	
SO3967	8	10	7	6	12	14	4	3	molybdenum ABC transporter, periplasmic molybdenum-binding protein, putative
SO3969	11	18	17	19	16	11	15	19	OmpA family protein
SO3973		4	6	4	3	4	5	4	RIO1/ZK632.3/MJ0444 family, putative
SO3974	4					2		2	conserved domain protein
SO3980	18	15	22	24	13	15	8	12	cytochrome c552 nitrite reductase
SO3981					2				nitrate/nitrite sensor protein NarQ (narQ)
SO3982	3		3		4	2			DNA-binding nitrate/nitrite response regulator
SO3984	6	5	3	2	4		2	8	magnesium transporter, putative
SO3988	23	26	27	28	28	27	30	26	aerobic respiration control protein ArcA (arcA)
SO3990	5	6	6	2	8		4	3	dipeptidyl peptidase IV
SO3991	10	14	11	13	11	7	9	11	fructose-1,6-bisphosphatase (fbp)
SO3994	8	7	11	12	7	4	12	12	hypothetical protein
SO4002	2	6	3	5	7	6	7	6	sensory transduction histidine kinase
SO4003	2	3	4	3	5	2	7	7	response regulator
SO4006	3	3	3		3	3	4	4	hypothetical protein
SO4007	2	4	3	2		3	2	2	hypothetical protein
SO4008	39	58	34	51	43	49	37	45	hypothetical protein
SO4011	2		2		3				conserved hypothetical protein
SO4012	2	2	3		3	4	3	2	hypothetical protein
SO4013	8	8	9	9	8	6	8	10	hypothetical protein
SO4014	19	28	17	17	24	22	24	21	AcrB/AcrD/AcrF family protein
SO4015	7	6	9	11	4	8	3	5	conserved hypothetical protein
SO4016	2	3	2	2	3			2	conserved hypothetical protein
SO4017	11	15	16	14	12	15	13	17	transglycosylase, Slt family
SO4018	2		2						hypothetical protein
SO4019			2		5				hypothetical protein
SO4022	3			2	3	3		2	peptidase, M16 family
SO4028	9	12	5	9	8	9	4	4	single-strand binding protein (ssb)
SO4029								2	transporter, putative
SO4030	15	19	22	19	23	7	10	20	excinuclease ABC, A subunit (uvrA)
SO4034	58	55	39	42	48	42	52	48	ATP-dependent RNA helicase DeaD (deaD)
SO4036	2	2	2		5		2	4	hypothetical protein

Locus	45 min Control		45 min Cr		90 min Control		90 min Cr		Description
	Run 1	Run 2	Run 1	Run 2	Run 1	Run 2	Run 1	Run 2	
SO4038	2		2		5		2	3	hypothetical protein
SO4043	2	2		3	3				TonB domain protein
SO4047	4	6	6	5	6	4		2	cytochrome c family protein
SO4048	2	3	3	4	4	3			cytochrome c family protein
SO4052						2			transcriptional regulator, MarR family
SO4053	13	12	4	7	19	11	6	9	methyl-accepting chemotaxis protein
SO4054				2			2	4	5,10-methylenetetrahydrofolate reductase (metF)
SO4055			4	4	3		3	2	aspartokinase II/homoserine dehydrogenase, methionine-sensitive (metL)
SO4057	2	2	3	3	2		4	4	met repressor (metJ)
SO4062			2						polysulfide reductase, subunit A (psrA)
SO4066	21	22	16	15	15	11	10	12	phosphoribosylaminoimidazole-succinocarboxamide synthase, putative
SO4068	9	14	18	16	17	15	14	18	hypothetical protein
SO4070	4	3	6	7	4	5	6	7	conserved hypothetical protein
SO4072	6	11	7	12	8	3	6	6	MiaB-like putative RNA modifying enzyme YliG (yliG)
SO4077	8	7	15	14	5	5	19	21	TonB-dependent receptor, putative
SO4078	6	4	5	4	9			5	pmbA protein (pmbA)
SO4079	4	10	7	15	4	6	6	16	conserved hypothetical protein
SO4080	21	24	19	18	22	21	20	14	conserved hypothetical protein
SO4085		2		2			3		chitinase A (chiA)
SO4089	10	14	14	13	12	11	15	18	HlyD family secretion protein
SO4090	4	2	6	4	2	4	6	5	outer membrane efflux protein
SO4091	6	9	9	6	3	7	6	5	tldD protein (tldD)
SO4093	3	2	2	2	3	5	2	3	conserved hypothetical protein
SO4094	7	4	6	6	5	5	7	5	ribonuclease G (cafA)
SO4095					3				maf protein (maf)
SO4097	10	12	13	12	8	9	9	6	rod shape-determining protein MreC (mreC)
SO4098	18	25	25	28	23	19	27	28	rod shape-determining protein MreB (mreB)
SO4100		2	3	3		2	2		MSHA biogenesis protein MshQ (mshQ)
SO4102			2					2	MSHA biogenesis protein MshO (mshO)
SO4105	21	18	25	22	19	20	23	25	MSHA pilin protein MshA (mshA)
SO4106	6	8	11	11	7	7	9	10	MSHA pilin protein MshB (mshB)

Locus	45 min Control		45 min Cr		90 min Control		90 min Cr		Description
	Run 1	Run 2	Run 1	Run 2	Run 1	Run 2	Run 1	Run 2	
SO4107					2				hypothetical protein
SO4108	4	4	6	7	7	3	6	5	MSHA biogenesis protein MshG (mshG)
SO4109	9	15	8	12	13	7	6	10	MSHA biogenesis protein MshE (mshE)
SO4110	5	11	8	8	11	11	7	9	MSHA biogenesis protein MshN, putative
SO4111	6	3	3	4	3	7		2	MSHA biogenesis protein MshM (mshM)
SO4112	4	4	7	12	9	3	8	6	MSHA biogenesis protein MshL (mshL)
SO4113	3		2		4	2	2		MSHA biogenesis protein MshK (mshK)
SO4114	6	5	5	8	4	4	6	4	MSHA biogenesis protein MshJ (mshJ)
SO4116	2	2			3			2	MSHA biogenesis protein MshH (mshH)
SO4118	13	14	13	12	9	8	9	13	malate oxidoreductase, putative
SO4120	6	6	7	8	4	3	8	11	ribosomal protein L31 (rpmE)
SO4121		2		2	4			3	hypothetical protein
SO4122	3	2		3	2			2	primosomal protein N' (priA)
SO4123	12	13	7	6	9	6	12	4	arginyl-tRNA synthetase (argS)
SO4124	8	3	4	6	11	8	6	4	cell division protein FtsN, putative
SO4128	18	19	21	13	23	14	20	24	SPFH domain/Band 7 family protein
SO4129	24	33	27	29	26	17	28	30	SPFH domain/Band 7 family protein
SO4130		2							conserved hypothetical protein
SO4131	3			2	2				conserved hypothetical protein
SO4133	10	11	13	14	16	12	16	12	uridine phosphorylase (udp)
SO4134		2		2	4	5	9	7	conserved hypothetical protein
SO4135			2	3				3	ISSo7, transposase
SO4138		2		2	2				conserved hypothetical protein
SO4139	15	24	16	19	20	20	20	27	conserved domain protein
SO4140		2	3		3		2		transcriptional regulator, LysR family
SO4141	2	5	3	3	5		5	6	oxidoreductase, short-chain dehydrogenase/reductase family
SO4149	2								RTX toxin, putative
SO4151			2				3	3	polysaccharide deacetylase family protein
SO4154		3							transcriptional regulator, LysR family
SO4155	4				4	4			sensor histidine kinase
SO4157	2				3				DNA-binding response regulator
SO4160				2					flagellar biosynthesis protein, putative

Locus	45 min Control		45 min Cr		90 min Control		90 min Cr		Description
	Run 1	Run 2	Run 1	Run 2	Run 1	Run 2	Run 1	Run 2	
SO4162	5	7	10	9	7	6	9	8	ATP-dependent protease HslV (hslV)
SO4163	42	48	51	59	38	43	54	57	heat shock protein HslVU, ATPase subunit HslU (hslU)
SO4164	2	4	3	4	2		2	4	conserved hypothetical protein
SO4173	4	5	4	5	5	5	3	3	sensor histidine kinase
SO4177	2			2			2	2	hypothetical protein
SO4178	2	4	2	6		5	3	2	conserved hypothetical protein
SO4181	2	4							RNA pseudouridylate synthase family protein
SO4189		2		3			3		conserved hypothetical protein
SO4190	16	15	10	13	11	6	12	10	inorganic pyrophosphatase, manganese-dependent (ppaC)
SO4193	5	5	3	5	4	4	6	6	conserved hypothetical protein
SO4199	17	20	15	22	21	20	15	23	ubiquinone/menaquinone biosynthesis methytransferase UbiE (ubiE)
SO4200	3	2	2		4	3			conserved hypothetical protein
SO4201	11	9	6	11	6	10	10	12	ubiquinone biosynthesis protein AarF (aarF)
SO4202	6	9	7	6	6	7	7	11	Sec-independent protein translocase protein TatA (tatA)
SO4203	5	12	5	7	10	7	9	10	Sec-independent protein translocase protein TatB (tatB)
SO4205						2			hypothetical protein
SO4206	2								hydrolase, TatD family
SO4207	4	11	3	4	3	8	3		GGDEF domain protein
SO4208	10	11	5	7	9	8	5	7	delta-aminolevulinic acid dehydratase (hemB-2)
SO4211	97	110	101	118	117	95	111	128	preprotein translocase, SecA subunit (secA)
SO4212			2						peptidase, M23/M37 family
SO4214	2								UDP-3-0-acyl N-acetylglucosamine deacetylase (lpxC)
SO4215	16	23	27	25	16	17	29	23	cell division protein FtsZ (ftsZ)
SO4216	14	16	20	17	17	10	15	16	cell division protein FtsA (ftsA)
SO4217	2	4	3	2	3	3	4	3	cell division protein FtsQ (ftsQ)
SO4218	5	6	9	5	8	2	4	8	UDP-N-acetylmuramate--alanine ligase (murC)
									UDP-N-acetylglucosamine--N-acetylmuramyl-(pentapeptide)
									pyrophosphoryl-undecaprenol N-acetylglucosamine transferase
SO4219	21	21	21	16	17	17	25	28	(murG)
SO4221	4	2	7	6	7		6	7	UDP-N-acetylmuramoylalanine--D-glutamate ligase (murD)
									UDP-N-acetylmuramoylalanine--D-glutamyl-2,6-diaminopimelate--D-
SO4223	6	14	10	14	8	6	10	16	alanyl-D-alanyl ligase (murF)

Locus	45 min Control		45 min Cr		90 min Control		90 min Cr		Description
	Run 1	Run 2	Run 1	Run 2	Run 1	Run 2	Run 1	Run 2	
SO4224		2	2	4	3		2	2	UDP-N-acetylmuramoylalanyl-D-glutamate--2,6-diaminopimelate ligase (murE)
SO4225	11	12	8	11	8	7	8	10	peptidoglycan synthetase FtsI (ftsI)
SO4226		2				3			cell division protein FtsL (ftsL)
SO4227	7	13	8	6	9	8	4	7	conserved hypothetical protein TIGR00006
SO4228		2	2	3	2		2		conserved hypothetical protein TIGR00242
SO4230	2		2	2				7	glycerol kinase (glpK)
SO4232			2	3				4	long-chain fatty acid transport protein
SO4233		3					2		3-isopropylmalate dehydratase, small subunit (leuD)
SO4234					2		2		3-isopropylmalate dehydratase, large subunit (leuC)
SO4235			2	2					3-isopropylmalate dehydrogenase (leuB)
SO4236		2							2-isopropylmalate synthase (leuA)
SO4241					3				ATP-dependent DNA helicase RecQ (recQ)
SO4244		4	3	2		5			hypothetical protein
SO4246	6	8	9	12	7	9	7	8	ribosomal protein L33 (rpmG)
SO4247	11	11	12	15	12	10	12	14	ribosomal protein L28 (rpmB)
SO4249	10	10	8	7	7	8		6	DNA/pantothenate metabolism flavoprotein (dfp)
SO4250	4	7	2	5	5	2	2	5	deoxyuridine 5-triphosphate nucleotidohydrolase (dut)
SO4251		2	3		2	2	2		transcriptional regulator, TetR family
SO4252		6	2		2		3		prolyl oligopeptidase family protein
SO4254	8	7	7	6	8	6	5	5	GTP cyclohydrolase I (folE)
SO4255	3	6	8	6	7	4	8	10	orotate phosphoribosyltransferase (pyrE)
SO4256	8	10	4	6	5	9	7	6	ribonuclease PH (rph)
SO4257	12	9	8	10	8	9	9	7	conserved hypothetical protein TIGR00255
SO4258	5	7	12	13	5	2	11	10	site-specific recombinase, phage integrase family
SO4261		2							hypothetical protein
SO4262					2		2	2	hypothetical protein
SO4263				2	2		2		conserved hypothetical protein
SO4264	7	7	6	8	13	4	3	8	type I restriction-modification system, S subunit (hsdS-2)
SO4265	12	12	10	10	14	9	12	18	type I restriction-modification system, M subunit (hsdM-2)
SO4266		2							conserved hypothetical protein
SO4267				2				3	type I restriction-modification system, R subunit (hsdR-2)
SO4270			2						hypothetical protein

Locus	45 min Control		45 min Cr		90 min Control		90 min Cr		Description
	Run 1	Run 2	Run 1	Run 2	Run 1	Run 2	Run 1	Run 2	
SO4280				2					hypothetical protein
SO4281		2			2				potassium uptake protein KtrA, putative
SO4283		3	2		3	4	4		apbE family protein
SO4284	4	3	3		2	4	3	2	ISSo5, transposase
SO4286	2	3		5		3	2	3	chemotaxis motB protein (motB)
SO4289		2	3	2	2				phosphate ABC transporter, ATP-binding protein (pstB-2)
SO4299					2			2	chloramphenicol acetyltransferase (cat)
SO4308	2	2	4	2	3		2		diaminopimelate epimerase (dapF)
SO4309	4	2	2	4	4	4	3	5	diaminopimelate decarboxylase (lysA)
SO4310								3	hypothetical protein
SO4311	4	4	5	4	5	3	4	5	cyay protein (cyaY)
SO4313	12	15	11	17	15	16	10	14	porphobilinogen deaminase (hemC)
SO4315	19	33	23	31	24	30	29	28	hemX protein (hemX)
SO4316	12	18	16	21	18	19	18	18	hemY protein, putative
SO4317	3	7	3	5	7	2	6	6	RTX toxin, putative
SO4318	9	8	7	7	10	13	8	6	toxin secretion ATP-binding protein (rtxB)
SO4319	17	18	17	17	26	15	11	12	HlyD family secretion protein
SO4320	40	46	21	32	43	34	28	34	agglutination protein (aggA)
SO4321	15	16	22	17	11	15	17	16	OmpA family protein
SO4323	9	14	10	8	19	15	8	10	GGDEF domain protein
SO4325		4		2			4	6	ATP-dependent DNA helicase Rep (rep)
SO4326	2			3					transcriptional regulator, TetR family
SO4327	21	25	24	27	21	21	20	30	HlyD family secretion domain protein
SO4329	10	13	13	7	8	14	8	8	conserved hypothetical protein
SO4334	5	2	3	6	6	5	6	4	inner membrane protein, putative
SO4340	5	9	9	5	8	7	8	5	conserved hypothetical protein
SO4343	4	7	6	6	4	2	9	9	aminotransferase, class V
SO4344		4	2	2	2	2			threonine dehydratase (ilvA)
SO4345		2	5		3		2		dihydroxy-acid dehydratase (ilvD)
SO4349	4	6	2	8	5		9	11	ketol-acid reductoisomerase (ilvC)
SO4350	2		2		2			2	transcriptional regulator ilvY (ilvY)
SO4351	3	5	2	3		2		3	CBS domain protein

Locus	45 min Control		45 min Cr		90 min Control		90 min Cr		Description
	Run 1	Run 2	Run 1	Run 2	Run 1	Run 2	Run 1	Run 2	
SO4356	7	13	9	5	12	7	11	10	conserved domain protein
SO4358	3		2	4		2		4	anaerobic dimethyl sulfoxide reductase, A subunit (dmaA-2)
SO4364		5	6	2	4		3	5	ATP-dependent DNA helicase RecG (recG)
SO4365	19	18	22	22	18	19	17	18	hypothetical protein
SO4367				2	2				acyltransferase family protein
SO4371	2					2		2	conserved hypothetical protein
SO4372	2								thioester dehydrase family protein
SO4373	8	12	4	4	8	10	7	10	glycosyl transferase, group 2 family protein
SO4374		6	2	3		4		4	histidine ammonia-lyase, putative
SO4377	2	4	4	4	3	2	3	5	membrane protein, putative
SO4378	2	3	3	4	3	2	2	4	FAD-binding protein
SO4380							2		3-oxoacyl-(acyl-carrier-protein) synthase II, putative
SO4381				2					thioester dehydrase family protein
SO4382	5	3	2	7	4	4	6	5	3-oxoacyl-(acyl-carrier-protein) reductase (fabG-2)
SO4383		2		2	3			2	3-oxoacyl-(acyl-carrier-protein) synthase II (fabF-2)
SO4384	28	30	22	23	22	27	12	22	hypothetical protein
SO4385				2					von Willebrand factor type A domain protein
SO4391	5	3	3	5	6	5	8	9	hypothetical protein
SO4393				2					acetyltransferase, GNAT family
SO4394		2							phage shock protein E (pspE-2)
SO4396			2	3	2		3	3	acyl carrier protein phosphodiesterase (acpD)
SO4397					2				conserved hypothetical protein
SO4398				2					conserved hypothetical protein TIGR00256
SO4399	6	11	10	5	8	5	9	11	hypothetical protein
SO4403	5	14	11	8	5	13	9	10	hypothetical protein
SO4405					2	2			catalase/peroxidase HPI (katG-2)
SO4408	22	31	24	22	29	20	15	27	virulence regulator BipA (bipA)
SO4410	22	30	15	24	25	21	33	28	glutamine synthetase, type I (glnA)
SO4414				3			3		conserved domain protein
SO4418		2	2	3		2	2	3	trypanothione synthetase domain protein
SO4420	2	2		3	3	3	3	2	peptidase, M23/M37 family
SO4426	2	2					2		RNA pseudouridylate synthase family protein

Locus	45 min Control		45 min Cr		90 min Control		90 min Cr		Description
	Run 1	Run 2	Run 1	Run 2	Run 1	Run 2	Run 1	Run 2	
SO4427			2	2	3			3	sensor histidine kinase
SO4428	5	8	7	8	9		5	8	DNA-binding response regulator
SO4438			3	2	3		2	2	hypothetical protein
SO4439								2	conserved hypothetical protein
SO4443						2			hypothetical protein
SO4445	2								response regulator/sensor histidine kinase
SO4446	5	3	2	3	3		3	2	molybdenum ABC transporter, ATP-binding protein
									molybdenum ABC transporter, periplasmic molybdenum-binding protein
SO4448		2	2	5	2				
SO4449	4	4	6	5	5		8	9	molybdenum cofactor biosynthesis protein E (moaE)
SO4450	2	2		2					molybdenum cofactor biosynthesis protein D (moaD)
SO4451		6	6	2		3	3	4	molybdenum cofactor biosynthesis protein C (moaC)
SO4452		3	2	3	2		3	3	molybdenum cofactor biosynthesis protein A (moaA)
SO4453	24	21	17	17	24	16	16	20	electron transfer flavoprotein-ubiquinone oxidoreductase, putative
SO4454	10	12	5	16	15	11	10	13	methyl-accepting chemotaxis protein
SO4456			2		3		3	2	conserved hypothetical protein
SO4457		3					3	3	GGDEF domain protein
SO4465			2						conserved domain protein
SO4466	3	2			2		2		methyl-accepting chemotaxis protein
SO4469	2	4	7	5	5		5		alcohol dehydrogenase, iron-containing
SO4470				3	2		2		conserved hypothetical protein
SO4471						2			nitrogen regulation protein (ntrB)
SO4472			3	3			5	3	nitrogen regulation protein NR(I) (ntrC)
SO4473		3		2			3	2	outer membrane protein, putative
SO4475								2	cation efflux family protein
SO4476		3							spheroplast protein y precursor, putative
SO4477	2						3	2	transcriptional regulatory protein CpxR (cpxR)
SO4478			4		2		4	3	sensor protein CpxA (cpxA)
SO4479	3				2		2	3	sigma-54 dependent transcriptional regulator
SO4480			4	2	3		6	11	aldehyde dehydrogenase (aldA)
SO4488	2							2	sensor histidine kinase
SO4490							2		hypothetical protein
SO4492	8	7	6	9	10	5	6	9	conserved hypothetical protein

Locus	45 min Control		45 min Cr		90 min Control		90 min Cr		Description
	Run 1	Run 2	Run 1	Run 2	Run 1	Run 2	Run 1	Run 2	
SO4497	4	3	3		2	4	3	2	ISSo5, transposase
SO4503	2		2						formate dehydrogenase accessory protein FdhD, putative
SO4505	5	7	7	8	5	6	6	6	conserved hypothetical protein
SO4506	10	7	3	6	11	3	3	3	iron-sulfur cluster-binding protein
SO4509	38	50	44	51	38	32	38	38	formate dehydrogenase, alpha subunit
SO4510	8	5	5	8	6	2	6	8	formate dehydrogenase, iron-sulfur subunit (fdhB-1)
SO4511	2			2	2				formate dehydrogenase, C subunit, putative
SO4513	16	18	5	3	48	36	4	3	formate dehydrogenase, alpha subunit
SO4514	4	2	4	3	5		3	4	formate dehydrogenase, iron-sulfur subunit (fdhB-2)
SO4516	6	10	15	10		3	15	12	ferric vibriobactin receptor (viuA)
SO4520	24	24	20	20	36	15	20	20	oxygen-independent coproporphyrinogen III oxidase, putative
SO4523	28	41	40	44	20	26	63	63	iron-regulated outer membrane virulence protein (irgA)
SO4525						2	2		conserved hypothetical protein
SO4529	5	7		6	3		5	5	RNA methyltransferase, TrmH family, group 2
SO4537	12	13	10	11	14	14	5	11	peptidase, putative
SO4557	13	23	17	24	17	19	20	23	methyl-accepting chemotaxis protein
SO4558				2				3	hypothetical protein
SO4559					3				conserved domain protein
SO4561	8	5	4	7	5	7			conserved hypothetical protein
SO4564						2			TonB2 protein, putative
SO4567								2	transcriptional regulator, AsnC family
SO4573	4	4		3	2		3	4	2-succinyl-6-hydroxy-2,4-cyclohexadiene-1-carboxylic acid synthase/2-oxoglutarate decarboxylase (menD)
SO4575	3	7	4	4	6		3	8	O-succinylbenzoate-CoA synthase (menC)
SO4583	2							2	RNA polymerase sigma-32 factor (rpoH)
SO4584	2	7	2	3	4	5	3	4	cell division permease protein FtsX (ftsX)
SO4585	10	10	13	15	8	7	9	12	cell division ATP-binding protein FtsE (ftsE)
SO4586	24	31	41	41	25	29	38	41	cell division protein FtsY (ftsY)
SO4587		2	2	2	2		2	2	conserved hypothetical protein TIGR00095
SO4591	3	3	3	2	6	7		4	tetraheme cytochrome c (cymA)
SO4593					3	4	2	4	hypothetical protein
SO4597		2	3	3	5	9	2	4	heavy metal efflux system protein, putative
SO4598		4	2	3	8	8	3	5	heavy metal efflux pump, CzcA family

Locus	45 min Control		45 min Cr		90 min Control		90 min Cr		Description
	Run 1	Run 2	Run 1	Run 2	Run 1	Run 2	Run 1	Run 2	
SO4599	5	4	6	4	4		3	5	ribonuclease, T2 family
SO4602	35	53	37	39	40	44	43	40	glycerol-3-phosphate acyltransferase (plsB)
SO4603	4		4	4	5	2		2	LexA repressor (lexA)
SO4615				2					SCO1/SenC family protein
SO4616		2					2		polysaccharide deacetylase family protein
SO4618					2				prolyl oligopeptidase family protein
SO4619	5	9	6	10	7	7	6	10	yhgI protein (yhgI)
SO4620	4	2	5	3	9	10	3	7	fumarate reductase, flavoprotein subunit precursor (ifcA-2)
SO4626					2				bioH protein (bioH)
SO4628	13	11	10	16	11	11	9	10	sulfatase
SO4629	21	22	22	20	19	14	26	27	conserved hypothetical protein
SO4633	4	5	7	4	3	3	2	5	transcriptional regulatory protein OmpR (ompR)
SO4634	3	5	5	3	4	3	3	5	osmolarity sensor protein EnvZ (envZ)
SO4635		2					2	2	methyl-accepting chemotaxis protein
SO4637				2				3	DNA-binding response regulator
SO4638	2			2	2		2	2	sensor histidine kinase
SO4640	11	15	10	9	10	9	11	13	antioxidant, AhpC/Tsa family
SO4642				2		2		2	conserved hypothetical protein
SO4643		3	3		2	3	3	3	hypothetical protein
SO4645		2			2				hypothetical protein
SO4647	2	2				3	3	2	DNA-binding response regulator
SO4648			2	2		2		2	sensor histidine kinase
SO4650								4	conserved hypothetical protein
SO4651			3	5			4	6	conserved hypothetical protein
SO4652			10	10			13	24	sulfate ABC transporter, periplasmic sulfate-binding protein (sbp)
SO4653								2	sulfate ABC transporter, permease protein (cysT-2)
SO4655	3	6	19	11			26	26	sulfate ABC transporter, ATP-binding protein (cysA-2)
SO4656		2		2					hypothetical protein
SO4658	2	2				2	2		conserved hypothetical protein
SO4659	6	6	4	6	2	5	7	5	conserved hypothetical protein
SO4661	2	4		2	2	6	2		hypothetical protein
SO4662	6	10	7	12	10	7	10	11	lemA protein

Locus	45 min Control		45 min Cr		90 min Control		90 min Cr		Description
	Run 1	Run 2	Run 1	Run 2	Run 1	Run 2	Run 1	Run 2	
SO4666	22	27	23	22	23	18	18	19	cytochrome c (cytC)
SO4667	8	8	3	6	5	9	7	7	GTP-binding protein EngB (engB)
SO4669	11	17	15	12	17	8	14	12	DNA polymerase I (polA)
SO4670	3	4	4	5	3		4	3	enhancing lycopene biosynthesis protein (elbB)
SO4672			3	3	2			2	glpE protein (glpE)
SO4673	9	7	12	11	14	4	11	7	threonine 3-dehydrogenase (tdh)
SO4674	13	13	16	12	15	10	13	17	2-amino-3-ketobutyrate coenzyme A ligase (kbl)
SO4675				2					transcriptional regulator, TetR family
SO4676	7	6	6	6	6	7	5	9	3-deoxy-D-manno-octulosonic-acid (KDO) transferase (kdtA)
SO4677	4	8	3	6	5	7	4	4	conserved hypothetical protein
SO4678	11	8	4	10	9	12	13	10	heptosyl transferase, glycosyltransferase family 9 protein
SO4679	19	19	16	16	15	21	16	21	glycosyl transferase, group 1 family protein
SO4680	13	15	17	14	15	13	17	16	conserved hypothetical protein
SO4681	21	23	20	21	25	19	19	19	glycosyl transferase, group 1 family protein
SO4682	3	3	2	3	5		6	4	glycosyl transferase, group 1 family protein
SO4684	5	6	5	2	2	3	2	5	phosphopantetheine adenylyltransferase (coaD)
SO4685	15	24	16	14	13	16	19	21	conserved hypothetical protein
SO4686			2		2				NAD dependent epimerase/dehydratase family protein
SO4687	2								UDP-glucose 6-dehydrogenase (ugd)
SO4688					2	2		4	glycosyl transferase, group 2 family protein
SO4690					2	2			conserved hypothetical protein
SO4692	35	40	33	39	25	28	31	36	AcrB/AcrD/AcrF family protein
SO4693	40	47	42	44	39	44	44	46	multidrug resistance protein, AcrA/AcrE family
SO4696			2		2		2		conserved hypothetical protein
SO4697							2		glutathione S-transferase (gst)
SO4699	10	15	15	14	13	5	14	16	oligopeptidase A (prlC)
SO4702	13	15	13	11	14	4	9	15	glutathione reductase (gor)
SO4704						2			hypothetical protein
SO4711		3							HD domain protein
SO4712				2					ABC transporter, ATP-binding protein, putative
SO4713		2			2		2		menaquinone-specific isochorismate synthase, putative
SO4716							2		acetyltransferase, GNAT family

Locus	45 min Control		45 min Cr		90 min Control		90 min Cr		Description
	Run 1	Run 2	Run 1	Run 2	Run 1	Run 2	Run 1	Run 2	
SO4717	10	8	4	5	3	5	6	12	sensor histidine kinase
SO4718	8	10	6	8	8	6	5	12	sigma-54 dependent response regulator
SO4719	31	36	31	30	24	35	18	19	conserved hypothetical protein
SO4721	3	2			2	2	4	2	ABC transporter, ATP-binding protein
SO4722	2			3	2	2		2	molybdopterin-guanine dinucleotide biosynthesis protein (mobA)
SO4723	16	20	11	13	13	11	12	12	molybdopterin biosynthesis MoeA protein, putative
SO4724		2		2		2			molybdenum cofactor biosynthesis protein A, putative
SO4725	3	5	3	4	4	6	3	3	conserved hypothetical protein
SO4726	5	4	4	3	7	2	2	3	formamidopyrimidine-DNA glycosylase (mutM)
SO4728	5	6	9	8	9	6	6	10	conserved hypothetical protein
SO4729	9	7	8	12	6	4	7	11	conserved hypothetical protein
SO4730	4	10	9	8	13	3	13	11	oxygen-independent coproporphyrinogen III oxidase (hemN)
SO4731		4	5	5	5		5	8	adenosine deaminase (add)
SO4732	7	12	6	9	7	6	7	8	conserved hypothetical protein
SO4733	7	4	4	6	5	5	5	5	lysophospholipase L2 (lypA)
SO4734			3				2	2	sensory box protein
SO4737	3	5	2	3	7	2	3	5	iron-sulfur cluster-binding protein
SO4738	4	3	2	4	3	4	4	4	hypothetical protein
SO4739	8	4	2	10	7	6	12	9	naphthoate synthase (menB)
SO4741	12	19	12	18	16	9	14	19	glucosamine--fructose-6-phosphate aminotransferase (isomerizing) (glmS)
SO4742	4	3	5	6	3	3	2		transcriptional regulator, DeoR family
SO4743	46	64	55	58	29	32	63	63	TonB-dependent receptor, putative
SO4745	11	11	7	6	4	7	8	12	UDP-N-acetylglucosamine pyrophosphorylase (glmU)
SO4746	12	12	16	15	12	12	17	15	ATP synthase F1, epsilon subunit (atpC)
SO4747	72	82	78	75	81	64	86	79	ATP synthase F1, beta subunit (atpD)
SO4748	49	51	46	45	49	51	50	43	ATP synthase F1, gamma subunit (atpG)
SO4749	94	106	94	95	102	103	98	105	ATP synthase F1, alpha subunit (atpA)
SO4750	16	17	16	15	14	18	15	12	ATP synthase F1, delta subunit (atpH)
SO4751	40	47	41	42	39	43	41	45	ATP synthase F0, B subunit (atpF)
SO4755	11	16	13	10	12	9	14	19	ParB family protein
SO4756			3	3			3	2	ParA family protein
SO4757	3	7		4	6		2	3	glucose-inhibited division protein B (gidB)

Locus	45 min Control		45 min Cr		90 min Control		90 min Cr		Description
	Run 1	Run 2	Run 1	Run 2	Run 1	Run 2	Run 1	Run 2	
SO4758	29	35	28	34	26	30	27	32	glucose-inhibited division protein A (gidA)
SOA0003	10	4	8	6	9	3	7	5	type II restriction endonuclease, putative
SOA0004	12	9	6	16	8	4	9	14	type II DNA modification methyltransferase
SOA0005		2		3	4		2	3	hypothetical protein
SOA0006					2		2	3	ParA family protein
SOA0008			2						hypothetical protein
SOA0011	5	5	6	4	4	3		5	conserved hypothetical protein
SOA0018	2				2	2		4	TnSon1, conserved hypothetical protein
SOA0019	5	5	2	6	4	4	3	3	TnSon1, resolvase
SOA0022			2				2	2	proteic killer active protein (higB)
SOA0023	3		2	3	2	3		2	proteic killer suppressor protein (higA)
SOA0031			3				3	6	partition protein, ParB family, putative
SOA0032		2				2			conserved hypothetical protein
SOA0033		2	2	2			2	3	hypothetical protein
SOA0040							3	2	hypothetical protein
SOA0041	5	7	5	5	9	6	7	5	transcriptional regulator, PemK family
SOA0042	3		5	6			4	4	hypothetical protein
SOA0045						2			site-specific recombinase, phage integrase family
SOA0048	18	22	26	23	24	17	23	24	prolyl oligopeptidase family protein
SOA0049	4	5	3		7	5	4	6	toxin secretion ABC transporter, ATP-binding subunit/permease
SOA0051	9	10	8	10	6	8	6	7	protein, putative
SOA0056		2	2	2				2	hypothetical protein
SOA0059	2	2	5	4	3	6		2	hypothetical protein
SOA0060	3	5	8	7	4	3	6	8	conserved hypothetical protein
SOA0061	4	4	7	5	3	7	6	6	acetyltransferase, GNAT family
SOA0062	7		4	6	4	4	4	3	parA protein, putative
SOA0067							2		hypothetical protein
SOA0069								3	hypothetical protein
SOA0070	3		7		3		5		conserved hypothetical protein
SOA0075						2			hypothetical protein
SOA0077	3	4	3	3	2		2	2	hypothetical protein
SOA0079			2	2			2		site-specific recombinase, resolvase family
									conserved hypothetical protein

Locus	45 min Control		45 min Cr		90 min Control		90 min Cr		Description
	Run 1	Run 2	Run 1	Run 2	Run 1	Run 2	Run 1	Run 2	
SOA0080			6	3				4	hypothetical protein
SOA0086		2	2			4		2	site-specific recombinase, resolvase family
SOA0088			3		2				plasmid stabilization protein ParE, putative
SOA0095	3	4	3	6	6	2	5	10	partitioning protein A
SOA0096	11	14	14	13	13	14	15	15	partitioning protein B
SOA0099	6	4	12	7	8	4	6	11	conserved hypothetical protein
SOA0100	7	17	21	26	17	9	21	19	conserved hypothetical protein
SOA0106	26	28	22	28	18	22	28	23	methyl-accepting chemotaxis protein
SOA0108								2	hypothetical protein
SOA0110	14	19	18	24	24	22	18	24	lipoprotein, putative
SOA0112	18	21	24	32	29	23	26	31	lipoprotein, putative
SOA0114	15	20	17	18	16	23	23	20	outer membrane protein A (ompA)
SOA0115	18	21	24	32	29	23	26	31	lipoprotein, putative
SOA0119								2	ISSo13, transposase
SOA0131				2			3	3	hypothetical protein
SOA0132	3	2	3	3	5	2	5	2	conserved hypothetical protein
SOA0135	6	5	6	4	6	5	7	6	hypothetical protein
SOA0138	12	11	12	11	11	6	12	10	hypothetical protein
SOA0139		2	2	3	2		2		hypothetical protein
SOA0140	33	35	30	19	31	19	30	30	hypothetical protein
SOA0141	15	16	4	2	11	6		3	hypothetical protein
SOA0142								2	ISSo13, transposase
SOA0149				2				3	conserved hypothetical protein
SOA0150	2	3	2	2	3	3	3	5	hypothetical protein
SOA0151								2	ISSo13, transposase
SOA0153		3	2	4	12	11	7	6	heavy metal efflux pump, CzcA family
SOA0154			3	3	13	13	8	10	heavy metal efflux protein, putative
SOA0157	2				2	2			hypothetical protein
SOA0160	3	5	8	5	11		5	4	esterase, putative
SOA0161	6	6	8	8	7	3	9	13	zinc-binding dehydrogenase
SOA0164				3				3	iron-containing alcohol dehydrogenase
SOA0165	11	11	12	8	14	9	7	13	transcriptional regulator, LysR family

Locus	45 min Control		45 min Cr		90 min Control		90 min Cr		Description
	Run 1	Run 2	Run 1	Run 2	Run 1	Run 2	Run 1	Run 2	
SOA0169	2				2	2		4	TnSon1, conserved hypothetical protein
SOA0170	5	5	2	6	4	4	3	3	TnSon1, resolvase
SOA0171	3	8	3	2	2	3	2	3	hypothetical protein
SOA0172		2		4	4				site-specific recombinase, resolvase family
SOA0173			3	6	2		4	3	hypothetical protein

VITA

Melissa Renee Thompson was born Melissa Renee Rugen on February 23, 1979 in Columbia, Mo. She spent her early childhood in the town of Green Ridge, Mo. Melissa started elementary school in Mexico, Mo attending Hawthorne Elementary School. She then transferred to Butler, Mo. attending Butler Elementary followed by Albany, Mo. for grades second thru fourth attending Virginia E. George Elementary. She finished her elementary and secondary education in California, Mo. graduating Salutatorian of her class from California High School in May of 1997. In December of 2001, she completed her Bachelor's of Science degree in Biological Sciences with Minors in Chemistry and Spanish from the University of Missouri-Columbia. After finishing her degree, she worked as a Senior Laboratory Technician for Dr. Kathleen Newton at the University of Missouri-Columbia. Her work with Dr. Newton included assisting in annotating the wild-type *Zea mays* mitochondrial genome, which was published in 2004.

In August of 2003, she enrolled in the Graduate School of Genome Science and Technology, a joint program between the University of Tennessee-Knoxville and Oak Ridge National Laboratory where she pursued a Doctoral of Philosophy degree in Life Sciences completing the degree in 2007. After graduation she moved to St. Louis, Mo to pursue a Post-Doctoral Fellow with Pfizer, Inc.